Title
Common Era records of Santa Barbara Basin benthic foraminifera reveal nineteenth and twentieth century shifts in reproductive life history, body size, and community structure

Author
Kahanamoku-Meyer, Sara Segura

Publication Date
2022

Peer reviewed|Thesis/dissertation

Common Era records of Santa Barbara Basin benthic foraminifera reveal nineteenth and twentieth century shifts in reproductive life history, body size, and community structure

by

Sara Segura Kahanamoku-Meyer

A dissertation submitted in partial satisfaction of the

requirements for the degree of

Doctor of Philosophy

in

Integrative Biology

in the

Graduate Division

of the

University of California, Berkeley

Committee in charge:

Professor Seth Finnegan, Chair
Professor Carl Boettiger
Professor Ivo Albert Paul Duijnstee

Fall 2022

Abstract

Common Era records of Santa Barbara Basin benthic foraminifera reveal nineteenth and twentieth century shifts in the reproductive life history, body size, and community structure

by

Sara Segura Kahanamoku-Meyer

Doctor of Philosophy in Integrative Biology

University of California, Berkeley

Professor Seth Finnegan, Chair

Past ecological information is critical for contextualizing the rapid, decadal to centennial-scale climate changes characteristic of novel human regimes—such as colonialism, industrialization, and urbanization. Yet these changes occur over 1-100 year "invisible timescales," making them difficult to resolve with traditional biological and paleontological methods. In this dissertation, I use a highly temporally-resolved fossil record from an extraordinary system, benthic foraminifer fossils preserved in the marine varves of the Santa Barbara Basin (SBB), to examine the short-term impacts of environmental shifts on individuals and communities over the Common Era, an interval that includes both environmental stasis and rapid change.

Here I use the largest dataset of benthic foraminifera images and morphometric measurements generated to date to assess trends in life history reproduction, intra- and interspecific body size, and community-level diversity and abundance. In Chapter 1, I introduce benthic foraminifera from the SBB as an extraordinary system for high-resolution paleoecology. In Chapter 2, I detail the high-throughput imaging method I employ to produce a dataset of over 20,000 foraminifer images and measurements. In Chapter 3, I use these data to document the reproductive life history of biserial *Bolivina* foraminifera from ~50 CE to 2008 CE to examine the range of natural variation in reproductive mode and how reproduction is correlated with environmental variables. In Chapter 4, I apply a ~760-year-long dataset of individual measurements to characterize connections between intraspecific and community body size and whether size is modulated by life history and environmental variation. In Chapter 5, I undertake a multivariate analysis of diversity, biomass, and environmental data to assess how benthic foraminifer communities are structured from ~1834-2008 CE. Finally, I synthesize my findings in Chapter 6 and outline a vision for how paleoecology and the historical sciences more broadly can be in conversation with other disciplines to better understand the impacts of social and ecological change on the ocean.

I find that all aspects of ecology examined—life history, body size, abundance, and community structure—undergo state changes in the 19th and 20th centuries. The timing of change corresponds to major shifts in human-environment interactions that accompanied the colonization and industrialization of California. Taken together, these findings suggest that not only do SBB benthic foraminifera communities change towards the present day, but that modern communities are more changeable than those of the past, demonstrating heightened variability in individual characteristics that have species- and community-scale ecological consequences.

Dedication

To my ʻohana
To my lāhui
To my ʻāina
And to Moananuiākea, the ocean that connects us all

Table of Contents

List of Figures and Tables

Acknowledgements

It is difficult to find the appropriate words to thank all who have, in countless ways over countless years, supported me in my academic journey.

I will begin in the place I know best: my one hānau of Haleʻiwa and Waialua. To Ke Iki, the beach that raised me, and the piko of my existence: mahalo for teaching me to watch the ocean, to look for the waves on the horizon and the currents under the surface, to be confident in the water while also knowing that it deserves our utmost respect. You were the first place I looked for stories of the past, and you will be the place to which I return when I am ready to become one of those stories. To the waters and lands of Koʻolauloa and Waialua: you are where I learned the meaning of abundance. To the moku of Oʻahualua: you taught me that all places are sacred, that akua live in each of the verdant corners of this land, that the call will be answered when it is given. To the moku of Hawaiʻi, Moku o Keawe, my ʻāina kūlāiwi: mahalo for always, without hestiation, making me feel held. I am fortunate beyond measure to know that Ko Hawaiʻi Pae ʻĀina is and will always be my home.

Even as Hawaiʻi is my piko, my genealogies extend beyond this place. Through my father, my family extends across Moananuiākea to Māʻohi Nui, the hundreds of islands currently known as French Polynesia. While I have much work to do in reconstructing these geneologies, I currently know that my relatives come from the fenua of Niʻa Mataʻi and Tuamotu. Through my mother, my family crosses the world, where her lineage has remained in Catalunya for many generations. I am blessed to have a strong connection to my mom's family, her nine brothers and sisters, their spouses, and the over thirty cousins that all remain in or near Catalunya. I thank all of these homelands for the grounding that they provide and the connections to past, present, and future that they keep open.

Many people have contributed in the dreaming, doing, writing, and finishing of my PhD. It is almost impossible to go through four years of university schooling plus five and a half years of graduate work in places many thousands of miles away from home without having the support of abundant communities of people, whether near or far. I hope to thank as many of them as possible here, but know that I may have left some names out in the haze of finishing this document. To these people, I apologize, and hope someday I can share my thanks in a more conscientious way.

To my mom, Marta Segura, who is the firmest foundation in my life: thank you, mahalo, gràcies, for raising me exactly the way that you did. I can't remember a time when you didn't believe in me *and* help me take the first steps in making my dreams a reality. There were some heavy obstacles in your way, but you crashed right through them to make sure that I know that I could do anything I wanted to in this life. In my most impactful mentorship moments, I find myself repeating to my students advice that you have given me (you should really be getting the teaching credits there). I am grateful that you always cheer me on, and that the bigger the mistakes I make, the more celebratory you are. Thank you for teaching me to learn from my failures and revel in challenges. My favorite compliment to get is when people meet you and tell me how they "can see where I get it from."

To my partner, Gregory Kahanamoku-Meyer: after nearly a decade together, I am still regularly made speechless by the way that you unfailingly and joyfully grow with me through all of our phases in life. You have helped to shape me into the person that I am today, and have accepted me at every stage with the most effervescent love. It's a little unhinged that we decided to go to grad school at the same time, but through all of this academic stress you've affirmed again and again that our most important and meaningful task in life is to love others, and to love well. Thank you for giving me what I needed to finish this work, and thank you for moving with me back to Hawai'i—five thousand miles from your home—to support my dream of returning to mine. You are everything.

This work would not have been possible without the undergraduate research and work-study students who spent years at the microscope alongside (and sometimes without) me. These students worked with me as first-years and as seniors, through a pandemic and as we navigated new ways to be together in lab. Sarah Kamel and Da'shaun Stewart: thank you for putting in countless hours to pick and identify thousands of tiny fossils. Heather McCandless, Jared Richards, and Max Titcomb: it was a gift to work with you on theses and REU projects and it is even more so to see how you have taken your talents into your graduate work. R. Cheyenne Bridge, Sapon Chupongstimun, Nina Jager, Leah Kahn, Kate Kennedy, Sophie Li, Judah Marsden, Heather Ramsey, Lily Ruiz, Carolina Sinco, and Mindy Yan: Thank you for dealing with rapidly changing research conditions and the stresses of college and still managing to do incredible work.

To my labmates, Maya Samuels-Fair, Joshua Zimmt, Ryan Yohler, and Kayli Nelson (and those who got out first: Emily Orzechowski and Larry Taylor): thank you for keeping me laughing and for always being willing to hash out an idea. I am so lucky to have you as colleagues. Maya, thank you for being a collaborator on this work and for being willing to talk forams, regardless of how busy you are. I admire all of my labmates for their tireless efforts to make the university a better place for us all.

A million thanks to my dissertation chair and advisor, Seth Finnegan. You are one of those people who encouraged me to dream up wild ideas and supported me in the work of chasing them. I don't know if this is a rarity in academia, but it certainly is a blessing. Thanks to you, we now have more forams than anyone really knows what to do with… and I can only imagine the grand questions you'll come up with that springboard from this work. To Ivo Duijnstee, who is not on paper but is in reality my secondary advisor, I can't express my gratitude for all that you've done in the saga of this work. You're a jack of all trades who has mastery of what seems to be nearly all of them, and you share this knowledge in the warmest way. Thank you for making the many intellectual and physical spaces you inhabit welcoming for me, no matter what. To my committee, Carl Boettiger and Tessa Hill, thank you for broadening my perspective and helping to shape my research trajectory into something that is not only academically interesting, but also supports my future goals, and for doing so with the utmost kindness and enthusiasm.

While through most of graduate school I have been physically present in xućyun (Huichin, the land of the Muwekma Ohlone Tribe and related descendants which UC Berkeley presently occupies), much of my work has expanded beyond this place and been generated and supported by collaborations with some of the scientists to whom I look up the most. Many of these projects

did not end up in this dissertation, but deserve to be recognized nonetheless. To the team of colleagues and friends working to shed light on racial disparities in scientific funding—Christine Yifeng Chen, Aradhna Tripati, Rosie Alegado, Vernon Morris, Karen Andrade, and Justin Hosbey—when Christine and I met on a geology field trip many years ago, I couldn't have foreseen what we'd get up to and how we would be uplifted in these endeavors by you all. Thank you for your support, and thanks to Aradhna for the financial backing of this work in the form of a fellowship from the Center for Diverse Leadership in Science at UCLA.

I am fortunate beyond measure to have a hui of ʻŌiwi scholars and allies who took me in as a younger student and helped me to learn how to navigate the incommensurabilities and complexities of academia. Mahalo nunui to Aurora Kagawa-Viviani, Rosie Alegado, Haunani Kāne, Katie Kamelamela, Brittany Kamai, Marissa Loving, Kawela Farrant, Keolu Fox, and countless others who have spent time with me to kūkākūkā about how we can bring forth ʻŌiwi futures. To the Ulana ʻIke Center: Rosie Alegado and Katy Hintzen, mahalo piha for welcoming me in and showing me how to do the work of building connections and uplifting Indigenous peoples across Moananuiākea and beyond. If in reading through you have noticed the name Rosie Alegado come up multiple times, good eye! Special thanks to Rosie for being a mentor, friend, co-conspirator, and my future postdoc advisor. Without you I do not know when—or if—I would have made it home. Mahalo palena ʻole.

To the abundant community of Indigenous scholars I am blessed to call my friends: mahalo for your radical friendship, for sharing food from faraway homelands, for being instigators and perpetuators, for cracking jokes and laughing in the loud and expansive way only Natives can. Mahalo to the Natives at Cal who brought me into their circle exactly when I needed it most: Breylan Martin, Jesus Nazario, Summer Lewis, Talia Dixon, Sierra Hampton, Nani Conklin, McKalee Steen, and everyone else in IGSA. Mahalo to the Indigenous scholars before us who provided a firm foundation for us ʻōpio to stand on. Mahalo to the contemporaries whose written and spoken encouragement helped me make it, day by day, through this PhD. I am awed by the revolutionary and fiery love each of you embodies in your work. I am blessed to create new worlds alongside you every day.

To Kahanamoku, Tenamoeata, Paoa, and the countless other watery ancestors and man-eating sharks from whom I trace my lineage: mahalo for the profundity and sharpness you bring to my work, and for the gurgling and joyful insights that bubble up unexpectedly in the darkest of seas. To all those who have come before: you are the droplets that form the swirling currents connecting our sea of islands; out of your waters, I am nothing.

1 The invisible timescales of global change

1.1 Resolving the history of climate change impacts on ecosystems

Novel human activity in the last several generations[1]—specifically, colonialism, industrialization, and the rise of global capitalism (Davis and Todd 2017)—is responsible for global heating and widespread environmental degradation, resulting in rising sea levels, an acidifying and deoxygenating ocean, losses of arable land, more frequent and intense droughts, fires, storms, coastal erosion, and severe declines in global biomass and biodiversity (Barnosky et al. 2011, 2012, IPCC 2018, IPCC 2019). These dramatic earth system changes have taken place in less than 200 years, reversing a 50-million-year-long trend of global cooling in a timespan that amounts to a geological instant (Westerhold et al. 2020). Reconstruction of these changes, as well as the global climate and ecosystem baselines that preceded them, involves nuanced understanding of the variability inherent to the Earth system on multiple timescales. The paleo sciences—including paleoclimatology, paleobiology, and historical ecology—are instrumental for the collection and interpretation of data on the long-term climate, environmental, and evolutionary history of earth, and in many cases provide ability to constrain the anticipated severity and extent of change across multiple systems. Taken together, paleo data is both powerful and critical for understanding the planetary implications of climate change (Dietl et al. 2015, Dietl 2019).

Yet many of the global reorganizations observed over the past one to three centuries taken place on timescales that are close to the limits of the resolving power of the fossil record (Kidwell 2015). In other words, rapid changes similar to those that have occurred in the recent past are very unlikely to be recorded in geological archives, thus limiting the predictive power that can be garnered from fossil records, as well as making holistic interpretations of future impacts difficult. In particular, changes that have occurred since the beginning of the Great Acceleration—the period of time beginning in the mid-20th century that corresponds with rapid, continuous, and simultaneous surges across multiple indicators of human activity[2]—have occurred on timescales

[1] This period is increasingly referred to by western scientists as the "Anthropocene," a term which seeks to capture the magnitude, variety, and longevity of human-induced changes on Earth's ecosystems and climate (Lewis and Maslin 2015). Conflicting opinions around the necessity and the timing of a new epoch are, at their core, driven by the conflicting ways that different parties assign responsibility to which groups for human-induced climate changes. As noted by Davis and Todd (2017), designating the Anthropocene a geological epoch "has political implications beyond the bounds of the discipline of geology, for stating that we are living in a geologic epoch determined by the detritus, movement, and actions of humans is itself a political act" (p. 762). The term Anthropocene is itself political, as it ascribes universal responsibility for the climate crisis—verbiage that is used to deflect from the historical and ongoing context of climate change (McGregor et al. 2020) and ignores that "anthropogenic climate change is an intensified repetition of anthropogenic environmental change inflicted on Indigenous peoples via colonial practices that facilitated capitalist industrial expansion" (Whyte 2017, p. 156; see also Whyte 2020 and the conclusion of this dissertation). Further, the positioning of the Anthropocene as a future apocalypse erases the ways that Black and Indigenous peoples have survived and resisted the ecological collapses associated with colonialism (Whyte 2016, 2018), themselves a "settler anthropocene" (Todd 2015). Because of this, I do not refer to the Anthropocene in this dissertation, preferring instead to refer to specific periods of time by their calendar year dates, or using commonly-known terms (e.g., "Great Acceleration," "Industrial Revolution") in an attempt to refrain from ascribing universal responsiblity for major eco-environmental reorganizations.

[2] These include earth-system indicators such as atmospheric CO_2, terrestrial and sea surface temperature, atmospheric ozone concentration, ocean acidification, plastic particle pollution, and overfishing; and socioeconomic

so rapid that even the majority of fossil studies that cover the recent past (e.g., Dietl et al. 2015, Kidwell 2015, Tomasovych and Kidwell 2017) lack the necessary resolving power to fully disentangle the impacts of these changes.

Modern ecological data are also unable to fill this invisible timescale gap. The earliest climatological instrumental records begin around 1880 CE, many decades into the Industrial Revolution and centuries beyond the expansion of settler colonial regimes into the New World (Davis and Todd 2017). Information on ecosystem interactions is even more limited, as multi-year ecological monitoring projects rarely extend back past 1970 CE. While historical ecology can provide some insight into long-term ecosystem-level trends and human impacts (e.g., fishery reconstructions; McClenachan et al. 2006, 2012, Ward-Paige et al. 2010, Thurstan et al. 2015) quantitative data from these studies are often necessarily focused on one aspect of ecosystem diversity, limiting the scope of the scientific studies that can be undertaken using these records.

As a result, the Earth system and ecological impacts of modern climate change exist in the space between the timescales assessed for ecological studies (10^{-8} to 10^{0} years) and those typically preserved in the fossil record (10^{3} to 10^{6} years; Estes et al. 2018)—a space I refer to as "invisible timescales" (Figure 1.1).[3] Because imminent changes will unfold over timescales that are effectively invisible in many fossil records, our ability to understand ecosystem baselines, identify the nature and extent of ecosystem responses to climate- and human-driven impacts, and predict near-term consequences is limited.

In this dissertation, I use a highly temporally-resolved fossil record from the Santa Barbara Basin to examine ecological and biotic shifts among benthic microfossils—namely, benthic foraminifera—over a period revelant to invisible timescales and modern-day understandings of global change. In this introduction, I detail how extraordinary fossil records can be used to shed light on these issues, and overview benthic foraminifera as a useful system in which to assess ecological impacts on individuals and populations through a period of time that contains both stasis and rapid environmental change.

1.2 The Santa Barbara Basin: An extraordinary record of ecosystem change over invisible timescales

One aspect of particular interest in the characterization of the nature and timing of climate and ecosystem reorganization is that of the impact of European colonialism in driving transformations in human-environment interactions across the globe (Lightfoot et al. 2013, Whyte 2017, 2020, McGregor et al. 2020). There is broad documentation of the changing land-use structures resulting from colonialism, such as mission agrarian systems and plantations, and their impacts on the composition of terrestrial flora and fauna populations and ecological processes worldwide. Yet fewer studies have focused on the impacts of colonialism on oceanic

indicators such as the size of the global human population, GDP, energy use, water use, transportation, tourism, and many other factors.

[3] I was introduced to this term by Dr. Peter Roopnarine, a paleoecologist whose work made it clear that the timescales of ecosystem variation are often not captured in fossil or modern ecological studies, which present "snapshots" rather than a full, dynamic picture of ecosystem variability. The term also appears to be in use by Dr. Jon Bergengren (http://ecodiversity.org/notes.html), and has been referenced in the archaeological literature (Murray 2002).

ecosystems (with the notable exceptions of commercial fishing and whaling ventures; see, e.g., Jackson et al. 2001, Pershing et al. 2010, Tulloch et al. 2018, Watson and Tidd 2018).

The scientific studies that do examine the impacts of colonial pressures on ocean ecosystems suggest a coordinated timing of change (Lightfoot et al. 2013), even if the mechanism for these changes are wide-ranging and vastly different. On the California coast, there is evidence that the disruption of the traditional ecological relationships of California Indigenous peoples during the mission period, and the concomitant introduction of cattle, led to a rapid collapse of benthic filter-feeding bivalves and brachiopods on the continental shelf in the mid-19th century (Tomasovych and Kidwell 2017). This loss of an entire filter-feeding fauna was complete by the start of the Great Acceleration in the mid-20th century, indicating that modern ecological studies would not have reconstructed this event, even if California benthic marine monitoring records were comprehensive and complete in the 20th century.

While the invisible and rapid timescales over which ecological changes have taken place make it difficult to characterize the responses of ecosystems to the pressures of human impacts (both traditional and colonial), select natural systems can preserve records that make analyses of this nature possible. Marine microfossils are one such famous system; these include the sub-millimeter-scale shelly remains of small organisms like foraminifera, ostracodes, diatoms, radiolarians, coccolithophores, and dinoflagellates, as well as the skeletonized parts of larger animals (e.g. the teeth, vertebrae, scales, and otoliths of fish; shark dermal denticles). Because shelly marine microfossils can be preserved in high resolution (10^0 to 10^6 years per sample; Kucera 2007, Yasuhara et al. 2015), in high numbers (for planktic foraminifera, in the millions for each cubic centimeter of sediment; Hsiang et al. 2017), and have a long fossil record (spanning back to the Early Cambrian; Pawlowski et al. 2003), they serve as an ideal system with which to cut across the disparate timescales of macro- and paleoecology. In addition, they represent a wide variety of ecological niches, and have long been used by paleo scientists as environmental proxies and biostratigraphic indicators. The high temporal resolution and preservation potential of microfossils make them ideal for quantitative and comparative paleoecological approaches.

Marine microfossils are among the highest-resolution paleontological systems known, yet only a small portion of marine sites at which microfossils are found preserve these assemblages at sub-annual to decadal resolution. These extremely high-resolution systems are ideal for exploring invisible timescales, as they record a wealth of environmental and biological information needed to assess climate and anthropogenic impacts on ecosystems over extremely short periods of time. One such extraordinary site is the Santa Barbara Basin (SBB), which captures seasonal, annual, and decadal records of marine ecosystem change that span the Common Era. The SBB is one of the most well-studied marine sediment systems, as its high-resolution varved sediments, where each layer can represent days to months of sediment accumulation, have made it a well-studied locality for paleoclimate variability reconstruction.

The SBB is a semi-enclosed basin that is bounded by the Santa Barbara coastline to the north and the Channel Islands to the south, with relatively high northeastern (230 m) and southwestern (475 m) sill depths (Figure 1.2). The topography of the basin and the nearby upwelling zone work together to produce low-oxygen bottom waters that exclude large bioturbators (Emery and

Hülsemann 1961, Soutar and Crill 1977, Thunell et al. 1995, Hendy et al. 2013, 2015, Du et al. 2018, Pak et al. 2018). High seasonal sedimentation rates into the basin, on the order of 140 cm ky^{-1}, produce the SBB's distinctive layered couplets. In these, dark siliciclastic sediments are formed as a result of terrigenous sediment delivery via rainfall during winter months, and light biogenic sediments are deposited during spring and summertime increases in primary productivity (Thunell et al. 1995, Schimmelmann and Lange 1996, Hendy et al. 2013, Du et al. 2018). The dysoxic bottom waters (below 500 m) of the SBB result in part from the way in which the basin's bathymetry restricts the movement of well-oxygenated waters into its center; these low oxygen conditions are further enhanced by overlying surface productivity driving respiration at depth (Bray et al. 1999, Moffitt et al. 2014). The extreme to severe hypoxia (<0.1 to 0.5 ml L^{-1}) that often results in the deepest parts of the SBB typically serves to exclude bioturbators (though not always; Schimmelmann et al. 1992, Burke et al. 1996). These compounding environmental phenomena result in the deposition and preservation of millimeter-scale sub-annual resolution of the fossiliferous dark-light varve couplet pairs for which the Basin is famous (Kennett and Ingram 1995).

Each of the sediment layers in the SBB preserve microfossils (including fish otoliths (Jones and Checkley 2019); planktic foraminifera (Field et al. 2006); and benthic foraminifera (Roach 2010); among others) and these fossiliferous, high-resolution layers are continuous for millennia. To date, researchers have studied the Santa Barbara Basin to understand environmental variation and human impacts in the California Current System over annual, decadal, centennial, millennial, and glacial-interglacial timescales. Numerous long-term records of climate variability have been generated from SBB cores, with data from microfossil assemblages, charcoal, oxygen and carbon isotopes, biomarker records, redox indicators, and numerous other proxies providing a broad picture of climatological and ecological shifts over the wide-ranging timescales recorded in the basin. All of these factors converge to make the SBB an extraordinary setting for high-resolution paleoecology.

1.3 Reproductive life history of benthic foraminifera

The high-resolution nature of samples from the SBB also allow for ecological studies that go beyond the typical possibilities of the fossil record, such as the investigation of individual variation, population dynamics, and select aspects of life history. Of these, life history is among the least studied over long timescales. Life history is, at its core, about the tradeoffs that organisms make regarding resource allocation through their lifespansm and how this impacts their growth, reproduction, and survival (Stearns 1992). A major aspect of this is the tradeoffs that surround reproduction. In species that can alternate between modes of reproduction (e.g., sexual vs. asexual), a prediction that can be made is that in times of low stress, asexual reproduction should occur more often as organisms seek to efficiently produce large numbers of genetically homogeneous In other words, when individuals are adapted to their environment, asexual reproduction allows for continuation of these well-adapted genotypes in a less energetically costly way than recombination (Butlin 2002). In contrast, stress tends to increase sexual reproduction, as organisms seek to produce genetically diverse offspring. While sexual reproduction is more costly than asexual reproduction, it allows maladapted individuals to utilize recombination to produce potentially better-adapted progeny (Otto and Lenormand 2002). Under this framework, novel climatic stressors and heightened environmental variability should induce

higher amounts of sexual reproduction, as these shifts to the environment likely increase the need for recombination.

Most direct observations of life history have been in cultured organisms or modern environments, particularly in species with short lifespans. This is true, too, for foraminifera, where recent examples of asexual reproduction were observed in a laboratory setting (Davis et al. 2020, Takagi et al. 2020) and manipulations of environmental conditions—such as modulating temperture and the types of food resources available—have been shown to induce differential modes of reproduction (Nigam and Caron 2000, Barras et al. 2009). However, in some microfossil taxa—such as diatoms (Sims et al. 2006), bryozoans (O'Dea 2006), and, of course, foraminifera—reproductive life history tradeoffs need not explicitly be observed, but can rather be gleaned from morphological features preserved in their shells.

Foraminifera generally undergo lifecycles that involve alternation of generations between a haploid, sexually-reproducing stage and a diploid, asexually reproducing stage. While many are thought to have a simple dimorphic lifecycle—in which gamonts (cells that are capable of producing gametes) alternate with agamonts (cells which undergo asexual reproduction)—some are thought to undergo a trimorphic life cycle, with the haploid gamont stage undergoing sexual reproduction via the production of gametes for recombination (Dettmering et al. 1998), and the diploid agamont and schizont stages undergoing asexual reproduction via multiple fission (Figure 1.3). Benthic foraminifer shells (commonly referred to as tests) preserve morphological indicators of the mode of reproduction by which the individual test was produced. Microspheric benthic foraminifer tests with a small first chamber (i.e., proloculus) are produced through sexual reproduction, while megalospheric benthic foraminifer tests with a large proloculus are produced via asexual reproduction (representing either the gamont or, in some cases, the schizont forms; Figure 1.3).

As a result, proloculus size differences reflect the method by which the individual was produced. Shells with large proloculi, or megalospheres—produced via asexual reproduction—correspond to the gamont and/or schizont phases (Figure 1.3). While the gamont represents a haploid form, it is notably uncertain whether schizonts are haploid or diploid (Figure 1.3; Dettmering et al. 1998). Regardless, the morphology of gamonts and schizonts are similar; thus, while the life cycle phase is indistinguishable, megalospheres always represent asexual reproduction. In contrast, shells with small proloculi, or microspheres, are produced via sexual reproduction and correspond to the diploid agamont phase (Figure 1.3).

Thus, foraminifer tests are a simple system through which to examine reproduction, where megalospheric tests represent asexually-produced offspring and microspheric tests represent sexually-produced offspring. These simple morphological features can provide clues to the life history of the individual organisms preserved in the fossil record, as well as offer insight into the variability inherent in foraminifer reproduction through time. Further, because foraminifera are already intensively studied to understand past climate, many foraminfer records are directly or closely associated with the environmental records needed to test life history theories about how reproduction responds to environmental change.

In this dissertation I utilize benthic foraminifer records from the Santa Barbara Basin to assess the extent of reproductive life history variation through time and determine whether environmental changes throughout the Common Era (0 CE-present) affect reproductive mode as preserved in foraminifer tests. These data on life history characteristics provide an unparalleled opportunity to investigate long-term, baseline reproductive trends, and can be used to gain insight into the effects of recent and rapid change on reproductive dynamics within benthic foraminifera in the SBB.

1.4 Examining individual body size variation

Body size distributions can vary widely among different communities, and this variation has important implications for ecological dynamics, energetics, and evolutionary history (Blueweiss et al. 1978, Peters and Peters 1986, Brown 1995, Smith et al. 2016). Body size is correlated with a wide variety of ecologically-important characteristics, such as metabolic rate (Peters and Peters 1986, Brown et al. 2004); offspring number, size, and longevity (Yampolsky and Scheiner 1996, Caval-Holme et al. 2013, Shama 2015, Marshall et al. 2018, Dallago et al. 2022); population-level abundance (White et al. 2007); and even high-level metrics such as diversity and species richness (Isaac et al. 2005) and the structure and dynamics of food webs (Woodward et al. 2005).

Given the large number of correlates between species traits and body size, it is considered a fundamental complex variable in ecology that can be used to examine macroecological trends across large spatial and temporal scales, alongside geographic range size and population density (Brown 1995). Because the fossil record can provide information on all three variables, paleontology is uniquely positioned to study macroecology in deep time (Lyons and Smith 2010). As a result, much is known about the evolution of body size within and across lineages through time and in response to a variety of Earth system states and environmental changes (Labarbera 1986, Smith et al. 2016).

Yet because individual-level measurements have traditionally been time- and labor-intensive to collect, most studies of body size in both neontological and paleontological records utilize summary measurements (e.g., maximum, mean, or median size) or derive size distributions from limited samples of individuals (e.g., Roy et al. 2001, Heim et al. 2015, Keating-Bitonti and Payne 2018a, Gearty and Payne 2020). While these methodologies can be highly useful—both in terms of illuminating interspecific size trajectories and ensuring that size records that span the history of life on Earth can be feasibly compiled (Heim et al. 2015, 2017, Smith et al. 2016)—they also serve to compress individual variation and thus limit the types of questions that can be addressed with these data (Liboiron 2021).

The consequences of ignoring individual-level variation are profound. From the earliest days of evolutionary biology, researchers noted the variation inherent in the traits of conspecific individuals, and this variation is recognized as the raw material on which selection acts (Wallace 1858, Darwin 1859). Further, intraspecific variation is considered to affect ecological dynamics, where complex and dynamic trait-environment interactions can modulate how individuals interact with each other and their surrounding environment (Brown 1995, Bolnick et al. 2011). The limited information on intraspecific variation gathered in typical paleontological datasets means that understanding of how such variation has affected life history, population dynamics, community assembly, and evolutionary outcomes over long timescales remains elusive.

Recent advances in paleontological data collection techniques have helped to ease these issues (Cunningham et al. 2014, Hsiang et al. 2016, 2017a). With high-throughput imaging methods, morphology can be quantified for individuals through time, and large datasets—touted as important for resolving central questions in community ecology and enhancing the power of the biological sciences to understand complexity (Hampton et al. 2013, Farley et al. 2018, Muñoz and Price 2019)—can be generated from fossil records that span long timescales. These data can be used to provide a morphological view of assemblage dynamics that reflects minute changes in individuals through time (Pavoine and Bonsall 2011, Bolnick et al. 2011, Mittelbach and Schemske 2015). They can also be applied to answer questions about the interplay between individual life histories (e.g., growth and reproduction), body size, and community-level size dynamics, all of which reflect and respond to external environmental forcing as well as intrinsic biotic pressures.

In this dissertation I apply these methods to generate individual measurements of size and morphology for foraminifera from the SBB. This work represents the first time an annual record of morphological change has been compiled for industrial- and modern-era marine assemblages in the Santa Barbara Basin. High-resolution fossil records of this period are necessary to establish pre-industrial ecological baselines and therby constrain the effects of recent human impacts.

1.5 Building a record of past ecological change on human timescales

This dissertation seeks to expand on previous studies of foraminifer diversity to build records of individual-level variation in life history and morphology and dissect the relationship between changes in community composition and within-species morphological and life history variation over the Common Era and in response to climate changes and other intensifying stressors on these foraminifera in the 19th through 21st centuries. In this dissertation, I focus on three central questions, which apply to each of the chapters presented. These guiding questions are:

1. What is the natural variability present in benthic foraminifera over ecologically-revelant timescales (decades to milennia)?
2. How are benthic foraminifera affected by natural and human-induced environmental changes in the Santa Barbara Basin?
3. How do individual-level data on benthic foraminifer life history and aspects of morphology capture the impacts of these changes?

In Chapter 2, I provide an overview of the relatively novel method—high-throughput imaging and automated, image-based morphometrics—that I use to examine variation in benthic foraminifer morphology through time. In Chapter 3, I present a 2,000 year-long record of reproductive life history in the benthic foraminifer genus *Bolivina*, examining whether benthic foraminifer reproductive investments (via sexual and asexual reproduction) vary at the population level through time, and use these samples to examine whether—and how—environmental changes impact reproductive choices. Chapter 4 examines the record of benthic foraminifer body size throughout a portion of the Common Era interval (~1240-2008 CE) to understand how size is structured within species, and whether size shifts are correlated with

biological and environmental factors throughout this period. Chapter 5 assesses how community ecology in benthic foraminifera is structured in samples from 1834-2008 CE, over a period which encompasses major socio-ecological changes across California and throughout the world more broadly. Finally, I synthesize my findings in Chapter 6 and outline a vision for how paleoecology and the historical sciences more broadly can be in conversation with other disciplines, such as Indigenous environmental studies and political ecology, to gain a full understanding of the myriad impacts of settler colonialism on California's oceans.

Chapter 1 Figures

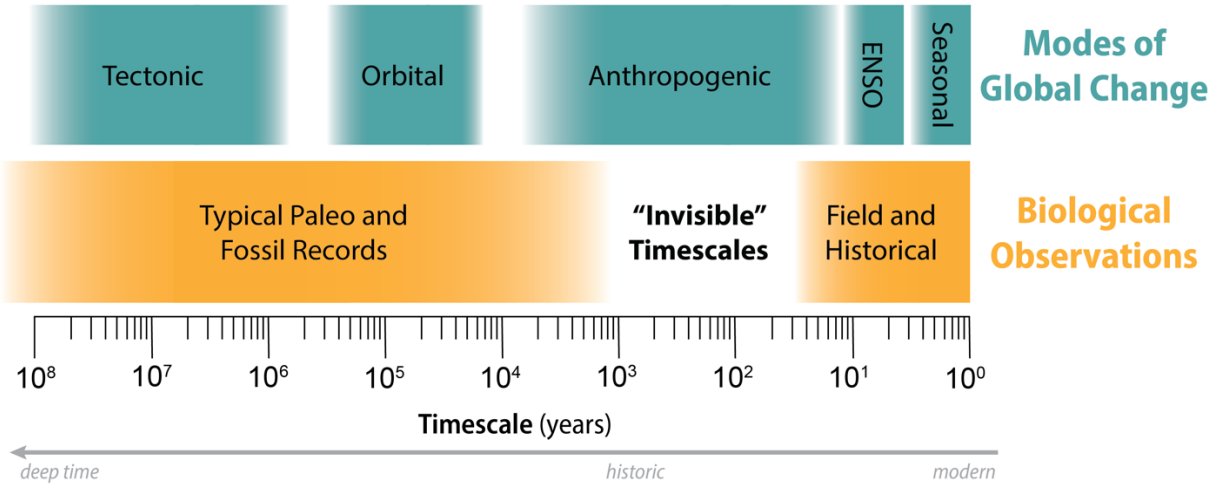

Figure 1.1: The disparate timescales of global change and biological observations. Field and historical observations typically span annual to decadal timescales, appropriate for observations of seasonal (summer-winter) to decadal (ENSO, PDO) modes of global change. In contrast, the normal fossil record captures tens of thousands to hundreds of millions of years, appropriate for studies of orbital (Milankovitch) to tectonic (continental drift) modes of global change. Invisible timescales lie in the "gap" between field and historical observations and the fossil record, yet are needed to elucidate anthropogenic impacts.

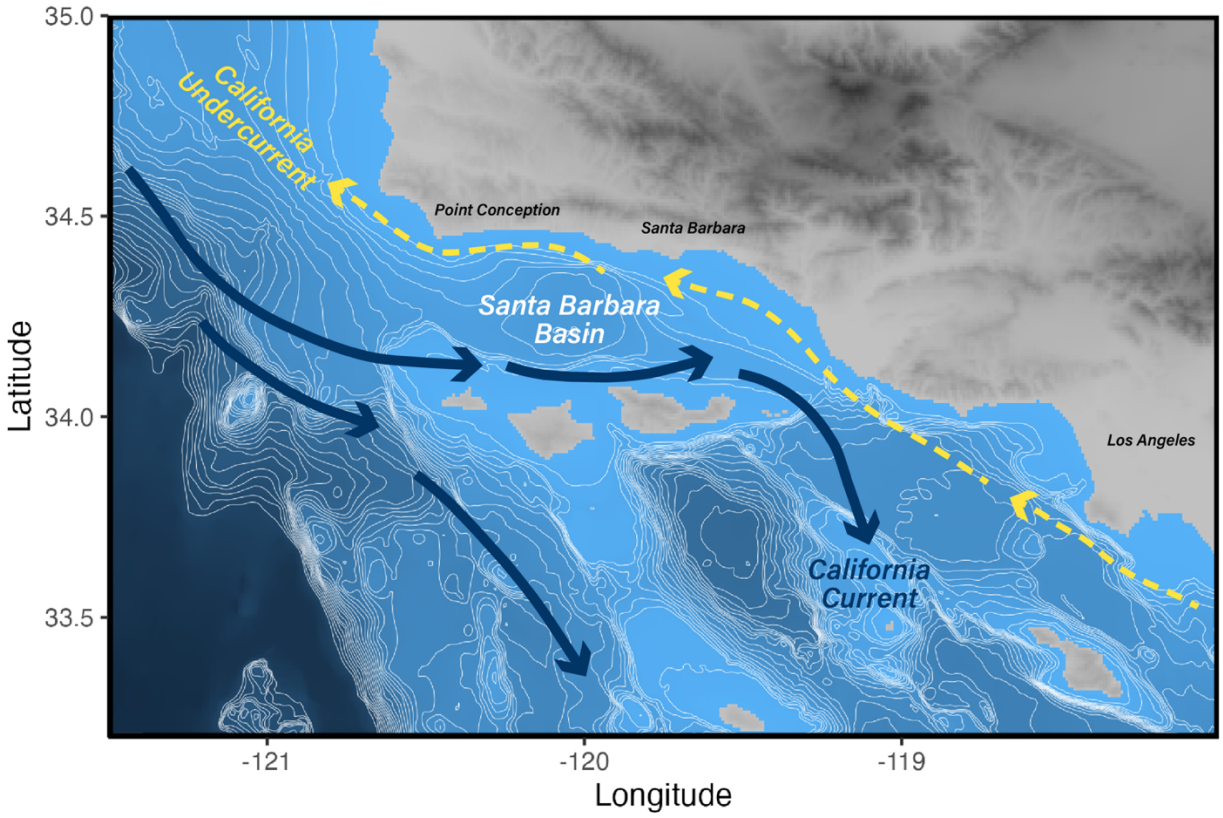

Figure 1.2: Santa Barbara Basin bathymetry and regional setting.
Basin bathymetry shows the asymmetric heights of the eastern (230 m) and western (475 m) sills. The general directions of the California Current (blue solid arrows) and Undercurrent (yellow dashed arrows) are shown. Greyscale areas represent the height of above-water terrestrial features (the California coast and the Channel Islands), where darker colors denote higher topographical features. Major population centers and points of interest are marked on the map. Bathymetric and topographic data courtesy of USGS (Barnard and Hoover 2010).

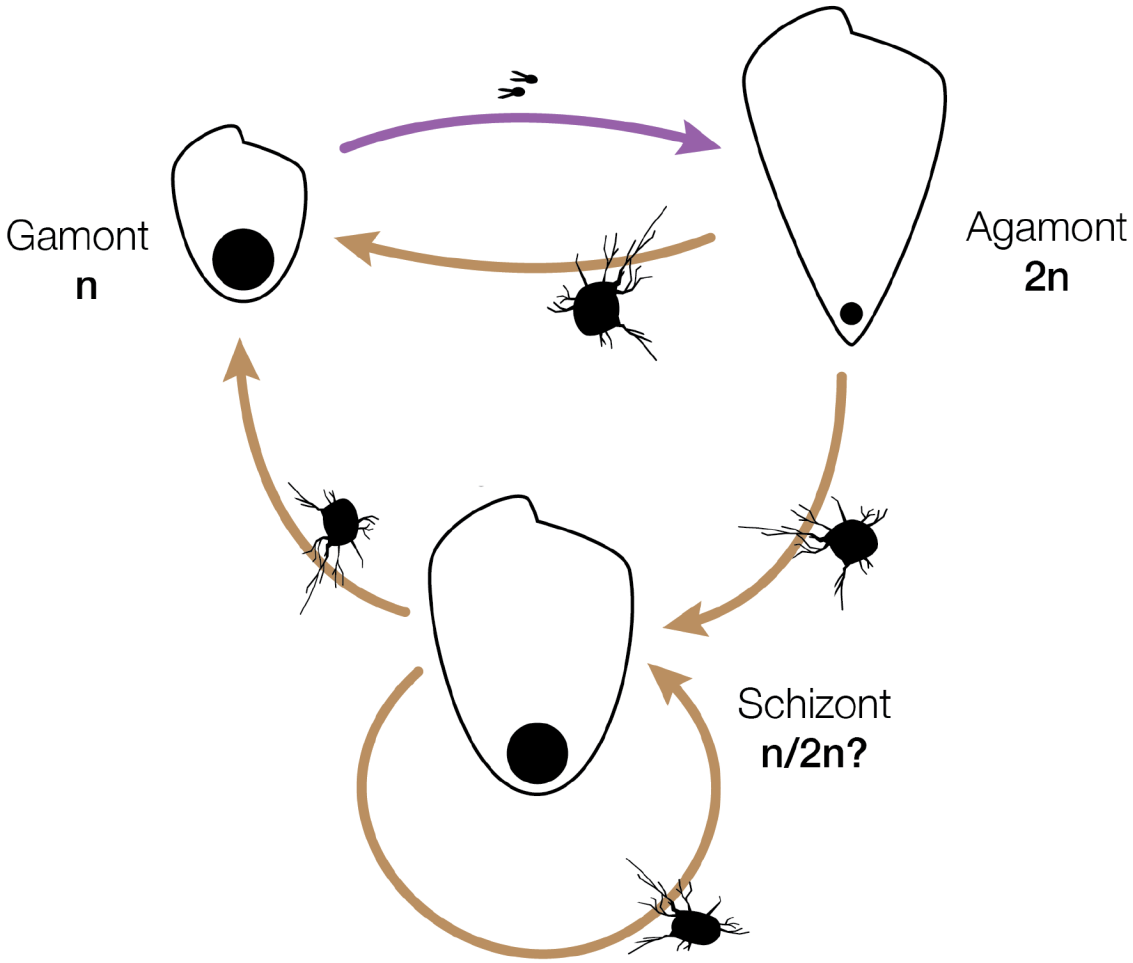

Figure 1.3: A model of the life cycle of foraminifera.
While numerous potential foraminifer lifecycles have been proposed, the tricyclic life cyle is currently the most accepted. Here this cycle is represented using the benthic foraminifer *Bolivina argentea*. Regular alternation is considerd to occur between the haploid, megalospheric gamont form, which reproduces via sexual reproduction, and the microspheric, diploid agamont form, which reproduces asexually via multiple fission. In addition to this dimorphic alternation, a number of benthic foraminifera have been observed to undergo a tricyclic cycle, with the megalospheric schizont form occurring between the agamont and the gamont phases and reproducing via cyclic schizogony. Brown lines with protoplasm indicate asexual reproduction, while purple lines with gametes indicate sexual reproduction; n denotes haploid; 2n denotes diploid; and n/2n? denotes haploid and/or diploid. Proloculus, gametes, and offspring are slighly enlarged relative to the test. Figure courtesy of Ivo Duijnstee.

1.6 Chapter 1 References

Barnard, P. L., and D. Hoover. 2010. A Seamless, High-Resolution, Coastal Digital Elevation Model (DEM) for Southern California. Page A Seamless, High-Resolution, Coastal Digital Elevation Model (DEM) for Southern California. USGS Numbered Series, U.S. Geological Survey.

Barnosky, A. D., E. A. Hadly, J. Bascompte, E. L. Berlow, J. H. Brown, M. Fortelius, W. M. Getz, J. Harte, A. Hastings, P. A. Marquet, N. D. Martinez, A. Mooers, P. Roopnarine, G. Vermeij, J. W. Williams, R. Gillespie, J. Kitzes, C. Marshall, N. Matzke, D. P. Mindell, E. Revilla, and A. B. Smith. 2012. Approaching a state shift in Earth's biosphere. Nature 486:52–58.

Barnosky, A. D., N. Matzke, S. Tomiya, G. O. U. Wogan, B. Swartz, T. B. Quental, C. Marshall, J. L. McGuire, E. L. Lindsey, K. C. Maguire, B. Mersey, and E. A. Ferrer. 2011. Has the Earth's sixth mass extinction already arrived? Nature 471:51 EP-.

Barras, C., E. Geslin, J.-C. Duplessy, and F. J. Jorissen. 2009. Reproduction and growth of the deep-sea benthic foraminifer Bulimina marginata under different laboratory conditions. The Journal of Foraminiferal Research 39:155–165.

Belanger, C. L. 2022. Volumetric analysis of benthic foraminifera: Intraspecific test size and growth patterns related to embryonic size and food resources. Marine Micropaleontology 176:102170.

Blueweiss, L., H. Fox, V. Kudzma, D. Nakashima, R. Peters, and S. Sams. 1978. Relationships between body size and some life history parameters. Oecologia 37:257–272.

Bolnick, D. I., P. Amarasekare, M. S. Araújo, R. Bürger, J. M. Levine, M. Novak, V. H. W. Rudolf, S. J. Schreiber, M. C. Urban, and D. A. Vasseur. 2011. Why intraspecific trait variation matters in community ecology. Trends in Ecology & Evolution 26:183–192.

Boltovskoy, E., D. B. Scott, and F. S. Medioli. 1991. Morphological variations of benthic foraminiferal tests in response to changes in ecological parameters: a review. Journal of Paleontology 65:175–185.

Brandon, J. A., W. Jones, and M. D. Ohman. 2019. Multidecadal increase in plastic particles in coastal ocean sediments. Science Advances 5:eaax0587–eaax0587.

Bray, N. A., A. Keyes, and W. M. L. Morawitz. 1999. The California Current system in the Southern California Bight and the Santa Barbara Channel. Journal of Geophysical Research: Oceans 104:7695–7714.

Brown, J. H. 1995. Macroecology. University of Chicago Press.

Brown, J. H., J. F. Gillooly, A. P. Allen, V. M. Savage, and G. B. West. 2004. TOWARD A METABOLIC THEORY OF ECOLOGY. Ecology 85:1771–1789.

Burke, S., R. Dunbar, and W. Berger. 1996. Benthic and pelagic Foraminifera of the Macoma layer, Santa Barbara Basin. Oceanographic Literature Review 1:64–65.

Butlin, R. 2002. The costs and benefits of sex: new insights from old asexual lineages. Nature Reviews Genetics 3:311–317.

Caval-Holme, F., J. Payne, and J. M. Skotheim. 2013. Constraints on the Adult-Offspring Size Relationship in Protists. Evolution 67:3537–3544.

Cunningham, J. A., I. A. Rahman, S. Lautenschlager, E. J. Rayfield, and P. C. J. Donoghue. 2014. A virtual world of paleontology. Trends in Ecology & Evolution 29:347–357.

Dallago, G. M., R. I. Cue, K. M. Wade, R. Lacroix, and E. Vasseur. 2022. Birth conditions affect the longevity of Holstein offspring. Journal of Dairy Science 105:1255–1264.

Darwin, C. 1859. On the origin of species by means of natural selection, or preservation of favoured races in the struggle for life. John Murray, London.
Davis, C. V., C. M. Livsey, H. M. Palmer, P. M. Hull, E. Thomas, T. M. Hill, and C. R. Benitez-Nelson. 2020. Extensive morphological variability in asexually produced planktic foraminifera. Science Advances 6:eabb8930.
Davis, H., H. Davis, and Z. Todd. 2017. On the Importance of a Date, or, Decolonizing the Anthropocene. ACME: An International Journal for Critical Geographies 16:761–780.
Dettmering, C., R. Röttger, J. Hohenegger, and R. Schmaljohann. 1998. The trimorphic life cycle in foraminifera: Observations from cultures allow new evaluation. European Journal of Protistology 34:363–368.
Dietl, G. P. 2019. Conservation palaeobiology and the shape of things to come. Philosophical Transactions of the Royal Society B 374:20190294.
Dietl, G. P., S. M. Kidwell, M. Brenner, D. A. Burney, K. W. Flessa, S. T. Jackson, and P. L. Koch. 2015. Conservation Paleobiology: Leveraging Knowledge of the Past to Inform Conservation and Restoration. Annual Review of Earth and Planetary Sciences 43:79–103.
Douglas, R. G., and H. L. Heitman. 1979. Slope and basin benthic foraminifera of the California borderland.
Douglas, R. G., J. Liestman, C. Walch, G. Blake, and M. L. Cotton. 1980. The Transition from Live to Sediment Assemblage in Benthic Foraminifera from the Southern California Borderland:257–280.
Du, X., I. Hendy, and A. Schimmelmann. 2018. A 9000-year flood history for Southern California_ A revised stratigraphy of varved sediments in Santa Barbara Basin. Marine Geology 397:29–42.
Duijnstee, I., S. Ernst, and G. Van der Zwaan. 2003. Effect of anoxia on the vertical migration of benthic foraminifera. Marine Ecology Progress Series 246:85–94.
Elder, L. E., A. Y. Hsiang, K. Nelson, L. C. Strotz, S. S. Kahanamoku, and P. M. Hull. 2018. Sixty-one thousand recent planktonic foraminifera from the Atlantic Ocean. Scientific Data 5:180109–180112.
Emery, K. O., and J. Hülsemann. 1961. The relationships of sediments, life and water in a marine basin. Deep Sea Research (1953) 8:165-IN2.
Farley, S. S., A. Dawson, S. J. Goring, and J. W. Williams. 2018. Situating Ecology as a Big-Data Science: Current Advances, Challenges, and Solutions. BioScience 68:563–576.
Field, D. B., T. R. Baumgartner, C. D. Charles, V. Ferreira-Bartrina, and M. D. Ohman. 2006. Planktonic Foraminifera of the California Current Reflect 20th-Century Warming. Science 311:63 LP – 66.
Foster Laura C., Schmidt Daniela N., Thomas Ellen, Arndt Sandra, and Ridgwell Andy. 2013. Surviving rapid climate change in the deep sea during the Paleogene hyperthermals. Proceedings of the National Academy of Sciences 110:9273–9276.
Gearty, W., and J. L. Payne. 2020. Physiological constraints on body size distributions in Crocodyliformes. Evolution 74:245–255.
Hampton, S. E., C. A. Strasser, J. J. Tewksbury, W. K. Gram, A. E. Budden, A. L. Batcheller, C. S. Duke, and J. H. Porter. 2013. Big data and the future of ecology. Frontiers in Ecology and the Environment 11:156–162.
Heim, N. A., M. L. Knope, E. K. Schaal, S. C. Wang, and J. L. Payne. 2015. Cope's rule in the evolution of marine animals. Science 347:867–870.

Heim, N. A., J. L. Payne, S. Finnegan, M. L. Knope, M. Kowalewski, S. K. Lyons, D. W. McShea, P. M. Novack-Gottshall, F. A. Smith, and S. C. Wang. 2017. Hierarchical complexity and the size limits of life. Proceedings of the Royal Society B: Biological Sciences 284:20171039–20171039.

Hendy, I. L., L. Dunn, A. Schimmelmann, and D. K. Pak. 2013. Resolving varve and radiocarbon chronology differences during the last 2000 years in the Santa Barbara Basin sedimentary record, California. Quaternary International 310:155–168.

Hendy, I. L., T. J. Napier, and A. Schimmelmann. 2015. From extreme rainfall to drought: 250 years of annually resolved sediment deposition in Santa Barbara Basin, California. Quaternary International 387:3–12.

Hsiang, A. Y., L. E. Elder, and P. M. Hull. 2016. Towards a morphological metric of assemblage dynamics in the fossil record: a test case using planktonic foraminifera. Philosophical Transactions of the Royal Society B: Biological Sciences 371:20150224–20150227.

Hsiang, A. Y., K. Nelson, L. E. Elder, E. C. Sibert, S. S. Kahanamoku, J. E. Burke, A. Kelly, Y. Liu, and P. M. Hull. 2017a. AutoMorph: Accelerating morphometrics with automated 2D and 3D image processing and shape extraction. Methods in Ecology and Evolution 9:605–612.

Hsiang, A. Y., K. Nelson, L. E. Elder, E. C. Sibert, S. S. Kahanamoku, J. E. Burke, A. Kelly, Y. Liu, and P. M. Hull. 2017b. AutoMorph: Accelerating morphometrics with automated 2D and 3D image processing and shape extraction. Methods in Ecology and Evolution 9:605–612.

IPCC. 2019. IPCC Special Report on the Ocean and Cryosphere in a Changing Climate. Page (D. C. R. H.-O. Pörtner V. Masson-Delmotte, P. Zhai, M. Tignor, E. Poloczanska, K. Mintenbeck, M. Nicolai, A. Okem, J. Petzold, B. Rama, N. Weyer, Ed.).

IPCC, V. Masson-Delmotte, P. Zhai, H.-O. Pörtner, D. Roberts, J. Skea, P. R. Shukla, A. Pirani, W. Moufouma-Okia, C. Pean, R. Pidcock, S. Connors, J. B. R. Matthews, Y. Chen, X. Zhou, M. I. Gomis, E. Lonnoy, T. Maycock, M. Tignor, and T. Waterfield. 2018. Global warming of 1.5˚C. Pages 1–32.

Isaac, N. J. B., K. E. Jones, J. L. Gittleman, and A. Purvis. 2005. Correlates of Species Richness in Mammals: Body Size, Life History, and Ecology. The American Naturalist 165:600–607.

Jackson, J. B. C., M. X. Kirby, W. H. Berger, K. A. Bjorndal, L. W. Botsford, B. J. Bourque, R. H. Bradbury, R. Cooke, J. Erlandson, J. A. Estes, T. P. Hughes, S. Kidwell, C. B. Lange, H. S. Lenihan, J. M. Pandolfi, C. H. Peterson, R. S. Steneck, M. J. Tegner, and R. R. Warner. 2001. Historical overfishing and the recent collapse of coastal ecosystems. Science 293:629–637.

Jones, W. A. 2016. The Santa Barbara Basin Fish Assemblage in the Last Two Millennia Inferred from Otoliths in Sediment Cores:1–141.

Jones, W. A., and D. M. Checkley. 2019. Mesopelagic fishes dominate otolith record of past two millennia in the Santa Barbara Basin. Nature Communications 10:4564.

Kahanamoku, S. S., P. M. Hull, D. R. Lindberg, A. Y. Hsiang, E. C. Clites, and S. Finnegan. 2018. Twelve thousand recent patellogastropods from a northeastern Pacific latitudinal gradient. Scientific Data 5:170197–170197.

Keating-Bitonti, C. R., and J. L. Payne. 2017. Ecophenotypic responses of benthic foraminifera to oxygen availability along an oxygen gradient in the California Borderland. Marine Ecology 38:e12430.

Keating-Bitonti, C. R., and J. L. Payne. 2018a. Environmental influence on growth history in marine benthic foraminifera. Paleobiology 44:736–757.
Keating-Bitonti, C. R., and J. L. Payne. 2018b. Environmental influence on growth history in marine benthic foraminifera. Paleobiology 44:736–757.
Kennett, J. P., and B. L. Ingram. 1995. A 20,000-year record of ocean circulation and climate change from the Santa Barbara basin. Nature 377:510–514.
Kidwell, S. M. 2015. Biology in the Anthropocene: Challenges and insights from young fossil records. Proceedings of the National Academy of Sciences 112:4922–4929.
Kucera, M. 2007. Chapter Six Planktonic Foraminifera as Tracers of Past Oceanic Environments BT - Proxies in Late Cenozoic Paleoceanography. Pages 213–262 Proxies in Late Cenozoic Paleoceanography. Elsevier.
Kuroyanagi, A., T. Irie, S. Kinoshita, H. Kawahata, A. Suzuki, H. Nishi, O. Sasaki, R. Takashima, and K. Fujita. 2021. Decrease in volume and density of foraminiferal shells with progressing ocean acidification. Scientific Reports 11:19988.
Labarbera, M. 1986. The Evolution and Ecology of Body Size. Dahlem Konjerenzen:69–98.
Lewis, S. L., and M. A. Maslin. 2015. Defining the Anthropocene. Nature 519:171–180.
Liboiron, M. 2021. Pollution is colonialism. Page Pollution Is Colonialism. Duke University Press.
Lightfoot, K. G., L. M. Panich, T. D. Schneider, and S. L. Gonzalez. 2013. European colonialism and the Anthropocene: A view from the Pacific Coast of North America. Anthropocene 4:101–115.
LUTZE, G. F. 1964. Statistical investigations on the variability of Bolivina argentea Cushman. Contribution from the Cushman Foundation for Foraminiferal Research 15:105–116.
Lyons, S. K., and F. A. Smith. 2010. Using a Macroecological Approach to Study Geographic Range, Abundance and Body Size in the Fossil Record. The Paleontological Society Papers 16:117–141.
Marshall, D. J., A. K. Pettersen, and H. Cameron. 2018. A global synthesis of offspring size variation, its eco-evolutionary causes and consequences. Functional Ecology 32:1436–1446.
McClenachan, L., F. Ferretti, and J. K. Baum. 2012. From archives to conservation: why historical data are needed to set baselines for marine animals and ecosystems. Conservation Letters 5:349–359.
McClenachan, L., J. B. Jackson, and M. J. Newman. 2006. Conservation implications of historic sea turtle nesting beach loss. Frontiers in Ecology and the Environment 4:290–296.
McGregor, D., S. Whitaker, and M. Sritharan. 2020. Indigenous environmental justice and sustainability. Current Opinion in Environmental Sustainability 43:35–40.
Mittelbach, G. G., and D. W. Schemske. 2015. Ecological and evolutionary perspectives on community assembly. Trends in Ecology & Evolution 30:241–247.
Moffitt, S. E., T. M. Hill, K. Ohkushi, J. P. Kennett, and R. J. Behl. 2014. Vertical oxygen minimum zone oscillations since 20 ka in Santa Barbara Basin: A benthic foraminiferal community perspective. Paleoceanography 29:44–57.
Muñoz, M. M., and S. A. Price. 2019. The Future is Bright for Evolutionary Morphology and Biomechanics in the Era of Big Data. Integrative and Comparative Biology 59:599–603.
Murray, T. 2002. Evaluating evolutionary archaeology. World Archaeology 34:47–59.
Nigam, R., and D. A. Caron. 2000. Does temperature affect dimorphic reproduction in benthic foraminifera? A culture experiment on Rosalina leei. Indian Academy of Sciences.

O'Dea, A. 2006. Asexual propagation in the marine bryozoan Cupuladria exfragminis. Journal of Experimental Marine Biology and Ecology 335:312–322.
Otto, S. P., and T. Lenormand. 2002. Resolving the paradox of sex and recombination. Nature Reviews Genetics 3:252–261.
Pak, D. K., I. L. Hendy, J. C. Weaver, A. Schimmelmann, and L. Clayman. 2018. Foraminiferal proxy response to ocean temperature variability and acidification over the last 150 years in the Santa Barbara Basin (California). Quaternary International 469:141–150.
Pavoine, S., and M. B. Bonsall. 2011. Measuring biodiversity to explain community assembly: a unified approach. Biological Reviews 86:792–812.
Pershing, A. J., L. B. Christensen, N. R. Record, G. D. Sherwood, and P. B. Stetson. 2010. The Impact of Whaling on the Ocean Carbon Cycle: Why Bigger Was Better. PLOS ONE 5:e12444.
Peters, R. H., and R. H. Peters. 1986. The ecological implications of body size. Cambridge university press.
Roach, L. D. 2010. Climate change in the Pacific North America region over the past millennium : development and application of novel geochemical tracers. UC San Diego.
Roy, K., D. Jablonski, and J. W. Valentine. 2001. Climate change, species range limits and body size in marine bivalves. Ecology Letters 4:366–370.
Santana, B. F. de B. B., T. R. Freitas, J. Leonel, and C. Bonetti. 2021. Biometric and biomass analysis of Quaternary Uvigerinidae (Foraminifera) from the Southern Brazilian continental slope. Marine Micropaleontology 169:102041.
Saraswat, R., A. Deopujari, R. Nigam, and P. J. Heniriques. 2011. Relationship between abundance and morphology of benthic foraminifera Epistominella exigua: Paleoclimatic implications. Journal of the Geological Society of India 77:190–196.
Schimmelmann, A., I. L. Hendy, L. Dunn, D. K. Pak, and C. B. Lange. 2013. Revised ~2000-year chronostratigraphy of partially varved marine sediment in Santa Barbara Basin, California. GFF 135:258–264.
Schimmelmann, A., and C. B. Lange. 1996. Tales of 1001 varves: a review of Santa Barbara Basin sediment studies. Geological Society, London, Special Publications 116:121–141.
Schimmelmann, A., C. B. Lange, W. H. Berger, A. Simon, S. K. Burke, and R. B. Dunbar. 1992. Extreme climatic conditions recorded in Santa Barbara Basin laminated sediments: the 1835–1840Macoma event. Marine Geology 106:279–299.
Schimmelmann, A., C. B. Lange, E. B. Roark, and B. L. Ingram. 2006. Resources for Paleoceanographic and Paleoclimatic Analysis: A 6,700-Year Stratigraphy and Regional Radiocarbon Reservoir-Age (ΔR) Record Based on Varve Counting and 14C-AMS Dating for the Santa Barbara Basin, Offshore California, U.S.A. Journal of Sedimentary Research 76:74–80.
Schmidt, D. N., E. Thomas, E. Authier, D. Saunders, and A. Ridgwell. 2018. Strategies in times of crisis—insights into the benthic foraminiferal record of the Palaeocene–Eocene Thermal Maximum. Philosophical Transactions of the Royal Society A: Mathematical, Physical and Engineering Sciences 376:20170328.
Shama, L. N. S. 2015. Bet hedging in a warming ocean: predictability of maternal environment shapes offspring size variation in marine sticklebacks. Global Change Biology 21:4387–4400.
Sibert, E. C., and R. D. Norris. 2015. New Age of Fishes initiated by the Cretaceous−Paleogene mass extinction. Proceedings of the National Academy of Sciences 112:8537–8542.

Sibert, E. C., and L. D. Rubin. 2021. An early Miocene extinction in pelagic sharks. Science 372:1105–1107.
Sibert, E., M. Friedman, P. Hull, G. Hunt, and R. Norris. 2018. Two pulses of morphological diversification in Pacific pelagic fishes following the Cretaceous–Palaeogene mass extinction. Proceedings of the Royal Society B: Biological Sciences 285:20181194–20181197.
Sims, P. A., D. G. Mann, and L. K. Medlin. 2006. Evolution of the diatoms: insights from fossil, biological and molecular data. Phycologia 45:361–402.
Smith, F. A., J. L. Payne, N. A. Heim, M. A. Balk, S. Finnegan, M. Kowalewski, S. K. Lyons, C. R. McClain, D. W. McShea, P. M. Novack-Gottshall, P. S. Anich, and S. C. Wang. 2016. Body Size Evolution Across the Geozoic. Annual Review of Earth and Planetary Sciences 44:523–553.
Soutar, A., and P. A. Crill. 1977. Sedimentation and climatic patterns in the Santa Barbara Basin during the 19th and 20th centuries. Geological Society of America Bulletin 88:1161–1161.
Stearns, S. C. 1992. The evolution of life histories. Oxford university press Oxford.
Takagi, H., A. Kurasawa, and K. Kimoto. 2020. Observation of asexual reproduction with symbiont transmission in planktonic foraminifera. Journal of Plankton Research 42:403–410.
Tetard, M., L. Licari, K. Tachikawa, E. Ovsepyan, and L. Beaufort. 2021. Toward a global calibration for quantifying past oxygenation in oxygen minimum zones using benthic Foraminifera. Biogeosciences Discussions:1–17.
Thunell, R. C., E. Tappa, and D. M. Anderson. 1995. Sediment fluxes and varve formation in Santa Barbara Basin, offshore California. Geology 23:1083–1083.
Thurstan, R. H., L. McClenachan, L. B. Crowder, J. A. Drew, J. N. Kittinger, P. S. Levin, C. M. Roberts, and J. M. Pandolfi. 2015. Filling historical data gaps to foster solutions in marine conservation. Ocean and Coastal Management 115:31–40.
Todd, Z. 2015. Indigenizing the anthropocene. Art in the Anthropocene: Encounters among aesthetics, politics, environments and epistemologies:241–54.
Tomasovych, A., and S. M. Kidwell. 2017. Nineteenth-century collapse of a benthic marine ecosystem on the open continental shelf. Proceedings of the Royal Society B: Biological Sciences 284:20170328–20170329.
Tulloch, V. J. D., É. E. Plagányi, R. Matear, C. J. Brown, and A. J. Richardson. 2018. Ecosystem modelling to quantify the impact of historical whaling on Southern Hemisphere baleen whales. Fish and Fisheries 19:117–137.
Wallace, A. R. 1858. On the tendency of varieties to depart indefinitely from the original type. Proceedings of the Linnean Society of London 3:53–62.
Ward-Paige, C. A., C. Mora, H. K. Lotze, C. Pattengill-Semmens, L. McClenachan, E. Arias-Castro, and R. A. Myers. 2010. Large-Scale Absence of Sharks on Reefs in the Greater-Caribbean: A Footprint of Human Pressures. PLOS ONE 5:e11968.
Watson, R. A., and A. Tidd. 2018. Mapping nearly a century and a half of global marine fishing_ 1869–2015. Marine Policy 93:171–177.
Westerhold, T., N. Marwan, A. J. Drury, D. Liebrand, C. Agnini, E. Anagnostou, J. S. K. Barnet, S. M. Bohaty, D. De Vleeschouwer, F. Florindo, T. Frederichs, D. A. Hodell, A. E. Holbourn, D. Kroon, V. Lauretano, K. Littler, L. J. Lourens, M. Lyle, H. Pälike, U. Röhl, J. Tian, R. H. Wilkens, P. A. Wilson, and J. C. Zachos. 2020. An astronomically dated record of Earth's climate and its predictability over the last 66 million years. Science 369:1383–1388.

White, E. P., S. K. M. Ernest, A. J. Kerkhoff, and B. J. Enquist. 2007. Relationships between body size and abundance in ecology. Trends in Ecology & Evolution 22:323–330.
Whyte, K. 2016, September 8. Our Ancestors' Dystopia Now: Indigenous Conservation and the Anthropocene. SSRN Scholarly Paper, Rochester, NY.
Whyte, K. 2017. Indigenous climate change studies: Indigenizing futures, decolonizing the Anthropocene. English Language Notes 55:153–162.
Whyte, K. 2020. Too late for indigenous climate justice: Ecological and relational tipping points. WIREs Climate Change 11:e603.
Whyte, K. P. 2018. Indigenous science (fiction) for the Anthropocene: Ancestral dystopias and fantasies of climate change crises. Environment and Planning E: Nature and Space 1:224–242.
Woodward, G., B. Ebenman, M. Emmerson, J. M. Montoya, J. M. Olesen, A. Valido, and P. H. Warren. 2005. Body size in ecological networks. Trends in Ecology & Evolution 20:402–409.
Yampolsky, L. Y., and S. M. Scheiner. 1996. Why Larger Offspring at Lower Temperatures? A Demographic Approach. The American Naturalist 147:86–100.
Yasuhara, M., D. P. Tittensor, H. Hillebrand, and B. Worm. 2015. Combining marine macroecology and palaeoecology in understanding biodiversity: microfossils as a model. Biological Reviews 92:199–215.

2 Materials and Methods: Twenty-two thousand recent benthic foraminifera from the Santa Barbara Basin

Sara S. Kahanamoku[1*], Maya Samuels-Fair[1], Sarah M. Kamel[2], Da'shaun Stewart[3], Leah Kahn[1,4], Max Titcomb[5], Yingyan Alyssa Mei[1], R. Cheyenne Bridge[6], Yuerong Sophie Li[3], Carolina Sinco[7], J.T. Epino[8], Gerson Gonzalez-Marin[3,4], Chloe Latt[4], Heather Fergus[3], Seth Finnegan[1]

Affiliations

1. Department of Integrative Biology and Museum of Paleontology, University of California, Berkeley, CA
2. Department of Psychology, University of California, Berkeley, CA
3. Department of Environmental Science, Policy, and Management, University of California, Berkeley, CA
4. Department of Earth and Planetary Science, University of California, Berkeley, CA
5. Scripps Institution of Oceanography, University of California, San Diego, CA
6. College of Chemistry, University of California, Berkeley, CA
7. Department of Molecular and Cell Biology, University of California, Berkeley, CA
8. Department of Sociology, University of California, Berkeley, CA

The Santa Barbara Basin is an extraordinary archive of environmental and ecological change. The varved sediments preserved in the hypoxic setting of the basin provide an annual to decadal record of the population dynamics of the benthic and pelagic organisms that inhabit surrounding ecosystems. Of the microfossils preserved in these sediments, benthic foraminifera are the most abundant seafloor-dwelling organisms within the basin. While they have been extensively studied for geochemical and palaeoceanographic work, studies of their morphology are lacking. Here we provide a large image and 2D shape dataset of recent benthic foraminifera from two core records sampled from the center of the Santa Barbara Basin that span an ~800-year-long interval during the Common Era (1249-2008 CE). Information on more than 36,000 objects is included, of which more than 22,000 are complete or partially damaged benthic foraminifera. Biogenic objects classified also include planktonic foraminifera, ostracods, pteropods, diatoms, radiolarians, fish teeth and skeletal structures, shark dermal denticles, and benthic foraminifer test fragments. The image dataset was produced using a high-throughput imaging method (*AutoMorph*) designed to extract 2D data from photographic images of fossils. We describe our sample preparation, imaging, and identification techniques, and outline potential uses for the data.

2.1 Background and Summary

Morphological data are the primary phenotypic data preserved in the fossil record. Yet until recently, information on morphological variation within fossil assemblages was limited by the laborious nature of manual morphological data collection. Recent advancements in data collection and processing techniques, such as the adoption of rapid two- and three-dimensional imaging techniques, have greatly accelerated the pace with which researchers can gather large morphological datasets. However, even with the aid of technological advancements, the collection of individual morphological information at the population, community, or assemblage scale remains relatively rare, as assessment of trends at these levels requires large amounts of

individual data that remains time-intensive to collect. To address this gap, paleontologists have developed high-throughput approaches for extracting 2D and 3D shape information from photographic images of entire populations or assemblages. One of these approaches, *AutoMorph*, which is used primarily for the creation of large microfossil datasets, has led to an explosion of big data in micropaleontology, as datasets generated with this method contain thousands to tens of thousands of individuals (Kahanamoku et al. 2018, Elder et al. 2018). These data have subsequently driven major scientific discoveries, including the identification of a previously unknown potential extinction event in sharks (Sibert and Rubin 2021) and a morphological diversification event in fishes (Sibert and Norris 2015, Sibert et al. 2018).

While big datasets have been generated for a number of marine microfossil groups, benthic foraminifera have largely been left out of the paleo big data revolution. No major morphological datasets have been generated for benthic foraminifera, and the vast majority of studies employ manual counting or description of morphotypes (Lutze 1964, Boltovskoy et al. 1991), labor-intensive morphometry techniques (Foster et al. 2013, Schmidt et al. 2018, Tetard et al. 2021), or rely on species- or genus-level exemplar specimens to describe trends within benthic foraminifer assemblages through time (Keating-Bitonti and Payne 2018). These manual techniques are not only time-consuming, but are also difficult to replicate without specialized knowledge and access to the physical samples used in a given study.

Benthic foraminifera are a useful focus group for the development of large, individual-level morphological datasets, as these unicellular protists have calcium carbonate tests that are distributed throughout the benthos of the modern global ocean, and are cosmopolitan within marine sediments, living anywhere from littoral to deep-water environments (Kucera 2007). The abundant fossil record of benthic foraminifera spans back to the early Cambrian (Culver 1991, Pawlowski et al. 2003), and as a result has been extensively utilized to examine both past environmental conditions (using species distribution data and shell chemistry, among other proxies; Zachos et al. 2001, 2008, Kucera 2007, Hönisch et al. 2012) and ecological and evolutionary trends (using genus- and species-level diversity data, classification of ecophenotypes, and quantitative assessments of lineage diversification and extinction; Ezard et al. 2011, Norris et al. 2013, Hull 2017). While there is a history of (semi-) automated approaches being used on benthic foraminifer taxa to extract information such as size (Santana et al. 2021), 2D shape (Lutze 1964, Keating-Bitonti and Payne 2017), calcite thickness (Kuroyanagi et al. 2021), life history variation (Saraswat et al. 2011, Schmidt et al. 2018), and biovolume through ontogeny (Keating-Bitonti and Payne 2018, Belanger 2022), these datasets are rarely publicly available in their raw forms. This combined lack of data on individual-level trends and a lack of accessibility for those data that do exist have limited the ability of additional studies to build on previous results and describe trends at population and community scales. As biologists increasingly strive to elucidate the impacts of climate change on marine life at all scales, large, individual-level datasets that span across historic periods of environmental change are critical both for building ecosystem baselines that place modern change into context and for leveraging the predictive power of the fossil record to understand the range of biological responses expected under projected climate scenarios.

Existing workflows can be used to address benthic foraminifer data gaps and begin to build large, open-access datasets that collect information on the individual-level intraspecific

morphological trait distributions needed to reconstruct community ecological characteristics. Here we provide an image library of individual benthic foraminifera and high-resolution 2D assemblage images, individual images, coordinate data, and morphometric measurements from Santa Barbara Basin sediment core samples. Images of 27,508 complete and damaged benthic foraminifera are provided along with 2D morphometric data. Images and shape data for an additional ~1,000 objects are also provided, encompassing general categories including planktonic foraminifera, ostracods, pteropods, diatoms, radiolarians, fish teeth and skeletal structures, shark dermal denticles, and foraminiferal test fragments (see Methods for further information). Benthic foraminifera are identified to species, and classifications of reproductive mode (sexual vs. asexual offspring production) are included for four biserial species with significant and visible dimorphism that allows for examination of life history trends among reproductive morphotypes.

2.2 Methods

2.2.1 Core sampling

As part of previous studies (Brandon et al. 2019, Jones and Checkley 2019), a kasten core and a box core from the center of the SBB (Southern California) were collected in 2010 at station MV1012-ST46.9 (34˚17.228'N, 120˚02.135'W) at approximately 580m water depth (Figure 1). This station was chosen as a re-occupation of Ocean Drilling Program Site 893 (Baldauf and Lyle 1995) and was designated as Station 46.9 following the station naming convention of the California Cooperative Oceanic Fisheries Investigations (CalCOFI; Bograd et al. 2003, CalCOFI 2022). 2 cm vertical core slices from each subcore were X-radiographed and scanned at 1-mm intervals in a linear, non-rotational scan (Brandon et al. 2019, Jones and Checkley 2019). Composite X-radiographs were used with color photographs to develop a high-resolution chronology for each core (Figure S1). The age model for the kasten core MV1012-KC1 was adapted from Hendy et al. (2013) and Schimmelmann et al. (2013); dates assigned to each sample were the average of the dates of the upper and lower surfaces of the sample transverse section. Box core MV1012-BC1 was sufficiently shallow to use traditional varve chronology [65–67] for couplet dating; a regression model was used to assign dates to the sediment stratigraphy prior to 1871, thus extending the chronology to 1834 CE (Brandon et al. 2019).

Subcore cross-sections were cut transversely every 0.5 cm to create transverse sections of 97.5cm^3, and these were stored at -80˚C prior to further processing. Core transverse sections were then dried overnight at 50˚C, washed in distilled water, and wet-sieved over a 104- and 63-μm mesh to create samples for analysis. The >104 μm fraction of these samples was picked under a dissecting microscope for fish otoliths (Jones and Checkley 2019) and plastic particles (Brandon et al. 2019) and used in separate analyses.

2.2.2 Chronology development

To develop the chronology used in the present analysis, Jones (2016) identified major tie points between kasten core MV1012-KC1 and kasten core SPR0901-06KC, which was sampled at the same location and has been used for extensive calibration of Common Era SBB chronology methods (Hendy et al. 2013, Schimmelmann et al. 2013). This methodology created a final chronostratigraphy for MC1012-KC1 with 0.5 cm resolution that excluded near-instantaneous event layers and incorporated cross-dating. Dates assigned to each sample were the average of the dates of the upper and lower surfaces of the sample transverse section.

Box core MV1012-BC was covered by a bacterial mat of ~1-2 cm thickness (Supplemental Figure S1), indicating that the surficial sediments were intact (Brandon et al. 2019). This core was sufficiently shallow to use traditional varve chronology (as outlined in Schimmelmann et al. 2006 and corroborated by Hendy et al. 2013 and Schimmelmann et al. 2013) for couplet dating. A regression model was used to assign dates to the sediment stratigraphy prior to 1871, thus extending to chronology to 1834 CE (Brandon et al. 2019).

2.2.3 Sample preparation

Prior to the present study, subcore cross-sections were cut transversely at every 0.5 cm, and near-instantaneous event layers were combined with chronologically-correlated transverse sections to create larger samples. These sections were dried overnight, washed in distilled water, and wet-sieved over a 104- and 63-μm mesh. Two previous studies, Jones and Checkley (2019) and Brandon et al. (2019) picked the >104 μm fractions for fish otoliths and plastic particles, respectively. To generate the present dataset, we picked samples from the 63-104 and >104 μm fractions for benthic foraminifera. These fractions were combined to create a single > 63 μm fraction for all cores. Kasten core samples were dry split using a sediment splitter to achieve approximately equivalent sample volumes for picking, while box core samples were processed in their entirety. Kasten core samples were picked exclusively for biserial benthic foraminifera, while box core samples were picked for all benthic foraminifer individuals present within a given sample. Split fractions and community data types (biserial only, or representative of the full benthic foraminifer community) are reported in Table 1.

2.2.4 Imaging

We imaged all benthic foraminifera picked from entire samples or representative split fractions. Benthic foraminifera were manually picked from each sample or split under a Leica EZ4 dissecting microscope at 16x magnification, and were arranged for imaging on matte black coated brass plates. Arranging ensured that individual foraminifera and other objects were not touching, a critical step for simplified post-processing using high-throughput imaging techniques (Hsiang et al. 2017). On the few occasions that all sample material did not fit within the boundaries of a single plate, multiple plates were imaged and named accordingly (e.g., MV1012-BC-40_1, MV1012-BC-40_2, etc.). Arranged samples were imaged in bulk using a Keyence VHX-7000 digital imaging microscope at 150x magnification, and the same lighting setting were used across samples to improve comparability.

2.2.5 AutoMorph (automated morphometric post-processing)

Bulk images were processed with the *AutoMorph* software package (Hsiang et al. 2017), an open-access bioinformatics pipeline designed to segment individual objects from light microscope and camera images and extract 2D and 3D shape information. The *AutoMorph* protocol contains four modules for 2D and 3D image processing: *segment, focus, run2Dmorph,* and *run3Dmorph*. For this study, the *segment* module was used to identify all unique objects in a 2D EDF bulk image, extract these objects and label them with sample metadata, and save these slices in unique directories. Because the bulk images used for this study were already compiled into extended-depth-of-focus (EDF) images, the *focus* module, which is designed to compile z-slices into EDF images, was not needed. Once images were segmented, we used the *run2dmorph* module to extract shape coordinates and basic measurements in 2D and create images of 2D

shape extraction for visual quality control. The *AutoMorph* software package and documentation is freely available on GitHub and can be accessed at https://github.com/HullLab/AutoMorph. The software suite and resultant datasets are described in detail in several publications (Hsiang et al. 2017, Kahanamoku et al. 2018, Elder et al. 2018). *AutoMorph* is adapted to run on local computers and supercomputer clusters; for this study, a laptop computer with a 2.6 GHz Quad-Core Intel i7 processor was sufficient to process all samples.

2.2.6 Image identification

Individual images produced by the *segment* module were used to identify all unique objects to one of X categories (Figure X) using a custom-made application for image viewing and the assignment of general object information to images, including the certainty of object classification. This application, called classifier, is a modified version of *classify-specify* (https://github.com/HullLab/Classify-Specify) designed for use on unix systems. The classifier application and documentation can be accessed at https://github.com/GregDMeyer/classifier. For samples with multiple bulk images, object numbers for each image following the first were modified, typically by adding an additional number to the beginning (e.g., obj. 00001 of the second bulk image becomes obj. 10001; for the third, obj. 20001, etc.) to avoid overlapping numbers. These allowed for smooth classification using the classifier application.

2.3 Data Records

We provide metadata, image, and shape data for all 36,275 objects in the dataset, of which 27,508 are complete and damaged benthic foraminifera, identified to species, and 26,399 for which shape information was successfully extracted using *AutoMorph*. The tables within this data report provide relevant metadata, summary statistics, and technical validation information. The coring location and an overview of core chronology are shown in Figure 1, and sample ages and split fractions are reported in Table 1. The workflow employed for sample preparation, imaging, and processing with *AutoMorph* is shown in Figure 2. Supplementary Table 1 provides references for taxonomic identifications and common synonyms, and reference images can be found in Figures 3 and 4. All data products of this study are available on Zenodo (Data citation 1); this repository contains 8 distinct data types uploaded as distinct files, and includes the following:

i) *bulk_images.zip*: Bulk images with objects identified by *segment* boxed in red
ii) *individual_images.zip*: EDF images of individual objects within the dataset
iii) *identification_files.zip*: Classifications for individual objects, including both general categories and species-specific classifications (when possible) for benthic foraminifera
iv) *cleaning_scripts.zip*: Directory containing R scripts used to clean object category misspellings or inconsistencies
v) *outline_images.zip*: EDF images of objects successfully extracted for 2D outlines and measurements; included for quality control. This includes one text file (unextracted_objects_2D.txt) listing objects with failed extractions
vi) *2d_coordinates.zip*: CSV files containing all extracted outline coordinates for each of the samples imaged, a text file of failed 2D extractions (unextracted_objects_2D.txt), and a summary CSV file including coordinates for all extracted objects (all_coordinates.csv)
vii) *2d_properties.zip*: 2D measurements for all objects

viii) *metadata_tables.zip*: Tables 1, 2, and 3 and Supplementary Table 1 from this publication, describing sample metadata, including site coordinates, sample names, object information, and summary statistics

2.3.1 Technical Validation

Technical validation occurred at several steps in the image processing pipeline to ensure that measurements were consistent across samples, and that all measurements were extracted from outlines that were true to the original sample shape. The major validation steps occurred at the object selection, shape extraction and size measurement, and object classification phases.

2.3.2 Object selection

The *AutoMorph* `segment` module produces a bulk image overview that provides an object number for each individual segmented object, which is boxed in red for ease of identification (Figure 2; full sample set of boxed images available in data citation). Full-sample images taken on the Keyence VHX-7000 digital imaging microscope were output as extended-depth-of-focus (EDF) images, and these EDF images were passed to the segment module in 'sample' mode to produce a series of boxed images, which denoted the object numbers for each segmented individual, for visual validation prior to finalizing the segmentation output. Each boxed image was visually checked to verify that most, if not all, microfossils were identified and segmented from each image. If this visual check failed—i.e., some or many microfossils were excluded from the segmentation—image selection parameters were adjusted in segment to optimize segmentation. Once an optimal parameter was identified, the segment module was run in 'final' mode to create individual images of each of the objects identified from the full-sample image. These individual images provide the basis for the *run2dmorph* module, which produces 2D measurements, and for taxonomic identification.

2.3.3 Shape extraction

2D shape extraction occurred via the *AutoMorph* `run2dmorph` module, which takes as input individual 2D EDF images and produces outline coordinates, measurements, and validation images with outlines overlain atop the input image. The quality of 2D shape extraction was checked visually for the first 100 objects in a slide using these outline-object overlays. `run2dmorph` also outputs a list of objects with failed outline extractions for each sample processed; these are provided alongside 2D shape data in the Data Citation. When a majority of complete benthic foraminifera failed to extract, the run2dmoprh routine was re-run with adjusted image extraction parameters to attain the best possible extraction.

Successful shape extractions can sometimes produce outlines that do not reflect the true outline of the specimen. To account for these errors, outline-based measurements can be filtered by using a rugosity threshold. Because the threshold of filtering needed may vary based on the data application, we provide all outline-based measurements in the Data Citation. See **Usage Notes** for suggested filtering thresholds.

2.3.4 Size measurements

The accuracy of 2D size extraction was confirmed by measuring individuals with successful shape extraction on a Keyence VHX-7000 imaging microscope. Table 3 contains 10 benthic foraminifera from 6 species used to check 2D size extraction. Individuals were measured along their major and minor axes and outline-based area measurements were collected using ImageJ

measurement software. We find that automated and "human" measurements are comparable, such that *AutoMorph* measurements range, on average, from 97% to 104% of hand measurements. Average differences between major and minor axes was ~5 μm. Extended technical evaluations of *AutoMorph* measurements can be found in publications associated with the software suite (Hsiang et al. 2017, Kahanamoku et al. 2018, Elder et al. 2018).

2.3.5 Object classification

6 individual researchers worked simultaneously to classify objects from images. These researchers were undergraduate students without prior knowledge of foraminiferal morphology or taxonomy. In order to ensure inter-identifier consistency, all were trained to identify objects using a set of samples pre-identified by me, building on object categories outlined in Elder et al. (2018). Each sample was not considered completely identified until at least two unique identifiers provided classifications for all objects within the sample. These object classifications were then compared, and disagreements between identifiers were checked by me, who provided the final classification. Additionally, all identifiers provided a confidence (scale of 1-3, from least to most confident) for each object classification, which allowed for identifications with low confidence to be checked and updated. In cases where objects remained difficult to identify with certainty, the object classification was changed to 'unknown' to prevent misidentification. Errors are described briefly here, with each classification category described in more detail in **Usage Notes**. Most misidentifications were for species-level taxonomic classifications of benthic foraminifera (see below). For general object classification, classification errors included misidentification of non-benthic objects, including radiolaria, planktonic foraminifera, diatoms, and pteropods, which, when classified in error, were typically identified as 'benthic foraminifer fragments' or 'junk.' Images that contained multiple objects (e.g., had not been properly arranged during the sample preparation step and as a result were touching, or had overlapping outlines) were also misclassified when individual classifiers chose to identify one or more objects rather than classify them as 'touching'. Chunks of consolidated sediment were typically poorly classified, and as a result, were assigned to the 'unknown' category. In cases where individual images were of large individuals, the segmented image boundary occasionally contained other, smaller individuals (which typically were captured within their own segmented images), some of which were erroneously classified alongside the larger individual. To remedy inconsistent object classifications, visual checks (as described above) were used to reassign object categories. Following visual checks, automated cleaning scripts were employed to remedy misspellings or inconsistent spellings among object categories. These scripts are included within Data Citation 1.

2.3.6 Taxonomic classification

Taxonomic classification of benthic foraminifera occurred during the same classification step as general object classification (see Table S1.1 for taxonomic references). Benthic foraminifera were identified to species whenever possible, and identifiers were trained to make species-level identifications were using a set of reference images classified by me. Reference images for twelve of the most common species can be found in Figures 3 and 4. During object classification, identifiers classified benthic foraminifera to species and provided a confidence level for their classification. While the majority of confident classifications were for benthic foraminifera with complete or partially-damaged shells, on occasion classifications could be made from fragmentary pieces of shell (see **Usage Notes** for suggestions on how to filter out these

specimens when using morphometrics data). In total, ~60 unique species were identifiable from all samples, and are listed in Supplementary Table 1.

2.4 Usage Notes

Following their collection and preparation, many of the samples used in this study were picked for fish otoliths and plastic particles prior to the present study. However, the remainder of objects, including the benthic foraminifera on which we focus, were, to our knowledge, unbiased by previous research efforts undertaken on this material. It is worth noting that the benthic foraminifera that we observe for this study represent death assemblages, and as such may not be fully representative of the composition of living communities at the time of sediment layer deposition.

In studies of nearby sites in the Southern California Borderlands, death assemblages of benthic foraminifera are shown to differ in species composition, proportion, and distribution when compared to living assemblages (Douglas et al. 1980). However, these studies have lower temporal resolution than the present contribution, and may be observing time-averaged differences in assemblages that result from changes to shelf, slope, and basin environments that have taken place over the last several hundred years (Douglas and Heitman 1979). Yet even within the well-resolved sediments of the Santa Barbara Basin, there may be migration of benthic foraminifera between sediment layers. Some species undertake daily to seasonal migrations between the sediment-water interface and the uppermost centimeters of sediment (Duijnstee et al. 2003, Koho et al. 2011), and as a result, sediment layers of a given age may contain individuals from younger populations. Because vertical migration may be less pronounced during periods of anoxia (Duijnstee et al. 2003), the dysoxic waters of the Santa Barbara Basin may serve to limit this effect. Regardless, we caution that any analyses that utilize these data take benthic foraminifer ecology and the broader environmental and temporal setting of these samples into account.

The samples imaged for this study were washed over sieves, the smallest of which was 63 μm. While this size limit can be considered a general lower bound, some smaller particles may have slipped through size filter during the processing stage. These smaller objects should not be considered representative of the <63 μm fraction and should be excluded from the majority of data applications. In addition, while objects other than benthic foraminifera are included within these data, the majority were not intentionally picked out of the larger sample and should not be considered representative. However, a few classes were picked within intentionality and can be considered a representative fraction. These include pteropods, fish teeth, shark dermal denticles, and small (including larval) gastropod shells. These, alongside the benthic foraminifera, are the only objects that should be considered for future systematic and ecological studies that employ these data.

Each object was classified by a human observer (i.e., identifier) and placed into one of 15 categories along with an indication of confidence in the classification (1: not confident, 2: somewhat confident, 3: very confident). Broad classification categories are defined following Elder et al. (2018). ‘Junk’ denotes any fibers, inorganic crystalline structures, sand, rocks, captured images of light reflecting off of the background imaging plate, and other unidentifiable, non-biological forms. ‘Planktic’ indicates any planktonic foraminifer, and includes shells that are

complete, damaged, and fragmented. ‘Fragment’ includes any fragment of a benthic foraminifer that is not easily identifiable to species. ‘Gastropod’ denotes any gastropod shell, other than pteropods. ‘Pteropod’ denotes any pteropod shell, and includes shells that are complete, damaged, and fragmented. ‘Bivalve’ denotes small (potentially larval) bivalve shells. ‘Fish tooth’ denotes any fish dental structure, but does not include shark dermal denticles. ‘Dermal Denticle’ denotes any shark dermal denticle of any species. The ‘Radiolaria’ category contains radiolarians, ‘Diatom’ contains diatom frustules, ‘Echinoid’ contains echinoid fragments (including spines), ‘Spicule’ contains sponge spicules, and ‘Ostracod’ contains ostracods. In each of these categories, complete or larger individuals in clear, well-focused images were typically identified with greater confidence than broken or smaller objects, or those in out-of-focus images. Finally, ‘Touching’ denotes any images of multiple objects, which cannot be given a single identification. Objects in direct or very near contact are unable to be used for accurate 2D size and shape extraction, and should be excluded from any morphometric analyses.

Morphometric data should be checked prior to analyses according to the given use case. For example, data used for a study of body size may be filtered to remove poorly-extracted outlines by applying a rugosity filter, where objects with a rugosity greater than 1.2 are excluded from analyses (e.g., Chapter 4 of this dissertation). Other morphometric outputs that can aid in automated cleaning include aspect ratio and the outline coordinates.

Objects for which 2D size and shape extraction failed are listed in each relevant measurement file. Metadata including pixel sizes used for automated measurement can be found in the labels attached to each bulk and individual image provided in data file X of Data Citation 1. These pixel sizes can be used for future measurement via *AutoMorph* or other morphometric software. Additional metadata provided via image labels includes the sample name, object number, age, locality name, where images were processed, and the identity of the individual who processed the images. This metadata is permanently associated with images to ensure that no information is lost should these images be separated from other data files.

Acknowledgements
This work was partially supported by NSF/GSA Graduate Student Geoscience Grant #12739-20, which is funded by NSF Award No. 1949901 to SSK. SSK was also supported by an NSF Graduate Research Fellowship under Grant No. DGE 2146752 and a UC Berkeley Chancellor’s fellowship. The authors thank Jenni Brandon, William Jones, and Richard Norris for providing washed core samples and age models. We also thank Pincelli Hull, Alison Hsiang, Leanne Elder, and Kaylea Nelson for their development of and assistance with the *AutoMorph* software suite, and Gregory Kahanamoku-Meyer for writing the classify software used for identification.

Author Contributions
SSK and SF conceived and coordinated the study, selected samples for analysis, drafted the manuscript, and created figures. SSK, MSF, SMK, DS, LK, MT, YAM, JTE, GGM, CL, and HF picked samples for benthic foraminifera. SSK and MSF performed all imaging, technical validations, image processing, morphometric analyses, and dataset compilation. SSK, MSF, SMK, YSL, CS, and RCB classified objects, and SSK performed taxonomic verifications to ensure that classifications were consistent among identifiers. All authors contributed to the final writing of the manuscript.

Chapter 2 Figures

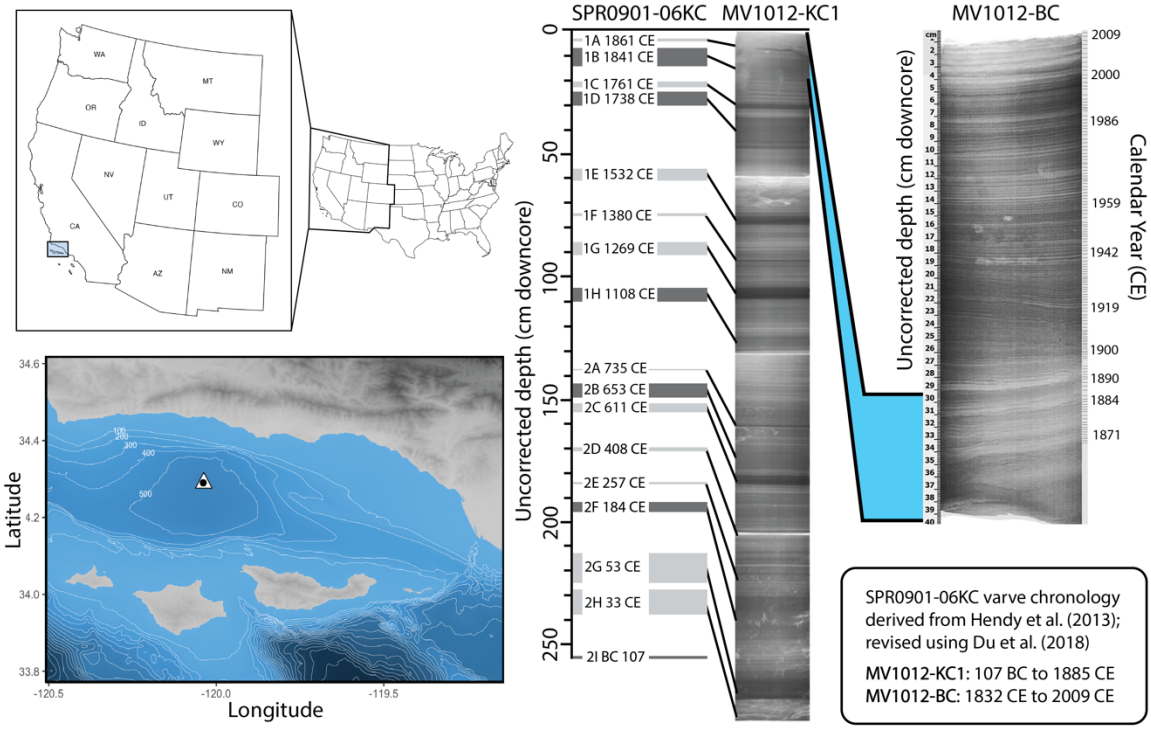

Figure 2.1: Sampling location and core chronology.
(A) The sampling location for kasten and box cores, site MV1012-ST46.9, (34˚17.228'N, 120˚02.135'W), is denoted by a white triangle. The sampling location was chosen as a reoccupation of Ocean Drilling Program site 893 (34.2875 N, 120.036 W, 577 m water depth), denoted by a black circle. Contour lines indicate seafloor depth (m). (B) Core chronology for box core MV1012-BC-1 and kasten core MV1012-KC1. Core images modified from Jones 2016 and Brandon et al. 2019.

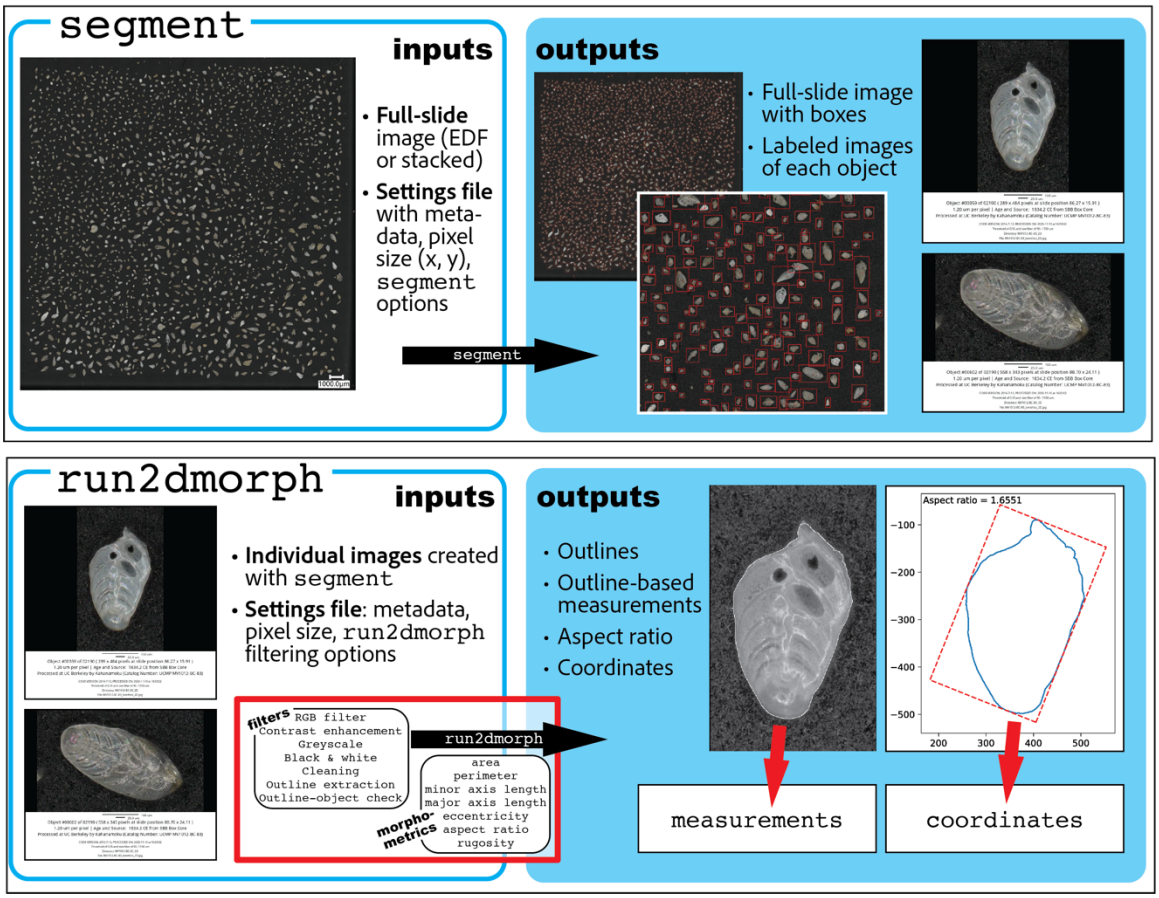

Figure 2.2: High-throughput imaging and AutoMorph image processing protocols. *AutoMorph* is an open-source software suite used for high-throughput image processing and automated morphometric measurements. For this study, two *AutoMorph* modules were used: segment (top panel) and run2dmorph (bottom panel). Segment takes as an input a full slide image and a settings file with metadata (sample name, age, location of collection, catalog number, etc.), size information (typically expressed as pixel size, e.g. microns per pixel), and settings flags. Segment outputs include a full-slide image with boxed and numbered individual objects, which correspond to individual images of objects, which are labeled with metadata as well as a scale bar. Run2dmorph takes as input the individual images created with segment (for this study, EDF images) as well as a settings file with measurement and filtering flags. Run2morph processes individual images through filters to create outlines, and uses outlines to generate outline-based measurements of area, perimeter, major and minor axis length, eccentricity, aspect ratio, and rugosity. Outlines and aspect ratios are output as images for visual checks, and measurements and outline coordinates are output as CSV files.

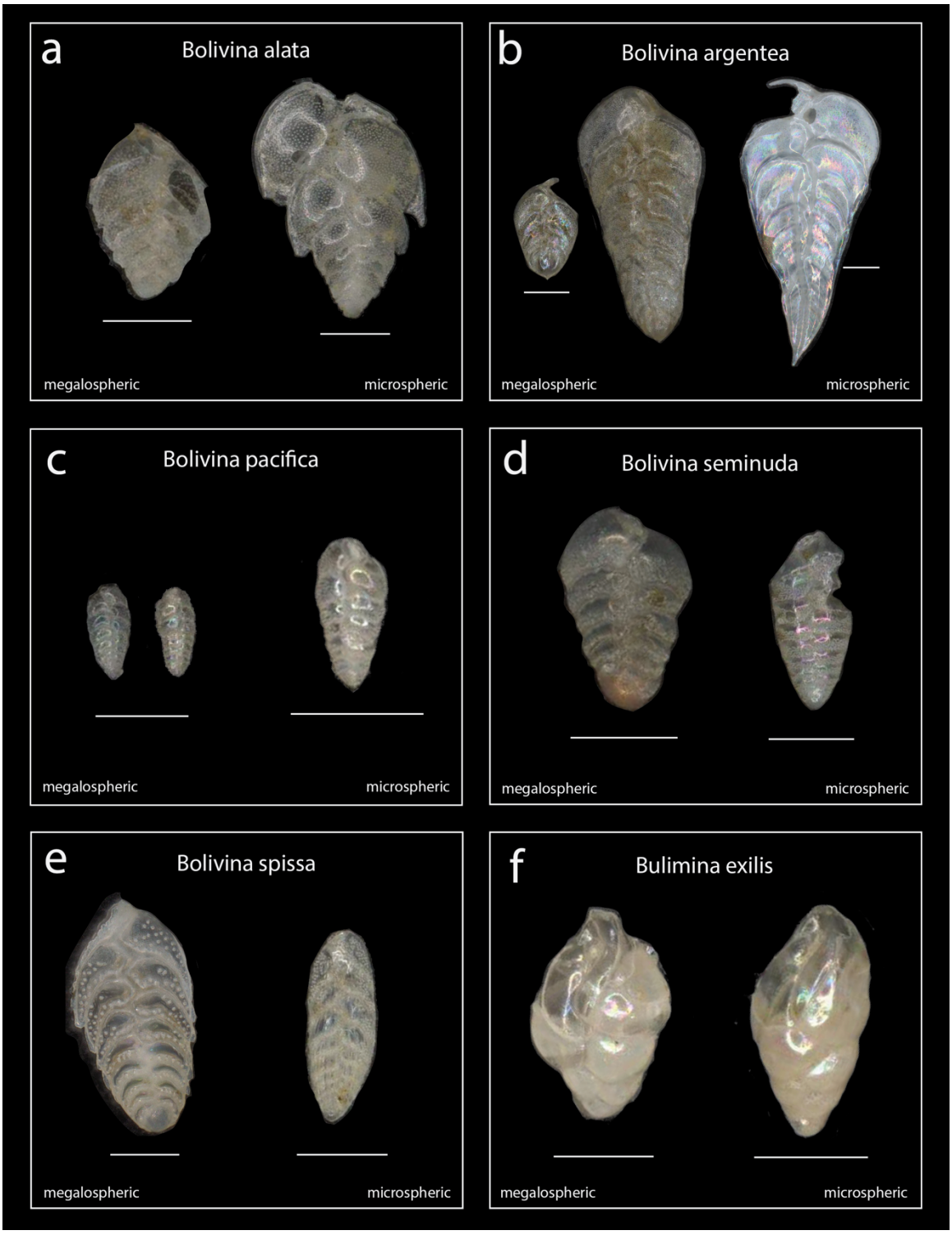

Figure 2.3: Common biserial benthic foraminifera from site MV1012.
(a) *Bolivina alata*; (b) *B. argentea*; (c) *B. pacifica*; (d) *B. seminuda*; (e) *B. spissa*; (f) *Bulimina exilis.* Megalospheric and microspheric morphotypes within each species are denoted; all individuals are arranged with the proloculus (first chamber) facing downwards. Scale bars denote 100 μm.

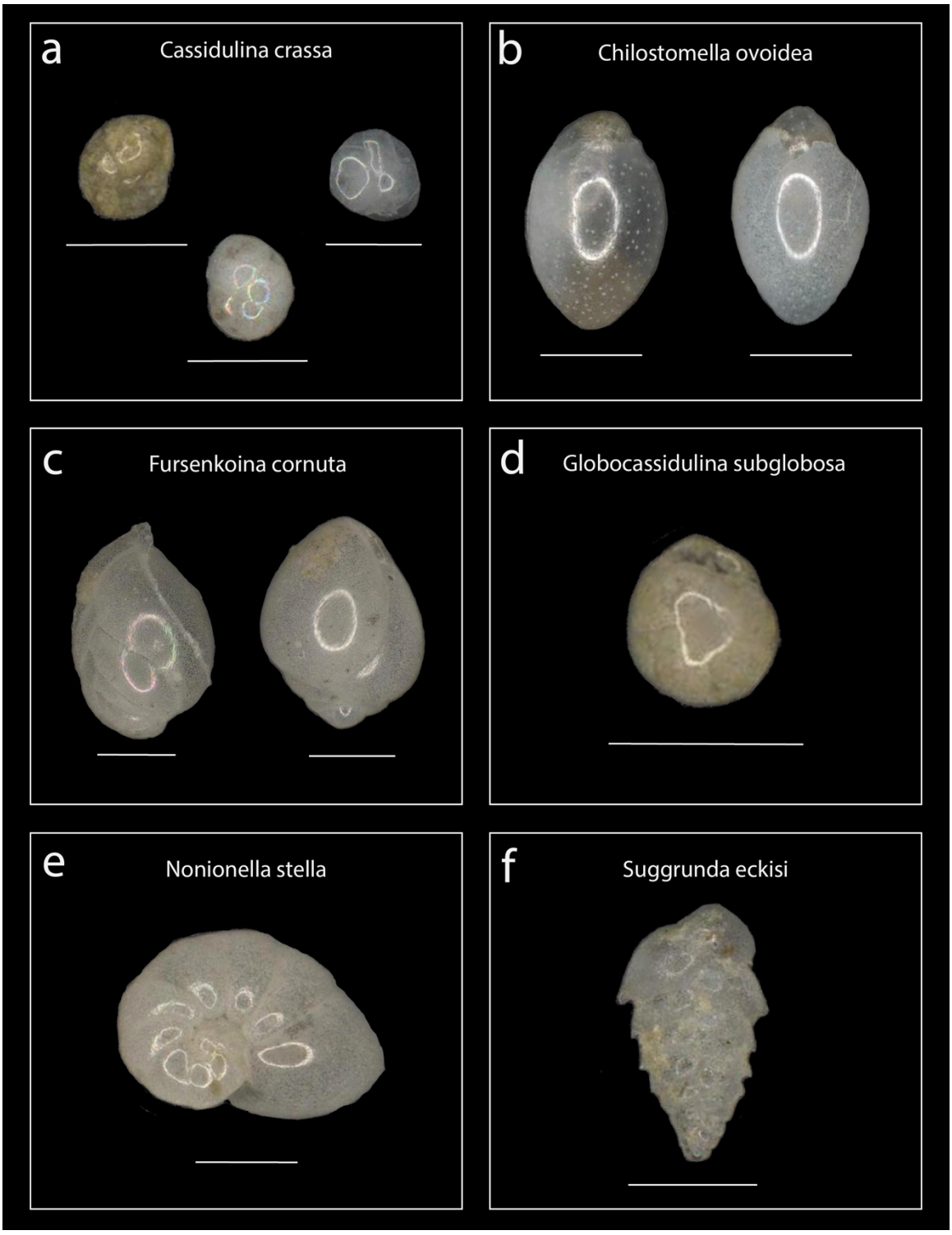

Figure 2.4: Common benthic foraminifera from site MV1012.
(a) *Cassidulina crassa*, with individuals show variation in shell coloration; (b) *Chilostomella ovoidea*, with individuals showing variation in coloration and porosity; (c) *Fursenkoina cornuta*, with individuals rotated ~180˚ opposite one another; (d) *Globocassidulina subglobosa*; (e) *Nonionella stella*; and (f) Suggrunda eckisi. Scale bars denote 100 μm.

LIST OF TABLES

Table 2.1: Sample ages and split fractions.

Site	Core Type	Sample	Calendar Year CE	Assemblage Type	Split Size
MV1012	Box	MV1012-BC-2	2007.9	All	1
MV1012	Box	MV1012-BC-3	2006.7	All	1
MV1012	Box	MV1012-BC-4	2005.6	All	1
MV1012	Box	MV1012-BC-5	2004.4	All	1
MV1012	Box	MV1012-BC-6	2003.3	All	1
MV1012	Box	MV1012-BC-7	2002.1	All	1
MV1012	Box	MV1012-BC-8	2001	All	1
MV1012	Box	MV1012-BC-9-10	1998.4	All	1
MV1012	Box	MV1012-BC-11	1995.8	All	1
MV1012	Box	MV1012-BC-12	1994	All	1
MV1012	Box	MV1012-BC-14	1990.5	All	1
MV1012	Box	MV1012-BC-15	1988.8	All	1
MV1012	Box	MV1012-BC-16	1987	All	1
MV1012	Box	MV1012-BC-17	1984.8	All	1
MV1012	Box	MV1012-BC-19	1980.5	All	1
MV1012	Box	MV1012-BC-20	1978.4	All	1
MV1012	Box	MV1012-BC-22	1974.1	All	1
MV1012	Box	MV1012-BC-25	1967.6	All	1
MV1012	Box	MV1012-BC-26	1965.5	All	1
MV1012	Box	MV1012-BC-27	1963.3	All	1
MV1012	Box	MV1012-BC-32	1952.6	All	1
MV1012	Box	MV1012-BC-36	1944.1	All	1
MV1012	Box	MV1012-BC-41	1931.8	All	1
MV1012	Box	MV1012-BC-42	1929.2	All	1
MV1012	Box	MV1012-BC-48	1913.6	All	1
MV1012	Box	MV1012-BC-53	1900	All	1
MV1012	Box	MV1012-BC-57	1890.9	All	1
MV1012	Box	MV1012-BC-70	1862.3	All	1
MV1012	Kasten	KC1-1-25	1841	Biserial only	1/32
MV1012	Box	MV1012-BC-82	1836.3	All	1
MV1012	Box	MV1012-BC-83	1834.2	All	1
MV1012	Kasten	KC1-1-52	1820	Biserial only	1/32
MV1012	Kasten	KC1-1-64	1769	Biserial only	1/16
MV1012	Kasten	KC1-1-103	1712	Biserial only	1/128

Site	Core Type	Sample	Calendar Year CE	Assemblage Type	Split Size
MV1012	Kasten	KC1-1-117	1666	Biserial only	1/16
MV1012	Kasten	KC1-1-124	1643	Biserial only	1/32
MV1012	Kasten	KC1-2-9	1610	Biserial only	1/64
MV1012	Kasten	KC1-2-28	1548	Biserial only	1/32
MV1012	Kasten	KC1-2-49	1478	Biserial only	1/32
MV1012	Kasten	KC1-2-59	1429	Biserial only	1/32
MV1012	Kasten	KC1-2-64	1405	Biserial only	1/16
MV1012	Kasten	KC1-2-68	1385	Biserial only	1/128
MV1012	Kasten	KC1-2-80	1325	Biserial only	1/32
MV1012	Kasten	KC1-2-87	1289	Biserial only	1/16
MV1012	Kasten	KC1-2-103	1249	Biserial only	1/32

Table 2.2: Major object classification categories and brief definitions.

Classification Category	Definition
Junk	Fibers, imaging plate background, rocks, inorganic crystalline structures, and poorly-extracted partial images of benthic foraminifera
Planktic	Whole, damaged, or partial planktonic foraminifera, including shell wall fragments identifiable as planktic
Fragment	Fragments of benthic foraminifera unidentifiable to species or too incomplete to serve as a morphological specimen
Gastropod	Microgastropods or any gastropod fragments; does not include pteropods
Fish Tooth	Whole, damaged, or partial fish teeth
Dermal Denticle	Shark dermal denticles or placoid scales
Diatom	Whole, partial, or damaged diatom frustule
Spicule	Sponge spicules, typically microscleres
Echinoid	Whole or fragmented echinoid spines
Pteropod	Whole, damaged, or partial pteropod shells
Radiolarian	Whole, damaged, or partial radiolarian tests
Ostracod	Whole, damaged, or partial ostracode valves or carapaces
Touching	Segmented images of multiple objects, typically objects with overlapping outlines
Bivalve	Larval bivalve shells, small whole bivalve specimens, or identifiable shell fragments

Table 2.3: Technical validation measurements.

Sample Name	Obj. Num.	Species	ImageJ			AutoMorph			Minor Axis Difference	Major Axis Difference	Area Difference
			Minor Axis (µm)	Major Axis (µm)	Area (µm2)	Minor Axis (µm)	Major Axis (µm)	Area ($µm^2$)			
MV1012-BC-3	5	*Globo-cassidulina subglobossa*	110.5	126.4	10798	112.1	129.5	11369	1.014	1.025	1.053
MV1012-BC-3	7	*Suggrunda eckisi*	96.6	194.9	14173	99	195.2	14764	1.025	1.002	1.042
MV1012-BC-3	14	*Suggrunda eckisi*	98	169.1	11609	95.7	157	11524	0.977	0.928	0.993
MV1012-BC-3	16	*Bolivina pacifica*	73.5	144	7678	75	141.2	8118	1.02	0.981	1.057
MV1012-BC-3	9	*Suggrunda eckisi*	116.6	194.4	16652	115.8	182.8	16315	0.993	0.94	0.98
MV1012-BC-3	4	*Bulimina exilis*	111.5	133.9	10155	109.8	128.9	10986	0.985	0.963	1.082
MV1012-BC-4	20	*Bolivina argentea*	297.4	928.9	207898	320.4	890.8	213158	1.077	0.959	1.025
MV1012-BC-4	53	*Fursenkoina cornuta*	324.9	461.2	107255	328.8	460.8	118560	1.012	0.999	1.105
MV1012-BC-4	31	*Bolivina argentea*	198.4	263.8	37737	198.4	249.7	38499	1	0.947	1.02
								Mean Diff.	1.01	0.97	1.04

Chapter 2 Supplementary Figures and Tables

Supplementary Table 2.1: Taxonomic references and synonyms for benthic foraminifera at site MV1012.

Species	Life Science Identifier	Taxonomic Reference
Alabaminella wedellensis	113350	Earland 1936
Angulogerina angulosa	113749	Williamson 1858
Anomalinoides larseni	1038726	Huber 1988
Anomalinoides minimus	113402	Förster 1892
Astrononion stellatum	954368	Terquem 1882
Bolivina alata	112964	Seguenza 1862
Bolivina argentea	852154	Cushman 1926
Bolivina interjuncta	926387	Cushman 1926
Bolivina ordinaria	112978	Phleger & Parker 1952
Bolivina pacifica	112979	Cushman & McCulloch 1942
Bolivina seminuda	417913	Cushman 1911; Cushman & McCulloch 1942
Bolivina spissa	814781	Cushman 1926
Bolivinita minuta	1551292	Natland 1938
Buccella peruviana	736489	d'Orbigny 1839
Bulimina exilis (=Eubulimina exilis)	417980	Brady 1884
Cassidulina auka	1324195	Boltovskoy & Theyer 1970
Cassidulina carinata	183041	Silvestri 1896
Cassidulina crassa	397221	Orbigny 1839
Cassidulina delicata	522689	Cushman 1927
Cassidulina minuta (=Paracassidulina minuta)	113078	Cushman 1933
Chilostomella ovoidea	113554	Reuss 1850
Cibicidoides wuellerstorfi	112890	Schwager 1866
Epistominella exigua	113334	Brady 1884
Epistominella obesa	522226	Bandy & Arnal 1957
Epistominella pacifica (=Pseudoparrella pacifica)	849701	Cushman 1927
Epistominella pulchella	761687	Husezima & Maruhasi 1944

Species	Life Science Identifier	Taxonomic Reference
Epistominella sandiegoensis	522137	Uchio 1960
Epistominella smithi	862706	Stewart & Stewart 1930
Fursenkoina complanata	466392	Egger 1893
Fursenkoina cornuta	862715	Cushman 1913
Fursenkoina pauciloculata	417966	Brady 1884
Globobulimina barbata	1551161	Cushman 1927
Globobulimina ovata	1551163	d'Orbigny 1846
Globobulimina pacifica	417928	Cushman 1927
Globocassidulina neomargareta	1059294	Finger & Lipps 1990
Globocassidulina pacifica (=Burseolina pacifica)	417960	Cushman 1925
Globocassidulina subglobosa	113091	Brady 1881
Gyroidina subtenera (?)	1551069	Galloway & Wissler 1927
Lagena striata	113507	d'Orbigny 1839
Melonis affinis	418046	Reuss 1851
Melonis pompilioides	113564	Fichtel & Moll 1798
Nonionella decora (=Pseudononion decorum)	522930	Cushman & McCulloch 1940
Nonionella digitata	113600	Nørvang 1945
Nonionella stella	113604	Cushman & Moyer 1930
Nonionoides turgidus	466471	Williamson 1858
Oolina squamosa	113227	Montagu 1803
Parafissurina malcomsonii	417886	Wright 1911
Praeglobobulimina spinescens	113063	Brady 1884
Pullenia bulloides	113110	d'Orbigny 1846
Pullenia elegans	764129	Cushman & Todd 1943
Pyrgo murrhina	112593	Schwager 1866
Quinqueloculina seminula	112674	Linnaeus 1758
Suggrunda eckisi	521635	Natland 1950
Triloculina trihedra	163643	Loeblich & Tappan 1953
Uvigerina auberiana	113763	d'Orbigny 1839
Uvigerina interruptacostata	907135	LeRoy 1944
Uvigerina peregrina	113773	Cushman 1923
Uvigerina senticosa	417951	Cushman 1927

Data Citation

Kahanamoku, Sara S., Samuels-Fair, M., Kamel, S.M., Stewart, D., Kahn, L., Titcomb, M., Mei, Y.A., Bridge, R.C., Li, Y.S., Sinco, C., Epino, J.T., Gonzalez-Marin, G., Latt, C., Fergus, H., and Finnegan, S. Twenty-two thousand Common Era benthic foraminifera from the Santa Barbara Basin [Data set]. Zenodo. https://doi.org/10.5281/zenodo.7274658

2.5 Chapter 2 References

Baldauf, J., and M. Lyle. 1995. Proceedings of the Ocean Drilling Program, Scientific Results. Vol. 146, Part 2. Santa Barbara Basin: covering Leg 146 of the cruises of the Drilling Vessel" Joides Resolution", Santa Barbara Channel, California, Site 893, 20 September-22. Texas A & M University, Ocean Drilling Program.

Belanger, C. L. 2022. Volumetric analysis of benthic foraminifera: Intraspecific test size and growth patterns related to embryonic size and food resources. Marine Micropaleontology 176:102170.

Bograd, S. J., D. A. Checkley Jr, and W. S. Wooster. 2003. CalCOFI: a half century of physical, chemical, and biological research in the California Current System. Deep Sea Research Part II: Topical Studies in Oceanography 50:2349–2353.

Boltovskoy, E., D. B. Scott, and F. S. Medioli. 1991. Morphological variations of benthic foraminiferal tests in response to changes in ecological parameters: a review. Journal of Paleontology 65:175–185.

Brandon, J. A., W. Jones, and M. D. Ohman. 2019. Multidecadal increase in plastic particles in coastal ocean sediments. Science Advances 5:eaax0587–eaax0587.

CalCOFI. 2022. CalCOFI – California Cooperative Oceanic Fisheries Investigations. https://calcofi.org/.

Culver, S. J. 1991. Early Cambrian foraminifera from west Africa. Science 254:689–691.

Douglas, R. G., and H. L. Heitman. 1979. Slope and basin benthic foraminifera of the California borderland.

Douglas, R. G., J. Liestman, C. Walch, G. Blake, and M. L. Cotton. 1980. The Transition from Live to Sediment Assemblage in Benthic Foraminifera from the Southern California Borderland:257–280.

Duijnstee, I., S. Ernst, and G. Van der Zwaan. 2003. Effect of anoxia on the vertical migration of benthic foraminifera. Marine Ecology Progress Series 246:85–94.

Elder, L. E., A. Y. Hsiang, K. Nelson, L. C. Strotz, S. S. Kahanamoku, and P. M. Hull. 2018. Sixty-one thousand recent planktonic foraminifera from the Atlantic Ocean. Scientific Data 5:180109–180112.

Ezard, T. H. G., T. Aze, P. N. Pearson, and A. Purvis. 2011. Interplay between changing climate and species' ecology drives macroevolutionary dynamics. Science 332:349–351.

Foster Laura C., Schmidt Daniela N., Thomas Ellen, Arndt Sandra, and Ridgwell Andy. 2013. Surviving rapid climate change in the deep sea during the Paleogene hyperthermals. Proceedings of the National Academy of Sciences 110:9273–9276.

Hendy, I. L., L. Dunn, A. Schimmelmann, and D. K. Pak. 2013. Resolving varve and radiocarbon chronology differences during the last 2000 years in the Santa Barbara Basin sedimentary record, California. Quaternary International 310:155–168.

Hönisch, B., A. Ridgwell, D. N. Schmidt, E. Thomas, S. J. Gibbs, A. Sluijs, R. Zeebe, L. Kump, R. C. Martindale, S. E. Greene, W. Kiessling, J. Ries, J. C. Zachos, D. L. Royer, S. Barker,

T. M. Marchitto, R. Moyer, C. Pelejero, P. Ziveri, G. L. Foster, and B. Williams. 2012. The Geological Record of Ocean Acidification. Science 335:1058–1063.
Hsiang, A. Y., K. Nelson, L. E. Elder, E. C. Sibert, S. S. Kahanamoku, J. E. Burke, A. Kelly, Y. Liu, and P. M. Hull. 2017. AutoMorph: Accelerating morphometrics with automated 2D and 3D image processing and shape extraction. Methods in Ecology and Evolution 9:605–612.
Hull, P. M. 2017. Emergence of modern marine ecosystems. Current Biology 27:R466–R469.
Jones, W. A. 2016. The Santa Barbara Basin Fish Assemblage in the Last Two Millennia Inferred from Otoliths in Sediment Cores:1–141.
Jones, W. A., and D. M. Checkley. 2019. Mesopelagic fishes dominate otolith record of past two millennia in the Santa Barbara Basin. Nature Communications 10:4564.
Kahanamoku, S. S., P. M. Hull, D. R. Lindberg, A. Y. Hsiang, E. C. Clites, and S. Finnegan. 2018. Twelve thousand recent patellogastropods from a northeastern Pacific latitudinal gradient. Scientific Data 5:170197–170197.
Keating-Bitonti, C. R., and J. L. Payne. 2017. Ecophenotypic responses of benthic foraminifera to oxygen availability along an oxygen gradient in the California Borderland. Marine Ecology 38:e12430.
Keating-Bitonti, C. R., and J. L. Payne. 2018. Environmental influence on growth history in marine benthic foraminifera. Paleobiology 44:736–757.
Koho, K. A., E. Piña-Ochoa, E. Geslin, and N. Risgaard-Petersen. 2011. Vertical migration, nitrate uptake and denitrification: survival mechanisms of foraminifers (Globobulimina turgida) under low oxygen conditions. FEMS Microbiology Ecology 75:273–283.
Kucera, M. 2007. Chapter Six Planktonic Foraminifera as Tracers of Past Oceanic Environments BT - Proxies in Late Cenozoic Paleoceanography. Pages 213–262 Proxies in Late Cenozoic Paleoceanography. Elsevier.
Kuroyanagi, A., T. Irie, S. Kinoshita, H. Kawahata, A. Suzuki, H. Nishi, O. Sasaki, R. Takashima, and K. Fujita. 2021. Decrease in volume and density of foraminiferal shells with progressing ocean acidification. Scientific Reports 11:19988.
LUTZE, G. F. 1964. Statistical investigations on the variability of Bolivina argentea Cushman. Contribution from the Cushman Foundation for Foraminiferal Research 15:105–116.
Norris, R. D., S. K. Turner, P. M. Hull, and A. Ridgwell. 2013. Marine Ecosystem Responses to Cenozoic Global Change. Science 341:492–498.
Pawlowski, J., M. Holzmann, C. Berney, J. Fahrni, A. J. Gooday, T. Cedhagen, A. Habura, and S. S. Bowser. 2003. The evolution of early Foraminifera. Proceedings of the National Academy of Sciences 100:11494–11498.
Santana, B. F. de B. B., T. R. Freitas, J. Leonel, and C. Bonetti. 2021. Biometric and biomass analysis of Quaternary Uvigerinidae (Foraminifera) from the Southern Brazilian continental slope. Marine Micropaleontology 169:102041.
Saraswat, R., A. Deopujari, R. Nigam, and P. J. Heniriques. 2011. Relationship between abundance and morphology of benthic foraminifera Epistominella exigua: Paleoclimatic implications. Journal of the Geological Society of India 77:190–196.
Schimmelmann, A., I. L. Hendy, L. Dunn, D. K. Pak, and C. B. Lange. 2013. Revised ~2000-year chronostratigraphy of partially varved marine sediment in Santa Barbara Basin, California. GFF 135:258–264.
Schimmelmann, A., C. B. Lange, E. B. Roark, and B. L. Ingram. 2006. Resources for Paleoceanographic and Paleoclimatic Analysis: A 6,700-Year Stratigraphy and Regional Radiocarbon Reservoir-Age (ΔR) Record Based on Varve Counting and 14C-AMS Dating

for the Santa Barbara Basin, Offshore California, U.S.A. Journal of Sedimentary Research 76:74–80.
Schmidt, D. N., E. Thomas, E. Authier, D. Saunders, and A. Ridgwell. 2018. Strategies in times of crisis—insights into the benthic foraminiferal record of the Palaeocene–Eocene Thermal Maximum. Philosophical Transactions of the Royal Society A: Mathematical, Physical and Engineering Sciences 376:20170328.
Sibert, E. C., and R. D. Norris. 2015. New Age of Fishes initiated by the Cretaceous−Paleogene mass extinction. Proceedings of the National Academy of Sciences 112:8537–8542.
Sibert, E. C., and L. D. Rubin. 2021. An early Miocene extinction in pelagic sharks. Science 372:1105–1107.
Sibert, E., M. Friedman, P. Hull, G. Hunt, and R. Norris. 2018. Two pulses of morphological diversification in Pacific pelagic fishes following the Cretaceous–Palaeogene mass extinction. Proceedings of the Royal Society B: Biological Sciences 285:20181194–20181197.
Tetard, M., L. Licari, K. Tachikawa, E. Ovsepyan, and L. Beaufort. 2021. Toward a global calibration for quantifying past oxygenation in oxygen minimum zones using benthic Foraminifera. Biogeosciences Discussions:1–17.
Zachos, J. C., G. R. Dickens, and R. E. Zeebe. 2008. An early Cenozoic perspective on greenhouse warming and carbon-cycle dynamics. Nature 451:279–283.
Zachos, J., M. Pagani, L. Sloan, E. Thomas, and K. Billups. 2001. Trends, rhythms, and aberrations in global climate 65 Ma to present. science 292:686–693.

3 A 2-kyr record of abundance and reproductive mode in benthic foraminifera from the Santa Barbara Basin shows a nineteenth-century change

Sara S. Kahanamoku[1*], Maya Samuels-Fair[1*], Jared C. Richards[2], Ivo A.P. Duijnstee[1], Richard Norris[3], Seth Finnegan[1]

1) Department of Integrative Biology and Museum of Paleontology, University of California, Berkeley, CA; 2) Department of Organismal Biology, Harvard University, Cambridge, MA; 3) Scripps Institution of Oceanography, University of California, San Diego, CA

*Co-first authorship

Abstract

Life history is a critical determinant of the eco-evolutionary success of populations and lineages. While obtaining direct indicators of life history information from the fossil record is difficult, some groups preserve morphological indicators of reproductive mode that allow for study of life history through time. We examined ~45,000 individuals from *Bolivina* benthic foraminifera, scoring each as the product of either sexual or asexual reproduction, then examined changes in individual accumulation rate and prevalence of reproductive mode in 70 samples from a core spanning the past 2 kyr in the Santa Barbara Basin, California. Across four different *Bolivina* species, increases in accumulation rate tend to be associated with increases in the proportion of asexual reproduction, suggesting clonal blooms during permissive environmental conditions. Increasing accumulation rates tend to coincide with El Niño events, likely in response to reduced upwelling productivity and increased ventilation. However, in the mid-19th century these relationships break down, and both abundance and the proportion offspring of asexual reproduction drop and remain low through the present day. The timing of change in *Bolivina* life history corresponds with changes in environmental conditions as inferred from historical data and proxy records (ENSO variance, SST, productivity and oxygenation state), but also with major shifts in human-environmental interactions that accompanied the intensifying colonization of California. Our study suggests that the impacts of intensified settler colonialism and industrialization, which began in the mid-19th century and continue to present, may have induced a state change in Californian marine ecosystems even in environments that are far from direct impact.

3.1 Introduction

Life history choices–how resources are allocated through ontogeny–modulate key individual traits, such as size at birth (Blueweiss et al. 1978, Yampolsky and Scheiner 1996, Shama 2015, Marshall et al. 2018, Dallago et al. 2022), growth rate (Hutchings 1993, Angilletta Jr et al. 2004, Dmitriew 2011), maturation age (Stearns and Koella 1986, Ridgway et al. 2011, Shuter et al. 2016), fecundity and reproductive success (Darwin 1871, Llodra 2002, Pincheira-Donoso and Hunt 2017), and overall lifespan (Stearns 2000, Wilkinson and South 2002, De Magalhaes and Costa 2009). Variations in individual life histories and their resulting trade-offs (Stearns 1992, Christie et al. 2018) in turn impact population growth rates (Cole 1954, Caswell 1978, Beckerman et al. 2002, Carson et al. 2010) and the available range of genetic and morphological variation within populations (Cole 1954, Beckerman et al. 2002, Carson et al. 2010, Ji et al. 2022), which over time compound to determine the success of entire evolutionary lineages (Olsen et al. 2004, Hutchings et al. 2012, Hellmair and Kinziger 2014).

Life history evolution has been challenging to study on long timescales, with the majority of direct studies of life history variation examining the progression of at most a few generations (Miloslavich et al. 2018, Montero-Serra et al. 2018, Estes et al. 2018, Cusser et al. 2021). The lack of studies that incorporate historical data to understand how long-term trends in individual life history choices affect eco-evolutionary lineages stems in part from the difficulty of quantifying life history choices in fossil and historical records. Morphological traits have long been used as a proxy for life history choices and their macro-scale ecological and evolutionary impacts, providing insights into characteristics driven by life history choices, such as body size (LaBarbera 1989, Jablonski et al. 1996, Malerba et al. 2017) and growth rate (Moss et al. 2016). However, studies that focus on direct aspects of life history evolution, such as reproductive strategies or fecundity, are more rare (but see O'Dea and Jackson 2009, Di Martino and Liow 2021). Long-term data on reproductive dynamics are needed in order to understand baseline variation in reproductive trends and how observations align with theoretical models predicting the outcomes of life history trade-offs. Without these data, accurate identification of the impacts of major episodes of climate and environmental change on reproductive life history choices, and thus lineage-specific extinction risk under present and projected future climate scenarios (e.g., Pearson et al. 2014, García et al. 2019, De Kort et al. 2021) is inhibited.

Some lineages preserve morphological indicators of life history choices relating to reproduction, thus allowing for the generation of time series from fossil records with resolutions that span from decades to millions of years (Moran 2004, O'Dea et al. 2007, O'Dea and Jackson 2009, Siveter et al. 2014, Yamaguchi et al. 2017, Schmidt et al. 2018). Among these, foraminifera–unicellular protists that make calcium carbonate tests with high preservation potential (Kucera 2007)–have a rich, cosmopolitan, and highly temporally-resolved fossil record (Yasuhara et al. 2015) which has fostered a long history of study of the linkages between morphological variation and environmental factors (Lutze 1964, Hallock 1985, Schmidt et al. 2018, Keating-Bitonti and Payne 2018). As far as we know, foraminifera generally undergo lifecycles that involve switching between a haploid, sexually-reproducing stage (the gamont) and a diploid, asexually-reproducing stage (the agamont) or multiple, successive haploid (and/or diploid) stages corresponding with asexual reproduction (Dettmering et al. 1998). Sexual versus asexual reproductive allocation is therefore a critical aspect of foraminiferan life history evolution.

Foraminifer offspring preserve morphological indicators of the mode of reproduction by which they were produced in the size of their proloculus, or first chamber: microspheric individuals (small proloculi) are produced by sexual reproduction, and megalospheric individuals (large proloculi) are produced by asexual reproduction (Sen Gupta 2003, Davis et al. 2020). Across foraminifera, reproductive mode is thought to respond to a variety of abiotic factors as well as population dynamics: while sexual reproduction has been considered to be favorable under variable conditions, both sexual and asexual reproduction is possible and, in different groups, observed with varying frequency (Lehtonen et al. 2012, Yang and Kim 2016, Burke and Bonduriansky 2017). Under stable conditions, asexual reproduction often accounts for most reproductive events (Hallock 1985). In benthic foraminifera, the prevalence of asexual reproduction may be impacted by environmental conditions such as bottom-water temperature (Nigam and Rao 1987) or oxygenation (Lutze 1964). However, a general lack of research into life history variation in foraminifera has hindered understanding of the reproductive dynamics and capacities of foraminifer populations, both under stable baseline conditions and periods of

rapid environmental change. Few direct observations or laboratory experiments of foraminifera undergoing reproductive events exist (but see Takagi et al. 2020, Davis et al. 2020), and little is known about the potential link of reproductive mode, and thus proloculus size, to environmental variability (Schmidt et al. 2018).

A number of foraminifera within the biserial benthic genus *Bolivina* exhibit strong bimodality in their highly visible proloculi (Douglas and Staines-Urias 2007, Staines-Urías and Douglas 2009), and these morphological traits are readily preserved. As a result, this system is a rare case in which life history patterns can be explored without real-time observation of reproduction. Within the SBB, the fossil record of *Bolivina* spans back millennia, thus making this system ideal for the examination of life history patterns both through periods of stability and environmental change. Here we use high-throughput imaging methods to generate individual-level data for *Bolivina* foraminifera from the Santa Barbara Basin of Southern California (SBB), an area with high levels of primary productivity, seasonal upwelling, and low-oxygen bottom waters that minimize bioturbation and allow for preservation of millimeter scale seasonal to annual laminae (varves; Figure 3.1, Figure S3.1).

Here we present a 2-kyr record of reproductive life history in the Santa Barbara Basin biserial benthic foraminifer genus *Bolivina* to examine baseline trends in reproductive mode and during the Common Era. We further assess which common oceanographic factors may influence reproductive life history variation, and explore potential mechanisms that drive a mid-19th century change in *Bolivina* life history.

3.2 Materials and Methods

3.2.1 Core Sampling

A kasten core and a box core from the center of the Santa Barbara Basin (Southern California; SBB) were collected in 2010 at station MV1012-ST46.9 (34˚17.228'N, 120˚02.135'W) at approximately 580m water depth (Figure 3.1). 2 cm vertical core slices from each subcore were X-radiographed and scanned at 1-mm intervals in a linear, non-rotational scan (Brandon et al. 2019, Jones and Checkley 2019). Composite X-radiographs were used with color photographs to develop a high-resolution chronology for each core (Figure S3.1). The age model for kasten core MV1012-KC1 was adapted from Hendy et al. (Hendy et al. 2013) and Schimmelman et al. (Schimmelmann et al. 2013); dates assigned to each sample were the average of the dates of the upper and lower surfaces of the sample transverse section. Box core MV1012-BC1 was sufficiently shallow to use traditional varve chronology (Hendy et al. 2013, Schimmelmann et al. 2013, 2006) for couplet dating; a regression model was used to assign dates to the sediment stratigraphy prior to 1871, thus extending the chronology to 1834 CE (Brandon et al. 2019).

Prior to the present study, subcore cross-sections were cut transversely every 0.5 cm to create transverse sections of 97.5cm^3, and these were stored at -80˚C prior to further processing. Core transverse sections were then dried overnight at 50˚C, washed in distilled water, and wet-sieved over a 104- and 63-µm mesh to create samples for analysis. The >104 µm fraction of these samples was picked under a dissecting microscope for fish otoliths (Jones and Checkley 2019) and plastic particles (Brandon et al. 2019) and used in separate analyses. For the present analysis, samples from the 63-104 and >104 µm fraction of kasten cores MV1012-KC1 were dry split

using a sediment splitter to achieve approximately equivalent sample volumes for ease of picking (Table S3.1). Samples from box core MV1012-BC were processed in their entirety due to their small overall volumes (Table S3.1), and all analyses were standardized to sample volume.

3.2.2 Sample processing

70 samples from ~50 to 2008 CE were selected for this analysis. Of these, 36 samples were picked for all *Bolivina* foraminifera present within the sample (*Bolivina alata*, *B. argentea*, *B. pacifica*, *B. seminuda*, *B. seminuda var. humilis*, and *B. spissa*; Table S3.1) under a Leica EZ4 dissecting microscope at 16x magnification, arranged on coated brass picking plates, and imaged in bulk using a Keyence VHX-7000 digital imaging microscope following high-throughput imaging techniques outlined in Hsiang et al. (Hsiang et al. 2017a). Bulk images were segmented into individual images using the *AutoMorph* protocol (Hsiang et al. 2017a) (Figure S3.2; see Chapter 2 of this dissertation). Images of individual segmented objects formed the basis of analysis for these samples (Figure S3.3); in total, over 36,000 individual *Bolivina* foraminifera were imaged and classified for subsequent analyses. The remaining 34 samples were picked solely for *Bolivina argentea* (Table S3.1, Figure S3.4); these were not imaged, but were manually scored for reproductive mode by visually classifying proloculus size to place individuals into the megalospheric or microspheric category. Over 9,000 individual *B. argentea* were scored manually.

3.2.3 Taxonomic identification and scoring for reproductive mode

Individuals were identified to species (Figure S3.3, Table S3.2) and scored for reproductive mode, either from individual images or during manual sample processing (Table S3.1). To track changes in overall abundances, species-specific accumulation rates were calculated for each sample by normalizing the total number of picked *Bolivina* by species to the sedimentation rate for a given sample (foraminifera per volume per year; Figure S3.5). Visual identification of proloculus size allowed for binary classification of megalospheric (large proloculus) and microspheric (small proloculus) individuals (Figure S3.6). Individuals with broken, non-visible, or unmeasureable proloculi were classified as "unknown," as were taxa without known bimodality in proloculus size, and excluded from analyses.

While previous studies have shown that the kasten and box core can be combined and analyzed as single continuous record (Jones 2016, Jones and Checkley 2019), reproductive mode classifications and species-specific accumulation rates from samples within the overlap portion of the kasten and the box core (1834-1885 CE) were compared as an additional check of core compatibility. We find that samples within this overlap period have similar proportions of asexual individuals and accumulation rates (Figure S3.7; see supplemental materials for further discussion).

We considered only biserial benthic foraminifera with clear proloculus size dimorphism. All foraminifera from genera other than *Bolivina* were excluded from the final dataset, as were individuals within *Bolivina* that were not confidently identifiable to species. Within *Bolivina*, we excluded *Bolivina intercostata* as this species was rare and no clear dimorphism in proloculus size was observed. We also excluded *Bolivina pacifica* from analyses due to the small sample size for this species, as well as the low variation in proloculus size for this species, which resulted in low confidence in identifications and reproductive mode classification. We combined

Bolivina seminuda and *Bolivina seminuda var. humilis* into a single species category, *B. seminuda* (Table S3.2, Figure S3.3) to reflect how many studies done in the SBB classify this species (see supplemental for further discussion). Images and data for all *Bolivina* species are included in the dataset alongside the reduced dataset used for this analysis (Kahanamoku et al. 2022).

3.2.4 Environmental data

Sediments in the SBB have been used in numerous studies of Common Era paleoclimate (Kennett and Ingram 1995, Bull et al. 2000, Robert 2004, White et al. 2013, Du et al. 2018) and ecological trends (Soutar and Isaacs 1974, Baumgartner 1992, Cannariato et al. 1999, Field et al. 2006, Barron et al. 2010, Jones and Checkley 2019), allowing for robust reconstruction of proxies for ocean temperature (Zhao et al. 2000), oxygenation (Wang et al. 2017b, Wang and Hendy 2021a), and sedimentary carbon and nitrogen (Wang et al. 2019) with annual to decadal resolution over the past two millennia. We compiled data on common oceanographic proxies, including sea surface temperature, ENSO index, total nitrogen and carbon, and oxygenation proxies from paleoclimate studies across the 2-kyr sample interval and compiled these data into a common temporal framework (Table S3.3). We supplemented missing data with the interpolation techniques most commonly used for each data type (Table S3.3).

3.2.5 Statistical analysis

We first undertook a pilot study to test whether the number of megalospheric and microspheric *B. argentea*, the most abundant bolivinid with the most pronounced bimodal distribution of proloculus size, differ through time. We counted *B. argentea* abundance and classified reproductive mode from proloculus size in 34 samples from ~50 to 1861 CE (Table S3.1, Figure S3.4). Confidence intervals on estimated megalospheric and microspheric *B. argentea* abundance in each sample were bootstrapped and adjusted according to the sample split fraction. We used a linear regression to test whether the proportion of *B. argentea* that are megalospheric is correlated with the log of *B. argentea* abundance. Following this pilot study, we then investigated whether proportion megalospheric was correlated with abundance for three other bolivinids, *B. alata*, *B. seminuda*, and *B. spissa* in 35 samples from 1249 to ~2008 CE (Figure S3.4). To see whether reproductive mode changes synchronously across bolivinids, we tested for correlations in proportion megalospheric between all pairwise combinations of the four species. To test for potential correlations between environmental parameters and *Bolivina* life history dynamics, we used environmental data as predictors for both abundance and proportion megalospheric in linear and logistic mixed models, respectively, with species as a random effect. We performed model selection via ANOVA to determine which best explained variation in *Bolivina* abundance and reproduction.

3.3 Results

3.3.1 Bolivina reproductive mode versus accumulation rate and time

All *Bolivina* have positive correlations between accumulation rate and the proportion of megalospheric individuals (here, referred to as “asexual individuals” or “asexual morphs”) throughout the composite core interval (Figure 3.2). The proportion of megalospheric individuals is significant and positively correlated with accumulation rate across the 2,000-year time series in a quasi-binomial (Shoukri and Aleid 2022) regression model (*B. alata*, *B. argentea*, and *B.*

seminuda: $p << 0.001$, pseudo $R^2 = 0.46$, 0.58, and 0.42, respectively; *B. spissa*: $p = 0.01$, pseudo $R^2 = 0.21$). Data for *B. argentea* is more temporally extensive than data for the other *Bolivina* species (Figure S3.8), yet trends remain similar across species. The positive correlations observed suggest that samples with high accumulation rate represent asexual blooms during facultative conditions.

Overall the proportion of asexually-produced individuals is correlated with abundance for all species examined for this study, but across the core interval, samples with low abundance have large variation in the proportion of asexual individuals (Figure 3.3). They range from no to many asexual morphs for a given species, while samples with very high abundance have a high proportion of asexual individuals and few sexual morphs. In other words, when a given species of *Bolivina* is more abundant, a greater proportion of individuals have been produced asexually. Some species exhibit wider ranges in the proportion of asexual individuals in high-abundance samples (e.g., ranging from approximately 0.5 to 1 in *B. alata* and *B. argentea*), while others have nearly exclusively asexual morphs in these samples (ranging from approximately 0.85 to 1 in *B. seminuda*). We find that these large swings in the prevalence of asexual morphs can occur over relatively short intervals, with some samples being separated by as little as 10 years. Uncertainty in the proportion of asexual individuals across populations is at most 0.1, indicating that the drastic shifts we observe in populations' dominant reproductive strategy between most consecutive samples (Figure 3.2) is likely not an artifact of sampling, but represents a real phenomenon common among *Bolivina* species.

3.3.2 Blooming across species pairs and over time

While abundance and reproductive mode are correlated in all biserial foraminifera sampled throughout the timeseries, these trends may be synchronous or asynchronous amongst species throughout time. To test for interspecific correlations in reproductive mode, we examined correlations between each species' asexual abundances (i.e., the estimated total abundance for megalospheric individuals in each sample by species classification). The proportion of asexual individuals within samples is positively correlated for all species pairs (Spearman's ρ: 0.6-0.8 for pairwise correlation tests), suggesting that blooms were generally synchronous across all four species.

While we find that all *Bolivina* species with strong dimorphism undergo blooming throughout the entirety of the Common Era, there appears to be a shift in the relationship between reproductive mode and abundance that impacts *Bolivina* populations following the mid-19th century. To explore the timing of change, we performed a linear interpolation for abundance and the proportion of asexual individuals for each species for every year between 1249 and 2008 CE (the interval over which image data are available; Table S3.1). We then used this interpolated data for a breakpoint analysis (Figure S3.10) In models considering a single breakpoint, *B. alata*, *B. argentea*, and *B. seminuda* had similarly-timed breakpoints in the mid-19th century for both the time series of abundance (1859, 1868, and 1866 CE, respectively; Figure S3.10a) and proportion asexual (1835, 1878, and 1875 CE, respectively; Figure S3.10b) In a model considering two breakpoints, the most recent breakpoints for each species are similarly grouped in the mid- to late-19th century (Table S3.4). One species, *B. spissa* had a significantly earlier final breakpoint, which all models (1-3 breakpoints) placed within the 15th century (single breakpoint: 1666 and 1658 for abundance and proportion asexual, respectively). While this

breakpoint analysis relies on interpolated data, the coordination in the timing of breakpoints between most species suggests that there may be a common cause for the changes to each abundance and reproductive mode we observe.

To further examine the hypothesis that a shift in reproduction and abundance distributions occurred in the mid-19th century, we split our dataset at ~1850 and examined whether significant differences exist between older (pre-1850) and younger (post-1850) samples. We find that distributions of *Bolivina* abundance vs. asexual reproduction are significantly different in samples older than 1850 CE when compared to samples younger than 1850 CE (Figure 3.4). In a Welch two-sample t-test, we find that the samples prior to 1850 are significantly different than samples following 1850 ($p < 1x10^{-10}$), and that the pre-1850 mean proportion of asexual reproduction is higher than the post-1850 mean (90.45% vs. 56.59%, respectively). As a result, after the mid 19th century high proportions of asexual reproduction are not as strongly associated with high abundance (represented as accumulation rate, or sedimentation-rate- and volume-standardized foraminifer abundance). When a similar test is undertaken for *Bolivina* abundance, we also find significant differences between samples pre-1850 and post-1850 (Welch two-sample t-test $p = 0.0001$; pre-1850 mean abundance = 1186.2; post-1850 mean abundance = 14.4).

3.3.3 Influence of environmental variation on Santa Barbara Basin Bolivina *abundance*

The coordinated nature of asexual blooms across species throughout the core interval suggests that these blooms may be driven by a common external force throughout the majority of the core interval. Further, the timing of changes to abundance and the proportion of asexual individuals we observe for the majority of species occur during the mid- to late-19th century, suggesting that a change from normal–either via a shift in the driver of blooms or the introduction of a novel stressor–occurred around this time interval. To examine potential environmental drivers of blooming behavior, we utilized a dataset of common environmental proxies from the SBB that span the majority of the core interval (Table S3.3).

We used both raw and interpolated data (Supplemental Table S3.3) to test relationships between all variables and abundance, fitting linear mixed models that included species as a random effect. Of all variables tested, SST, ENSO variance, Ba_{excess}, and normalized Mo_{EF} were found to be significant ($p < 0.001$ for all variables except Ba_{excess}, for which $p < 0.05$). In a mixed effects model including all significant predictors of abundance, we find that all predictors (SST, ENSO amplitude, Ba_{excess}, and normalized Mo_{EF}) remain significant, and that the model's total explanatory power is substantial, with a conditional R^2 (i.e., including both fixed and random effects) of 0.82 and a marginal R^2 (i.e., including only fixed effects) of 0.32. We also examined relationships between these environmental variables and reproductive mode using a series of single-predictor logistic regression models, but found that none of the environmental variables examined are significant predictors of the proportion of asexual individuals within a sample (Table S3.5).

3.4 Discussion

The Santa Barbara Basin is an ideal system for examining high-resolution ecological trends over the Common Era, a period of time that includes both stable environmental conditions and unprecedented levels of environmental change. Here we use a novel dataset of individual

dimorphic *Bolivina* reproductive mode and abundance spanning ~2kyr and encompassing over 45,000 individual observations to assess life history variation at the population level. To our knowledge, this is the largest dataset of benthic foraminifer morphological features to date, and the first to compile morphological indicators of reproductive mode from image data. Using high-resolution life history information, we uncover individual- and population-scale variation that strongly suggests that correlations between reproductive mode and abundance are a primary feature of the Common Era record of the SBB, and that species' reproductive choices are correlated, such that asexual blooming events and lower-density sexual reproductive events occur within similar timing across *Bolivina*. These relationships between abundance and reproductive mode are a consistent feature of the Common Era record up until the nineteenth century CE, at which point they shift. The resulting low population growth rates we observe following the nineteenth century CE remain a feature of the record through the present day.

3.4.1 Blooming

The coincident blooms we observe within *Bolivina* from the SBB suggest that a widespread phenomenon is driving synchronous reproductive trends across species (at least at the temporal resolution of time averaging of our sampling of 2-4 years; here we cannot comment on potential differences in timing of short-lived blooms or bloom succession on the sub-sample scale). Further, we find that while blooms driven by asexual reproduction occur throughout the Common Era, they decrease in intensity towards present. The similar timing of changes to mean abundance and proportion of asexual individuals observed within samples suggests that either this common driver underwent a shift during the mid- to late-19th century, or that another environmental factor inhibits the blooms—with major impacts on *Bolivina* reproduction and, consequently, each species' abundances. Prior to the mid-19th century, blooms are a relatively consistent feature of the fossil record of *Bolivina* in the SBB, suggesting that blooming behavior is a feature of *Bolivina* life history strategies for the majority of the Common Era. With respect to the changes in mean reproductive mode in the mid-19th century, there are more extreme minimums in the prevalence of asexual reproduction in samples from the last ~170 years, such that the lowest proportions of asexual reproduction seen throughout the composite core interval come from this time period.

These long-term, persistent patterns in asexual blooms among *Bolivina* are consistent with the life history theory that asexual reproduction is a low-cost, high-output mode of reproduction that is often favored over sexual reproduction in species that can easily alter their reproductive strategy (Doncaster et al. 2000, Agrawal 2001, Lehtonen et al. 2012, Yang and Kim 2016, Burke and Bonduriansky 2017). However, understanding whether asexual reproduction is a strategy employed solely when conditions are favorable, and whether the favorability of environmental conditions differs across spatial and temporal scales and between species, is more difficult, particularly with regard to relatively understudied groups like benthic foraminifera. Various conditions may trigger asexual reproduction; for example, asexual blooms may occur both when food is bountiful and when food is limited, in the former to take advantage of abundant resource, and in the latter to escape a difficult situation (Van der Zwaan et al. 1999).

While blooming appears to be approximately coincident in our samples, it is possible that conditions that drive blooming behavior may differ between species, as demonstrated by studies noting that observations of blooms driven by opportunistic feeding were limited to a select

number of species (Gooday 1988). Previous studies of *Bolivina* have reported blooming behavior across the genus' range, with blooms often occurring in low-oxygen environments. *Bolivina* are thought to thrive in hypoxic conditions due to physiological adaptations (e.g., denitrification ability, plastids, and endobionts; Bernhard and Reimers 1991, Bernhard et al. 2000, 2012, Risgaard-Petersen et al. 2006, Piña-Ochoa et al. 2010, Koho et al. 2011, Woehle et al. 2022) that allow them to outcompete oxygen-limited foraminifera and evade predators (Phleger and Soutar 1973, Leutenegger and Hansen 1979). Studies of other species suggest that asexual blooming is shared among multiple lineages of benthic foraminifera, and that these blooms in oxygen-limited species may be driven by pulses of deep sea organic matter (Gooday 1988, Ohga and Kitazato 1997, Saraswat et al. 2011). Low-diversity, high-abundance foraminifer assemblages have been observed to inhabit phytodetritus layers, suggesting that some species of foraminifera are specialist feeders that bloom opportunistically given the presence of appropriate sources of food, while other species are wholly unaffected by food influx and have more cryptic drivers of blooming behavior, or lack thereof (Gooday 1988).

3.4.2 Coordinated blooms suggest an external driver

The coordinated blooms we observe within *Bolivina* from the SBB suggest that a widespread phenomenon is driving synchronous reproductive trends across species. Further, we find that while blooms occur throughout the Common Era, they decrease in intensity towards present. The similar timing of changes to mean abundance and proportion of asexual individuals observed within samples suggests that this common driver underwent a shift during the mid- to late-19th century, with major impacts on *Bolivina* reproduction and, consequently, each species' abundances. Prior to the mid-19th century, blooms are relatively consistent within the fossil record of *Bolivina* in the SBB, suggesting that blooming is a feature of *Bolivina* life history strategies for the majority of the Common Era. We observe a large reduction in the intensity of blooms between the period spanning the early Common Era through the mid-19th century (~500-1850 CE) and the period following 1850 CE, such that as samples approach the modern era, there is lower abundance and higher variation in the proportion of asexual individuals. Further, there are more extreme minimums in the prevalence of asexual reproduction in samples from the last ~170 years, such that the lowest proportions of asexual reproduction seen throughout the composite core interval come from this time period.

While we find a number of significant predictors of abundance, it remains difficult to pinpoint a single driver of blooming behavior given that none are significant predictors for proportional variation in reproductive mode, and the variance in abundance explained by environmental variables alone is moderate ($R^2 = 0.32$). Because low-oxygen waters often occur in areas with high nutrient availability, it remains unclear whether *Bolivina* blooms are the product of increased food availability or the onset of anoxic conditions (Ohga and Kitazato 1997). Within the SBB, food availability and anoxia are often coupled, with nutrient-rich upwelling promoting primary productivity and export production to the bottom of a poorly-ventilated basin (Kennett and Ingram 1995), making it difficult to untangle the two. Using proxies for oxygen availability (Mo_{EF}) and productivity (Ba_{excess}) (Wang et al. 2017b, Wang and Hendy 2021a), we find that both are significant predictors of abundance alongside surface-water temperature and ENSO amplitude, which together hold substantial explanatory power for species-specific abundance trends. Redox proxies (Figure 3.5) show that the coastal oxygen minimum zone (OMZ) on southern CA margin gradually intensifies following 1850, which, when coupled with 20th

century warming, leads to reduced oxygen solubility and greater stratification in the SBB (Wang et al. 2017b). At the same time, ENSO drives high-frequency interannual oscillations in oxygen, potentially rendering SBB environments less stable as ENSO variation increases in the 20th century (Li et al. 2011, Wang et al. 2017b).

We find no clear response to global warming within SBB benthic foraminifera. The decline in abundance associated with a decrease in asexual reproduction we observe in *Bolivina* occurs over a short time period in the mid- to late-19th century, following which abundance remains low and reproductive mode variation remains high. Accelerated climate impacts over the past ~50 years (e.g., heightened ENSO variability, declining oxygenation, increased food supply to the seafloor resulting from warming surface waters, increased stratification, and changes to deepwater nutrient supply; Field et al. 2006, Bograd et al. 2008, Chan et al. 2008, Rykaczewski and Dunne 2010, Abram et al. 2016, Pozo Buil et al. 2021) appear to have no correlation with these shifts, suggesting that the major drivers of change occurred earlier and may have pushed the system into a new state prior to the Great Acceleration (~1950 CE; Steffen et al. 2015).

3.4.3 Settler colonialism as a potential mid-19th century driver of SBB ecosystem change

The striking trend in *Bolivina* abundance we uncover suggests that a state change in abundance occurs around the mid-19th century and is followed by a marked decline in the prevalence of asexual reproduction across all species (Figure 3.3, Figure 3.4). These changes happened at a time when, across California more broadly, major shifts in human-environment interactions occurred as a result of intensified settler colonialism. Alterations to ENSO variability and other oceanographic factors also begin around this time period, which some attribute to an early onset of industrial-era warming (Abram et al. 2016). The breakpoint analysis we conducted suggests that the reproductive and abundance changes we observe occurred around the mid- to late-1800s CE for all species except *B. spissa* (mid-1600s; Supplemental Table S3.4).

The 19th century biotic changes observed in our data correspond to a period during which settler colonialism shifted land management regimes from Indigenous-led, localized systems to Eurocentric systems of management (Norgaard 2019). These coupled ecological-social disruptions resulted in the mass introduction of non-native species (Moyle 1976, Solow and Costello 2004), the conversion of the majority of California coasts to pastureland (Larson-Praplan 2014) and the enactment of fire suppression regimes (Anderson et al. 2013, Collins et al. 2019, Schweizer et al. 2020) which may have altered terrestrial-marine connections across the state. While few studies have directly examined the impacts of colonization on California's marine environments, historical records show that oceans were not spared from direct impact. These include state changes to hydrologic systems, from high-alpine lakes (Streib et al. 2021) to downstream sources of runoff (Napier and Hendy 2018) which impact sedimentation and nutrient delivery regimes in the ocean; shifts in marine ecosystem structure via trophic downgrading and cumulative use impacts on keystone species (Halpern et al. 2009, Maxwell et al. 2013) and invasive species introductions (Teck et al. 2010); as well as many other less visible impacts, the effects of which have likely both accumulated and increased over time (Halpern et al. 2019).

Our data raise the possibility that the accelerating land-use and climate changes have impacted fundamental *Bolivina* life history characteristics, i.e., reproductive and population growth

strategies, in the SBB. The cessation of large asexual blooms (i.e., drops in the frequency and/or magnitude of asexual reproduction events) beginning ~150 years ago may indicate that external factors impacted the preferred mode of reproduction as well as the frequency and magnitude of reproduction events within the basin. Perhaps external factors altered carrying capacity for benthic foraminifera; alternatively, altered environmental conditions may have resulted in increased stress, disturbance frequency, or the severity of extreme events. While the environmental variables we find to be significant predictors of abundance shifts–namely SST, ENSO variance, and redox proxies for oxygenation–undergo changes beginning in the 19th century (Figure 3.5; see also Abram et al. 2016), it is likely that additional factors play a role in driving biotic change in SBB foraminifera.

Regardless of the specific drivers of these changes, the shifted *Bolivina* reproductive and population dynamics we observe may indicate that a novel state was reached in the mid-19th century within the SBB. Pre- and post-1850 assemblages may represent alternative stable states, potentially driven by landscape-scale changes that are a characteristic feature of colonialism. If this complex-system threshold were reached, it could explain why we observe rapid and sustained changes rather than progressive shifts that correspond with continuously escalating nearshore impacts of colonialism, which began in the 17th century following European arrival, escalated during the era of Spanish missions and Mexican ranchos (in Santa Barbara: 1786 and 1842, respectively), and accelerated as a result of American colonization (1850-present). Though future work is needed to test this hypothesis, we suggest two potential mechanisms below that can serve as a starting point for further exploration.

While it may seem surprising that SBB benthic foraminifera–deepwater bottom-dwellers in an anoxic basin–are impacted by the ecosocial regime shifts that resulted from settler colonialism, a number of mechanisms may connect SBB forams to broader colonially-driven changes to terrestrial-marine connections. For example, changing fire regimes driven by the genocide of Indigenous peoples in California and the suppression of cultural burning (Anderson et al. 2013, Taylor et al. 2016) increased the prevalence and intensity of fires (Wahl et al. 2019), altering hydrologic regimes by increasing runoff and atmospheric particle delivery following fire events (Flint et al. 2019, Kelly et al. 2021). Studies in other areas along the California coast suggest that altered fire regimes lead to changes in terrigenous nutrient delivery and marine carbon (Leithold et al. 2005), a major food source for benthic ecosystems. Thus, one potential mechanism for the state changes we observe may be alterations in food availability (see Chapters 4 and 5 of this dissertation for further discussion).

Another potential mechanism is the rapid increases in sedimentation observed along the California coast during this time. Increases in sediment runoff in the 19th and 20th centuries began with changes in human land use due to forced removal of Indigenous peoples, settler introductions of non-native vegetation and large livestock, and wide scale deforestation, and continued as a result of the building of dams (Leithold et al. 2005, Tomasovych and Kidwell 2017, Napier and Hendy 2018, Rodriguez et al. 2020). These increases in sedimentation are directly observed in California marine systems, from salt marshes (Broadman et al. 2022) to the continental shelf (Tomašových and Kidwell 2017). Sediment delivery is shown to have driven extirpation events in other California marine ecosystems through cumulative effects of increased frequency and volume of suspended sediment on benthic organisms (Tomašových and Kidwell

2017). Within our samples, the abundance changes we observe roughly correlate with major shifts in sedimentation within the SBB. Previous work within the basin shows that sedimentary mass accumulation rates (MAR) spike ~150 years before present, representing the highest MAR over the past 9,000 years (Du et al. 2018). Benthic foraminifer accumulation rate (BFAR, which is normalized to sedimentation rate) also drops precipitously in our samples around the same time (Figure S3.5).

Given the host of concurrent changes observed in the mid-19th century, which continue through the 20th century and into the present day, it is possible that even in environments that are far from the direct impacts of colonization this time period represents a state change in California marine ecosystems broadly. To date, numerous studies have shown that settler colonialism (often inaccurately generalized as "human impact;" Davis et al. 2017) has had large and long-lasting effects on coastal and marine ecosystems around the world. Further, studies consistently place the onset of major impacts–which include ecosystem collapse, depopulation, and loss of ecosystem services–in North America at ~150 to 300 years ago, coinciding with the onset of settler colonial regimes across the continent (Worm et al. 2006, Lotze et al. 2006, Yasuhara et al. 2012).

We suggest that the Santa Barbara Basin is no different, and that SBB benthic foraminifera may too represent a system where settler colonial impacts are correlated with biotic change. Our data show that the reproductive choices made by some of the smallest and most cosmopolitan organisms in the ocean have changed significantly towards the present day, with large impacts on their abundances and, as a result, the structure and year-to-year dynamics of these ecological communities. To test the potential mechanisms outlined above, future research can examine whether nutrient delivery regimes are altered around the mid-19th century, either via changes to the primary source of terrigenous nutrients or changes to the residence time of these nutrients within the SBB. In addition, a record of mass accumulation that includes the past ~200 years could be assessed alongside more less direct markers of increased sediment delivery, such as examining the population of terrestrial livestock in the Santa Barbara watershed region (following Tomašových and Kidwell 2017). Future studies that more closely examine the timing and mechanism of SBB benthic foraminifer change could help to determine whether this offshore anoxic basin was affected by the impacts of settler colonialism and industrialization, which intensified in the 19th century in California and have continued to accelerate through the present day.

Chapter 3 Figures

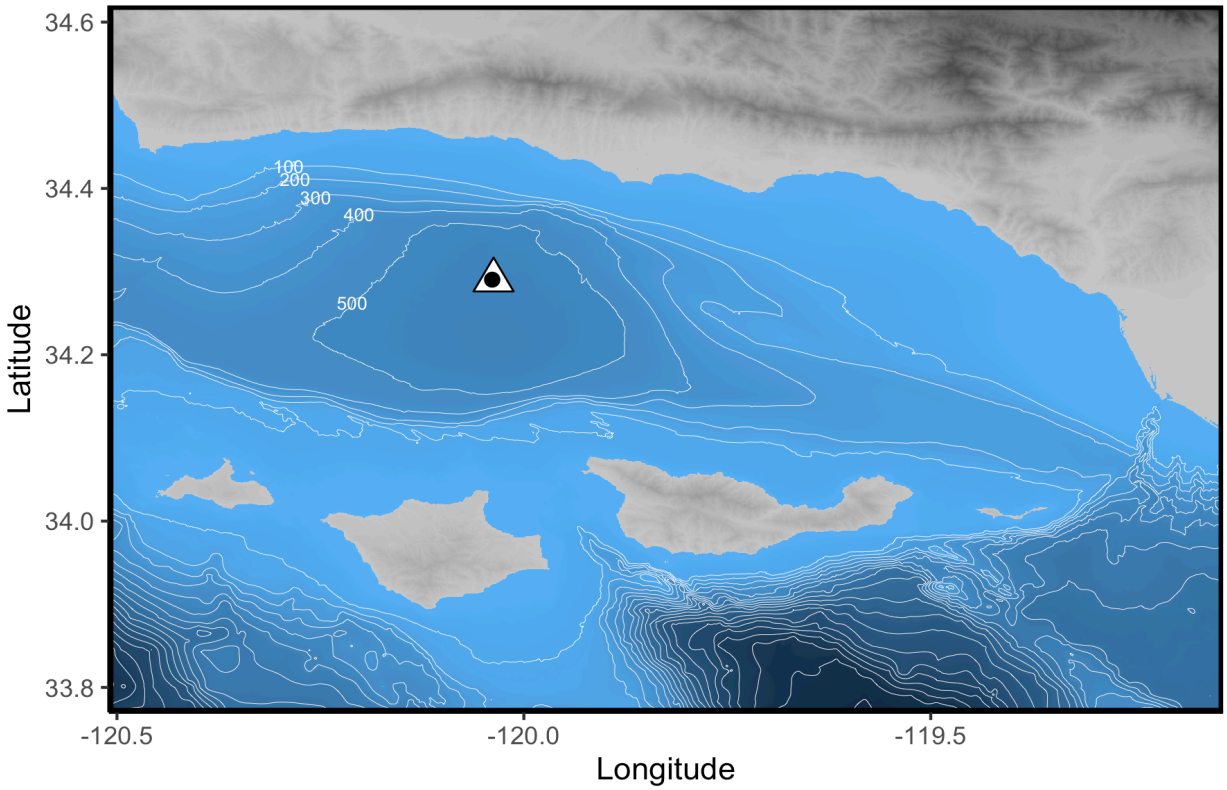

Figure 3.1: Map of the Santa Barbara Basin and surrounding area.
Site MV1012-ST46.9, (34˚17.228'N, 120˚02.135'W), the location at which both kasten cores (KC1 and KC2) and the box core (BC) were sampled, is denoted by a white triangle. The samping location was chosen as a reoccupation of Ocean Drilling Program site 893 (34.2875 N, 120.036 W, 577 m water depth, denoted by black circle). Contour lines indicate seafloor depth (m).

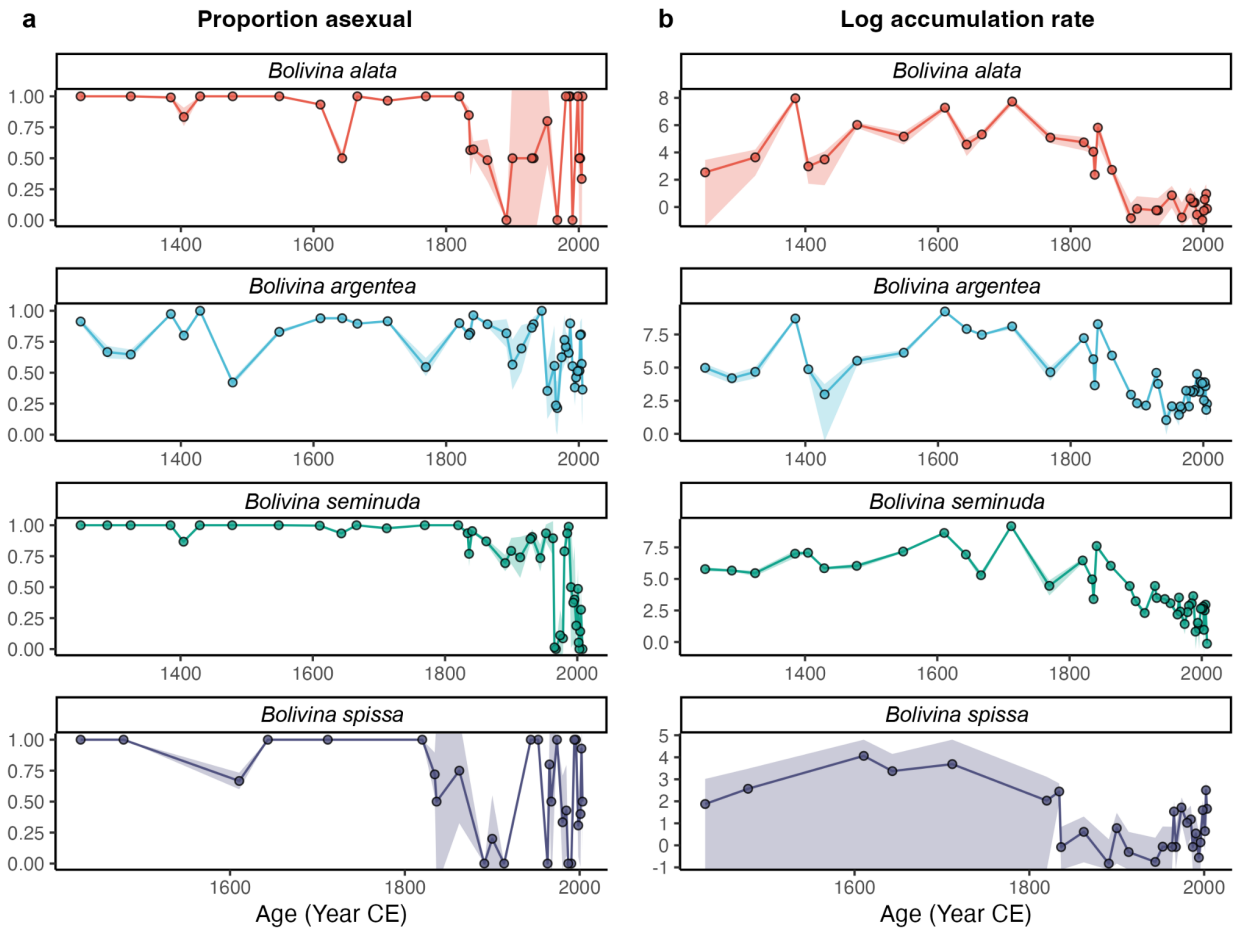

Figure 3.2: Proportion reproduction mode variation and accumulation rate of Bolivina foraminifera, 1249-2008 CE.
(a) Proportion asexual; (b) log-transformed accumulation rate (cm-2 yr-2); colors indicate species, while shaded areas indicate bootstrapped 95% confidence intervals. Breakpoints from a single-breakpoint analysis of interpolated time series data are indicated by colored dashed lines, where colors correspond with species identities.

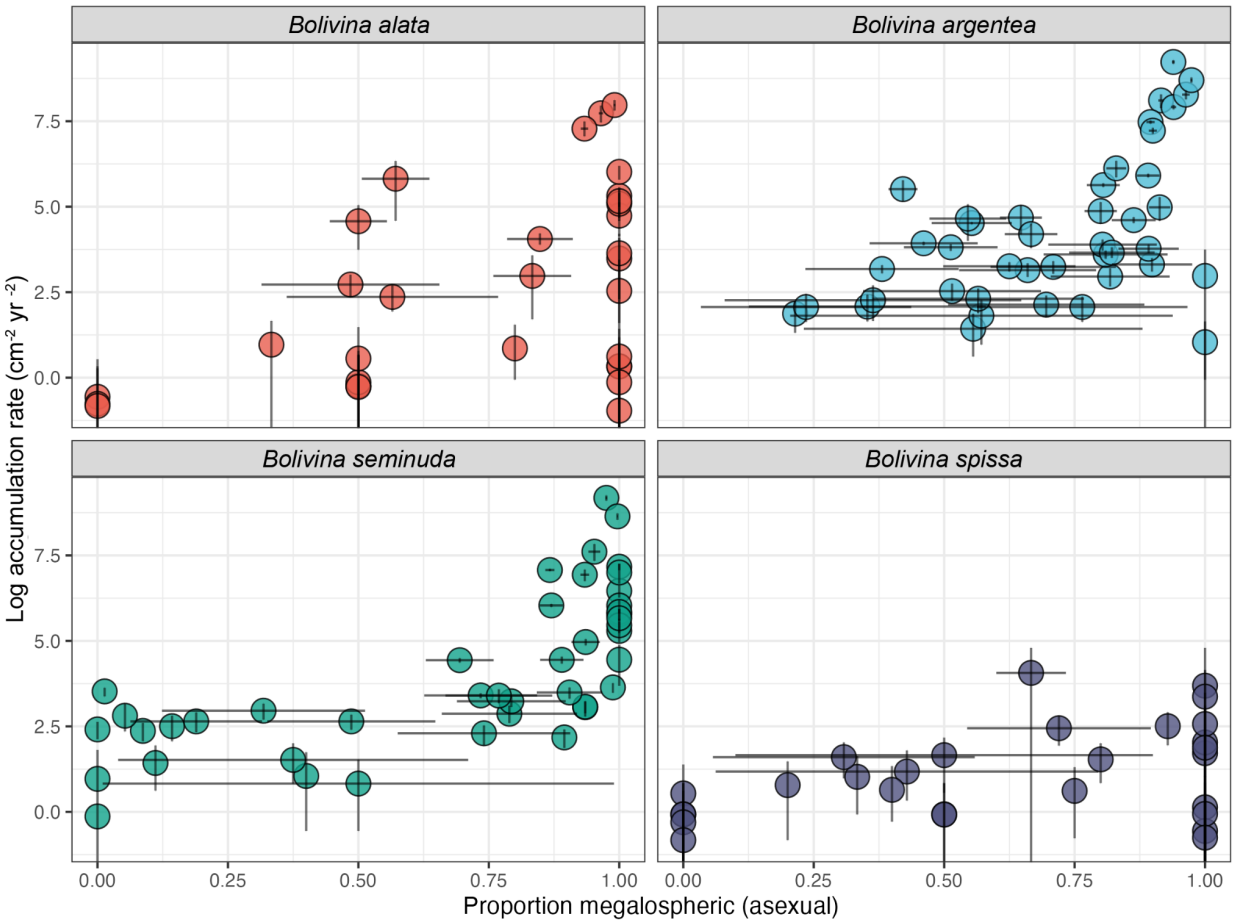

Figure 3.3: The proportion of asexual Bolivina in each sample covaries with abundance. Panels show the proportion of megalospheric individuals for a given log-transformed accumulation rate for Bolivina alata, Bolivina argentea, Bolivina seminuda, and Bolivina spissa. Error bars represent 95% confidence intervals.

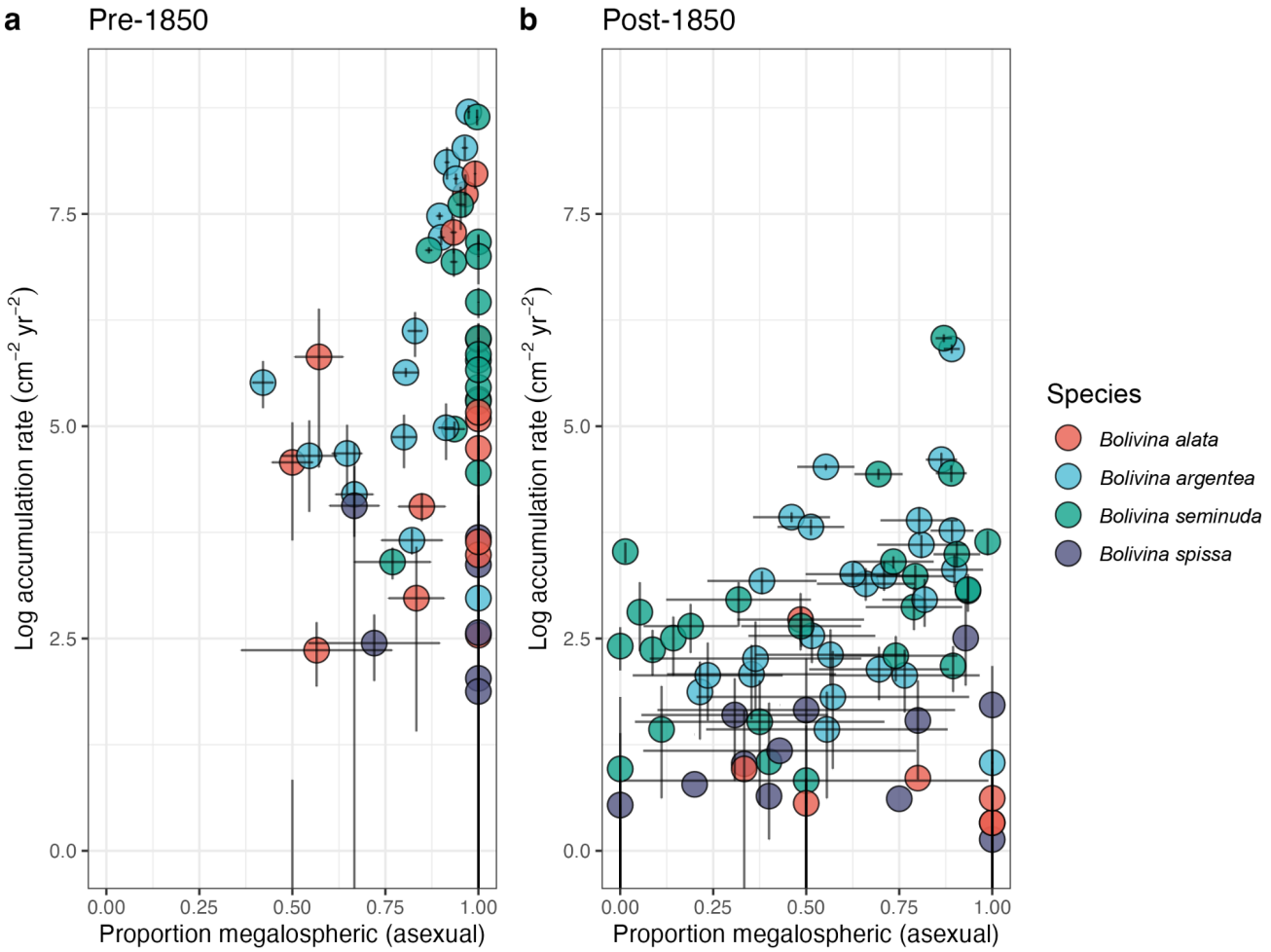

Figure 3.4: The abundance-reproduction relationship for Bolivina pre- and post-1850. The distribution of between *Bolivina* abundance and the proportion of asexual variation in each sample is significantly different in samples (a) older than 1850 CE vs. (b) samples younger than 1850 CE. After the mid 19th century, high proportions of asexual reproduction are not as strongly associated with high accumulation rate. The pre-1850 mean proportion of asexual reproduction is higher than the post-1850 mean ($p << 0.01$; 90.45% vs. 56.59%, respectively). Error bars represent 95% confidence intervals.

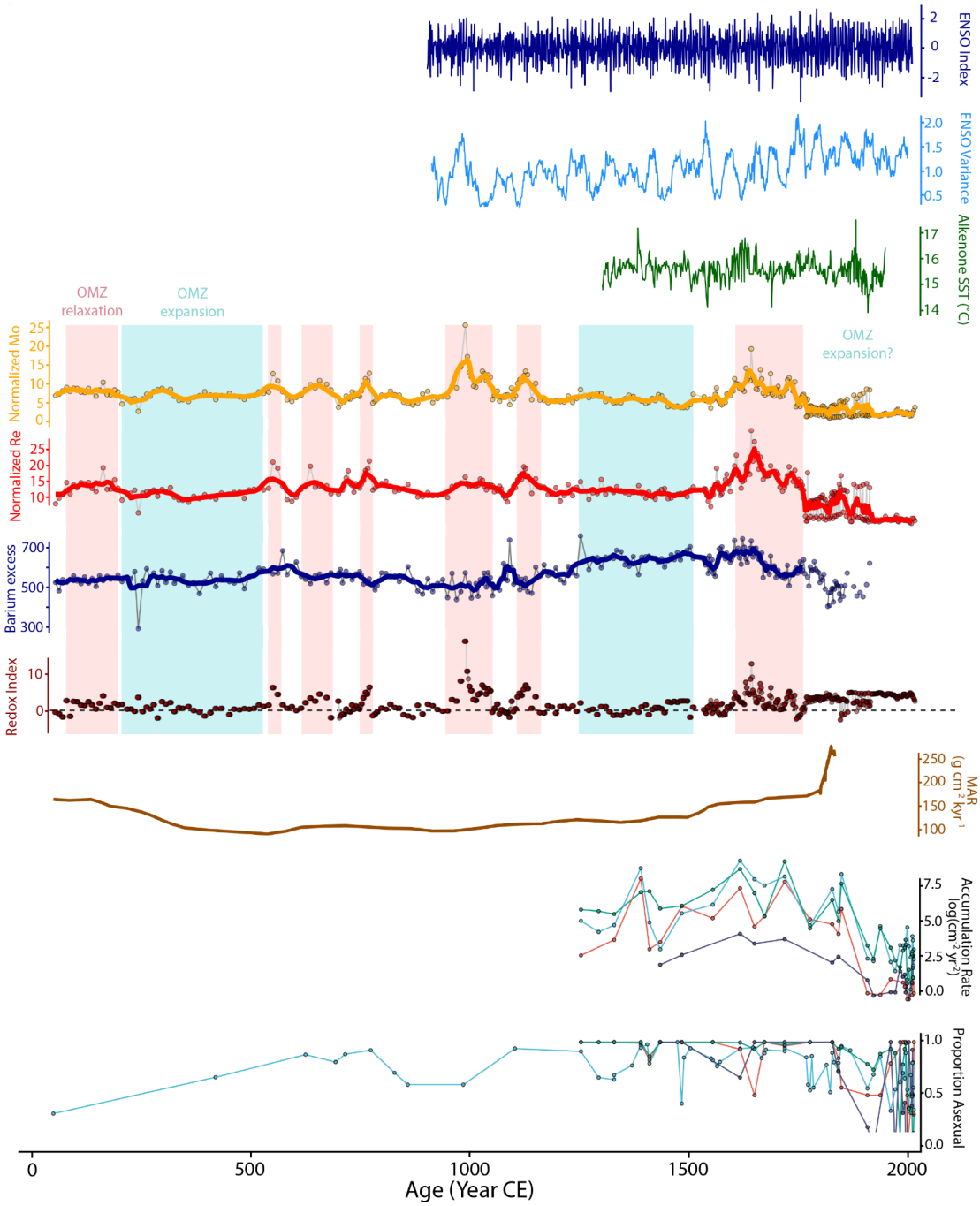

Figure 3.5: Comparison of oceanographic proxies and benthic foraminifer records. (a) ENSO index; (b) 21-year biweight ENSO variance (Li et al. 2011); (c) $U^{K'}_{37}$ (alkenone) Sea Surface Temperature (Zhao et al. 2000); (d-g) redox proxies, including: (d) Normalized Mo_{EF}, (e) Normalized Re_{EF}, (f) Barium excess, and (d) an index of reducing conditions, denoting intervals when High Mo_{EF} occurs alongside high Re_{EF}, such that positive values indicate reducing conditions (Wang et al. 2017b, Wang and Hendy 2021b); (h) Mass Accumulation Rate (g cm^{-2} kyr^{-1}; Du et al. 2018); (i) Log-transformed *Bolivina* accumulation rate (cm^{-2} yr^{-2}); and (j) proportion asexual of *Bolivina*.

3.5 Chapter 3 References

Abram, N. J., H. V. McGregor, J. E. Tierney, M. N. Evans, N. P. McKay, and D. S. Kaufman. 2016. Early onset of industrial-era warming across the oceans and continents. Nature 536:411–418.

Agrawal, A. F. 2001. Sexual selection and the maintenance of sexual reproduction. Nature 411:692–695.

Anderson, R. S., A. Ejarque, P. M. Brown, and D. J. Hallett. 2013. Holocene and historical vegetation change and fire history on the north-central coast of California, USA. The Holocene 23:1797–1810.

Angilletta Jr, M. J., T. D. Steury, and M. W. Sears. 2004. Temperature, growth rate, and body size in ectotherms: fitting pieces of a life-history puzzle. Integrative and comparative biology 44:498–509.

Barron, J. A., D. Bukry, and D. Field. 2010. Santa Barbara Basin diatom and silicoflagellate response to global climate anomalies during the past 2200 years. Quaternary International 215:34–44.

Baumgartner, T. R. 1992. Reconstruction of the history of the Pacific sardine and northern anchovy populations over the past two millenia from sediments of the Santa Barbara basin, California. CalCOFI Rep 33:24–40.

Beckerman, A., T. G. Benton, E. Ranta, V. Kaitala, and P. Lundberg. 2002. Population dynamic consequences of delayed life-history effects. Trends in Ecology & Evolution 17:263–269.

Bernhard, J. M., K. R. Buck, M. A. Farmer, and S. S. Bowser. 2000. The Santa Barbara Basin is a symbiosis oasis. Nature 403:77–80.

Bernhard, J. M., K. L. Casciotti, M. R. McIlvin, D. J. Beaudoin, P. T. Visscher, and V. P. Edgcomb. 2012. Potential importance of physiologically diverse benthic foraminifera in sedimentary nitrate storage and respiration. Journal of Geophysical Research: Biogeosciences 117.

Bernhard, J. M., and C. E. Reimers. 1991. Benthic foraminiferal population fluctuations related to anoxia: Santa Barbara Basin. Biogeochemistry 15:127–149.

Bernhard, J. M., B. K. Sen Gupta, and P. F. Borne. 1997. Benthic foraminiferal proxy to estimate dysoxic bottom-water oxygen concentrations; Santa Barbara Basin, U.S. Pacific continental margin. Journal of Foraminiferal Research 27:301–310.

Blueweiss, L., H. Fox, V. Kudzma, D. Nakashima, R. Peters, and S. Sams. 1978. Relationships between body size and some life history parameters. Oecologia 37:257–272.

Bograd, S. J., C. G. Castro, E. Di Lorenzo, D. M. Palacios, H. Bailey, W. Gilly, and F. P. Chavez. 2008. Oxygen declines and the shoaling of the hypoxic boundary in the California Current. Geophysical Research Letters 35.

Brandon, J. A., W. Jones, and M. D. Ohman. 2019. Multidecadal increase in plastic particles in coastal ocean sediments. Science Advances 5:eaax0587–eaax0587.

Broadman, E., L. Reidy, and D. Wahl. 2022. Late Holocene human-environment interactions on the central California coast, USA, inferred from Morro Bay salt marsh sediments. Anthropocene 38:100339.

Bull, D., A. E. S. Kemp, and G. P. Weedon. 2000. A 160-k.y.-old record of El Niño–Southern Oscillation in marine production and coastal runoff from Santa Barbara Basin, California, USA. Geology 28:1007–1010.

Burke, N. W., and R. Bonduriansky. 2017. Sexual Conflict, Facultative Asexuality, and the True Paradox of Sex. Trends in Ecology & Evolution 32:646–652.

Cannariato, K. G., J. P. Kennett, and R. J. Behl. 1999. Biotic response to late Quaternary rapid climate switches in Santa Barbara Basin: Ecological and evolutionary implications. Geology 27:63–66.
Cardich, J., M. Morales, L. Quipúzcoa, A. Sifeddine, and D. Gutiérrez. 2012. Benthic Foraminiferal Communities and Microhabitat Selection on the Continental Shelf Off Central Peru. Pages 323–340 *in* A. V. Altenbach, J. M. Bernhard, and J. Seckbach, editors. Anoxia: Evidence for Eukaryote Survival and Paleontological Strategies. Springer Netherlands, Dordrecht.
Carson, H. S., P. C. López-Duarte, L. Rasmussen, D. Wang, and L. A. Levin. 2010. Reproductive Timing Alters Population Connectivity in Marine Metapopulations. Current Biology 20:1926–1931.
Caswell, H. 1978. A general formula for the sensitivity of population growth rate to changes in life history parameters. Theoretical Population Biology 14:215–230.
Chan, F., J. A. Barth, J. Lubchenco, A. Kirincich, H. Weeks, W. T. Peterson, and B. A. Menge. 2008. Emergence of Anoxia in the California Current Large Marine Ecosystem. Science 319:920–920.
Christie, M. R., G. G. McNickle, R. A. French, and M. S. Blouin. 2018. Life history variation is maintained by fitness trade-offs and negative frequency-dependent selection. Proceedings of the National Academy of Sciences 115:4441–4446.
Cole, L. C. 1954. The population consequences of life history phenomena. The Quarterly review of biology 29:103–137.
Collins, B. M., J. D. Miller, E. E. Knapp, and D. B. Sapsis. 2019. A quantitative comparison of forest fires in central and northern California under early (1911–1924) and contemporary (2002–2015) fire suppression. International Journal of Wildland Fire 28:138–148.
Cusser, S., J. Helms IV, C. A. Bahlai, and N. M. Haddad. 2021. How long do population level field experiments need to be? Utilising data from the 40-year-old LTER network. Ecology Letters 24:1103–1111.
Dallago, G. M., R. I. Cue, K. M. Wade, R. Lacroix, and E. Vasseur. 2022. Birth conditions affect the longevity of Holstein offspring. Journal of Dairy Science 105:1255–1264.
Darwin, C. 1871. The descent of man. New York: D. Appleton.
Davis, C. V., C. M. Livsey, H. M. Palmer, P. M. Hull, E. Thomas, T. M. Hill, and C. R. Benitez-Nelson. 2020. Extensive morphological variability in asexually produced planktic foraminifera. Science Advances 6:eabb8930.
Davis, H., H. Davis, and Z. Todd. 2017. On the Importance of a Date, or, Decolonizing the Anthropocene. ACME: An International Journal for Critical Geographies 16:761–780.
De Kort, H., J. G. Prunier, S. Ducatez, O. Honnay, M. Baguette, V. M. Stevens, and S. Blanchet. 2021. Life history, climate and biogeography interactively affect worldwide genetic diversity of plant and animal populations. Nature communications 12:1–11.
De Magalhaes, J., and and J. Costa. 2009. A database of vertebrate longevity records and their relation to other life-history traits. Journal of evolutionary biology 22:1770–1774.
Dettmering, C., R. Röttger, J. Hohenegger, and R. Schmaljohann. 1998. The trimorphic life cycle in foraminifera: Observations from cultures allow new evaluation. European Journal of Protistology 34:363–368.
Di Martino, E., and L. H. Liow. 2021. Trait–fitness associations do not predict within-species phenotypic evolution over 2 million years. Proceedings of the Royal Society B: Biological Sciences 288:20202047.

Dmitriew, C. M. 2011. The evolution of growth trajectories: what limits growth rate? Biological Reviews 86:97–116.
Doncaster, C. P., G. E. Pound, and S. J. Cox. 2000. The ecological cost of sex. Nature 404:281–285.
Douglas, R., and F. Staines-Urias. 2007. Dimorphism, shell Mg/Ca ratios and stable isotope content in species of *Bolivina* (benthic foraminifera) in the Gulf of California, Mexico. Journal of Foraminiferal Research 37:189–203.
Du, X., I. Hendy, and A. Schimmelmann. 2018. A 9000-year flood history for Southern California_ A revised stratigraphy of varved sediments in Santa Barbara Basin. Marine Geology 397:29–42.
Elder, L. E., A. Y. Hsiang, K. Nelson, L. C. Strotz, S. S. Kahanamoku, and P. M. Hull. 2018. Sixty-one thousand recent planktonic foraminifera from the Atlantic Ocean. Scientific Data 5:180109.
Erdem, Z., and J. Schönfeld. 2017. Pleistocene to Holocene benthic foraminiferal assemblages from the Peruvian continental margin. Palaeontologia Electronica 20:Art-Nr.
Erdem, Z., J. Schönfeld, A. E. Rathburn, M.-E. Pérez, J. Cardich, and N. Glock. 2020. Bottom-water deoxygenation at the Peruvian margin during the last deglaciation recorded by benthic foraminifera. Biogeosciences 17:3165–3182.
Estes, L., P. R. Elsen, T. Treuer, L. Ahmed, K. Caylor, J. Chang, J. J. Choi, and E. C. Ellis. 2018. The spatial and temporal domains of modern ecology. Nature Ecology & Evolution 73:1–10.
Field, D. B., T. R. Baumgartner, C. D. Charles, V. Ferreira-Bartrina, and M. D. Ohman. 2006. Planktonic Foraminifera of the California Current Reflect 20th-Century Warming. Science 311:63 LP – 66.
Flint, L. E., E. C. Underwood, A. L. Flint, and A. D. Hollander. 2019. Characterizing the Influence of Fire on Hydrology in Southern California. Natural Areas Journal 39:108–121.
García, D., C. Smith, E. Machín, M. Loureiro, and M. Reichard. 2019. Changing patterns of growth in a changing planet: How a shift in phenology affects critical life-history traits in annual fishes. Freshwater Biology 64:1848–1858.
Gooday, A. J. 1988. A response by benthic foraminifera to the deposition of phytodetritus in the deep sea. Nature 332:70–73.
Hallock, P. 1985. Why are larger Foraminifera large? Paleobiology 11:195–208.
Halpern, B. S., M. Frazier, J. Afflerbach, J. S. Lowndes, F. Micheli, C. O'Hara, C. Scarborough, and K. A. Selkoe. 2019. Recent pace of change in human impact on the world's ocean. Scientific Reports 9:11609.
Halpern, B. S., C. V. Kappel, K. A. Selkoe, F. Micheli, C. M. Ebert, C. Kontgis, C. M. Crain, R. G. Martone, C. Shearer, and S. J. Teck. 2009. Mapping cumulative human impacts to California Current marine ecosystems. Conservation Letters 2:138–148.
Hellmair, M., and A. P. Kinziger. 2014. Increased Extinction Potential of Insular Fish Populations with Reduced Life History Variation and Low Genetic Diversity. PLOS ONE 9:e113139.
Hendy, I. L., L. Dunn, A. Schimmelmann, and D. K. Pak. 2013. Resolving varve and radiocarbon chronology differences during the last 2000 years in the Santa Barbara Basin sedimentary record, California. Quaternary International 310:155–168.
Hsiang, A. Y., K. Nelson, L. E. Elder, E. C. Sibert, S. S. Kahanamoku, J. E. Burke, A. Kelly, Y. Liu, and P. M. Hull. 2017a. AutoMorph: Accelerating morphometrics with automated 2D and 3D image processing and shape extraction. Methods in Ecology and Evolution 9:605–

612.
Hsiang, A. Y., K. Nelson, L. E. Elder, E. C. Sibert, S. S. Kahanamoku, J. E. Burke, A. Kelly, Y. Liu, and P. M. Hull. 2017b. AutoMorph: Accelerating morphometrics with automated 2D and 3D image processing and shape extraction. Methods in Ecology and Evolution 9:605–612.
Hutchings, J. A. 1993. Adaptive life histories effected by age-specific survival and growth rate. Ecology 74:673–684.
Hutchings, J. A., R. A. Myers, V. B. García, L. O. Lucifora, and A. Kuparinen. 2012. Life-history correlates of extinction risk and recovery potential. Ecological Applications 22:1061–1067.
Jablonski, D., D. Erwin, and J. Lipps. 1996. Body size and macroevolution. Evolutionary paleobiology. University of Chicago Press, Chicago:256–289.
Ji, Y., S. Feng, L. Wu, Q. Fang, A. Brüniche-Olsen, J. A. DeWoody, Y. Cheng, D. Zhang, Y. Hao, G. Song, Y. Qu, A. Suh, G. Zhang, S. J. Hackett, and F. Lei. 2022. Orthologous microsatellites, transposable elements, and DNA deletions correlate with generation time and body mass in neoavian birds. Science Advances 8:eabo0099.
Jones, W. A. 2016. The Santa Barbara Basin Fish Assemblage in the Last Two Millennia Inferred from Otoliths in Sediment Cores:1–141.
Jones, W. A., and D. M. Checkley. 2019. Mesopelagic fishes dominate otolith record of past two millennia in the Santa Barbara Basin. Nature Communications 10:4564.
Kahanamoku, S., M. Samuels-Fair, S. M. Kamel, D. Stewart, L. Kahn, M. Titcomb, Y. A. Mei, R. C. Bridge, Y. S. Li, C. Sinco, J. T. Epino, G. Gonzalez-Marin, C. Latt, H. Fergus, and S. Finnegan. 2022, November 2. Twenty-two thousand Common Era benthic foraminifera from the Santa Barbara Basin. Zenodo.
KAMINSKI, M. A., C. G. CETEAN, and J. TYSZKA. 2011. Nomenclature to describe the transition from multiserial to uniserial chamber arrangement in benthic foraminifera. Journal of Micropalaeontology 30:7.
Keating-Bitonti, C. R., and J. L. Payne. 2018. Environmental influence on growth history in marine benthic foraminifera. Paleobiology 44:736–757.
Kelly, R. L., X. Bian, S. J. Feakins, K. L. Fornace, T. Gunderson, N. J. Hawco, H. Liang, J. Niggemann, S. E. Paulson, P. Pinedo-Gonzalez, A. J. West, S.-C. Yang, and S. G. John. 2021. Delivery of Metals and Dissolved Black Carbon to the Southern California Coastal Ocean via Aerosols and Floodwaters Following the 2017 Thomas Fire. Journal of Geophysical Research: Biogeosciences 126:e2020JG006117.
Kennett, J. P., and B. L. Ingram. 1995. A 20,000-year record of ocean circulation and climate change from the Santa Barbara basin. Nature 377:510–514.
Koho, K. A., E. Piña-Ochoa, E. Geslin, and N. Risgaard-Petersen. 2011. Vertical migration, nitrate uptake and denitrification: survival mechanisms of foraminifers (Globobulimina turgida) under low oxygen conditions. FEMS Microbiology Ecology 75:273–283.
Kucera, M. 2007. Chapter Six Planktonic Foraminifera as Tracers of Past Oceanic Environments BT - Proxies in Late Cenozoic Paleoceanography. Pages 213–262 Proxies in Late Cenozoic Paleoceanography. Elsevier.
LaBarbera, M. 1989. Analyzing body size as a factor in ecology and evolution. Annual Review of Ecology and Systematics 20:97–117.
Larson-Praplan, S. 2014. History of Rangeland Management in California. Rangelands 36:11–17.

Lehtonen, J., M. D. Jennions, and H. Kokko. 2012. The many costs of sex. Trends in Ecology & Evolution 27:172–178.
Leithold, E. L., D. W. Perkey, N. E. Blair, and T. N. Creamer. 2005. Sedimentation and carbon burial on the northern California continental shelf: the signatures of land-use change. Continental Shelf Research 25:349–371.
Leutenegger, S., and H. Hansen. 1979. Ultrastructural and radiotracer studies of pore function in foraminifera. Marine biology 54:11–16.
Li, J., S.-P. Xie, E. R. Cook, G. Huang, R. D'Arrigo, F. Liu, J. Ma, and X.-T. Zheng. 2011. Interdecadal modulation of El Niño amplitude during the past millennium. Nature Climate Change 1:114–118.
Llodra, E. R. 2002. Fecundity and life-history strategies in marine invertebrates.
Lotze, H. K., H. S. Lenihan, B. J. Bourque, R. H. Bradbury, R. G. Cooke, M. C. Kay, S. M. Kidwell, M. X. Kirby, C. H. Peterson, and J. B. C. Jackson. 2006. Depletion, Degradation, and Recovery Potential of Estuaries and Coastal Seas. Science 312:1806–1809.
Lutze, G. F. 1964. Statistical investigations on the variability of Bolivina argentea Cushman. Contribution from the Cushman Foundation for Foraminiferal Research 15:105–116.
Malerba, M. E., C. R. White, and D. J. Marshall. 2017. Eco-energetic consequences of evolutionary shifts in body size. Ecology Letters 21:54–62.
Marshall, D. J., A. K. Pettersen, and H. Cameron. 2018. A global synthesis of offspring size variation, its eco-evolutionary causes and consequences. Functional Ecology 32:1436–1446.
Maxwell, S. M., E. L. Hazen, S. J. Bograd, B. S. Halpern, G. A. Breed, B. Nickel, N. M. Teutschel, L. B. Crowder, S. Benson, P. H. Dutton, H. Bailey, M. A. Kappes, C. E. Kuhn, M. J. Weise, B. Mate, S. A. Shaffer, J. L. Hassrick, R. W. Henry, L. Irvine, B. I. McDonald, P. W. Robinson, B. A. Block, and D. P. Costa. 2013. Cumulative human impacts on marine predators. Nature Communications 4:2688.
Miloslavich, P., N. J. Bax, S. E. Simmons, E. Klein, W. Appeltans, O. Aburto-Oropeza, M. Andersen Garcia, S. D. Batten, L. Benedetti-Cecchi, D. M. Checkley Jr., S. Chiba, J. E. Duffy, D. C. Dunn, A. Fischer, J. Gunn, R. Kudela, F. Marsac, F. E. Muller-Karger, D. Obura, and Y.-J. Shin. 2018. Essential ocean variables for global sustained observations of biodiversity and ecosystem changes. Global Change Biology 24:2416–2433.
Montero-Serra, I., J. Garrabou, D. F. Doak, L. Figuerola, B. Hereu, J.-B. Ledoux, and C. Linares. 2018. Accounting for Life-History Strategies and Timescales in Marine Restoration. Conservation Letters 11:e12341.
Moran, A. L. 2004. Egg Size Evolution in Tropical American Arcid Bivalves: The Comparative Method and the Fossil Record. Evolution 58:2718–2733.
Moss, D. K., L. C. Ivany, E. J. Judd, P. W. Cummings, C. E. Bearden, W.-J. Kim, E. G. Artruc, and J. R. Driscoll. 2016. Lifespan, growth rate, and body size across latitude in marine Bivalvia, with implications for Phanerozoic evolution. Proceedings of the Royal Society B: Biological Sciences 283:20161364–20161367.
Moyle, P. B. 1976. Fish introductions in California: History and impact on native fishes. Biological Conservation 9:101–118.
Napier, T. J., and I. L. Hendy. 2018. The impact of hydroclimate and dam construction on terrigenous detrital sediment composition in a 250-year Santa Barbara Basin record off southern California. Quaternary International 469:151–168.
Nigam, R., and A. S. Rao. 1987. Proloculus size variation in recent benthic Foraminifera: Implications for paleoclimatic studies. Estuarine, Coastal and Shelf Science 24:649–655.

Norgaard, K. M. 2019. Salmon and acorns feed our people: Colonialism, nature, and social action. Rutgers University Press.
O'Dea, A., and J. Jackson. 2009. Environmental change drove macroevolution in cupuladriid bryozoans. Proceedings of the Royal Society B: Biological Sciences 276:3629–3634.
O'Dea, A., J. B. C. Jackson, H. Fortunato, J. T. Smith, L. D'Croz, K. G. Johnson, and J. A. Todd. 2007. Environmental change preceded Caribbean extinction by 2 million years. Proceedings of the National Academy of Sciences 104:5501–5506.
Ohga, T., and H. Kitazato. 1997. Seasonal changes in bathyal foraminiferal populations in response to the flux of organic matter (Sagami Bay, Japan). Terra Nova 9:33–37.
Olsen, E. M., M. Heino, G. R. Lilly, M. J. Morgan, J. Brattey, B. Ernande, and U. Dieckmann. 2004. Maturation trends indicative of rapid evolution preceded the collapse of northern cod. Nature 428:932–935.
Páez, M., O. Zúñiga, J. Valdés, and L. Ortlieb. 2001. Foraminíferos bentónicos recientes en sedimentos micróxicos de la bahía Mejillones del Sur (23º S), Chile. Revista de biología marina y oceanografía 36:129–139.
Palmer, H. M., T. M. Hill, P. D. Roopnarine, S. E. Myhre, K. R. Reyes, and J. T. Donnenfield. 2020. Southern California margin benthic foraminiferal assemblages record recent centennial-scale changes in oxygen minimum zone. Biogeosciences 17:2923–2937.
Pearson, R. G., J. C. Stanton, K. T. Shoemaker, M. E. Aiello-Lammens, P. J. Ersts, N. Horning, D. A. Fordham, C. J. Raxworthy, H. Y. Ryu, and J. McNees. 2014. Life history and spatial traits predict extinction risk due to climate change. Nature Climate Change 4:217–221.
Phleger, F. B., and A. Soutar. 1973. Production of benthic foraminifera in three east Pacific oxygen minima. Micropaleontology:110–115.
Piña-Ochoa, E., S. Høgslund, E. Geslin, T. Cedhagen, N. P. Revsbech, L. P. Nielsen, M. Schweizer, F. Jorissen, S. Rysgaard, and N. Risgaard-Petersen. 2010. Widespread occurrence of nitrate storage and denitrification among Foraminifera and Gromiida. Proceedings of the National Academy of Sciences 107:1148–1153.
Pincheira-Donoso, D., and J. Hunt. 2017. Fecundity selection theory: concepts and evidence. Biological Reviews 92:341–356.
Pozo Buil, M., M. G. Jacox, J. Fiechter, M. A. Alexander, S. J. Bograd, E. N. Curchitser, C. A. Edwards, R. R. Rykaczewski, and C. A. Stock. 2021. A Dynamically Downscaled Ensemble of Future Projections for the California Current System. Frontiers in Marine Science 8.
Ridgway, I., C. Richardson, and S. Austad. 2011. Maximum shell size, growth rate, and maturation age correlate with longevity in bivalve molluscs. Journals of Gerontology Series A: Biomedical Sciences and Medical Sciences 66:183–190.
Risgaard-Petersen, N., A. M. Langezaal, S. Ingvardsen, M. C. Schmid, M. S. M. Jetten, H. J. M. Op den Camp, J. W. M. Derksen, E. Piña-Ochoa, S. P. Eriksson, L. Peter Nielsen, N. Peter Revsbech, T. Cedhagen, and G. J. van der Zwaan. 2006. Evidence for complete denitrification in a benthic foraminifer. Nature 443:93–96.
Robert, C. 2004. Late Quaternary variability of precipitation in Southern California and climatic implications: clay mineral evidence from the Santa Barbara Basin, ODP Site 893. Quaternary Science Reviews 23:1029–1040.
Rodriguez, A. B., B. A. McKee, C. B. Miller, M. C. Bost, and A. N. Atencio. 2020. Coastal sedimentation across North America doubled in the 20th century despite river dams. Nature Communications 11:3249.
Rykaczewski, R. R., and J. P. Dunne. 2010. Enhanced nutrient supply to the California Current

Ecosystem with global warming and increased stratification in an earth system model. Geophysical Research Letters 37.
Saraswat, R., A. Deopujari, R. Nigam, and P. J. Heniriques. 2011. Relationship between abundance and morphology of benthic foraminifera Epistominella exigua: Paleoclimatic implications. Journal of the Geological Society of India 77:190–196.
Schimmelmann, A., I. L. Hendy, L. Dunn, D. K. Pak, and C. B. Lange. 2013. Revised ~2000-year chronostratigraphy of partially varved marine sediment in Santa Barbara Basin, California. GFF 135:258–264.
Schimmelmann, A., and C. B. Lange. 1996. Tales of 1001 varves: a review of Santa Barbara Basin sediment studies. Geological Society, London, Special Publications 116:121–141.
Schimmelmann, A., C. B. Lange, E. B. Roark, and B. L. Ingram. 2006. Resources for Paleoceanographic and Paleoclimatic Analysis: A 6,700-Year Stratigraphy and Regional Radiocarbon Reservoir-Age (ΔR) Record Based on Varve Counting and 14C-AMS Dating for the Santa Barbara Basin, Offshore California, U.S.A. Journal of Sedimentary Research 76:74–80.
Schmidt, D. N., E. Thomas, E. Authier, D. Saunders, and A. Ridgwell. 2018. Strategies in times of crisis—insights into the benthic foraminiferal record of the Palaeocene–Eocene Thermal Maximum. Philosophical Transactions of the Royal Society A: Mathematical, Physical and Engineering Sciences 376:20170328.
Schweizer, D., T. Nichols, R. Cisneros, K. Navarro, and T. Procter. 2020. Wildland Fire, Extreme Weather and Society: Implications of a History of Fire Suppression in California, USA. Pages 41–57 *in* R. Akhtar, editor. Extreme Weather Events and Human Health: International Case Studies. Springer International Publishing, Cham.
Sen Gupta, B. 2003. Modern Foraminifera.
Shama, L. N. S. 2015. Bet hedging in a warming ocean: predictability of maternal environment shapes offspring size variation in marine sticklebacks. Global Change Biology 21:4387–4400.
Shoukri, M. M., and M. M. Aleid. 2022. Quasi-Binomial Regression Model for the Analysis of Data with Extra-Binomial Variation. Open Journal of Statistics 12:1–14.
Shuter, B. J., H. C. Giacomini, D. de Kerckhove, and K. Vascotto. 2016. Fish life history dynamics: shifts in prey size structure evoke shifts in predator maturation traits. Canadian Journal of Fisheries and Aquatic Sciences 73:693–708.
Siveter, D. J., G. Tanaka, Ú. C. Farrell, M. J. Martin, D. J. Siveter, and D. E. G. Briggs. 2014. Exceptionally Preserved 450-Million-Year-Old Ordovician Ostracods with Brood Care. Current Biology 24:801–806.
Solow, A. R., and C. J. Costello. 2004. Estimating the Rate of Species Introductions from the Discovery Record. Ecology 85:1822–1825.
Soutar, A., and J. D. Isaacs. 1974. Abundance of pelagic fish during the 19th and 20th centuries as recorded in anaerobic sediment off the Californias. Fishery Bulletin 72:257–273.
Staines-Urías, F., and R. G. Douglas. 2009. Environmental and intraspecific dimorphism effects on the stable isotope composition of deep-sea benthic foraminifera from the Southern Gulf of California, Mexico. Marine Micropaleontology 71:80–95.
Stearns, S. C. 1992. The evolution of life histories. Oxford university press Oxford.
Stearns, S. C. 2000. Life history evolution: successes, limitations, and prospects. Naturwissenschaften 87:476–486.
Stearns, S. C., and J. C. Koella. 1986. The evolution of phenotypic plasticity in life-history traits:

predictions of reaction norms for age and size at maturity. Evolution 40:893–913.
Steffen, W., W. Broadgate, L. Deutsch, O. Gaffney, and C. Ludwig. 2015. The trajectory of the Anthropocene: the great acceleration. The Anthropocene Review 2:81–98.
Streib, L. C., J. R. Stone, E. C. Lyon, H. H. Quang, K. M. Yeager, S. R. H. Zimmerman, and M. M. McGlue. 2021. Anthropogenic climate change has altered lake state in the Sierra Nevada (California, USA). Global Change Biology 27:6059–6070.
Takagi, H., A. Kurasawa, and K. Kimoto. 2020. Observation of asexual reproduction with symbiont transmission in planktonic foraminifera. Journal of Plankton Research 42:403–410.
Taylor, A. H., V. Trouet, C. N. Skinner, and S. Stephens. 2016. Socioecological transitions trigger fire regime shifts and modulate fire–climate interactions in the Sierra Nevada, USA, 1600–2015 CE. Proceedings of the National Academy of Sciences 113:13684–13689.
Teck, S. J., B. S. Halpern, C. V. Kappel, F. Micheli, K. A. Selkoe, C. M. Crain, R. Martone, C. Shearer, J. Arvai, B. Fischhoff, G. Murray, R. Neslo, and R. Cooke. 2010. Using expert judgment to estimate marine ecosystem vulnerability in the California Current. Ecological Applications 20:1402–1416.
Tomasovych, A., and S. M. Kidwell. 2017. Nineteenth-century collapse of a benthic marine ecosystem on the open continental shelf. Proceedings of the Royal Society B: Biological Sciences 284:20170328–20170329.
Tomašových, A., and S. M. Kidwell. 2017. Nineteenth-century collapse of a benthic marine ecosystem on the open continental shelf. Proceedings of the Royal Society B: Biological Sciences 284:20170328.
Uchimura, H., H. Nishi, R. Takashima, A. Kuroyanagi, Y. Yamamoto, and S. Kutterolf. 2017. Distribution of Recent Benthic Foraminifera off Western Costa Rica in the Eastern Equatorial Pacific Ocean. Paleontological Research 21:380–396.
Van der Zwaan, G., ab I. Duijnstee, M. Den Dulk, S. Ernst, N. Jannink, and T. Kouwenhoven. 1999. Benthic foraminifers: proxies or problems?: a review of paleocological concepts. Earth-Science Reviews 46:213–236.
Vandepitte, L., B. Vanhoorne, W. Decock, S. Dekeyzer, A. Trias Verbeeck, L. Bovit, F. Hernandez, and J. Mees. 2015. How Aphia—The Platform behind Several Online and Taxonomically Oriented Databases—Can Serve Both the Taxonomic Community and the Field of Biodiversity Informatics. Journal of Marine Science and Engineering 3:1448–1473.
Wahl, E. R., E. Zorita, V. Trouet, and A. H. Taylor. 2019. Jet stream dynamics, hydroclimate, and fire in California from 1600 CE to present. Proceedings of the National Academy of Sciences 116:5393–5398.
Wang, Y., and I. L. Hendy. 2021a. Reorganized Atmospheric Circulation During the Little Ice Age Leads to Rapid Southern California Deoxygenation. Geophysical Research Letters 48:e2021GL094469.
Wang, Y., and I. L. Hendy. 2021b. Reorganized Atmospheric Circulation During the Little Ice Age Leads to Rapid Southern California Deoxygenation. Geophysical Research Letters 48:e2021GL094469.
Wang, Y., I. L. Hendy, and R. Thunell. 2019. Local and Remote Forcing of Denitrification in the Northeast Pacific for the Last 2,000 Years. Paleoceanography and Paleoclimatology 34:1517–1533.
Wang, Y., I. Hendy, and T. J. Napier. 2017a. Climate and Anthropogenic Controls of Coastal Deoxygenation on Interannual to Centennial Timescales. Geophysical Research Letters 44:11,528-11,536.

Wang, Y., I. Hendy, and T. J. Napier. 2017b. Climate and Anthropogenic Controls of Coastal Deoxygenation on Interannual to Centennial Timescales. Geophysical Research Letters 44:11,511-528,536.
White, S. M., T. M. Hill, J. P. Kennett, R. J. Behl, and C. Nicholson. 2013. Millennial-scale variability to 735 ka: High-resolution climate records from Santa Barbara Basin, CA. Paleoceanography 28:213–226.
Wilkinson, G. S., and J. M. South. 2002. Life history, ecology and longevity in bats. Aging cell 1:124–131.
Woehle, C., A.-S. Roy, N. Glock, J. Michels, T. Wein, J. Weissenbach, D. Romero, C. Hiebenthal, S. N. Gorb, J. Schönfeld, and T. Dagan. 2022. Denitrification in foraminifera has an ancient origin and is complemented by associated bacteria. Proceedings of the National Academy of Sciences 119:e2200198119.
Worm, B., E. B. Barbier, N. Beaumont, J. E. Duffy, C. Folke, B. S. Halpern, J. B. Jackson, H. K. Lotze, F. Micheli, and S. R. Palumbi. 2006. Impacts of biodiversity loss on ocean ecosystem services. science 314:787–790.
Yamaguchi, T., R. Honda, H. Matsui, and H. Nishi. 2017. Sexual shape dimorphism and selection pressure on males in fossil ostracodes. Paleobiology 43:407–424.
Yampolsky, L. Y., and S. M. Scheiner. 1996. Why Larger Offspring at Lower Temperatures? A Demographic Approach. The American Naturalist 147:86–100.
Yang, Y. Y., and J. G. Kim. 2016. The optimal balance between sexual and asexual reproduction in variable environments: a systematic review. Journal of Ecology and Environment 40:12.
Yasuhara, M., G. Hunt, D. Breitburg, A. Tsujimoto, and K. Katsuki. 2012. Human-induced marine ecological degradation: micropaleontological perspectives. Ecology and Evolution 2:3242–3268.
Yasuhara, M., D. P. Tittensor, H. Hillebrand, and B. Worm. 2015. Combining marine macroecology and palaeoecology in understanding biodiversity: microfossils as a model. Biological Reviews 92:199–215.
Zhao, M., G. Eglinton, G. Read, and A. Schimmelmann. 2000. An alkenone (U37K′) quasi-annual sea surface temperature record (AD 1440 to 1940) using varved sediments from the Santa Barbara Basin. Organic Geochemistry 31:903–917.

3.6 Appendix
Supplemental Information for Chapter 3: A 2-kyr record of life history strategies in benthic foraminifera from the Santa Barbara Basin shows a nineteenth-century change

Sara S. Kahanamoku[1*], Maya Samuels-Fair[1*], Jared C. Richards[2], Ivo A.P. Duijnstee[1], Richard Norris[3], Seth Finnegan[1]

1) Department of Integrative Biology and Museum of Paleontology, University of California, Berkeley, CA; 2) Department of Organismal Biology, Harvard University, Cambridge, MA; 3) Scripps Institution of Oceanography, University of California, San Diego, CA

Supplemental Methods

Core Sampling and Chronology

Kasten core MV1012-KC1 and box core MV1012-BC were collected in October 2010 by members of the Scripps Institution of Oceanography Cal-ECHOES research cruise at station MV1012-ST46.9 (34˚17.228'N, 120˚02.135'W) at ~580m water depth (Brandon et al. 2019, Jones and Checkley 2019). This station was chosen as a re-occupation of Ocean Drilling Program Site 893, and was designated as Station 46.9 following the station naming convention of the California Cooperative Oceanic Fisheries Investigations (CalCOFI). The cores were photographed in color on deck prior to subcoring. Kasten cores were subcored into four end-to-end subcores on deck with rectangular acrylic core lines (76 cm x 15 cm) (Jones and Checkley 2019). The box core was subcored with a single rectangular plastic core liner of the same size (Brandon et al. 2019). All subcores were stored under anoxic conditions at 4˚C prior to sample processing. Composite X-radiographs were used with color photographs to develop a high-resolution chronology for each core (Supplementary Figure S3.1).

Several age models have been used to develop chronologies by assigning dates to Santa Barbara Basin (SBB) varved stratigraphy. These models relied on counting seasonal varve couplets (Schimmelmann and Lange 1996, Schimmelmann et al. 2006), which has since been calibrated with ^{14}C dates from planktonic foraminiferal carbonate and terrestrial-derived organic carbon from a kasten core, SPR0901-06KC, sampled at the same location as the cores used for the present analysis (Hendy et al. 2013, Schimmelmann et al. 2013). This ^{14}C calibration was used to show that the traditional varve couplet counting method is accurate from the modern back to ~1700 AD, following which its accuracy decreases due to varve undercounting (Hendy et al. 2013, Schimmelmann et al. 2013). A new chronostratigraphy for the SBB was established by Hendy et al. (Hendy et al. 2013) and Schimmelman et al. (Schimmelmann et al. 2013) following these ^{14}C dates that extended from BCE 107 to CE 1700, which was then adapted for the kasten core used in the present analysis during a prior study (Jones 2016, Jones and Checkley 2019). To adapt this chronology, Jones et al. (Jones 2016) identified major instantaneous sedimentation events characterized in kasten core SPR0901-06KC (which are recognizable as they form anomalously thick, homogenous gray or olive layers due to deposition on very short timescales as a result of flood or turbidite events; Hendy et al. 2013) within the kasten core MV1012-KC1 and assigned these events a single calendar date as age tie-points. The overall varve structure was cross-dated between each kasten core to aid in this chronology development, and the down-core chronology was corrected by removing the thicknesses of instantaneous events, and a series of linear regression equations between sequential instantaneous events were used to assign dates to the remaining stratigraphic structure (Hendy et al. 2013, Jones 2016). This methodology created

a final chronostratigraphy for MC1012-KC1 with 0.5 cm resolution that excluded near-instantaneous event layers and incorporated cross-dating to extend the chronology back to 8-53 C.E.; dates assigned to each sample were the average of the dates of the upper and lower surfaces of the sample transverse section.

Box core MV1012-BC was covered by a bacterial mat of ~1-2 cm thickness (Supplemental Figure S3.1), indicating that the surficial sediments were intact (Brandon et al. 2019). Box core MV1012-BC1 was sufficiently shallow to use traditional varve chronology (Hendy et al. 2013, Schimmelmann et al. 2013, 2006) (as outlined in Schimmelmann et al. 2006 and corroborated by Hendy et al. 2013) for couplet dating; a regression model was used to assign dates to the sediment stratigraphy prior to 1871, thus extending to chronology to 1834 AD (Brandon et al. 2019).

Kasten Core and Box Core Calibration

The varved couplets of MV1012-BC were counted from 2009 to 1871 CE, and correlated well with both traditional and ^{14}C-calibrated chronologies used to corroborate the varve-counting method in the SBB (Schimmelmann et al. 2006, 2013, Hendy et al. 2013). The top of MV1012-KC1 and the bottom of MV1012-BC overlap by ~10 cm, representing a shared interval from 1832-1885 CE. Previous work cross-dated core stratigraphies of MV1012-KC1 and MV1012-BC with one another and with the sediment core SPR0901-06KC, the most recently and accurately dated SBB core at the time of sample processing, to ensure the best possible match between varves and stratigraphies of separate cores (Hendy et al. 2013, Schimmelmann et al. 2013, Jones 2016, Jones and Checkley 2019). Within both previous studies (Jones and Checkley 2019) and the present analysis, the overlap between MV1012-KC1 and MV1012-BC show similar trends in all variables assessed.

However, when samples for this analysis are compared by core type, there is a greater range of variation within the box core for estimated abundances than within the kasten core (Figure S3.7), and each species has a mean abundance that is several orders of magnitude lower in the in the Box Core (1834-2008 CE) than the Kasten Core (~500-1871 CE, two-sample t-test $p < 0.05$). There is also increased variation in the proportion of asexual individuals between samples for each species and a shifted absolute and lower third-quartile minimum for each species across the two core intervals (Figure S3.7), suggesting that much less asexual reproduction takes place in the interval encompassed by the Box Core than in the Kasten Core interval. However, while there is a shifted mean in both abundance (H_0 = kasten > box; $p << 0.01$) and the proportion of asexual individuals within a sample (H_0 kasten > box; $p << 0.01$), abundance variation around these shifted mean remains correlated across species. These changes to mean abundance and the higher variation in the proportion of asexual individuals witin each species in Box Core samples suggests that a novel regime may be at play in the last ~150 years that differs from the majority of the Common Era interval. The large increase in variation in the prevalence of asexual morphs within Box Core samples may be driven in part by the smaller abundances of these samples (with higher uncertainty resulting from smaller sample sizes).

To assess whether differences between the box core are due to core differences or represent actual changes to biotic trends, we imaged an overlap sample from each core. These samples were used to assess within-sample diversity, species-level abundance trends, and reproductive

mode proportions to determine whether samples were comparable. Supplementary Figure S3.7 shows that MV1012-BC-70 (1862.3 CE) and MV1012-KC1-1-15 (1861 CE) have similar proportions of megalospheric B. argentea in each sample (0.89 vs 0.92, respectively) and identical calculated estimated abundance fluxes for B. argentea (2517 vs. 2517, respectively).

AutoMorph Workflow

AutoMorph (Hsiang et al. 2017b), the morphometrics software used to process bulk images to create individual images (Figure S3.2), is available on github at https://github.com/HullLab/AutoMorph. For additional information, see Chapter 2 of this dissertation.

Taxonomic references and images

For this study we examine biserial benthic foraminifera in the genus Bolivina. Biserial foraminifera have an evolute trochospiral chamber arrangement with approximately 180° between consecutive chambers (Kaminski et al. 2011). In other words, biserial foraminifera have an alternating chamber arrangement that creates two series of chambers. *B. alata, B. argentea, B. seminuda,* and *B. spissa* are true biserial forms, as the chambers comprising each row are separated by a common suture; in these species, the two series of rows create a 'zigzag' suture that separates each chamber series from the other (Kaminski et al. 2011).

B. seminuda var. humilis, currently accepted as *Bolivina humilis*, is considered to be a variety of the parent species *B. seminuda* (Table S3.2). During classification, these were treated as distinct morphotypes. However, classification was complicated due to the difficulty in distinguishing *B. seminuda* from *B. seminuda var. humilis* in their microspheric forms (Figure S3.3). To avoid conflicting identifications, we combined data for *B. seminuda* with *B. seminuda var. humilis*, thus treating these varieties as a single species for this analysis. In examining taxonomic references to determine how to treat these morphotypes, we found them to be inconsistent; while some treat *B. seminuda* as distinct from *B. seminuda var. humilis*, others treat them as a blended morphospecies, typically identifying all morphotypes under the single species name *B. seminuda*. Bernhard et al. (Bernhard et al. 1997) identify only *B. seminuda* (no *var. humilis*) within the Santa Barbara Basin, with a plate showing an SEM image of a single specimen. A number of studies of Southeastern Pacific fauna identified only *B. seminuda* but had no images of the species (Páez et al. 2001, Uchimura et al. 2017, Erdem et al. 2020). Others identified only *B. seminuda var. humilis* (or *B. humilis*) but provided no reference images (Cardich et al. 2012). Yet others distinguish between the two, but do not show morphological variation resulting from reproductive mode differences (e.g., megalospheric vs. microspheric) (Erdem and Schönfeld 2017).

For this analysis, we have chosen to treat these morphotypes as a single species, *B. seminuda*. The results of our analyses are not altered when we treat *B. seminuda* and its variety *B. seminuda var. humilis* as distinct species, nor does it change the results observed for either species individually.

Validation of reproductive mode classification

It is thought that foraminifera generally undergo lifecycles that involve alternation of generations between a haploid, sexually-reproducing stage and a diploid, asexually reproducing stage. While

many are thought to have a simple dimorphic lifecycle (in which gamonts alternate with agamonts), some are thought to undergo a trimorphic life cycle, with the haploid gamont stage undergoing sexual reproduction via the production of gametes for recombination, and the diploid agamont and schizont stages undergoing asexual reproduction via multiple fission. Regardless of the pathway by which alternation of generations is undertaken, foraminfera alternate between two major forms: a haploid, sexual stage and a diploid, non-sexual (asexual) stage or stages. While all foraminifera are thought to undergo this alternation, not all have easily visible dimorphism within their shells that corresponds to sexual or asexual reproductive modes. For this reason, we focus the analyses of the present study only on those which have visible and distinct dimorphism in proloculus (first chamber) size. The size of the proloculus is thought to correspond to the reproductive mode by with that individual was produced, with microspheric (small proloculi) individuals having been produced via sexual reproduction, and megalospheric (large proloculi) individuals having been produced via asexual reproduction. To validate the observed dimorphism between species, we measured chamber sizes of megalospheric and microspheric individuals to ensure that our visual classification of reproductive morphs was accurate (Figure S3.6).

Visual identification of foraminifera from images

We follow high-throughput morphometrics techniques developed and implemented by Hsiang et al. (2017) and Elder et al. (2018) to image samples of picked benthic foraminifera and identify individuals from these images. Because we use biserial benthic foraminifera for the present analysis, the orientation of a given individual when it is imaged does not affect the reliability or ease with which individuals can be identified, in large part because there are few differences in the morphology of umbilical vs. aperture-side chambers within biserial foraminifera. In other words, all morphological features of interest (i.e., proloculus, sutures between chambers, keel (if applicable), and the general overall growth pattern) are visible regardless of an individual's orientation due to the alternating chamber arrangement that produces two side-by-side rows of chambers within biserial benthic foraminifera during growth.

Statistical analysis

Where data are log-transformed within the text, natural log transformations (base *e*) are used.

Supplemental Text

(a) Regional setting

The Santa Barbara Basin of Southern California (SBB) is situated within the California Current System, an area of high levels of primary productivity and seasonal upwelling. Prevalent anaerobia in SBB bottom waters is due to the restriction of water movements by the bordering Santa Barbara Coastline to the north, the Channel Islands to the south, and the high sill depths of the eastern (230 m) and western (475 m) areas of the basin. These low-oxygen bottom waters minimize bioturbation, allowing for preservation of millimeter scale seasonal to annual laminae (varves; Figure 3.1; Figure S3.1).

(b) Assessing environmental predictors with linear and logistic mixed models

We compiled oceanographic and climatic data from a published literature (Main Text Table 3) to assess the impact of environmental change on *Bolivina* abundance and reproduction. For a

model including SST as a predictor, the total explanatory power of the model is substantial (conditional $R^2 = 0.55$) and the portion of the model related to SST alone (marginal R^2) is 0.19. Within this model, the effect of SST on foraminifer abundance is statistically significant and positive ($p < 0.001$). A model containing ENSO as a predictor returned ENSO variance (Li et al. 2011) as a significant and negative predictor of abundance ($p < 0.001$; conditional $R^2 = 0.46$; marginal $R^2 = 0.15$). A model containing Ba_{excess} and normalized Mo_{EF} as predictors returned both as significant ($p < 0.05$ and $p < 0.001$, respectively; conditional $R^2 = 0.62$, marginal $R^2 = 0.13$).

SST

SST data from Zhao et al. (2000) provides alkenone (Uk'37) measurements from a period covering the LIA through the mid-20th century (1297-1941 CE; Figure SX). These data are sub-pentadal, with measurements occurring irregularly every 1-5 years. In order to obtain data for each of the years represented in our dataset of *Bolivina* abundance and reproductive mode, we linearly interpolated these data to create annual measurements.

ENSO

ENSO data from Li et al. 2011 provides an 1100-year index of ENSO variability (910 - 2000 CE), covering nearly the entire span of the box and kasten cores at a yearly resolution. The data include ENSO variability for the past 1,100 years (variable name: Series), derived from the first principal component of tree-ring based North America Drought Atlas (NADA). This index comprises interannual ENSO variability only, as a 9-year Lanczos highpass filter was applied on time series at each NADA grid point. A 21-year running biweight variance was calculated to measure changes in ENSO amplitude. The authors use this technique in order to examine the interdecadal amplitude modulation of a time series while reducing bias that might be introduced by extreme outliers (Li et al. 2011 p. 20). To extend the time series, we merged the Li ENSO index with data from NOAA's Niño 3.4 SST Index (https://psl.noaa.gov/gcos_wgsp/Timeseries/Nino34/). To make these datasets comparable, we calculated a 21-year running biweight variance for these data, which allowed for extension of both the ENSO Index and the ENSO Variance time series.

Within the SBB, ENSO events correlate with weakened upwelling, which in turn results in decreased food supply to the seafloor, lower anaerobic activity, and higher oxygen within the basin. While there are generally higher abundances during more positive ENSO years, the relationship between ENSO Index and abundance is not significant. However, the relationship between ENSO Variance and abundance is highly significant as a predictor for both abundance ($p < 0.001$) and the prevalence of asexual reproduction ($p = 0.035$) in linear and logistic mixed-effects models, respectively, that hold species as a random effect.

Total Organic Carbon, Total Nitrogen, and δ15N

Total Nitrogen, Total Organic Carbon, and δ15N data are available through 1910 from Wang et al. (2019) (Wang et al. 2019). Data for TOC were extended to ~2008 by Wang et al. (2017) (Wang et al. 2017a), and these data were included in this analysis. When TN, TOC, and δ15N were included as predictors in mixed effects models, none emerged as significant predictors of either abundance or reproductive mode.

Redox Metals and OMZ indicators

Wang and Hendy (2021) use redox-sensitive metals to assess Oxygen Minimum Zone (OMZ) expansion and contraction over the Common Era (Wang and Hendy 2021b). They calculate metal enrichment factors by normalizing redox-sensitive trace metal concentrations to Aluminum ($Metal_{EF} = (Metal/Al)_{sample} / (Metal/Al)_{background}$). They also calculate Barium excess by correcting Barium for the detrital input ($Ba_{excess} = Ba_{sample} - (Ba/Al)_{background} \times Al_{sample}$) using background from Wang et al. (2017). These authors use authigenic enrichment factors of MoEF, ReEF, and BaEF with respect to the lithogenic background to reconstruct past oxygenation, and in their paper interpret co-occurrences of metal enrichment factors as indicators of past oxygenation states. These include indicators of:

- *Oxygen:* Molybdenum (Mo_{EF}) is used by Wang et al. 2021 as a major indicator for OMZ expansion or contraction, where OMZ intensification and relaxation rates are calculated based on the least-square linear regression of Mo_{EF}. Notably, "higher oxygen" intervals are defined by below average Mo_{EF} values, and "low oxygen" intervals are defined by above average Mo_{EF} values. As a result, Mo_{EF} values normalized to the average (i.e., $Mo_{norm} = Mo_{EF} - Mo_{EF\ avg}$) can be used as an indicator for high vs. low oxygen. Barium excess can also be used as an oxygen indicator when Mo_{EF} and Re_{EF} are low. This relationship is used to calculate an oxygen index using the equation $Ba_{excess} \times \text{sign}(Mo_{EF}) \times \text{sign}(Re_{EF})$. As a result, positive oxygen index values indicate periods of higher oxygen;
- *Productivity:* Ba_{EF} is often used as a productivity indicator for sediments dominated by biogenic input and with minimal terrestrial influences (Eagle et al., 2003); and
- *Reducing conditions:* High Mo_{EF} is an indicator of reducing measurements when Re_{EF} is also high. This relationship can be used to calculate a reducing index, by multiplying normalized Mo_{EF} by the sign of normalized Re_{EF}, using the equation $Mo_{norm} \times \text{sign}(Re_{EF})$. As a result, positive redox index values will indicate reducing conditions.

When we compare these indicators with *Bolivina* abundance, we find that normalized Mo_{EF} is strongly positively correlated with abundance, while Ba_{excess} and the oxygen index we calculate from Ba_{excess} and Mo_{EF}, Re_{EF} exhibit weaker positive relationships with abundance. Stronger reducing conditions, indicated by the redox index we calculate from Normalized Mo_{EF} and Re_{EF}, appear negatively correlated with *Bolivina* abundance. When we examine these regressions in a linear mixed effects model including all redox-sensitive and oxygen-sensitive variables as predictors of abundance, we find that Ba_{excess} (an indicator of productivity) is significant at $p = 0.009$; Mo_{EF} is significant at $p = 0.002$, while the redox index (an indicator of reducing conditions) is not significant. The conditional R^2 of this model (including species as a random effect) is 0.62, while the R^2 related to the fixed effects alone is 0.15. None of the redox indicators are significant predictors of reproductive mode in a logistic mixed effects model with species as a random effect.

Cross-correlations between environmental variables

Our data do not show cross-correlations between proxy variables. However, they are thought to be strongly connected: low temperatures indicate higher levels of upwelling, which drives increased productivity and decreased bottom-water oxygenation. Independently, both SST and ENSO data show a similar relationship with *Bolivina* abundance: higher temperatures and higher

ENSO intensity correlate with higher abundances of *Bolivina* (Figures SX and SX). It is likely that both SST and ENSO intensity are positively correlated with decreased upwelling and higher bottom-water oxygen in the SBB, though the long-term proxy records needed to corroborate this correlation are lacking.

We also note that SST variation within the SBB over the past ~640 years has remained relatively small, varying between 13.9˚C and 17.5˚C with a median and average of 15.5˚C across the entire primary data interval. Studies of the relationship between ENSO and SST in the Pacific suggest that while there is a strong correlation between these two variables, the strongest relationship occurs within the equatorial Pacific Warm Pool. The Santa Barbara Basin lies outside of this zone, and as such is affected via less well-understood teleconnections. Moreover, SST within the Santa Barbara Basin and the broader California Current system is impacted by the strength of upwelling, where in years with weakened upwelling the thermocline deepens, the warm Davidson current extends northwards, and the cold California current slows, thus resulting in a generally warmer SST and lower overall productivity (Zhao et al. 2000).

(c) Breakpoint analysis

The breakpoint analysis that we conducted should be considered an indicator of the potential timing of change, but should not be interpreted as the fixed point at which changes certainly occur. Because linearly-interpolated data were used to calculate the timing of this break, these data may influence the outcome of these breakpoint models, and additional primary data may change their final output. However, we find these breakpoint models to be a useful secondary tool with which to assess the likelihood that the mid-19th century represents an inflection point for *Bolivina alata, Bolivina argentea,* and *Bolivina seminuda*. These models return a significantly earlier timepoint for *Bolivina spissa*; note that while the data for *B. spissa* is less complete than the data for all other species, this earlier shift is intriguing, as it aligns with changes observed by previous studies that correspond with earlier events in the colonization of California (e.g., the arrival of European settlers and the establishment of permanent colonies beginning in the late 16th century; (Palmer et al. 2020)). Taken alongside our primary data, these models suggest that future work should focus on these time periods as potential points at which major shifts in foraminifera biological parameters occur.

(d) Limitations of the data

Samples were processed on >63 μm sieves, and as a result we analyze the size fraction for these analyses. While this is the standard size fraction used across micropaleontological studies, we note that young foraminifera or abnormally small species have likely been excluded from these analyses as a result of sample processing. In addition, because foraminifer species identifications are typically based on morphology rather than genetic information, these taxonomic units may not capture factors such as reproductive isolation. This lack of information about the genetic characteristics of foraminifera also limits our ability to undertake a cost-benefit analysis on the fitness of sexual and asexual reproduction. Future work that incorporates genetic variation could help to fill this longstanding gap in our understanding of the genetic determinants of foraminifer reproduction.

Chapter 3 Supplemental Figures

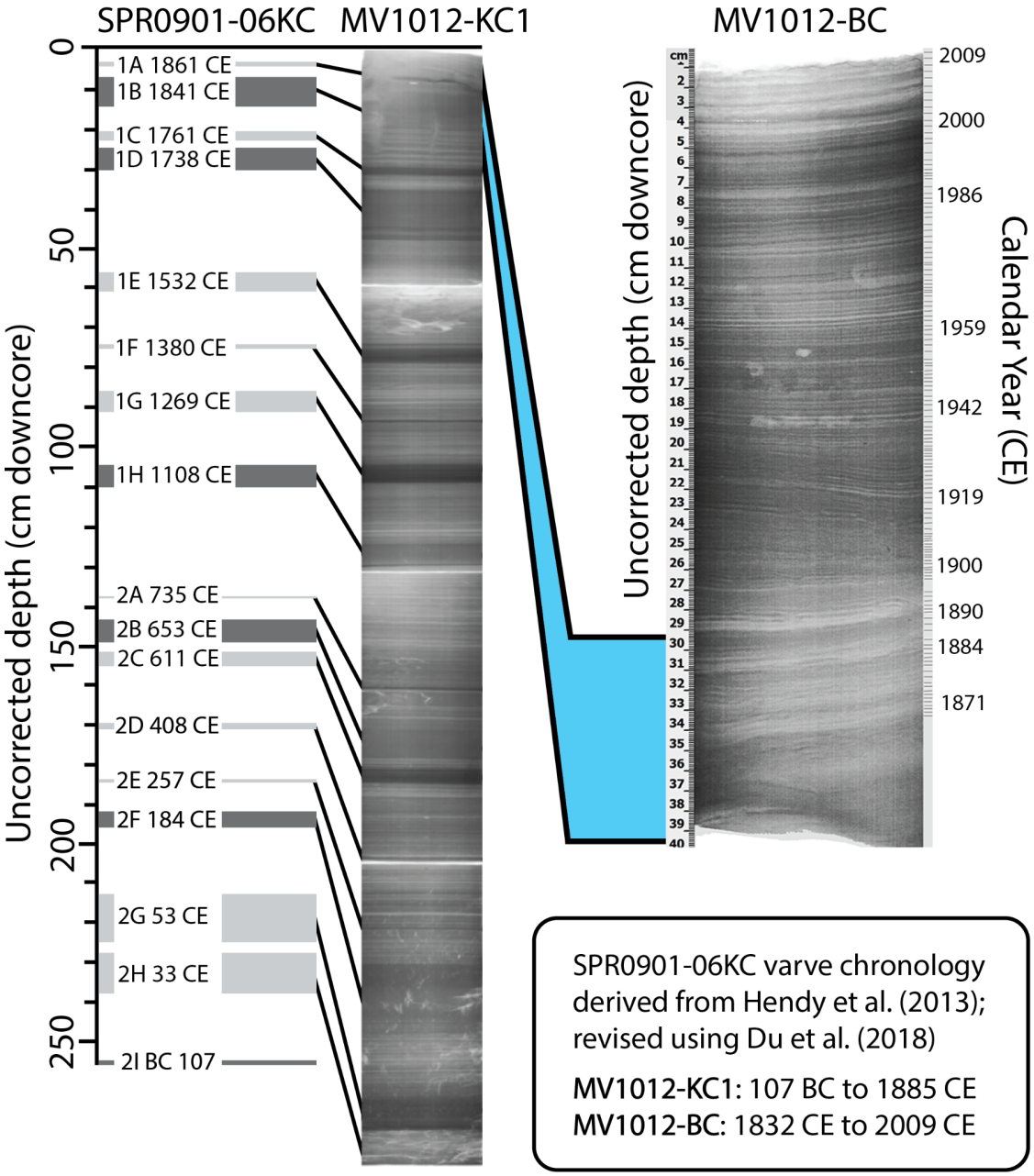

Supplementary Figure 3.1: Kasten and Box Core Core Chronology.
Kasten Core Chronology. X-radiograph images show Kasten and Box Cores collected from site MV1012 in the Santa Barbara Basin and individual varve couplets used to develop core chronology. Uncorrected depth in centimeters is indicated for each core. Instantaneous events are labeled according to notation used by Hendy et al. (2013) and Du et al. (2018); these distinct events were cross-dated between cores using core SPR0901-06KC to aid in chronology development. Stratigraphic overlap between the Kasten and Box Cores are denoted in blue. Figure modified from Jones and Checkley 2019 and Brandon et al. 2019.

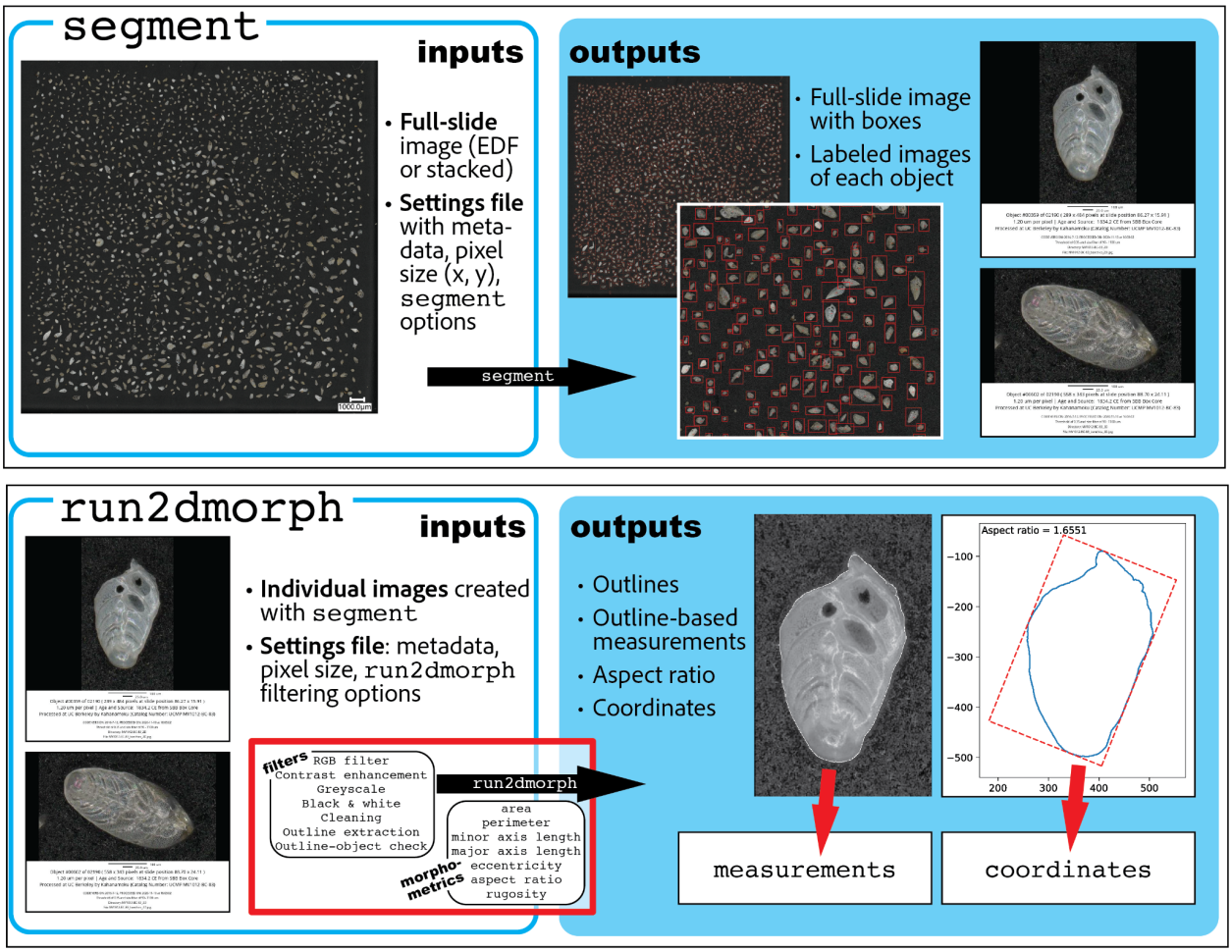

Supplementary Figure 3.2: AutoMorph image processing protocol.
AutoMorph is an open-source software suite used for high-throughput image processing and automated morphometric measurements. For this study, two AutoMorph modules were used: segment (top panel) and run2dmorph (bottom panel). Segment takes as an input a full slide image and a settings file with metadata (sample name, age, location of collection, catalog number, etc.), size information (typically expressed as pixel size, e.g. microns per pixel), and settings flags. Segment outputs include a full-slide image with boxed and numbered individual objects, which correspond to individual images of objects, which are labeled with metadata as well as a scale bar. Run2dmorph takes as input the individual images created with segment (for this study, EDF images) as well as a settings file with measurement and filtering flags. Run2morph processes individual images through filters to create outlines, and uses outlines to generate outline-based measurements of area, perimeter, major and minor axis length, eccentricity, aspect ratio, and rugosity. Outlines and aspect ratios are output as images for visual checks, and measurements and outline coordinates are output as CSV files.

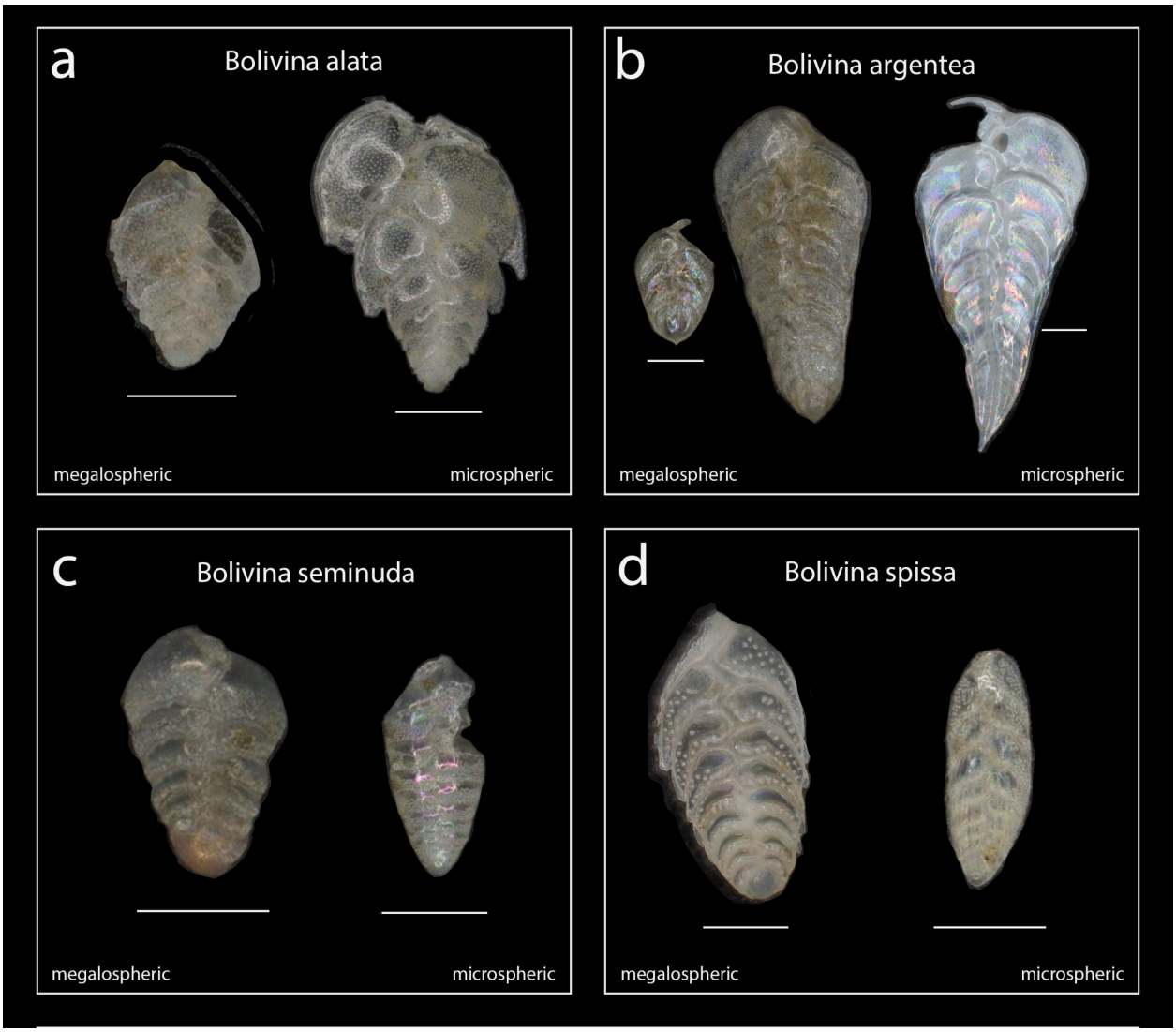

Supplementary Figure 3.3: Plate of taxonomic identifications used in this study.
(a) Bolivina alata; (b) Bolivina argentea; (c) Bolivina seminuda; (d) Bolivina spissa. Megalosphere and microsphere variation is shown for each species.

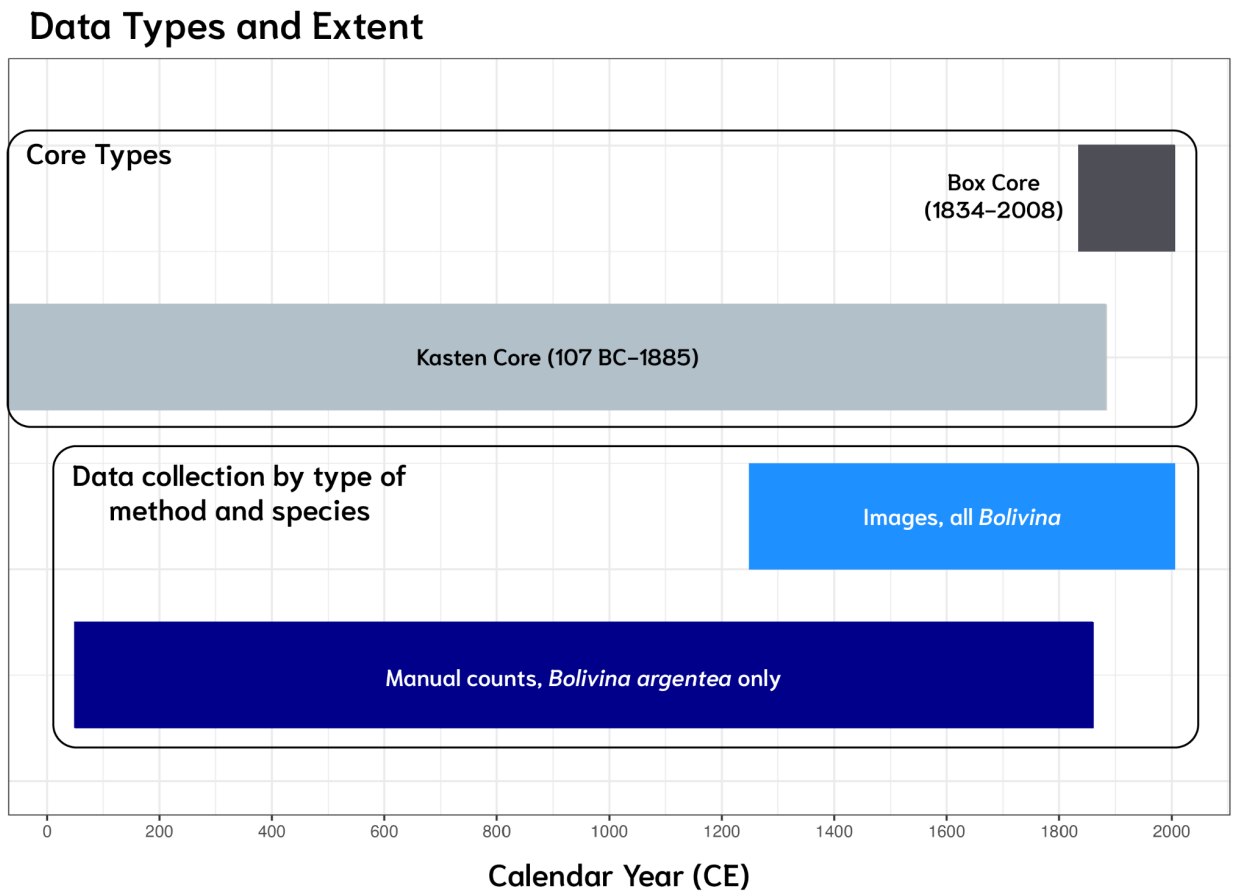

Supplementary Figure 3.4: Temporal span of data.
Core types and data collection types are denoted.

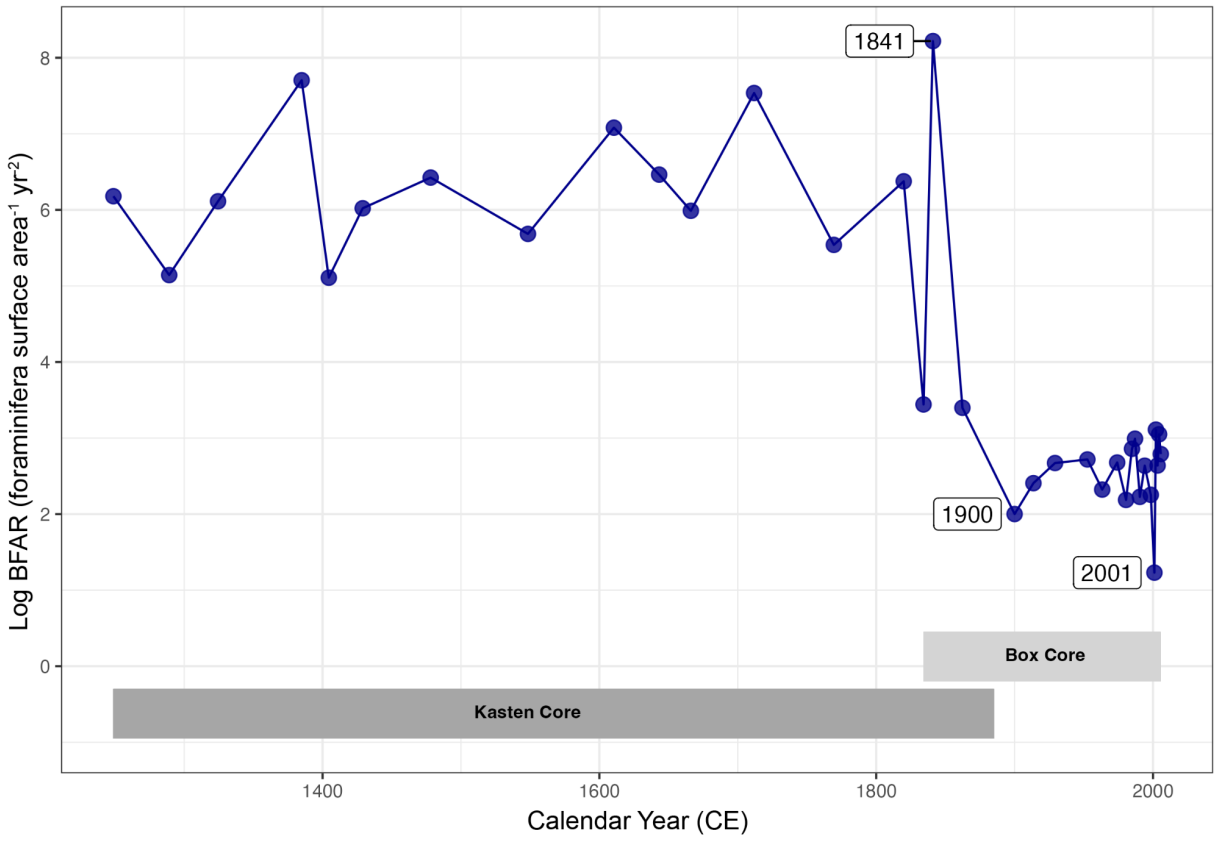

Supplementary Figure 3.5: Log-transformed Benthic Foraminifer Accumulation Rate. Data shown are for the composite core interval for samples picked for all *Bolivina* morphotypes. Foraminifer accumulation rate is calculated using the total number of benthic foraminifera, normalized to volume and years represented within a given sample (foraminifera per surface area per year).

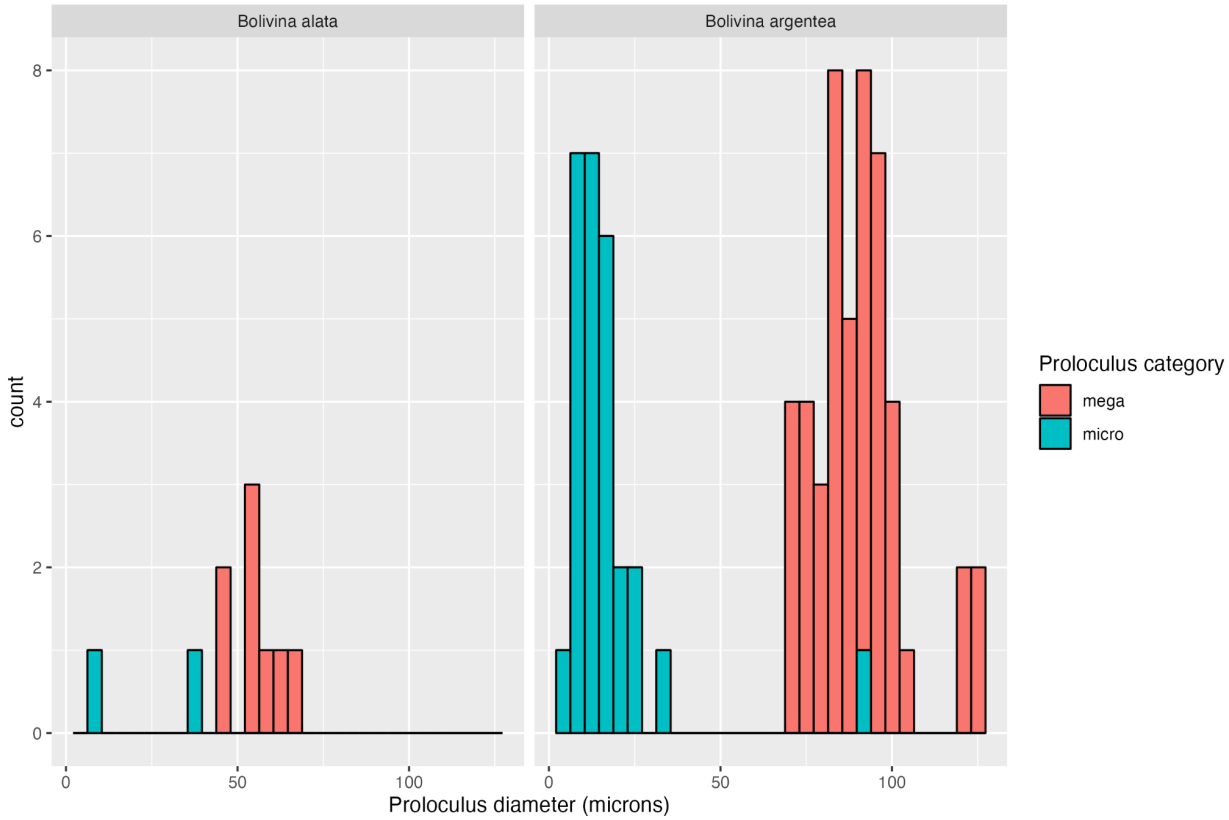

Supplementary Figure 3.6: Microsphere and megalosphere size distributions for B. alata and B. argentea.
Histograms show size-frequency distributions for proloculus diameters measured on a Keyence VHX-7000 digital imaging microscope. Distributions demonstrate that proloculus sizes are largely non-overlapping for the two species measured here.

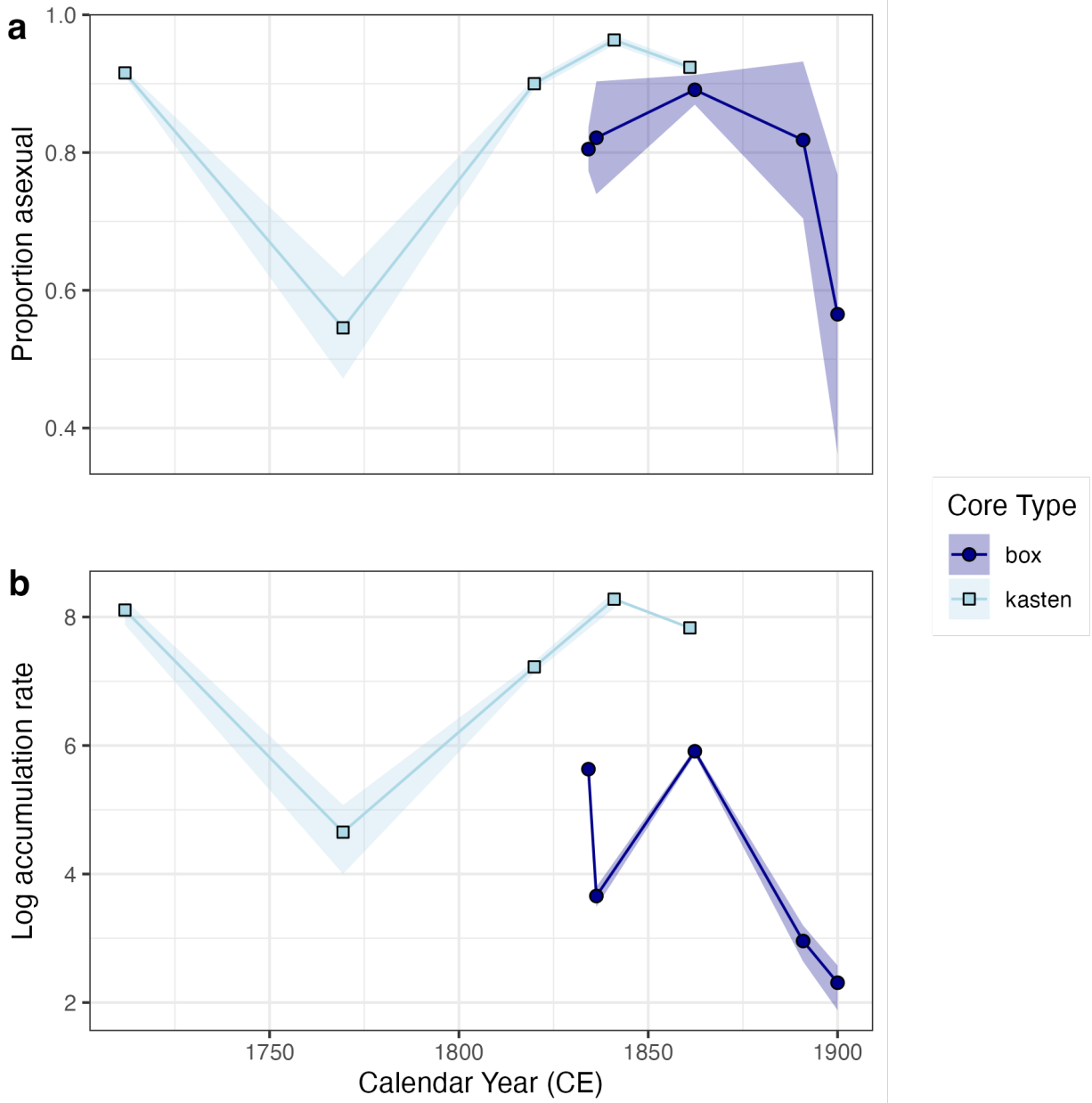

Supplementary Figure 3.7: Comparison of kasten and box core samples, 1700-1900 CE. (a) Proportion asexual; (b) accumulation rate. Due to kasten core processing, these data are only for *B. argentea*. Shaded regions show bootstrapped 95% confidence intervals.

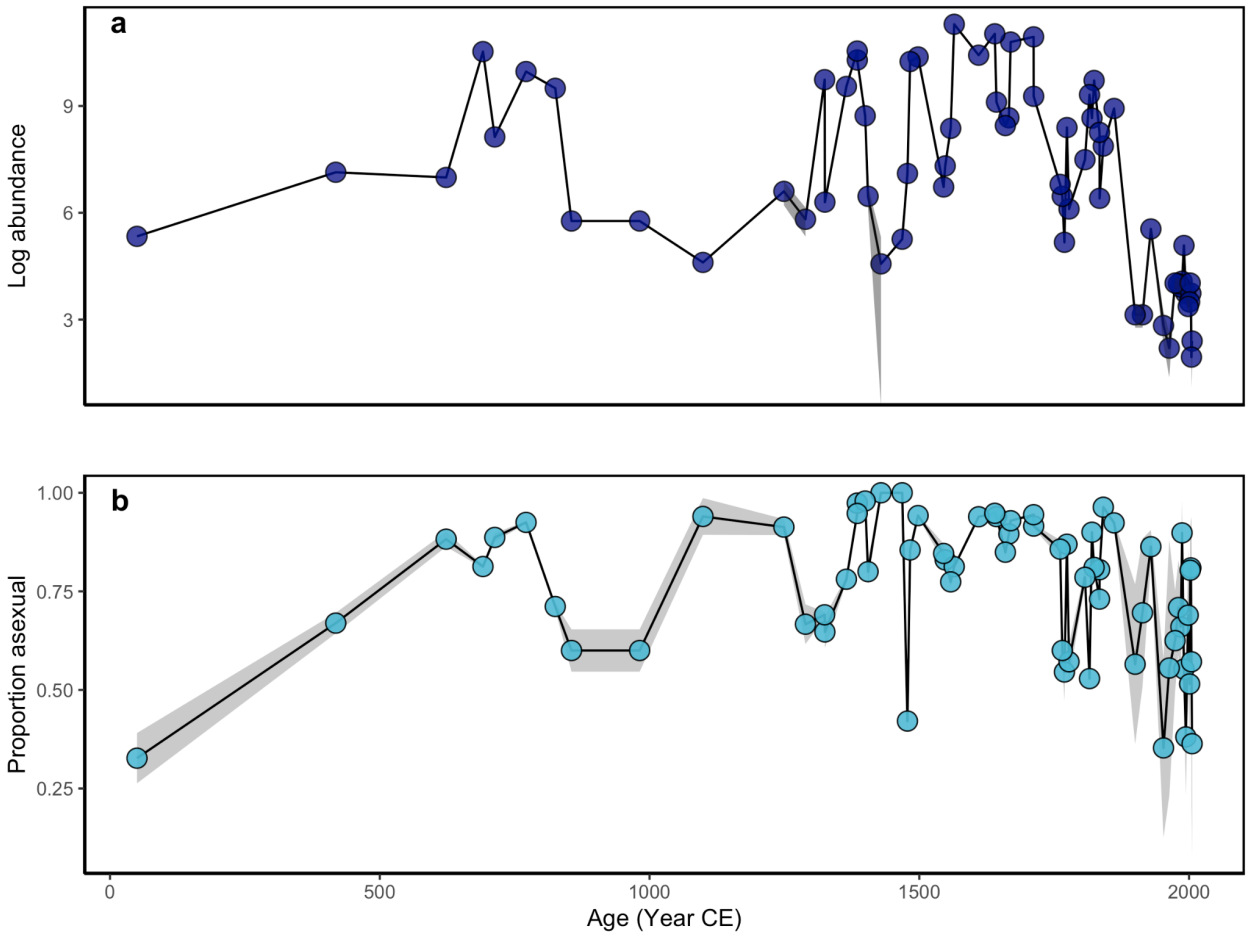

Supplementary Figure 3.8: Abundance and reproductive mode of B. argentea, 50-2008 CE. (a) Natural log-transformed accumulation rate and (b) proportion of asexual morphs of *Bolivina argentea*, the most abundant species with the most time series data, for the composite core interval (30 - 2008 CE). Shaded areas in panel (a) indicate bootstrapped 95% confidence intervals, while shaded areas in panel (b) denote 95% binomial confidence intervals.

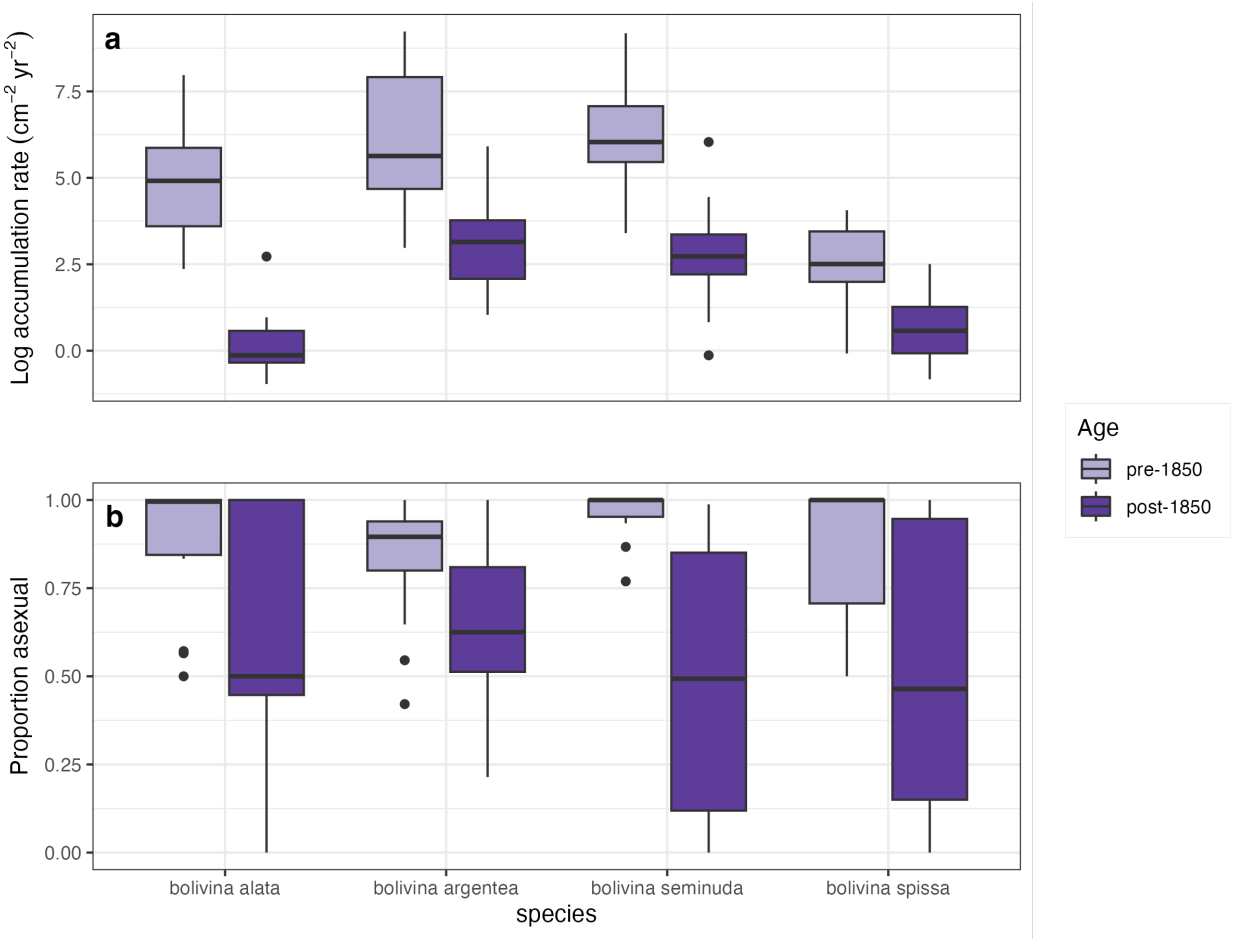

Supplementary Figure 3.9: Differences in abundance and proportion asexual by species between Box and Kasten Cores.
(a) Log accumulation rate; (b) proportion asexual. Colors denote core type. Boxes show interquartile range (IQR; where the bottom, middle, and top of boxes denote Q1, median, and Q2 values for each species); whiskers represent minimum and maximum values within 1.5 times the IQR, and points denote outliers.

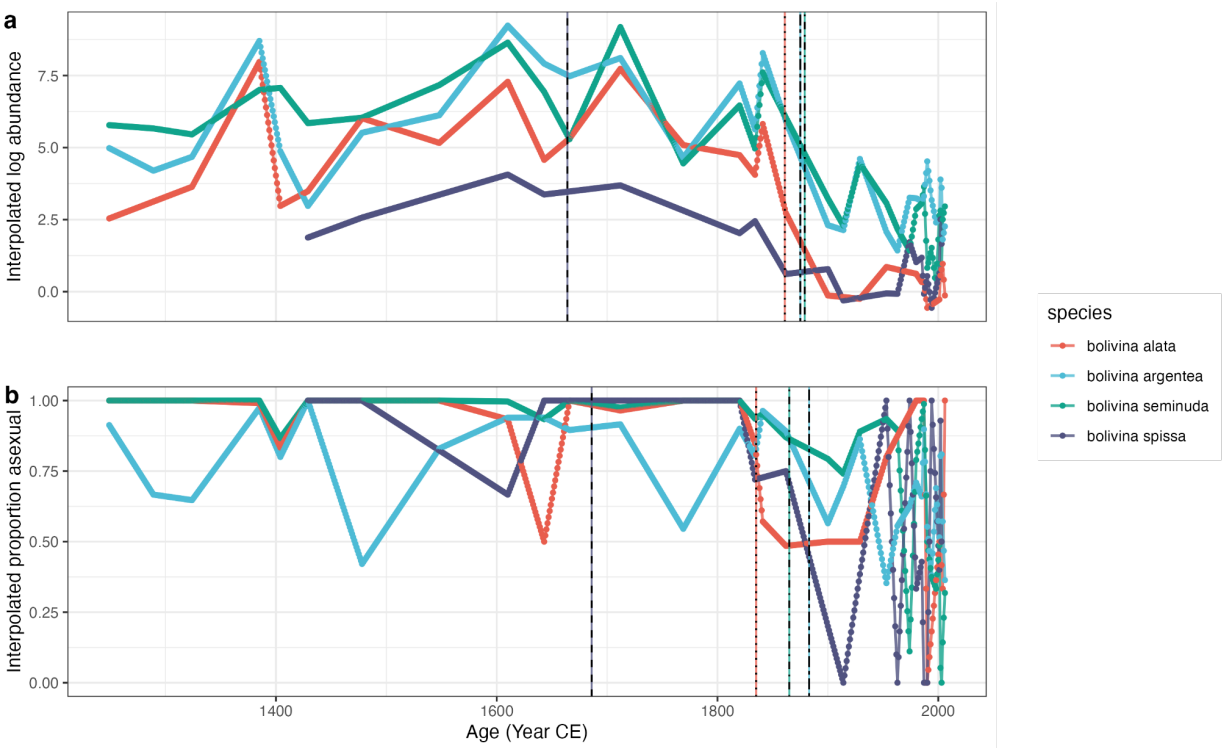

Supplementary Figure 3.10: Time series of linearly-interpolated Bolivina data.
(a) Interpolated log abundances by species and (b) proportions of asexual individuals by species, 1249-2008 CE. Colors denote species, and breakpoints calculated from a single-breakpoint model are shown by vertical lines.

LIST OF TABLES

Supplementary Table 3.1: Data types and split fractions by sample.
Samples were either imaged and fully picked for all *Bolivina* species used in this study, or were hand-picked for *B. argentea* and scored for reproductive mode (and thus have no associated image data).

Site	Core Type	Sample	Calendar Year CE	Age Range	Data Type	Sample Notes	Split Size
MV1012	Box	BC-2	2007.9		Image	Picked for bolivinids and imaged	1
MV1012	Box	BC-3	2006.7		Image	Picked for bolivinids and imaged	1
MV1012	Box	BC-4	2005.6		Image	Picked for bolivinids and imaged	1
MV1012	Box	BC-5	2004.4		Image	Picked for bolivinids and imaged	1
MV1012	Box	BC-6	2003.3		Image	Picked for bolivinids and imaged	1
MV1012	Box	BC-7	2002.1		Image	Picked for bolivinids and imaged	1
MV1012	Box	BC-8	2001		Image	Picked for bolivinids and imaged	1
MV1012	Box	BC-9-10	1998.4		Image	Picked for bolivinids and imaged	1
MV1012	Box	BC-12	1994		Image	Picked for bolivinids and imaged	1
MV1012	Box	BC-14	1990.5		Image	Picked for bolivinids and imaged	1
MV1012	Box	BC-16	1987		Image	Picked for bolivinids and imaged	1
MV1012	Box	BC-17	1984.8		Image	Picked for bolivinids and imaged	1
MV1012	Box	BC-19	1980.5		Image	Picked for bolivinids and imaged	1
MV1012	Box	BC-22	1974.1		Image	Picked for bolivinids and imaged	1
MV1012	Box	BC-27	1963.3		Image	Picked for bolivinids and imaged	1
MV1012	Box	BC-32	1952.6		Image	Picked for bolivinids and imaged	1
MV1012	Box	BC-42	1929.2		Image	Picked for bolivinids and imaged	1
MV1012	Box	BC-48	1913.6		Image	Picked for bolivinids and imaged	1
MV1012	Box	BC-53	1900		Image	Picked for bolivinids and imaged	1
MV1012	Kasten	KC1-1-15	1861		Count	Picked for *B. argentea*	1/64
MV1012	Kasten	KC1-1-25	1841		Image	Picked for bolivinids and imaged	1/32
MV1012	Box	BC-83	1834.2		Image	Picked for bolivinids and imaged	1
MV1012	Kasten	KC1-1-45	1834	1827-1841	Count	Picked for *B. argentea*	1/8
MV1012	Kasten	KC1-1-49	1832.58		Count	Picked for *B. argentea*	1/8

Site	Core Type	Sample	Calendar Year CE	Age Range	Data Type	Sample Notes	Split Size
MV1012	Kasten	KC1-1-51	1824	1820-1828	Count	Picked for *B. argentea*	1/64
MV1012	Kasten	KC1-1-52	1820		Image	Picked for bolivinids and imaged	1/32
MV1012	Kasten	KC1-1-53	1815.5	1811-1820	Count	Picked for *B. argentea*	1/64
MV1012	Kasten	KC1-1-55	1807	1803-1811	Count	Picked for *B. argentea*	1/64
MV1012	Kasten	KC1-1-62	1777.5	1773-1782	Count	Picked for *B. argentea*	1/64
MV1012	Kasten	KC1-1-63	1773.64		Count	Picked for *B. argentea*	1/64
MV1012	Kasten	KC1-1-64	1769		Image	Picked for bolivinids and imaged	1/16
MV1012	Kasten	KC1-1-65	1765	1761-1769	Count	Picked for *B. argentea*	1/64
MV1012	Kasten	KC1-1-69	1761		Count	Picked for *B. argentea*	1/64
MV1012	Kasten	KC1-1-103	1712		Image	Picked for bolivinids and imaged	1/128
MV1012	Kasten	KC1-1-103	1711.842		Count	Picked for *B. argentea*	1/64
MV1012	Kasten	KC1-1-116	1669.334		Count	Picked for *B. argentea*	1/64
MV1012	Kasten	KC1-1-117	1666		Image	Picked for bolivinids and imaged	1/16
MV1012	Kasten	KC1-1-119	1659.525		Count	Picked for *B. argentea*	1/64
MV1012	Kasten	KC1-1-124	1643		Image	Picked for bolivinids and imaged	1/32
MV1012	Kasten	KC1-1-125	1639.906		Count	Picked for *B. argentea*	1/64
MV1012	Kasten	KC1-2-9	1610		Image	Picked for bolivinids and imaged	1/64
MV1012	Kasten	KC1-2-23	1564.701		Count	Picked for *B. argentea*	1/64
MV1012	Kasten	KC1-2-25	1558.161		Count	Picked for *B. argentea*	1/8
MV1012	Kasten	KC1-2-28	1548		Image	Picked for bolivinids and imaged	1/32
MV1012	Kasten	KC1-2-29	1545.082		Count	Picked for *B. argentea*	1/64
MV1012	Kasten	KC1-2-45	1497.678		Count	Picked for *B. argentea*	1/64
MV1012	Kasten	KC1-2-48	1482.968		Count	Picked for *B. argentea*	1/64
MV1012	Kasten	KC1-2-49	1478		Image	Picked for bolivinids and imaged	1/32
MV1012	Kasten	KC1-2-51	1468.258		Count	Picked for *B. argentea*	1/64
MV1012	Kasten	KC1-2-59	1429		Image	Picked for bolivinids and imaged	1/32
MV1012	Kasten	KC1-2-64	1405		Image	Picked for bolivinids and imaged	1/16
MV1012	Kasten	KC1-2-65	1399.614		Count	Picked for *B. argentea*	1/64
MV1012	Kasten	KC1-2-68	1385		Image	Picked for bolivinids and imaged	1/128
MV1012	Kasten	KC1-2-68	1384.904		Count	Picked for *B. argentea*	1/64
MV1012	Kasten	KC1-2-72	1364.865		Count	Picked for *B. argentea*	1/64
MV1012	Kasten	KC1-2-80	1325		Image	Picked for bolivinids and imaged	1/32
MV1012	Kasten	KC1-2-79	1324.505		Count	Picked for *B. argentea*	1/64

Site	Core Type	Sample	Calendar Year CE	Age Range	Data Type	Sample Notes	Split Size
MV1012	Kasten	KC1-2-87	1289		Image	Picked for bolivinids and imaged	1/16
MV1012	Kasten	KC1-2-103	1249		Image	Picked for bolivinids and imaged	1/32
MV1012	Kasten	KC1-2-136	1149	1108-1190	Count	Picked for *B. argentea*	1/2
MV1012	Kasten	KC1-3-18	981.664		Count	Picked for *B. argentea*	1/64
MV1012	Kasten	KC1-3-39	855.328		Count	Picked for *B. argentea*	1/64
MV1012	Kasten	KC1-3-44	825.248		Count	Picked for *B. argentea*	1/64
MV1012	Kasten	KC1-3-53	771.104		Count	Picked for *B. argentea*	1/64
MV1012	Kasten	KC1-3-69	713.132		Count	Picked for *B. argentea*	1/64
MV1012	Kasten	KC1-3-73	691.264		Count	Picked for *B. argentea*	1/64
MV1012	Kasten	KC1-3-98	623		Count	Picked for *B. argentea*	1/64
MV1012	Kasten	KC1-3-143	418.415		Count	Picked for *B. argentea*	3/32
MV1012	Kasten	KC1-4-30	50	47-53	Count	Picked for *B. argentea*	1/4

Supplementary Table 3.2: Taxonomy references and synonyms.
Species names used within the main text and supplement are provided and associated with a Life Science Identifier (i.e., Aphia ID) (Vandepitte et al. 2015), as well as their synonymized names and the references upon which their taxonomic identification is based. The final column contains references used to corroborate identifications made via images.

Species	Life Science Identifier (Aphia ID)	Synonyms	Taxonomy References	Image ID References
Bolivina alata	112964	*Bolivina beyrichi var. alata*	Seguenza 1862	Erdem and Schönfeld 2017, Palmer et al. 2020
		Brizalina alata		
		Vulvulina alata		
Bolivina argentea	852154	*Brizalina argentea*	Cushman 1926	Lutze 1964, Erdem and Schönfeld 2017, Palmer et al. 2020
Bolivina seminuda	417913	*Bolivinella seminuda*	Cushman 1911	Erdem and Schönfeld 2017, Palmer et al. 2020
		Bolivinellina seminuda		
		Brizalina seminuda		
Bolivina seminuda var. humilis	816071	*Bolivina humilis* (accepted)	Cushman & McCulloch 1942	Erdem and Schönfeld 2017
		Bolivina seminuda var. humilis		
		Bolivinella humilis		
		Bolivinellina humilis		
		Brizalina humilis		
Bolivina spissa	814781	*Bolivina subadvena var. spissa*	Cushman 1926	Erdem and Schönfeld 2017, Palmer et al. 2020
		Brizalina spissa		
Bolivina pacifica	112979	*Bolivina acerosa var. pacifica*	Cushman & McCulloch 1942	Erdem and Schönfeld 2017
		Bolivinellina pacifica		
		Brizalina pacifica		

Supplementary Table 3.3: Common Era environmental proxies used and their source references.
Abbreviations, variable names, and the temporal extent of each dataset is listed alongside source publications. Data can be found in Data Citation.

Abbreviation	Variable	Calendar Range	Source	Interpolation used
ENSO	El Niño Southern Oscillation	910-2000 CE	Li et al. 2011	Linear interpolation
PDO	Pacific Decadal Oscillation	993-1996 CE	MacDonald and Case 2005	Linear interpolation
D15N	Bulk sedimentary d15N	170.5 BCE - 1910 CE	Wang et al. 2019	Moving 5-point window
TN	Bulk sedimentary total Nitrogen	170.5 BCE - 1910 CE	Wang et al. 2019	Moving 5-point window
TOC	Bulk sedimentary total organic carbon	170.5 BCE - 1910 CE	Wang et al. 2019	Moving 5-point window
SST Uk37	Alkenone Sea Surface Temperature	1297-1941 CE	Zhao et al. 2000	Linear interpolation on yearly averages
OMZ	OMZ reconstruction using redox-sensitive metals (Mo, Re, Ba)	165 BCE - 1904 CE	Wang et al. 2021, Wang et al. 2017	Moving 5-point window
MAR	Mass Accumulation Rate	70000 BCE - 1834 CE	Du et al. 2018	N/A

Supplementary Table 3.4: Breakpoint models and ages.
Breakpoints are shown for each species' abundance (denoted by "A") and proportion asexual individuals (denoted by "P"), calculated from interpolated data. Bayesian Information Criteria (BIC and ΔBIC) and shown for 1- through 5-breakpoint models.

Species	Type	1 Break	2 Breaks	3 Breaks	BIC 0	BIC 1	BIC 2	BIC 3	BIC 4	BIC 5	Δ BIC 1	Δ BIC 2	Δ BIC 3	Δ BIC 4	Δ BIC 5
Bolivina alata	A	1859	1361, 1857	1361, 1754, 1867	3460.9	2440	2301.1	2125.2	2090.2	2100.1	-1020.9	-138.9	-175.9	-35	9.9
	P	1835	1591, 1836	1552, 1665, 1835	-345.74	-999.17	-1026.15	-1094.84	-1084.44	-1066.17	-653.43	-26.98	-68.7	10.41	18.27
Bolivina argentea	A	1868	1551, 1864	1562, 1729, 1872	3170.2	2615	2480.1	2166.5	2136.9	2199.9	-555.2	-134.9	-313.6	-29.6	63
	P	1878	1546, 1729	1442, 1555, 1729	-772.51	-915.53	-1023.35	-1152.94	-1250.91	-1142.71	-143.02	-107.82	-129.6	-97.97	108.21
Bolivina seminuda	A	1866	1745, 1882	1530, 1742, 1882	3090.4	2251.8	1924.9	1775.3	1741.9	1724.8	-838.6	-326.9	-149.6	-33.4	-17.1
	P	1875			-865.51	-1347.14	-1342.21	-1331.73	-1320.09	-1309.35	-481.63	4.93	10.48	11.64	10.75
Bolivina spissa	A	1666	1612, 1698	1334, 1600, 1694	2062.31	1091.63	815.41	680.69	597.66	598.7	-970.68	-276.22	-134.72	-83.03	1.04
	P	1658	1455, 1653	1350, 1450, 1654	144.89	-428.13	-470.57	-544.76	-563.37	-550.89	-573.02	-42.44	-74.19	-18.61	12.48

Supplementary Table 3.5: Regression model outputs.
Models shown are the best-fit linear mixed model on abundance, and binomial logistic regression models for each species on proportion asexual.

Abundance					**Proportion Asexual**					
Predictors	*Estimates*	*CI*	*p*			*N*	*Predictors*	*Odds Ratios*	*CI*	*p*
(Intercept)	-16.84	-30.02 – -3.66	**0.014**	*	*B. alata*	20	(Intercept)	0		0.44
SST	2.17	1.28 – 3.06	**<0.001**	***			SST	2.42	0.07 – 121.71	0.59
ENSO amplitude	-2.39	-3.58 – -1.20	**<0.001**	***			ENSO amplitude	0.18	0.00 – 6.27	0.358
Mo_{EF}	0.35	0.15 – 0.56	**0.001**	**			Mo_{EF}	0.53	0.14 – 1.30	0.214
Ba_{excess}	-0.02	-0.02 – -0.01	**<0.001**	***			Ba_{excess}	1.02	0.99 – 1.05	0.257
Random Effects					*B. argentea*	*N*	*Predictors*	*Odds Ratios*	*CI*	*p*
σ^2	1.2					20	(Intercept)	0		0.61
τ_{00}	3.29 $_{species}$						SST	3.73	0.07 – 189.01	0.457
ICC	0.73						ENSO amplitude	1.06	0.01 – 240.35	0.981
N	4 $_{species}$						Mo_{EF}	1.54	0.62 – 5.98	0.416
							Ba_{excess}	0.99	0.96 – 1.02	0.501
Observations	49				*B. seminuda*	*N*	*Predictors*	*Odds Ratios*	*CI*	*p*
Marginal R^2 / Conditional R^2	0.318 / 0.818					20	(Intercept)	0		0.613
							SST	2.82	0.00 – 324.05	0.659
							ENSO amplitude	0.77	0.00 – 881.49	0.926
							Mo_{EF}	0.87	0.11 – 5.35	0.856
							Ba_{excess}	1.01	0.97 – 1.07	0.619
					B. spissa	*N*	*Predictors*	*Odds Ratios*	*CI*	*p*
						9	(Intercept)	0		0.88
							SST	1.23	0.00 – Inf	0.968
							ENSO amplitude	0.1	0.00 – Inf	0.826
							Mo_{EF}	0.62	0.02 – 22.34	0.749
							Ba_{excess}	1.02	0.95 – 1.12	0.59

Supplemental References

Bernhard, J. M., B. K. Sen Gupta, and P. F. Borne. 1997. Benthic foraminiferal proxy to estimate dysoxic bottom-water oxygen concentrations; Santa Barbara Basin, U.S. Pacific continental margin. Journal of Foraminiferal Research 27:301–310.

Brandon, J. A., W. Jones, and M. D. Ohman. 2019. Multidecadal increase in plastic particles in coastal ocean sediments. Science Advances 5:eaax0587–eaax0587.

Cardich, J., M. Morales, L. Quipúzcoa, A. Sifeddine, and D. Gutiérrez. 2012. Benthic Foraminiferal Communities and Microhabitat Selection on the Continental Shelf Off Central Peru. Pages 323–340 *in* A. V. Altenbach, J. M. Bernhard, and J. Seckbach, editors. Anoxia: Evidence for Eukaryote Survival and Paleontological Strategies. Springer Netherlands, Dordrecht.

Elder, L. E., A. Y. Hsiang, K. Nelson, L. C. Strotz, S. S. Kahanamoku, and P. M. Hull. 2018. Sixty-one thousand recent planktonic foraminifera from the Atlantic Ocean. Scientific Data 5:180109.

Erdem, Z., and J. Schönfeld. 2017. Pleistocene to Holocene benthic foraminiferal assemblages from the Peruvian continental margin. Palaeontologia Electronica 20:Art-Nr.

Erdem, Z., J. Schönfeld, A. E. Rathburn, M.-E. Pérez, J. Cardich, and N. Glock. 2020. Bottom-water deoxygenation at the Peruvian margin during the last deglaciation recorded by benthic foraminifera. Biogeosciences 17:3165–3182.

Hendy, I. L., L. Dunn, A. Schimmelmann, and D. K. Pak. 2013. Resolving varve and radiocarbon chronology differences during the last 2000 years in the Santa Barbara Basin sedimentary record, California. Quaternary International 310:155–168.

Hsiang, A. Y., K. Nelson, L. E. Elder, E. C. Sibert, S. S. Kahanamoku, J. E. Burke, A. Kelly, Y. Liu, and P. M. Hull. 2017. AutoMorph: Accelerating morphometrics with automated 2D and 3D image processing and shape extraction. Methods in Ecology and Evolution 9:605–612.

Jones, W. A. 2016. The Santa Barbara Basin Fish Assemblage in the Last Two Millennia Inferred from Otoliths in Sediment Cores:1–141.

Jones, W. A., and D. M. Checkley. 2019. Mesopelagic fishes dominate otolith record of past two millennia in the Santa Barbara Basin. Nature Communications 10:4564.

KAMINSKI, M. A., C. G. CETEAN, and J. TYSZKA. 2011. Nomenclature to describe the transition from multiserial to uniserial chamber arrangement in benthic foraminifera. Journal of Micropalaeontology 30:7.

Li, J., S.-P. Xie, E. R. Cook, G. Huang, R. D'Arrigo, F. Liu, J. Ma, and X.-T. Zheng. 2011. Interdecadal modulation of El Niño amplitude during the past millennium. Nature Climate Change 1:114–118.

Páez, M., O. Zúñiga, J. Valdés, and L. Ortlieb. 2001. Foraminíferos bentónicos recientes en sedimentos micróxicos de la bahía Mejillones del Sur (23º S), Chile. Revista de biología marina y oceanografía 36:129–139.

Palmer, H. M., T. M. Hill, P. D. Roopnarine, S. E. Myhre, K. R. Reyes, and J. T. Donnenfield. 2020. Southern California margin benthic foraminiferal assemblages record recent centennial-scale changes in oxygen minimum zone. Biogeosciences 17:2923–2937.

Schimmelmann, A., I. L. Hendy, L. Dunn, D. K. Pak, and C. B. Lange. 2013. Revised ~2000-year chronostratigraphy of partially varved marine sediment in Santa Barbara Basin, California. GFF 135:258–264.

Schimmelmann, A., and C. B. Lange. 1996. Tales of 1001 varves: a review of Santa Barbara

Basin sediment studies. Geological Society, London, Special Publications 116:121–141.
Schimmelmann, A., C. B. Lange, E. B. Roark, and B. L. Ingram. 2006. Resources for Paleoceanographic and Paleoclimatic Analysis: A 6,700-Year Stratigraphy and Regional Radiocarbon Reservoir-Age (ΔR) Record Based on Varve Counting and 14C-AMS Dating for the Santa Barbara Basin, Offshore California, U.S.A. Journal of Sedimentary Research 76:74–80.
Uchimura, H., H. Nishi, R. Takashima, A. Kuroyanagi, Y. Yamamoto, and S. Kutterolf. 2017. Distribution of Recent Benthic Foraminifera off Western Costa Rica in the Eastern Equatorial Pacific Ocean. Paleontological Research 21:380–396.
Vandepitte, L., B. Vanhoorne, W. Decock, S. Dekeyzer, A. Trias Verbeeck, L. Bovit, F. Hernandez, and J. Mees. 2015. How Aphia—The Platform behind Several Online and Taxonomically Oriented Databases—Can Serve Both the Taxonomic Community and the Field of Biodiversity Informatics. Journal of Marine Science and Engineering 3:1448–1473.
Wang, Y., and I. L. Hendy. 2021. Reorganized Atmospheric Circulation During the Little Ice Age Leads to Rapid Southern California Deoxygenation. Geophysical Research Letters 48:e2021GL094469.
Wang, Y., I. L. Hendy, and R. Thunell. 2019. Local and Remote Forcing of Denitrification in the Northeast Pacific for the Last 2,000 Years. Paleoceanography and Paleoclimatology 34:1517–1533.
Wang, Y., I. Hendy, and T. J. Napier. 2017. Climate and Anthropogenic Controls of Coastal Deoxygenation on Interannual to Centennial Timescales. Geophysical Research Letters 44:11,528-11,536.
Zhao, M., G. Eglinton, G. Read, and A. Schimmelmann. 2000. An alkenone (U37K′) quasi-annual sea surface temperature record (AD 1440 to 1940) using varved sediments from the Santa Barbara Basin. Organic Geochemistry 31:903–917.

4 Correlated trends and shifts in terminal shell size of foraminifera over the last 760 years

Sara S. Kahanamoku[1], Maya Samuels-Fair[1], Ivo Duijnstee[1], Seth Finnegan[1]

Affiliations

1. Department of Integrative Biology and Museum of Paleontology, University of California, Berkeley, CA
2. Department of Organismal Biology, Harvard University, Cambridge, MA

Abstract

Body size distributions within ecological communities reflect the influence of environmental forces and life history tradeoffs on these communities across space and through time. Yet many studies of body size use summary measurements (i.e., assume a standard size for each taxon) or focus on changes in mean size rather than shifts in the shape of individual body size distributions, which are indicative of ecologically-relevant shifts in population structure. Here we use a dataset of more than 21,000 measurements of individual body size from 12 species of benthic foraminifera from the Santa Barbara Basin (SBB) to examine how intraspecific and community-level body size trends have varied across a ~760-year interval that spans a period of significant environmental change. These data also include information on reproductive life history, revealing body size trajectories within and across reproductive morphotypes. We show that intraspecific body size variation within SBB benthic foraminifera is impacted by both life history and environmental parameters. Changes to intraspecific terminal size distributions produced community-level body size trends, which underwent a stepped decrease during the mid-20th century CE. We find that changes in size-frequency distributions tend to be positively correlated across species and driven in particular by changes in representation of smaller individuals, suggesting that these community-level size changes towards the recent correspond with even stronger body size correlations across species when compared to older samples. Reproductive mode is also shown to significantly affect overall terminal size in species with strong dimorphism between megalospheric (asexually-produced) and microspheric (sexually-produced) generations, with modern decreases in the prevalence of megalospheric individuals corresponding with the intraspecific size decreases we observe. Finally, we find that food and oxygenation proxies are significant predictors of size for some species within the basin, but no significant community-level environmental predictors of size were detected. These results suggest that the impacts of environmental change and life history on intraspecific benthic foraminifer size in the SBB are complex, yet community-level size decreases may be driven by species-specific responses to oceanographic changes within the California Current system.

4.1 Introduction

Organismal body size is a useful paleoenvironmental indicator (Brown 1995, Smith et al. 2016), as it can control access to ecological niches and modulate sensitivity to fundamental physiological processes (Peters and Peters 1986). In organisms with widely ranging life history options, body size may be dynamically modulated by the environment. As a result, body size is a trait that is responsive to many selective pressures, and is useful for tracking how changing ocean conditions affect individual biology and community ecology. Within marine environments, body size changes have been shown to correlate with warming (Hunt and Roy 2006, Schmidt et al. 2006, Gardner et al. 2011, Forster et al. 2012, Piazza et al. 2020), deoxygenation (Morten and Twitchett 2009, Piazza et al. 2020), changes to primary productivity (Vermeij 2012, Pyenson and Vermeij 2016), and shifts in food web structure (Woodward et al. 2005, Worm et al. 2006, Bryndum-Buchholz et al. 2019, Lotze et al. 2019), among other factors. While these impacts are not universal, as size-environment relationships are complex and spatially and temporally heterogeneous (Berke et al. 2013, Belanger 2022), changing environmental conditions affect both intraspecific and interspecific growth. These range from determining the trajectories of individual life histories (Blueweiss et al. 1978, Calder 1996) to the ability of ecological communities to weather perturbations, and these macroecological factors contribute to the evolutionary success of entire lineages (Payne and Heim 2020, Monarrez et al. 2021).

Body size has been shown to affect key life history characteristics, such as the number of offspring an individual can produce, the size of these offspring at birth and maturity (Caval-Holme et al. 2013, Shama 2015, Belanger 2022), and the range of ecophenotypic variation observed within offspring populations. Notably, in foraminifera the reverse is also true: life history choices strongly affect terminal body size as observed in the fossil record because reproduction commonly marks the end of the parent cell's lifespan. Phases of early reproduction thus result in smaller terminal body sizes. These life history factors shape population growth rates and overall abundance (White et al. 2007, Lohbeck et al. 2012, DeLong and Luhring 2018), as well as the success or failure of range expansion (Burton et al. 2010, Williams et al. 2019). As a result, body size can often serve as an indicator of the ways in which environmental change impacts not only the morphology of individuals, but also species-level potentials for growth, adaptation, and survival (Marshall 2008, Moczek et al. 2011, Murray et al. 2014, Schmidt et al. 2018).

Recently, both climate change (Daufresne et al. 2009, Sheridan and Bickford 2011) and novel human impacts (Barneche et al. 2018, Bryndum-Buchholz et al. 2019) have been shown to impact reproduction via their impacts on body size. While many studies have focused on the reproductive consequences of climate-and human-driven size shifts in large animals, unicellular organisms are also impacted by these stressors, and may be uniquely sensitive to environmental shifts due to the size-dependence of nutrient uptake and respiration (Zeuthen 1953, Banse 1976, Guderley 2004, Marañón et al. 2013). In addition, body size is often an important determinant of reproductive output in unicellular species. For example, body size affects whether reproduction can take place sexually (vs. asexually) in diatoms (Koester et al. 2007, Scalco et al. 2014, Kim et al. 2020), whereas in foraminifera, the internal volume of the test (i.e., the calcium carbonate shell) determines the total number of gametes that can be released during sexual reproduction (Bé and Anderson 1976) or how many propagules can be formed during schizogenous axesual reproduction.

Because foraminifera are readily preserved in marine sediments and have a cosmopolitan record that spans most of the Phanerozoic, these organisms are among the few that have been used to study how climate change and life history have determined body size distributions through time (Keating-Bitonti and Payne 2016 p., 2017, 2018, Belanger 2022). However, the majority of these studies (as well as the broader literature on fossil marine body size) have used summary measurements (i.e., assuming a standard size for each species) to characterize interspecific size, rather than measuring individuals and population size-frequency distributions. The use of genus- and species-level averages has precluded examination of trends in and external influences on intraspecific size through time. In particular, questions of how the life history strategies of both parents and offspring contribute to determining overall offspring size are difficult to examine using fossil data.

Here we use a dataset of 21,661 measurements of individual terminal body size from 12 species of benthic foraminifera from the Santa Barbara Basin to examine trends in intraspecific body size variation over a ~760-year interval that spans into the modern era. In addition, we inferred reproductive mode from morphology for 7,112 of these individuals (representing 4 species) which, together with size data, allows for examination of how organismal life history affects both body size and growth trajectories over many generations. When combined with instrumental records and environmental proxy data from the Santa Barbara Basin, these data allow us to evaluate relationships between environmental change, life history evolution, and body size distributions at high temporal resolution.

4.2 Materials and methods

4.2.1 Core Sampling and Chronology Development

Two cores–a kasten core (MV1012-KC1) and a box core (MV1012-BC)–were used for this study. Prior to the present analysis, these cores were collected in October 2010 by members of the Scripps Institution of Oceanography Cal-ECHOES research cruise at Santa Barbara Basin (SBB) station MV1012-ST46.9 (34˚17.228'N, 120˚02.135'W) at ~580m water depth (Brandon et al. 2019, Jones and Checkley 2019). Transverse sections from each core were cut every 0.5 cm to create sections of 97.5 cm^3. Composite X-radiographs and color photographs were used to develop a high-resolution chronology for each core (Figure S4.1) by counting seasonal varve couplets calibrated with radiocarbon dating to establish a chronology from 107 B.C. to 1700 C.E. (Hendy et al. 2013, Schimmelmann et al. 2013). Box core MV1012-BC was covered by a bacterial mat (Figure S4.1), indicating that the surficial sediments were intact (Brandon et al. 2019). Box core MV1012-BC was sufficiently shallow to use traditional varve-counting chronology (Hendy et al. 2013, Schimmelmann et al. 2013, 2006) for couplet dating, and a regression model was used to assign dates to the sediment stratigraphy prior to 1871, thus extending the box core chronology to 1834 AD (Brandon et al. 2019).

4.2.2 Sample processing

Prior to the present study, core transverse sections were dried, washed, and wet-sieved over a 104- and 63-μm mesh, and the >104 μm fraction of both kasten and box core transverse sections was picked under a dissecting microscope for fish otoliths (Jones and Checkley 2019) and plastic particles (Brandon et al. 2019). For this analysis, samples from the 63-104 and >104 μm fraction

of kasten cores MV1012-KC1 were dry split using a sediment splitter to achieve approximately equivalent sample volumes, while samples from box core MV1012-BC were processed in their entirety (Table S4.1).

Samples from kasten core MV1012-KC-1 were dry picked for all biserial benthic foraminifera, a majority of which were in the genus *Bolivina* and related genera. Following picking, samples were arranged on brass-coated matte black picking plates and imaged in bulk using a Keyence VHX-7000 digital imaging microscope at 150x magnification. These bulk images were taken using the Keyence 3D image stitch function, which generates stitched 2D EDF images and semi-3D scans (Figure S4.2). Samples from box core MV1012-BC were dry picked for all foraminifera within each sample, to capture the range of variation across full assemblages. As with kasten core samples, assemblages were arranged on picking plates and imaged in bulk, using the same magnification and lighting settings.

4.2.3 Morphometric analysis

Bulk 2D EDF images from both the kasten and box core were processed using the AutoMorph `segment` protocol (Hsiang et al. 2017) to create individual images of each object. Individual images formed the basis of subsequent morphometric analyses. The AutoMorph `run2dmorph` protocol was used to extract 2D shape parameters and outline coordinates from each image (Hsiang et al. 2017). 2D shape parameters include outline-based measurements of shell area, perimeter, major axis length (i.e., shell length), minor axis length (i.e., shell width), eccentricity, aspect ratio, and rugosity (a measurement of surface texture along an object edge, calculated by comparing unsmoothed and smoother perimeter lengths) (Hsiang et al. 2017). Broken shells were removed from the analysis using a filter based on the rugosity of the outlines extracted from images, which removed outliers that represent primarily fragmented and heavily broken shells (Figure S4.5). Visual checks were performed to ensure that a representative portion of the remaining samples had intact- or semi-intact outlines. To provide a secondary check, analyses done using shell area measurements were assessed against measurements of major axis length; all produced similar results, indicating that shell area measurements from outlines correspond to shell length, as expected given that shell area should vary as a function of minor axis length.

4.2.4 Species identification and reproductive mode classification

Individual 2D EDF images produced via `segment` were used to visually identify both benthic foraminifera species (Figures S4.3, S4.4) and non-foraminifer objects. Of these, 26,399 were benthic foraminiera were identifiable to species. Broken shells were identified to species, but heavily broken and poorly-extracted foraminifera were removed via outline-based filtering methods (Figure S4.5), thus reducing the dataset size to 22,341 individuals. Kasten core samples contained individuals from 7 species, which represented primarily *Bolivina* and other biserial benthic forms (Figure S4.3). In contrast, box core samples contained individuals from 65 unique species. The most common 12 species from the box core were retained for this analysis (Figures S4.3, S4.4; Table S4.2) in order to allow for statistical power in morphometric and ecological analyses. While this data reduction eliminated 53 species from our analysis, these were rare species that represented only 685 specimens within the overall dataset of over 22,000 individuals. Further, all 8 common kasten core species are also present within the reduced box core dataset, thus allowing for examination of species-specific morphology over the entirety of the composite core interval.

4.2.5 Environmental Data Collection

Proxies for major oceanographic and climate variables within the Santa Barbara Basin were compiled from published literature. These include time series of El Niño Southern Oscillation (ENSO; Li et al. 2011), Sea Surface Temperature (SST; Zhao et al. 2000), total organic carbon (TOC) and total nitrogen (TN; Wang et al. 2017), and redox metals used as proxies for oxygenation (Wang and Hendy 2021) (Table S4.3). Because these datasets were generated from core records that were sampled near to or at the sampling location of the cores used within these studies, all have comparable age models that allow for integration of these variables with our morphological and reproductive data.

Direct observational oceanographic data was obtained from the California Cooperative Fisheries Program (CalCOFI) online database for samples from the center of the SBB (Station 081.8 046.9; ~34.28˚N, 120.02˚W). Data from 1953-2008 CE was compiled for bottom water temperature; oxygen saturation state; and concentrations of nitrate, phosphate, and silicate from bottles collected at or below 500m water depth. Monthly data were then averaged to create a yearly record of each parameter at the deepest sections of the water column sampled by CalCOFI.

4.2.6 Statistical analysis

All statistical analyses were conducted in R (Team 2013). Temporal trends in mean body size–calculated using log-transformed individual data to create both sample and individual species-specific means–were assessed using the R package PaleoTS (Hunt and Carrano 2010, Hunt and Hunt 2019), which fits common evolutionary models to paleontological trait data. Four major rate models were tested: generalized random walk (Hunt 2006), Ornstein-Uhlenbeck (Hunt 2008a), stasis (Hunt 2007), and punctuated change (Hunt 2008b). Models were fit via maximum likelihood (Hunt and Roy 2006) and compared using log-likelihood and Akaike Information Criteria (AIC).

Scaled pairwise median size data for each well-sampled species (n > 10 individuals per sample) across both core intervals were examined using Spearman rank-order correlation tests to determine whether shell area and aspect ratio co-vary across samples, and linear regressions were used to determine relationships between body size and reproductive morphotypes: megalospheric, or asexually-produced individuals, and microspheric, or sexually-produced individuals (Figure S4.3). Environmental data and classifications of reproductive mode were tested as predictors for size and shape in both linear and linear mixed models with species held as a random effect. We examined the impact of environment on three distinct datasets: (1) a dataset from the composite core interval, containing 12 common species; (2) a dataset from the composite core interval, containing the 4 species of bolivinids with measured reproductive mode variation; and (3) a dataset from the box core interval, containing every benthic foraminifer species present.

4.3 Results

4.3.1 Stasis and punctuated change in intraspecific body size trends through time

Species mean shell areas (i.e., terminal body sizes) fluctuate through time, yet the range of individual body sizes remains relatively constant for most species picked from the entirety of the ~760-year-long record we examine (Figure 4.1). Across all species, interspecific mean shell areas (i.e., assemblage size means) show temporal variation with an overall decrease close to the present (Figure S4.6a). When models evaluating the mode of change are applied to these data, punctuated change is the best-fit model, with an overall breakpoint indicating a shift towards smaller interspecific (i.e., community-level) size means placed at 1963 CE (Figure S4.6b). Intraspecific mean sizes are also shown to be significantly different (and often smaller) in modern data when compared to the longer core interval (Figure S4.7, pre- vs. post-1950 CE; $p << 0.01$ in a Welch's two-sample t-test for each species).

When intraspecific mean shell areas are similarly examined, stasis is the favored model for three species (*Bolivina alata*, *B. spissa*, and *Bulimina exilis*), while a 1-step punctuated change model is favored for four species (*Bolivina argentea*, *B. pacifica*, *B. seminuda*, and *Suggrunda eckisi*; Figure 4.2). Of those species for which punctuated change is favored, two species (*B. argentea* and *B. seminuda*) decrease in size towards the present and have a shared estimated breakpoint at 1963 CE (similar to the overall mean shown in Figure S4.6). In contrast, *B. pacifica* and *S. eckisi* increase in size close to the present, with estimated breakpoints at 1980 CE and 1900 CE, respectively.

The emergence of both stasis and punctuated change as favored models for intraspecific size trends demonstrates how individual size trends structure community-level size within the basin. For example, *B. argentea* and *B. seminuda* are compositionally the most abundant species within pre-19th century samples, yet both decrease in abundance towards the recent (see Chapters 3 and 5 of this dissertation). As their relative abundance continues to decline throughout the 20th century, both species undergo size decreases. In contrast, species such as *S. eckisi* that increase in relative abundance towards the recent have the smallest size average distributions within the SBB assemblages we examine.

4.3.2 Correlated size changes across species

We find that interspecific median shell area is positively correlated across most species pairs through time (Figure 4.3; Table 4.1). Negative size correlations are contained within species pairings including *B. argentea* and *C. crassa*. When data are filtered by shell area percentile (i.e., 10th, 25th, 75th, and 90th size percentiles are examined), correlations are strongest for the lower percentiles and weakest for the highest percentiles (Figure S4.8; Table 4.1). This suggests that changes in the representation of small individuals tend to be more strongly correlated across species than changes in the representation of large individuals. The direction and strength of correlations does not change when we remove species using the lowest and highest 5% of the culling metric (see methods and Figure S4.5), nor does it change when we use major axis length as the primary indicator of size, indicating that size correlations are robust to the automated data processing techniques used here.

While size changes are correlated across species, shape changes (represented in the dataset by aspect ratio) are not (Figure S4.9). Species pairs with positive aspect ratio correlations (i.e., shape changes in the same direction) are primarily biserial foraminifera, which are foraminifera that grow by adding on chambers in an evolute trochospiral arrangement with ~180˚ between

consecutive chambers (i.e., chamber alternation; Kaminski et al. 2011), such that growth is almost always accompanied by changes to aspect ratio via elongation (Figure S4.10).

4.3.3 Megalospheric individuals are often larger than microspheric individuals

In *Bolivina* foraminifera with strongly visible reproductive mode variation (*B. alata*, *B. argentea*, *B. seminuda*, and *B. spissa*), megalospheric individuals are not always larger than microspheric individuals, but megalospheric individuals are larger on average in *B. argentea*, *B. seminuda*, and *B. spissa* ($p << 0.01$, Figure 4.4a). The largest shells by area are almost always megalospheric (i.e., asexually-produced) individuals. *B. alata* is the exception, showing an inverse trend ($p = 0.006$ in a Welch's two-sample t-test, Figure 4.4a). Time series of reproductive morphotype shell areas for each species show that significant temporal variation exists across both morphotypes (Figure S4.11). When shell lengths and widths are compared, megalospheric individuals have consistently larger widths than microspheric individuals of the same length (Figure 4.4b).

4.3.4 Reproductive mode contributes to Bolivina terminal body size distributions

Given that species with reproductive mode variation tend to covary in their reproductive mode choices (i.e., that all species choose similar reproductive modes at given points in time; see Chapter 1), it is possible that size changes are, too, driven by reproduction. To determine how reproductive mode may contribute to overall temporal size trends, we examined mean shell areas for reproductive morphotypes (asexually-produced megalospheres or sexually-produced microspheres) within each species in rate models (Figure S4.12). We find that stasis emerges as the favored model for both morphotypes of *B. alata* and *B. spissa*, mirroring results from pooled intraspecific analyses of size (Figure 4.2). For *B. argentea*, a 1-step punctuated change model is likewise favored, though breakpoints for megalospheric and microspheric morphotypes differ slightly from pooled data, with estimated dates at 1965 CE and 1820 CE, respectively (Figure S4.12). For *B. seminuda* microspheric morphotypes, stasis was the favored model (though small sample sizes likely affect this analysis; Figure S4.12). A 2-step punctuated change model was favored for *B. seminuda* megalospheric morphotypes, with the two breakpoints estimated at 1900 CE and 1978 CE (Figure S4.12).

We then examined whether median shell areas are correlated across species' morphotype pairs, and find that body size is weakly correlated among reproductive morphotypes through time (Figure S4.13). Changes in most species' reproductive morphotype shell areas are weakly positively correlated, though some morphotype pairs exhibit moderately strong negative correlations (Table S4.4). Correlations exist between all morphotype pairings (megalospheric-megalospheric, microspheric-microspheric, and megalospheric-microspheric). This is similar to our finding of correlated size shifts across all species within the core interval (Figure 4.3), though fewer strong correlations exist.

To test whether the mixing of morphotypes could contribute to overall size distributions, we examined the relationship between shell area and the prevalence of reproductive morphotypes (represented here as the proportion of megalospheric, or asexually-produced, individuals in a sample; Figure 4.5). We find that the prevalence of asexual reproductive mode is a significant predictor of mean shell area for all species in species-specific linear models ($p << 0.01$), explaining a moderate proportion of body size variation in *B. argentea* and *B. seminuda (*$R^2 = 0.25$ and 0.23, respectively) and fails to explain any body size variation in *B. alata* and *B. spissa*

($R^2 \approx 0$; Table 4.2). Within *B. argentea* and *B. seminuda*, more recent post-breakpoint samples often have lower amounts of asexually-produced individuals and correspond with smaller mean body sizes (Figure 4.5).

The temporal trends we observe in the reproductive morphotypes we examine suggest that strong size dimorphism in species *B. argentea* and *B. seminuda*, coupled with shifts in the prevalence of reproductive morphotypes within samples that occurs in the 19th century contribute to the size decreases observed in those species (Figure 4.2). Notably, both megalospheric and microspheric *B. argentea* morphotypes decrease in size towards the recent, while the megalospheric *B. seminuda* morphotype undergoes fluctuations before reaching a decreased mean following the mid-20th century breakpoint (Figure S4.12).

4.3.5 Environmental correlates of size

Food resource availability and oxygenation are often major determinants of body size in benthic foraminifera (Hallock 1985, Nigam and Rao 1987, Schmidt et al. 2018, Belanger 2022). As a proxy for food resource availability, we used data on total nitrogen (TN) (Table S4.3). In the specialized habitat of the SBB, benthic foraminifera are adapted to low-oxygen environments, and can use nitrate as an alternate electron acceptor in place of oxygen during respiration (Risgaard-Petersen et al. 2006, Piña-Ochoa et al. 2010). We used data on oxygenation state and redox state reconstructed from redox-sensitive metals alongside nitrogen isotope ratios ($\delta^{15}N$) as indications of oxygenation and respiration ability (Table S4.3).

We evaluated the impacts of food, oxygenation, and major environmental variables on body size for all species spanning the composite core interval (1249-2008 CE; Figure S4.14) using additive linear models. In these models, $\delta^{15}N$ was a significant ($p < 0.01$) predictor of long-transformed mean size for three of seven species (*B. alata*, *B. pacifica*, and *B. spissa*). For *Bolivina alata*, $\delta^{15}N$, a reducing environment index (Wang and Hendy 2021), and a 21-year running biweight ENSO variance (Li et al. 2011) were significant and positive predictors of size with an adjusted R^2 of 0.47. For *Bolivina pacifica*, only $\delta^{15}N$ was a significant and negative predictor of size ($R^2 = 0.48$), while for *Bolivina spissa*, $\delta^{15}N$ was a significant and positive predictor for size alongside TN ($R^2 = 0.47$). For all other species from the composite core interval (*B. argentea*, *B. seminuda*, *B. exilis*, and *B. eckisi*), no variables tested were significant predictors of size, and no models performed better than a null model in model comparisons (Table 4.2). Similar results were seen in linear mixed models with species held as a random effect (see Supplemental Information for linear mixed model results). When additional environmental variables were included as predictors (ENSO, PDO, SST) alongside an indicator of asexuality, none were significant, and the simpler model was preferred in model selection.

We perform similar model testing on box core data, which contained 5 additional species (*C. crassa*, *C. ovoidea*, *F. cornuta*, *G. sublobosa*, and *N. stella*) with data from the interval from 1834-2008 CE (Figure S4.15). In additive linear model testing, $\delta^{15}N$, TN, and an index for Pacific Decadal Oscillation (PDO; MacDonald and Case 2005) were significant predictors of body size ($p < 0.01$, $R^2 = 0.67$) for *C. crassa*. In *F. cornuta*, TN was a significant and positive predictor of body size ($R^2 = 0.23$). For all other species from the box core interval (*C. ovoidea, G. subglobosa, N. stella*), no variables tested were significant predictors of size, and no models performed better than a null model in comparisons (Table 4.2). For all other species from the

composite core interval (*C. ovoidea*, *G. subglobosa*, and *N. stella*), no variables tested were significant predictors of size, and no models performed better than a null model in model comparisons (Table 4.2).

Because our data span into the post-1950 era for which direct instrumental data is available, we can examine how direct measurements of food and oxygen availability from the CalCOFI database for a subset of the core (1953-2008 CE) impact body size in benthic foraminifera from the SBB (Figure S4.16). When we fit a linear model with oxygen saturation (O_2), phosphate (PO_4), nitrite (NO_2), nitrate (NO_3), and bottom water temperature as predictors of shell area (Figure S4.14), we find that none of these variables are significant predictors of species' mean shell areas in either model type (additive linear and linear mixed). Models including these variables were not favored over a null model in comparisons.

4.4 Discussion

The size distributions we generated allow for assessment of how species-specific trends in size affect community-level body size distributions over the ~760-year-long interval we examine. We find that intraspecific body size within SBB benthic foraminifera is affected by both life history and environmental parameters, and that changes to intraspecific size distributions due to these factors play a large role in structuring community-level body sizes towards the present day.

4.4.1 Relative stability of body size distributions through time, with recent shifts in some species

Species' overall shell area (i.e., body size) distributions are relatively stable through time, both within and across benthic foraminifer species (Figure 4.1). Yet interspecific mean sizes through time decrease by approximately a factor of three towards the present day (Figure S4.6), with the mode models we tested suggesting that a step change in community-level size occurs in the mid-20th century for biserial benthic foraminifera in the SBB.

Community-level changes are driven by mixed, species-specific size dynamics. A number of species exhibit stasis, with body sizes generally fluctuating around a common mean for the entirety of the interval we examine. While one of these species, *B. exilis*, is fairly common (Table S7), the others, *B. alata* and *B. spissa*, are less so. In contrast, the four species for which a punctuated change model is favored (*B. argentea*, *B. pacifica*, *B. seminuda*, and *S. eckisi*) are among the most abundant species in the SBB (Table S7). Notably, the two species who show stepped increases in body size (*B. pacifica* and *S. eckisi*) tend to be smaller than the other biserial species we examine, with mean shell areas that represent 83-92% of the average shell area of their congeners (Figure 4.2). The general tendency towards correlated size shifts, particularly at smaller sizes, suggests that size changes are much more likely to occur when species are smaller (Figure S4.8). This size decrease in prominent compositional species explains the community-level size changes we observe.

4.4.2 Changes in prevalent reproductive mode are an important influence on changes in size distributions in some species

We also find that reproductive mode affects overall size in species with reproductive mode dimorphism. Three species (*B. argentea*, *B. seminuda*, and *B. spissa*) with large variation in

reproductive mode have larger mean megalospheric individuals than mean microspheric individuals (Figure 4.4A). The difference in body size distributions we observe between megalospheric (asexually-produced) and microspheric (sexually-produced) individuals suggests that the external factors that drive reproductive mode ratios (i.e., the proportion of asexual reproduction within each sample) may also facilitate larger terminal sizes. Size differences seen through time (e.g., Figures 1, 2) may be a result of overall shell area being largely determined by proloculus area.

The differences in body size distributions we observe are generally consistent with predictions that arise from other studies of the relationship between foraminifer body size and proloculus size. A recent study by Belanger (2022) determined that individuals achieve large sizes by having a large initial chamber (proloculus) and not high growth rates; thus terminal size is a result of propagule size, and larger sizes should be seen primarily in asexually-produced individuals. This prediction is supported by our data: megalospheric individuals, which begin with a larger initial chamber, often have higher width-to-length ratios than microspheric individuals (with the exception of *B. alata*, which also tends towards larger microspheric individuals; Figure 4.4). Because each new chamber added has been shown to increase volume by a fixed proportion (Belanger 2022), individuals that begin with a larger proloculus subsequently have larger chambers than their conspecifics with smaller prolocuili. Another factor that may cause terminal size differences is differential timing of reproduction or death among the various generations. For instance, relatively rapid reproduction among the microspheric agamonts would transfer greater numbers of smaller-sized empty microspheric tests to the fossil pool.

Consequently, when there are high numbers of megalospheric individuals in a sample (i.e., asexual blooms due to multiple intermittent schizont generations), shell areas are generally larger for most of the biserial foraminifera we examine (Figure 4.5). The proportion of asexual individuals in a sample is a significant and positive predictor of shell area for all species across the composite core interval, but is a negative predictor for *B. spissa* in pre-1850 data and a negative predictor for *B. alata* in post-1850 data (Table 4.2). However, both *B. alata* and *B. spissa* have relatively low abundances in these samples, and as such further data may be required to verify these trends.

4.4.3 Reproductive mode structures community-level size distributions

Taken together, our data suggest that the changes to reproduction shown to occur in the mid-19th century (Chapter 3 of this dissertation) alter body size distributions within these species. For species with smaller differences between body size distributions of reproductive morphs (namely, *B. alata* and *B. spissa*), temporal trends in mean size exhibit stasis, with little changes to body size distributions in spite of the large shifts in the prevalence of reproductive mode that occur over this interval. However, species with strong positive relationships between reproductive mode and body size show significant size shifts towards the recent, suggesting that reproductive life history changes impact size distributions within these species.

The stepped decreases in size we observe for *B. argentea*, a species with strong dimorphism in proloculus size between reproductive morphotypes, is placed at 1820 CE for microspheric individuals and 1965 CE for megalospheric individuals (Figure S4.12). Notably, the 1820 CE

date for microspheric size decreases corresponds roughly with the mid-19th century changes in reproduction observed, suggesting that the shift towards smaller body sizes within microspheric individuals occurs at a time when microspheric individuals make up a higher proportion of *B. argentea* within the basin. Megalospheric *B. argentea* undergo a later size decrease, with the smallest megalospheric sizes observed over the past ~760 years occurring following this mid-20th century breakpoint. Further, *B. argentea* microspheric mean sizes are larger than megalospheric mean sizes following 1965 CE.

More complex trends are observed for *B. seminuda*. The best-fit maximum likelihood model for microspheric *B. seminuda* is one of stasis (Figure S4.12). However, few to no microspheric *B. seminuda* are observed prior to ~1800 CE, thus barring examination of longer-term trends for this morphotype. Yet the relative abundance of microspheric *B. seminuda* increases following the 19th century. Because microspheric *B. seminuda* have smaller average shell areas than their megalospheric counterparts, increases in microsphere abundances combined with the stepped size decrease we observe in megalospheric *B. seminuda* following the mid-20th century may contribute to overall size decreases we observe for this species (Figure 4.2). Notably, size dynamics with megalospheric *B. seminuda* suggest that this morphotype has undergone multiple stepped size shifts following ~1900 CE. While the data we use preclude analysis of ontogeny, it is important to note that these stepped size shifts could be driven by differences in assemblage age structure through time, and future work is needed to test the potential demographic drivers of size shifts. Regardless, these data indicate that morphotype-specific temporal dynamics (e.g., environmentally-induced shifts in timing of reproduction or death) can occasionally be more complex than species-level trajectories may imply.

The broader ecological implications of these shifted size distributions warrant further study. Increases in the proportion of microspheric individuals within modern samples during the mid-19th century are often followed by changes to body size within these same species, though size shifts may pre-date, occur synchronously, or lag far behind the timing of species-specific reproductive change. Though not all of the species we examine here have large size dimorphism among their reproductive morphs (and, as a result, their reproductive trends could not be studied in our data), the size-reproduction relationships we observe suggest that changed in the prevalence of reproductive modes play a role in shaping community-level biomass distributions within the SBB. Incorporating considerations of both body size and reproductive life history into future work investigating temporal ecosystem dynamics–though the collection and analysis of individual-level morphological data–may help to illuminate ecological shifts that may otherwise be overlooked.

4.4.4 Food and oxygenation play a role in structuring intraspecific size distributions

Our data also suggest that some, but not all, of the common species within the SBB exhibit significant correlations between body size distributions and food and oxygen availability. $\delta^{15}N$, a common significant predictor in our models, is typically interpreted as an oxygenation proxy, where more positive $\delta^{15}N$ indicates higher amounts of denitrification resulting from strengthened oxygen-deficient conditions (Davis et al. 2019, Xu et al. 2022). In *B. alata*, *B. spissa*, and *C. crassa*, $\delta^{15}N$ is positively correlated with body size, such that higher levels of denitrification, or lower levels of oxygen, correspond with larger body sizes in these species. In contrast, $\delta^{15}N$ is

negatively correlated with body size in *B. pacifica*, such that higher oxygenation corresponds with smaller body sizes in this species.

Oxygenation is known to structure species diversity within the Santa Barbara Basin (Bernhard and Reimers 1991, Bernhard et al. 1997, 2000, Hill et al. 2003, Moffitt et al. 2014, Myhre et al. 2017a, 2017b), but its impact on body size within hypoxia-tolerant species is less well established. The common benthic foraminifera we examine here are known to endure intermediate to strong hypoxia (e.g., <0.3 ml L^{-1} O_2), and some are considered hypoxic extremophiles (i.e., *N. stella*) that have been reported to survive for up to a month under strong hypoxic conditions (< 0.02 ml L^{-1} O_2) (Bernhard et al. 2000, 2012, Risgaard-Petersen et al. 2006, Piña-Ochoa et al. 2010). The most abundant species within the assemblages we examine are predominantly from clades within which denitrification is a common trait, and many have been directly shown to undergo denitrification (Woehle et al. 2022).

Our models suggest that some SBB species' body sizes may be impacted in complex and contrasting ways by increased hypoxia. We show that *B. alata*, *B. spissa*, and *C. crassa* increase in size with increasing amounts of hypoxia and denitrification, while *B. pacifica* decreases in size with increasing hypoxia. These relationships to oxygenation are intriguing, as they suggest that increasing levels of hypoxia projected in the California Current under high-emissions climate change scenarios (Chan et al. 2008, Pozo Buil et al. 2021) may alter biomass distributions within some common species within the SBB. Yet, notably, the majority of the species we examine have no significant relationship to oxygenation. These findings are consistent with a recent study which found that the largest foraminifera were found within samples with the lowest oxygen concentrations during a deglacial deoxygenation event, yet the significance of oxygen as a predictor of size varied across species (Belanger 2022).

In addition to oxygenation, the influx of food resources via particulate matter has been shown to structure benthic foraminifer assemblages in experimental settings (Duijnstee et al. 2003, Ernst et al. 2005), and is thought to be a major factor in determining species' biovolume distributions (Belanger 2022). Benthic foraminifera use surface sediments or particulate organic matter as food sources and are thought to uptake introduced carbon and nitrogen in differential amounts, likely dependent on their biomass and specific feeding preferences (Enge et al. 2014). In our models, we use total nitrogen (TN) as an indicator of food availability (and note that it is highly correlated with TOC, another common food indicator; Wang et al. 2019). TN is positively correlated with body size in three species: *B. spissa*, *C. crassa*, and *F. cornuta*, suggesting that increased amounts of food within the SBB system may drive body size increases among portions of the benthic foraminifer community. The influence of nitrogen supply on body size may increase under projected climate scenarios, which project increased nitrogen supply to the SBB throughout the 21st century (Rykaczewski and Dunne 2010).

It is likely that both oxygenation and food resource availability play a role in structuring benthic foraminifer size distributions, particularly in the time-averaged samples that come from SBB cores. While the SBB is renowned for its high-resolution sediments, the seasonal-to-annual resolution that these samples provide may collapse information about how foraminifera respond to short-term changes in oxygenation and food availability resulting from sub-seasonal organic matter flux. In experimental settings, oxygenation and organic flux have been shown to structure

species distributions across different scales: oxygen is considered to structure foraminiferal density and vertical distributions within sediment over short time periods (< 2 weeks), while organic flux is likely more important in maintaining species composition and density over longer time periods (> 4 weeks) (Ernst et al. 2005). Larger-scale climatic phenomena like ENSO and PDO (found to be significant predictors of size in two species, *B. alata* and *C. crassa*, respectively) also drive oxygenation and particulate matter influx on annual to decadal timescales. Higher-resolution, sub-seasonal data are needed to understand the complex interplay between seasonal oceanographic dynamics and foraminifer body size within the SBB, and how short-term drivers of community structure (such as oxygenation events) impact the growth trajectories of individuals across their lifetimes.

4.4.5 Stasis and punctuated change in benthic foraminifer body size trajectories

It is unsurprising that size stasis is a shared trend across a number of the species (Figure 4.2) and morphotypes (Figure S4.12) we examine. Stasis is commonly observed at the microevolutionary timescales relevant for population dynamics (Uyeda et al. 2011, Gotanda et al. 2015, Rollinson and Rowe 2015, Hunt et al. 2015). Some studies suggest that life history trade-offs may counteract potential directional size selection and play a role in stabilizing size distributions over time (Rollinson and Rowe 2015). The punctuated changes that we observe–where species undergo a step change in size distributions from one stasis state to another–may also be linked to shifts in life-history tradeoffs, as the species undergoing punctuated change show lagged or concurrent shifts in the prevalence of reproductive modes.

Because life history tradeoffs are directly recorded in the shell morphology of many benthic foraminifera (Nigam and Rao 1987, Saraswat et al. 2011, Schmidt et al. 2018), they are a rich study system in which to examine the impacts of these tradeoffs on size on both macroevolutionary and microevolutionary timescales. While volumetric and chamber-specific size analyses are outside of the scope of this work, future studies examining the relationship between individuals' proloculus sizes and overall growth trajectories in SBB benthic foraminifera could be useful for understanding the size impacts of life history tradeoffs on foraminifer communities.

Though there has been little previous work on benthic foraminifer body size within the SBB, previous studies of benthic foraminifer abundance and community-level diversity show that these organisms are affected by both climatic and anthropogenic stressors, both within the basin and in other systems worldwide (Yasuhara et al. 2012, 2016, Dey et al. 2012). The impacts of environmental change on body size among SBB benthic foraminifera we observe are species-specific, yet community-level body sizes changes indicate that modern (i.e., post mid-20th century) body sizes within the SBB are significantly different, and smaller, from those of the preceding ~700 years. Further work examining individual-level body size distributions among these species that extends the temporal duration of our data beyond 2008 CE is needed. Modern changes to the California Current system in which the SBB is located–which include intensifying hypoxia, increasing food supply to the seafloor resulting from warming surface waters, increased stratification, and changes to the deepwater nutrient supply (Chan et al. 2008, Rykaczewski and Dunne 2010, Pozo Buil et al. 2021)–will impact individual physiology and morphology and may drive further size decreases within SBB benthic foraminifera.

Our data suggest that these changes may be reflected in intraspecific and community-level biomass distributions within the basin and may be offset from significant changes to community-level diversity. The biomass shifts we observe are often lagged–sometimes earlier, sometimes later–in comparison to shifts in abundance (see Chapters 3 and 5 of this dissertation). Changes in body size variation may signal the impacts of environmental change prior to changes in species richness, and also serve as an indicator of the extent of these impacts on individual variation, life histories, and population dynamics.

Chapter 4 Figures

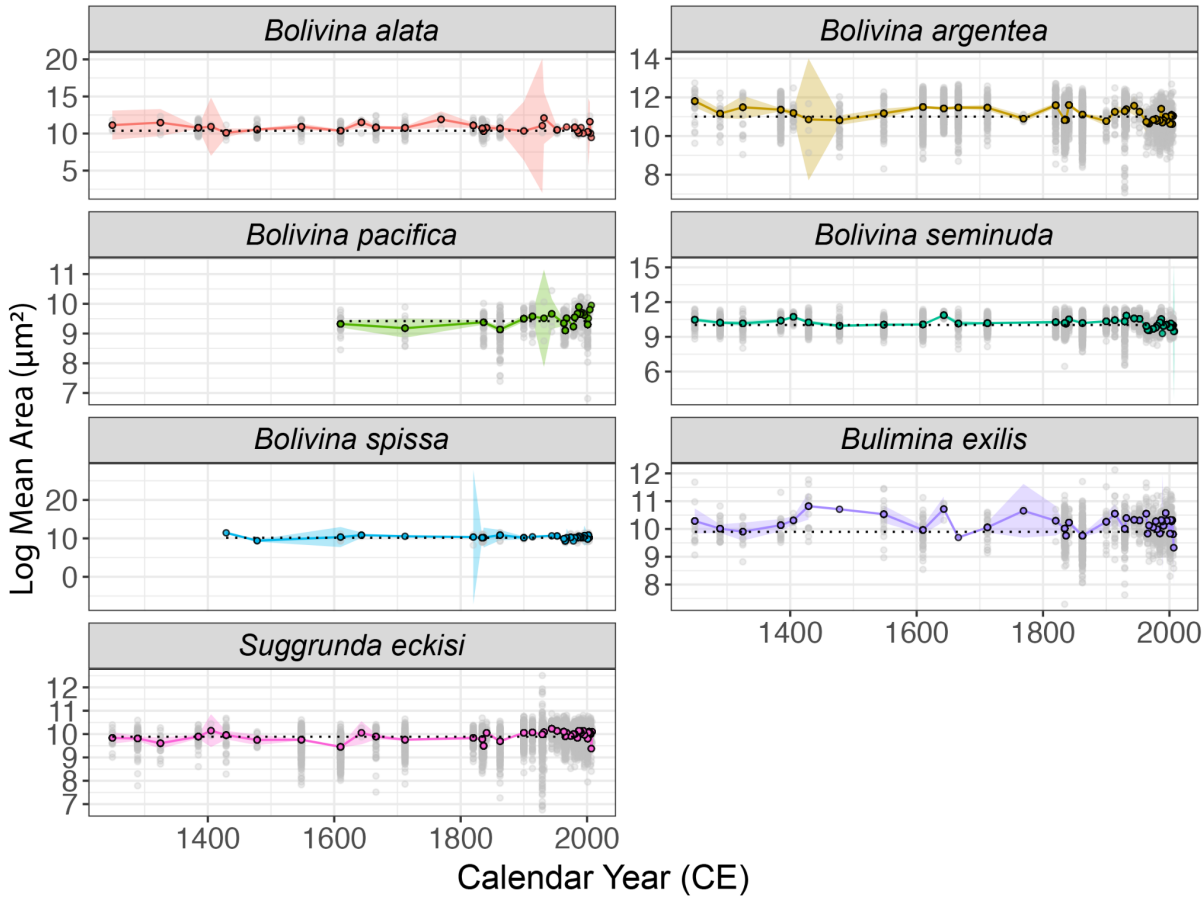

Figure 4.1: Time series of mean body size among species collected from the composite core sequence.
Colored points represent mean body size at each time point, while colored shaded regions represent 95% confidence intervals. Gray points denote individual size measurements; dashed lines indicate overall mean size for each species, calculated from composite data.

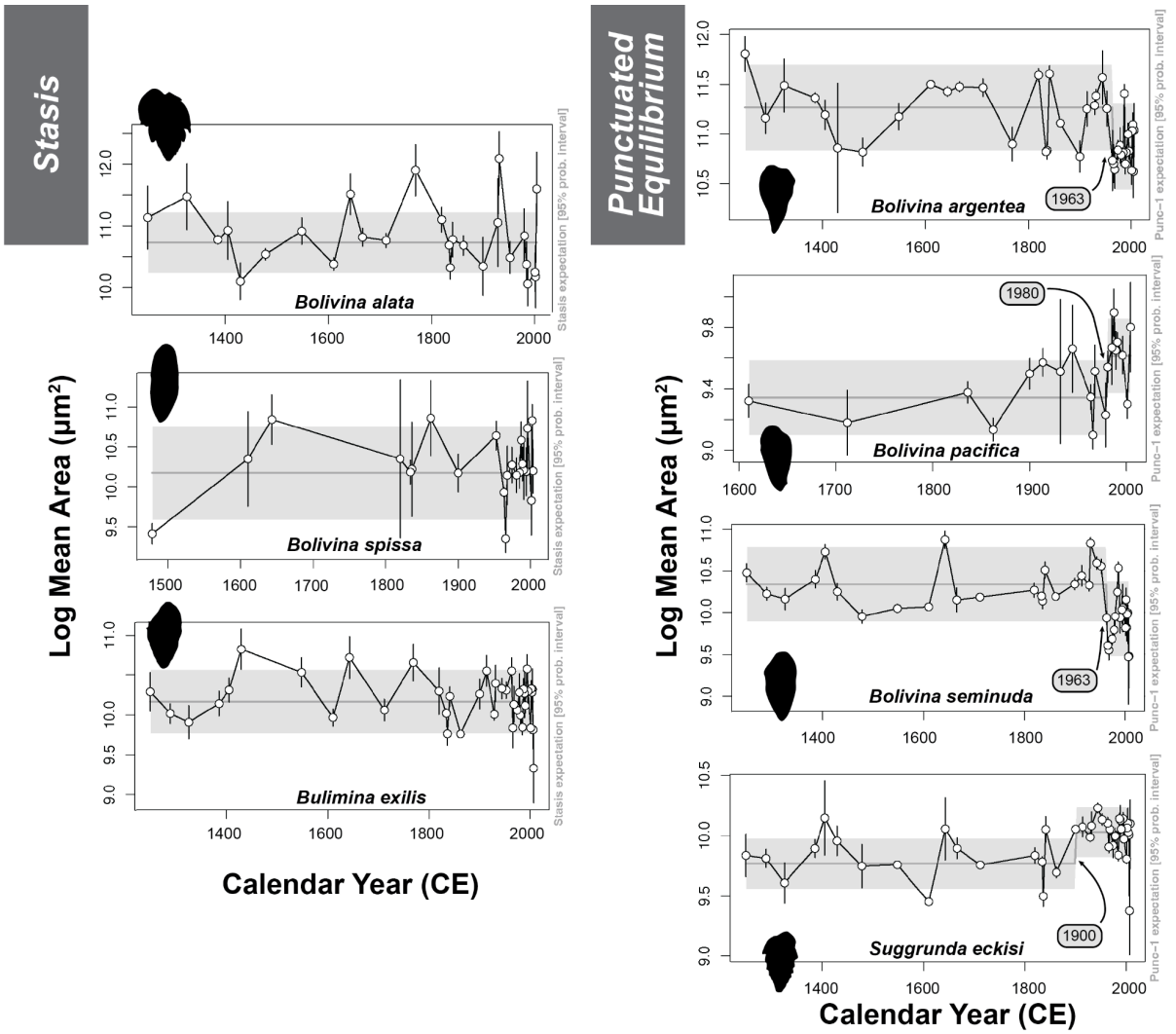

Figure 4.2: Best-fit models for ~760-year temporal trends of species' mean areas favor stasis and punctuated change.
Models were run only for those species for which individual-level data was collected beyond 1834 CE. Species-specific mean areas are denoted by open circles, with standard deviations marked by error bars. Solid grey lines indicate the overall model mean, while shaded grey areas denote 95% confidence intervals. Stasis is the best fit model for three species (*B. alata*, *B. seminuda*, and *B. exilis*), where species' body sizes at each time point fluctuate around a constant mean. A 1-step punctuated change model is the best fit for the remaining four species (*B. argentea*, *B. pacifica*, *B. seminuda*, and *S. eckisi*), where long periods of stasis around a mean are interrupted by sudden shifts to a new mean state. Estimated step-points are marked on each timeseries.

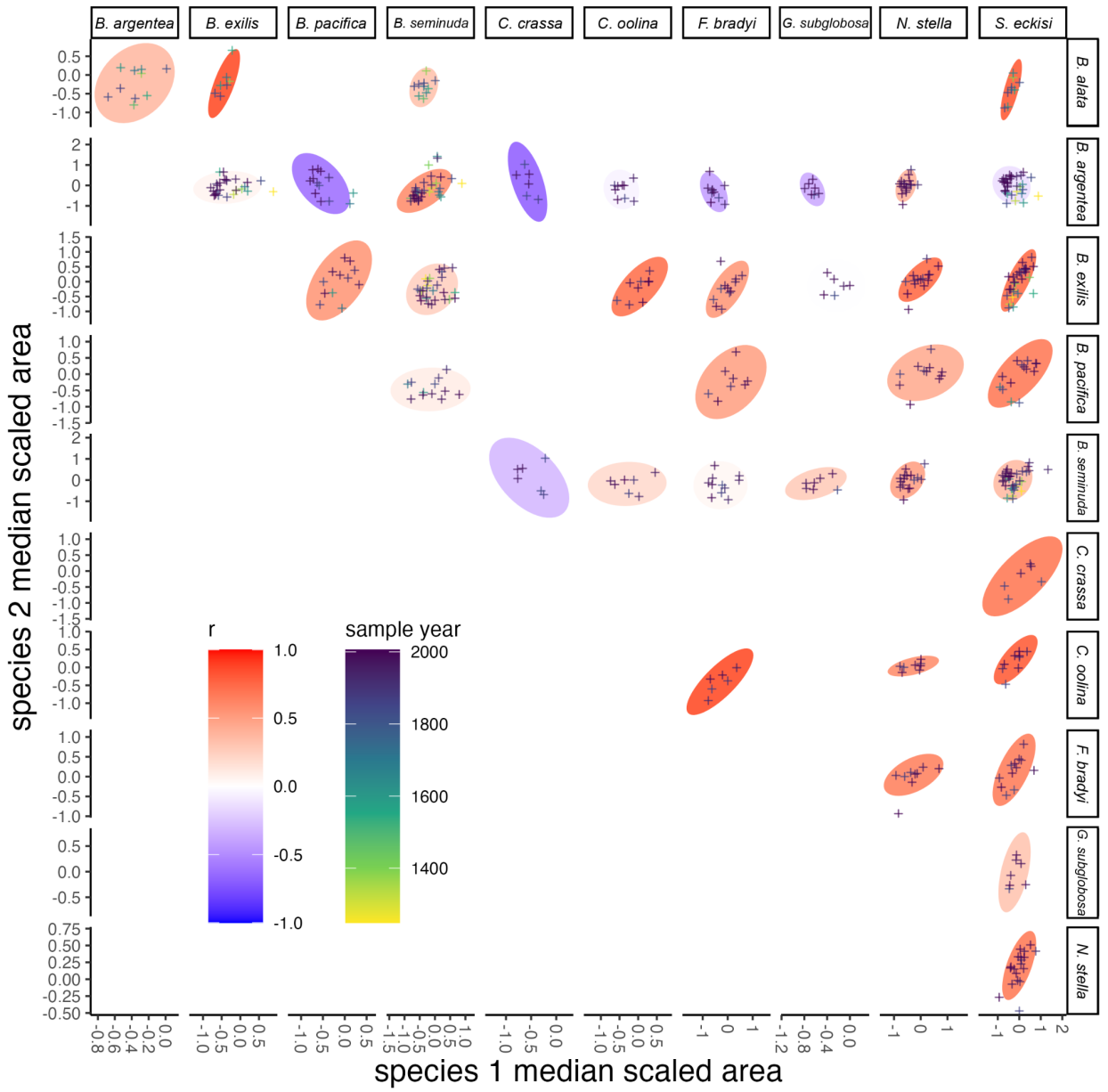

Figure 4.3: Median size is generally weakly to strongly positively correlated across species pairs through time.
Ellipse direction, aspect ratio, and color indicates the strength and direction of correlations between species pairs, with red colors denoting positive correlations (Spearman's ρ) and blue colors indicating negative correlations. Points indicate the number of samples in which species co-occur with sufficient numbers of individuals of both species, with point colors denoting the age of these samples (darker colors denote more recent samples, while lighter colors denote older samples). Missing ellipses denote species pairs for which samples were insufficient to calculate correlations. Pairings between most species and *B. argentea* and *C. crassa* are typically negatively correlated, a notable exception to the general trends towards positive correlations.

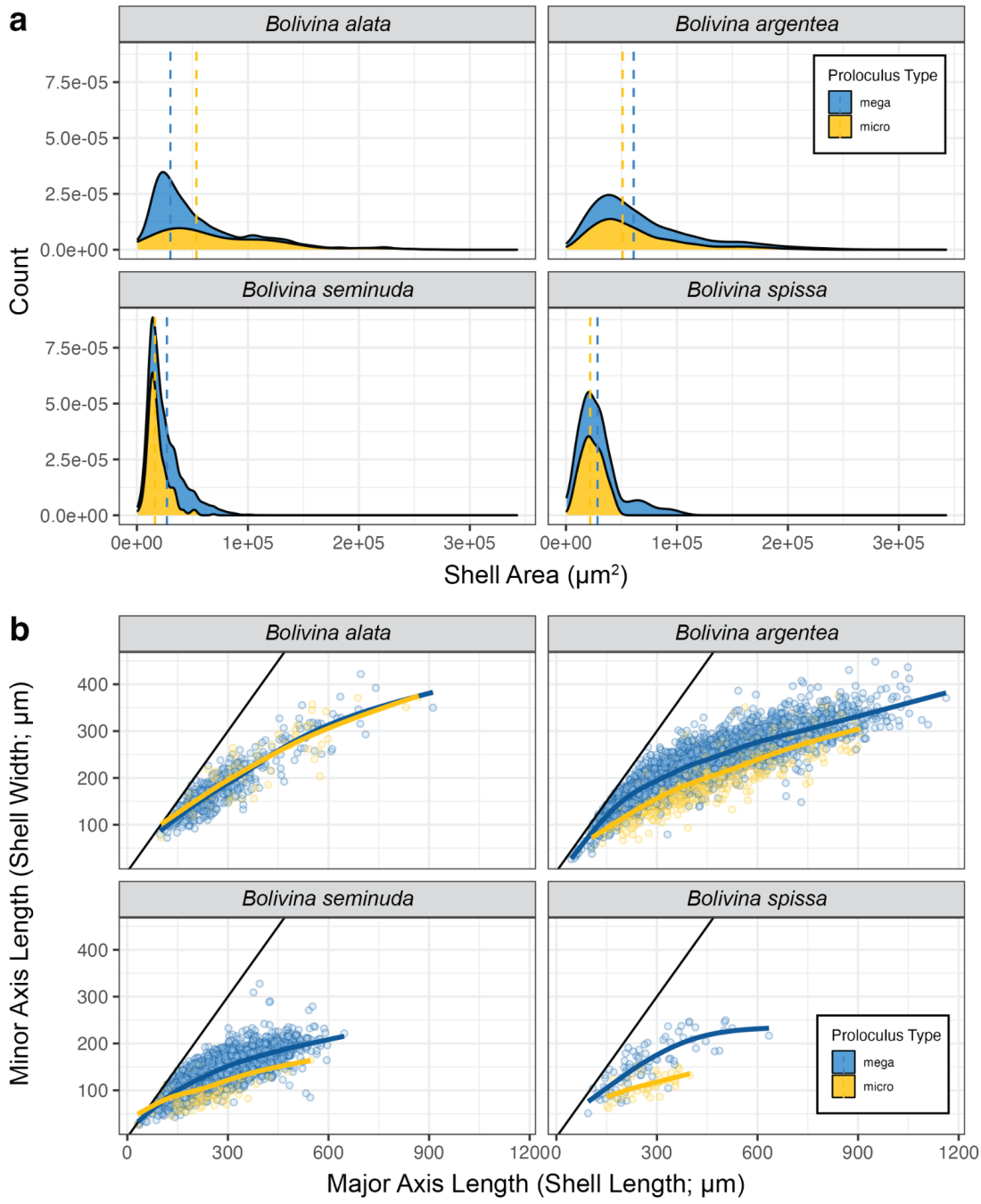

Figure 4.4: Megalosphere and microsphere areas differ across species.
(a) Stacked proportional frequency histograms show that most megalospheric *Bolivina* have larger body size distributions than microspheric conspecifics, with the exception of *B. alata*. Colors denote proloculus type; dashed lines indicate median size. (b) Shell length-width ratios show that reproductive morph area differences typically emerge via changes to shell widths; megalospheric individuals are often wider than microspheric individuals of a similar length. Solid colored lines indicate generalized additive model fits, while the identity line is denoted in black.

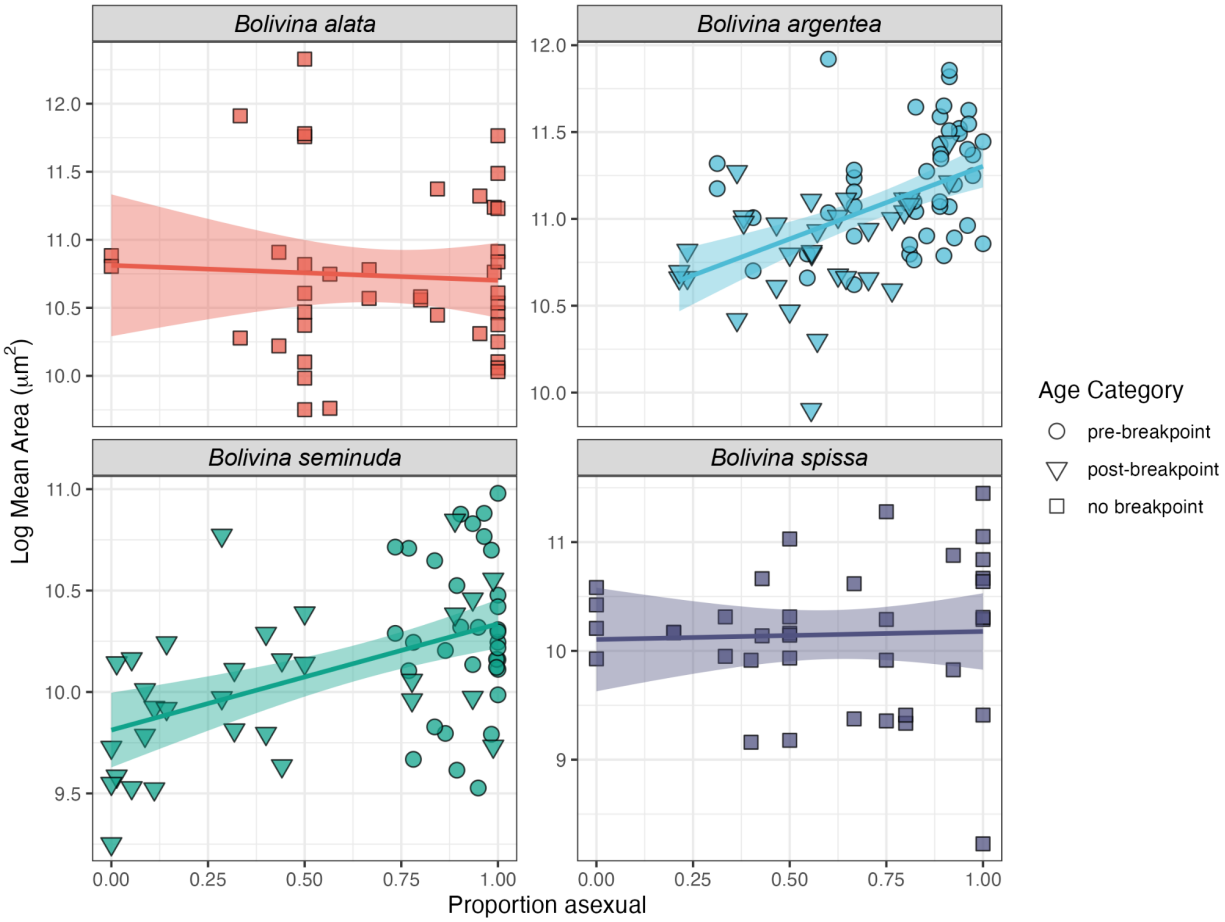

Figure 4.5: Mean body size distributions are positively correlated with the proportion of megalospheric (asexually-produced) individuals in a sample for some species.
Shapes denote data from punctuated change or stasis time steps for each species: circles show data points from steps prior to the species-specific breakpoints, while triangles show data points from steps following breakpoints. Squares denote species for which stasis was the favored model. Linear regressions are indicated by colored lines, with shaded regions showing the model 95% confidence interval ($p << 0.01$ for all species). In *B. argentea* and *B. seminuda*, post-breakpoint samples often have lower amounts of asexually-produced individuals alongside that correspond with smaller mean body sizes.

Chapter 4 Tables

Table 4.1: Correlations between species pairs for 50th (median) and 10th percentiles.

Species Pair	Percentile	Pair Count	r (Spearman's ρ)
C. oolina-F. bradyi	50% (median)	12	0.79
B. alata-B. exilis	50% (median)	14	0.78
B. alata-S. eckisi	50% (median)	18	0.73
C. oolina-S. eckisi	50% (median)	18	0.72
B. exilis-N. stella	50% (median)	30	0.66
B. exilis-S. eckisi	50% (median)	60	0.66
B. exilis-C. oolina	50% (median)	18	0.64
C. crassa-S. eckisi	50% (median)	12	0.61
B. pacifica-S. eckisi	50% (median)	28	0.6
N. stella-S. eckisi	50% (median)	38	0.6
F. bradyi-S. eckisi	50% (median)	24	0.59
F. bradyi-N. stella	50% (median)	18	0.57
B. argentea-B. seminuda	50% (median)	66	0.52
C. oolina-N. stella	50% (median)	16	0.52
B. exilis-B. pacifica	50% (median)	24	0.47
B. exilis-F. bradyi	50% (median)	24	0.47
B. seminuda-N. stella	50% (median)	32	0.44
B. pacifica-F. bradyi	50% (median)	16	0.43
B. pacifica-N. stella	50% (median)	22	0.39
B. argentea-N. stella	50% (median)	34	0.35
B. alata-B. argentea	50% (median)	20	0.32
B. seminuda-S. eckisi	50% (median)	68	0.32
B. alata-B. seminuda	50% (median)	20	0.28
G. subglobosa-S. eckisi	50% (median)	14	0.27
B. seminuda-G. subglobosa	50% (median)	14	0.24
B. exilis-B. seminuda	50% (median)	56	0.22
B. seminuda-C. oolina	50% (median)	14	0.17
B. pacifica-B. seminuda	50% (median)	24	0.09
B. argentea-B. exilis	50% (median)	54	0.05
B. seminuda-F. bradyi	50% (median)	22	0.04
B. exilis-G. subglobosa	50% (median)	12	0
B. argentea-C. oolina	50% (median)	18	-0.04
B. argentea-S. eckisi	50% (median)	66	-0.12

Species Pair	Percentile	Pair Count	r (Spearman's ρ)
B. seminuda-C. crassa	50% (median)	12	-0.27
B. argentea-G. subglobosa	50% (median)	14	-0.32
B. argentea-F. bradyi	50% (median)	20	-0.36
B. argentea-B. pacifica	50% (median)	26	-0.55
B. argentea-C. crassa	50% (median)	12	-0.61
C. oolina-N. stella	10%	16	0.88
B. seminuda-C. oolina	10%	14	0.87
F. bradyi-S. eckisi	10%	24	0.81
C. oolina-F. bradyi	10%	12	0.76
B. pacifica-S. eckisi	10%	28	0.74
C. crassa-S. eckisi	10%	12	0.74
B. pacifica-F. bradyi	10%	16	0.71
B. seminuda-F. bradyi	10%	22	0.71
B. argentea-C. oolina	10%	18	0.7
F. bradyi-N. stella	10%	18	0.67
B. alata-S. eckisi	10%	18	0.67
B. exilis-S. eckisi	10%	60	0.67
B. seminuda-N. stella	10%	32	0.67
B. exilis-B. seminuda	10%	56	0.66
B. exilis-F. bradyi	10%	24	0.64
B. argentea-N. stella	10%	34	0.63
C. oolina-S. eckisi	10%	18	0.62
B. argentea-B. seminuda	10%	66	0.62
B. pacifica-B. seminuda	10%	24	0.62
B. argentea-F. bradyi	10%	20	0.6
B. argentea-B. exilis	10%	54	0.57
N. stella-S. eckisi	10%	38	0.55
B. exilis-N. stella	10%	30	0.52
B. alata-B. exilis	10%	14	0.48
B. seminuda-S. eckisi	10%	68	0.48
B. exilis-B. pacifica	10%	24	0.48
B. alata-B. argentea	10%	20	0.43
B. seminuda-G. subglobosa	10%	14	0.43
B. pacifica-N. stella	10%	22	0.42
B. exilis-C. oolina	10%	18	0.36

Species Pair	Percentile	Pair Count	r (Spearman's ρ)
B. seminuda-C. crassa	10%	12	0.25
G. subglobosa-S. eckisi	10%	14	0.24
B. argentea-S. eckisi	10%	66	0.2
B. alata-B. seminuda	10%	20	0.08
B. argentea-B. pacifica	10%	26	0
B. argentea-C. crassa	10%	12	-0.02
B. exilis-G. subglobosa	10%	12	-0.19
B. argentea-G. subglobosa	10%	14	-0.33

Table 4.2: Regression outputs of species-specific linear models examining relationships between environmental predictors and body size.
The temporal extent of each species' record is indicated alongside the best-fit model and key parameters: Adjusted R^2, slope (β), and p-value. Outputs of model comparisons are shown for each species, alongside parameters used in model selection: number of model parameters (K), size-adjusted Akaike Information Criterion (AICc), differences between AICc values for each model (ΔAICc), and relative likelihood (AICc weight).

Species	Age Range	Best Model	Adj. R^2	β	p-value	Predictors	K	AICc	ΔAICc	AICc Wt
Bolivina alata	1249-2008	mean size ~ $\delta^{15}N$ + Reducing + ENSO variance	0.47	$\delta^{15}N$: +1.369 Reducing: +0.139 ENSO Variance: +0.628	$\delta^{15}N$*** Reducing* ENSO Variance*	$\delta^{15}N$, Reducing, ENSO variance	5	30.23	0	1
						$\delta^{15}N$, Reducing	4	50.36	20.1	0
						$\delta^{15}N$, TN	4	54.48	24.3	0
						$\delta^{15}N$	3	57.88	27.7	0
Bolivina argentea	1249-2008	None	-	-	-	-	-	-	-	-
Bolivina pacifica	1249-2008	mean size ~ $\delta^{15}N$	0.48	$\delta^{15}N$: -0.466	$\delta^{15}N$*	$\delta^{15}N$	3	4.01	0	1
						$\delta^{15}N$, PDO	4	33.28	29.3	0
Bolivina seminuda	1249-2008	None	-			-	-	-	-	-
Bolivina spissa	1249-2008	mean size ~ $\delta^{15}N$ + TN	0.47	$\delta^{15}N$: +0.552 TN: +5.200	$\delta^{15}N$* TN*	$\delta^{15}N$	4	27.51	0	0.55
						$\delta^{15}N$, TN	6	28.24	0.73	0.38
						$\delta^{15}N$, TN, ENSO index, ENSO variance	3	31.83	4.32	0.06
Bulimina exilis	1249-2008	None	-			-	-	-	-	-
Suggrunda eckisi	1249-2008	None	-			-	-	-	-	-
Cassidulina crassa	1843-2008	mean size ~ δ15N + TN + PDO	0.67	δ15N: +0.343 TN: +5.533 PDO: +0.420	δ15N** TN*** PDO**	$\delta^{15}N$, TN, PDO	5	0.42	0	0.97
						$\delta^{15}N$, TN	4	7.84	7.42	0.02
						$\delta^{15}N$, TN, ENSO variance	5	9.64	9.22	0.01

Species	Age Range	Best Model	Adj. R^2	β	p-value	Predictors	K	AICc	ΔAICc	AICc Wt
						$\delta^{15}N$	3	17.28	16.9	0
Chilostomella ovoidea	1843-2008	None	-	-	-	-	-	-	-	-
Fursenkoina cornuta	1843-2008	mean size ~ TN	0.23	TN: +2.525	TN**	TN	3	-6.79	0	0.77
						$\delta^{15}N$, TN	4	-4.32	2.47	0.23
Globo-cassidulina subglobosa	1843-2008	None	-	-	-	-	-	-	-	-
Nonionella stella	1843-2008	None	-	-	-	-	-	-	-	-
					* $p \leq 0.01$ ** $p \leq 0.001$ *** $p \approx 0$					

4.5 Chapter 4 References

Banse, K. 1976. Rates of Growth, Respiration and Photosynthesis of Unicellular Algae as Related to Cell Size—a Review1,2. Journal of Phycology 12:135–140.

Barneche, D. R., D. R. Robertson, C. R. White, and D. J. Marshall. 2018. Fish reproductive-energy output increases disproportionately with body size. Science 360:642–645.

Bé, A. W., and O. R. Anderson. 1976. Gametogenesis in planktonic foraminifera. Science 192:890–892.

Belanger, C. L. 2022. Volumetric analysis of benthic foraminifera: Intraspecific test size and growth patterns related to embryonic size and food resources. Marine Micropaleontology 176:102170.

Berke, S. K., D. Jablonski, A. Z. Krug, K. Roy, and A. Tomasovych. 2013. Beyond Bergmann's rule: size–latitude relationships in marine Bivalvia world-wide. Global Ecology and Biogeography 22:173–183.

Bernhard, J. M., K. R. Buck, M. A. Farmer, and S. S. Bowser. 2000. The Santa Barbara Basin is a symbiosis oasis. Nature 403:77–80.

Bernhard, J. M., K. L. Casciotti, M. R. McIlvin, D. J. Beaudoin, P. T. Visscher, and V. P. Edgcomb. 2012. Potential importance of physiologically diverse benthic foraminifera in sedimentary nitrate storage and respiration. Journal of Geophysical Research: Biogeosciences 117.

Bernhard, J. M., and C. E. Reimers. 1991. Benthic foraminiferal population fluctuations related to anoxia: Santa Barbara Basin. Biogeochemistry 15:127–149.

Bernhard, J. M., B. K. Sen Gupta, and P. F. Borne. 1997. Benthic foraminiferal proxy to estimate dysoxic bottom-water oxygen concentrations; Santa Barbara Basin, U.S. Pacific continental margin. Journal of Foraminiferal Research 27:301–310.

Blueweiss, L., H. Fox, V. Kudzma, D. Nakashima, R. Peters, and S. Sams. 1978. Relationships between body size and some life history parameters. Oecologia 37:257–272.

Brandon, J. A., W. Jones, and M. D. Ohman. 2019. Multidecadal increase in plastic particles in coastal ocean sediments. Science Advances 5:eaax0587–eaax0587.

Brown, J. H. 1995. Macroecology. University of Chicago Press.

Bryndum-Buchholz, A., D. P. Tittensor, J. L. Blanchard, W. W. L. Cheung, M. Coll, E. D. Galbraith, S. Jennings, O. Maury, and H. K. Lotze. 2019. Twenty-first-century climate change impacts on marine animal biomass and ecosystem structure across ocean basins. Global Change Biology 25:459–472.

Burton, O. J., B. L. Phillips, and J. M. J. Travis. 2010. Trade-offs and the evolution of life-histories during range expansion. Ecology Letters 13:1210–1220.

Calder, W. A. 1996. Size, function, and life history. Courier Corporation.

Caval-Holme, F., J. Payne, and J. M. Skotheim. 2013. Constraints on the Adult-Offspring Size Relationship in Protists. Evolution 67:3537–3544.

Chan, F., J. A. Barth, J. Lubchenco, A. Kirincich, H. Weeks, W. T. Peterson, and B. A. Menge. 2008. Emergence of Anoxia in the California Current Large Marine Ecosystem. Science 319:920–920.

Daufresne, M., K. Lengfellner, and U. Sommer. 2009. Global warming benefits the small in aquatic ecosystems. Proceedings of the National Academy of Sciences 106:12788–12793.

Davis, C. V., J. F. Ontiveros-Cuadras, C. Benitez-Nelson, A. Schmittner, E. J. Tappa, E. Osborne, and R. C. Thunell. 2019. Ongoing Increase in Eastern Tropical North Pacific

Denitrification as Interpreted Through the Santa Barbara Basin Sedimentary δ15N Record. Paleoceanography and Paleoclimatology 34:1554–1567.
DeLong, J. P., and T. M. Luhring. 2018. Size-dependent predation and correlated life history traits alter eco-evolutionary dynamics and selection for faster individual growth. Population Ecology 60:9–20.
Dey, M., D. Ganguly, C. Chowdhury, N. Majumder, and T. K. Jana. 2012. Intra-Annual Variation of Modern Foraminiferal Assemblage in a Tropical Mangrove Ecosystem in India. Wetlands 32:813–826.
Duijnstee, I., S. Ernst, and G. Van der Zwaan. 2003. Effect of anoxia on the vertical migration of benthic foraminifera. Marine Ecology Progress Series 246:85–94.
Enge, A. J., U. Witte, M. Kucera, and P. Heinz. 2014. Uptake of phytodetritus by benthic foraminifera under oxygen depletion at the Indian margin (Arabian Sea). Biogeosciences 11:2017–2026.
Ernst, S., R. Bours, I. Duijnstee, and B. van der Zwaan. 2005. Experimental effects of an organic matter pulse and oxygen depletion on a benthic foraminiferal shelf community. Journal of Foraminiferal Research 35:177–197.
Forster, J., A. G. Hirst, and D. Atkinson. 2012. Warming-induced reductions in body size are greater in aquatic than terrestrial species. Proceedings of the National Academy of Sciences 109:19310–19314.
Gardner, J. L., A. Peters, M. R. Kearney, L. Joseph, and R. Heinsohn. 2011. Declining body size: a third universal response to warming? Trends in Ecology & Evolution 26:285–291.
Gotanda, K. M., C. Correa, M. M. Turcotte, G. Rolshausen, and A. P. Hendry. 2015. Linking macrotrends and microrates: Re-evaluating microevolutionary support for Cope's rule. Evolution 69:1345–1354.
Guderley, H. 2004. Locomotor performance and muscle metabolic capacities: impact of temperature and energetic status. Comparative Biochemistry and Physiology Part B: Biochemistry and Molecular Biology 139:371–382.
Hallock, P. 1985. Why are larger Foraminifera large? Paleobiology 11:195–208.
Hendy, I. L., L. Dunn, A. Schimmelmann, and D. K. Pak. 2013. Resolving varve and radiocarbon chronology differences during the last 2000 years in the Santa Barbara Basin sedimentary record, California. Quaternary International 310:155–168.
Hill, T. M., J. P. Kennett, and H. J. Spero. 2003. Foraminifera as indicators of methane-rich environments: A study of modern methane seeps in Santa Barbara Channel, California. Marine Micropaleontology 49:123–138.
Hsiang, A. Y., K. Nelson, L. E. Elder, E. C. Sibert, S. S. Kahanamoku, J. E. Burke, A. Kelly, Y. Liu, and P. M. Hull. 2017. AutoMorph: Accelerating morphometrics with automated 2D and 3D image processing and shape extraction. Methods in Ecology and Evolution 9:605–612.
Hunt, G. 2006. Fitting and comparing models of phyletic evolution: random walks and beyond. Paleobiology 32:578–601.
Hunt, G. 2007. The relative importance of directional change, random walks, and stasis in the evolution of fossil lineages. Proceedings of the National Academy of Sciences 104:18404–18408.
Hunt, G. 2008a. Evolutionary patterns within fossil lineages: model-based assessment of modes, rates, punctuations and process. The Paleontological Society Papers 14:117–131.
Hunt, G. 2008b. Gradual or pulsed evolution: when should punctuational explanations be preferred? Paleobiology 34:360–377.

Hunt, G., and M. T. Carrano. 2010. Models and methods for analyzing phenotypic evolution in lineages and clades. The Paleontological Society Papers 16:245–269.
Hunt, G., M. J. Hopkins, and S. Lidgard. 2015. Simple versus complex models of trait evolution and stasis as a response to environmental change. Proceedings of the National Academy of Sciences 112:4885–4890.
Hunt, G., and M. G. Hunt. 2019. Package 'paleoTS.'
Hunt, G., and K. Roy. 2006. Climate change, body size evolution, and Cope's Rule in deep-sea ostracodes. Proceedings of the National Academy of Sciences 103:1347–1352.
Jones, W. A., and D. M. Checkley. 2019. Mesopelagic fishes dominate otolith record of past two millennia in the Santa Barbara Basin. Nature Communications 10:4564.
Kaminski, M. A., C. G. Cetean, and J. Tyszka. 2011. Nomenclature to describe the transition from multiserial to uniserial chamber arrangement in benthic foraminifera. Journal of Micropalaeontology 30:7.
Keating-Bitonti, C. R., and J. L. Payne. 2016. Physicochemical controls on biogeographic variation of benthic foraminiferal test size and shape. Paleobiology 42:595–611.
Keating-Bitonti, C. R., and J. L. Payne. 2017. Ecophenotypic responses of benthic foraminifera to oxygen availability along an oxygen gradient in the California Borderland. Marine Ecology 38:e12430.
Keating-Bitonti, C. R., and J. L. Payne. 2018. Environmental influence on growth history in marine benthic foraminifera. Paleobiology 44:736–757.
Kim, J. H., P. Ajani, S. A. Murray, J.-H. Kim, H. C. Lim, S. T. Teng, P. T. Lim, M.-S. Han, and B. S. Park. 2020. Sexual reproduction and genetic polymorphism within the cosmopolitan marine diatom Pseudo-nitzschia pungens. Scientific Reports 10:10653.
Koester, J. A., S. H. Brawley, L. Karp-Boss, and D. G. Mann. 2007. Sexual reproduction in the marine centric diatom Ditylum brightwellii (Bacillariophyta). European Journal of Phycology 42:351–366.
Li, J., S.-P. Xie, E. R. Cook, G. Huang, R. D'Arrigo, F. Liu, J. Ma, and X.-T. Zheng. 2011. Interdecadal modulation of El Niño amplitude during the past millennium. Nature Climate Change 1:114–118.
Lohbeck, K. T., U. Riebesell, and T. B. H. Reusch. 2012. Adaptive evolution of a key phytoplankton species to ocean acidification. Nature Geoscience 5:346–351.
Lotze, H. K., D. P. Tittensor, A. Bryndum-Buchholz, T. D. Eddy, W. W. L. Cheung, E. D. Galbraith, M. Barange, N. Barrier, D. Bianchi, J. L. Blanchard, L. Bopp, M. Büchner, C. M. Bulman, D. A. Carozza, V. Christensen, M. Coll, J. P. Dunne, E. A. Fulton, S. Jennings, M. C. Jones, S. Mackinson, O. Maury, S. Niiranen, R. Oliveros-Ramos, T. Roy, J. A. Fernandes, J. Schewe, Y.-J. Shin, T. A. M. Silva, J. Steenbeek, C. A. Stock, P. Verley, J. Volkholz, N. D. Walker, and B. Worm. 2019. Global ensemble projections reveal trophic amplification of ocean biomass declines with climate change. Proceedings of the National Academy of Sciences 116:12907–12912.
MacDonald, G. M., and R. A. Case. 2005. Variations in the Pacific Decadal Oscillation over the past millennium. Geophysical Research Letters 32.
Marañón, E., P. Cermeño, D. C. López-Sandoval, T. Rodríguez-Ramos, C. Sobrino, M. Huete-Ortega, J. M. Blanco, and J. Rodríguez. 2013. Unimodal size scaling of phytoplankton growth and the size dependence of nutrient uptake and use. Ecology Letters 16:371–379.
Marshall, D. J. 2008. Transgenerational Plasticity in the Sea: Context-Dependent Maternal Effects Across the Life History. Ecology 89:418–427.

Moczek, A. P., S. Sultan, S. Foster, C. Ledón-Rettig, I. Dworkin, H. F. Nijhout, E. Abouheif, and D. W. Pfennig. 2011. The role of developmental plasticity in evolutionary innovation. Proceedings of the Royal Society B: Biological Sciences 278:2705–2713.
Moffitt, S. E., T. M. Hill, K. Ohkushi, J. P. Kennett, and R. J. Behl. 2014. Vertical oxygen minimum zone oscillations since 20 ka in Santa Barbara Basin: A benthic foraminiferal community perspective. Paleoceanography 29:44–57.
Monarrez, P. M., N. A. Heim, and J. L. Payne. 2021. Mass extinctions alter extinction and origination dynamics with respect to body size. Proceedings of the Royal Society B: Biological Sciences 288:20211681.
Morten, S. D., and R. J. Twitchett. 2009. Fluctuations in the body size of marine invertebrates through the Pliensbachian–Toarcian extinction event. Palaeogeography, Palaeoclimatology, Palaeoecology 284:29–38.
Murray, C. S., A. Malvezzi, C. J. Gobler, and H. Baumann. 2014. Offspring sensitivity to ocean acidification changes seasonally in a coastal marine fish. Marine Ecology Progress Series 504:1–11.
Myhre, S. E., K. J. Kroeker, T. M. Hill, P. Roopnarine, and J. P. Kennett. 2017a. Community benthic paleoecology from high-resolution climate records: Mollusca and foraminifera in post-glacial environments of the California margin. Quaternary Science Reviews 155:179–197.
Myhre, S. E., D. Pak, M. Borreggine, J. P. Kennett, C. Nicholson, T. M. Hill, and C. Deutsch. 2017b. Oxygen minimum zone biotic baseline transects for paleoceanographic reconstructions in Santa Barbara Basin, CA. Deep-Sea Research Part II:0–1.
Nigam, R., and A. S. Rao. 1987. Proloculus size variation in recent benthic Foraminifera: Implications for paleoclimatic studies. Estuarine, Coastal and Shelf Science 24:649–655.
Payne, J. L., and N. A. Heim. 2020. Body size, sampling completeness, and extinction risk in the marine fossil record. Paleobiology 46:23–40.
Peters, R. H., and R. H. Peters. 1986. The ecological implications of body size. Cambridge university press.
Piazza, V., C. V. Ullmann, and M. Aberhan. 2020. Temperature-related body size change of marine benthic macroinvertebrates across the Early Toarcian Anoxic Event. Scientific Reports 10:4675.
Piña-Ochoa, E., S. Høgslund, E. Geslin, T. Cedhagen, N. P. Revsbech, L. P. Nielsen, M. Schweizer, F. Jorissen, S. Rysgaard, and N. Risgaard-Petersen. 2010. Widespread occurrence of nitrate storage and denitrification among Foraminifera and Gromiida. Proceedings of the National Academy of Sciences 107:1148–1153.
Pozo Buil, M., M. G. Jacox, J. Fiechter, M. A. Alexander, S. J. Bograd, E. N. Curchitser, C. A. Edwards, R. R. Rykaczewski, and C. A. Stock. 2021. A Dynamically Downscaled Ensemble of Future Projections for the California Current System. Frontiers in Marine Science 8.
Pyenson, N. D., and G. J. Vermeij. 2016. The rise of ocean giants: maximum body size in Cenozoic marine mammals as an indicator for productivity in the Pacific and Atlantic Oceans. Biology Letters 12:20160186.
Risgaard-Petersen, N., A. M. Langezaal, S. Ingvardsen, M. C. Schmid, M. S. M. Jetten, H. J. M. Op den Camp, J. W. M. Derksen, E. Piña-Ochoa, S. P. Eriksson, L. Peter Nielsen, N. Peter Revsbech, T. Cedhagen, and G. J. van der Zwaan. 2006. Evidence for complete denitrification in a benthic foraminifer. Nature 443:93–96.
Rollinson, N., and L. Rowe. 2015. Persistent directional selection on body size and a resolution

to the paradox of stasis. Evolution 69:2441–2451.
Rykaczewski, R. R., and J. P. Dunne. 2010. Enhanced nutrient supply to the California Current Ecosystem with global warming and increased stratification in an earth system model. Geophysical Research Letters 37.
Saraswat, R., A. Deopujari, R. Nigam, and P. J. Heniriques. 2011. Relationship between abundance and morphology of benthic foraminifera Epistominella exigua: Paleoclimatic implications. Journal of the Geological Society of India 77:190–196.
Scalco, E., K. Stec, D. Iudicone, M. I. Ferrante, and M. Montresor. 2014. The dynamics of sexual phase in the marine diatom Pseudo-nitzschia multistriata (Bacillariophyceae). Journal of Phycology 50:817–828.
Schimmelmann, A., I. L. Hendy, L. Dunn, D. K. Pak, and C. B. Lange. 2013. Revised ~2000-year chronostratigraphy of partially varved marine sediment in Santa Barbara Basin, California. GFF 135:258–264.
Schimmelmann, A., C. B. Lange, E. B. Roark, and B. L. Ingram. 2006. Resources for Paleoceanographic and Paleoclimatic Analysis: A 6,700-Year Stratigraphy and Regional Radiocarbon Reservoir-Age (ΔR) Record Based on Varve Counting and 14C-AMS Dating for the Santa Barbara Basin, Offshore California, U.S.A. Journal of Sedimentary Research 76:74–80.
Schmidt, D. N., D. Lazarus, J. R. Young, and M. Kucera. 2006. Biogeography and evolution of body size in marine plankton. Earth-Science Reviews 78:239–266.
Schmidt, D. N., E. Thomas, E. Authier, D. Saunders, and A. Ridgwell. 2018. Strategies in times of crisis—insights into the benthic foraminiferal record of the Palaeocene–Eocene Thermal Maximum. Philosophical Transactions of the Royal Society A: Mathematical, Physical and Engineering Sciences 376:20170328.
Shama, L. N. S. 2015. Bet hedging in a warming ocean: predictability of maternal environment shapes offspring size variation in marine sticklebacks. Global Change Biology 21:4387–4400.
Sheridan, J. A., and D. Bickford. 2011. Shrinking body size as an ecological response to climate change. Nature Climate Change 1:401–406.
Smith, F. A., J. L. Payne, N. A. Heim, M. A. Balk, S. Finnegan, M. Kowalewski, S. K. Lyons, C. R. McClain, D. W. McShea, P. M. Novack-Gottshall, P. S. Anich, and S. C. Wang. 2016. Body Size Evolution Across the Geozoic. Annual Review of Earth and Planetary Sciences 44:523–553.
Team, R. C. 2013. R: A language and environment for statistical computing.
Uyeda, J. C., T. F. Hansen, S. J. Arnold, and J. Pienaar. 2011. The million-year wait for macroevolutionary bursts. Proceedings of the National Academy of Sciences 108:15908–15913.
Vermeij, G. J. 2012. The evolution of gigantism on temperate seashores. Biological Journal of the Linnean Society 106:776–793.
Wang, Y., and I. L. Hendy. 2021. Reorganized Atmospheric Circulation During the Little Ice Age Leads to Rapid Southern California Deoxygenation. Geophysical Research Letters 48:e2021GL094469.
Wang, Y., I. L. Hendy, and R. Thunell. 2019. Local and Remote Forcing of Denitrification in the Northeast Pacific for the Last 2,000 Years. Paleoceanography and Paleoclimatology 34:1517–1533.
Wang, Y., I. Hendy, and T. J. Napier. 2017. Climate and Anthropogenic Controls of Coastal

Deoxygenation on Interannual to Centennial Timescales. Geophysical Research Letters 44:11,528-11,536.
White, E. P., S. K. M. Ernest, A. J. Kerkhoff, and B. J. Enquist. 2007. Relationships between body size and abundance in ecology. Trends in Ecology & Evolution 22:323–330.
Williams, J. L., R. A. Hufbauer, and T. E. X. Miller. 2019. How Evolution Modifies the Variability of Range Expansion. Trends in Ecology & Evolution 34:903–913.
Woehle, C., A.-S. Roy, N. Glock, J. Michels, T. Wein, J. Weissenbach, D. Romero, C. Hiebenthal, S. N. Gorb, J. Schönfeld, and T. Dagan. 2022. Denitrification in foraminifera has an ancient origin and is complemented by associated bacteria. Proceedings of the National Academy of Sciences 119:e2200198119.
Woodward, G., B. Ebenman, M. Emmerson, J. M. Montoya, J. M. Olesen, A. Valido, and P. H. Warren. 2005. Body size in ecological networks. Trends in Ecology & Evolution 20:402–409.
Worm, B., E. B. Barbier, N. Beaumont, J. E. Duffy, C. Folke, B. S. Halpern, J. B. Jackson, H. K. Lotze, F. Micheli, and S. R. Palumbi. 2006. Impacts of biodiversity loss on ocean ecosystem services. science 314:787–790.
Xu, H., D.-W. Li, H.-C. Li, M. Zhao, W. M. Berelson, G. Jin, L. Li, and S. Misra. 2022. Local and remote forcing on the interannual variations of the sedimentary δ15N in Santa Barbara Basin during the past 80 years. Frontiers in Marine Science 9.
Yasuhara, M., H. Doi, C.-L. Wei, R. Danovaro, and S. E. Myhre. 2016. Biodiversity–ecosystem functioning relationships in long-term time series and palaeoecological records: deep sea as a test bed. Philosophical Transactions of the Royal Society B: Biological Sciences 371:20150210–20150282.
Yasuhara, M., G. Hunt, D. Breitburg, A. Tsujimoto, and K. Katsuki. 2012. Human-induced marine ecological degradation: micropaleontological perspectives. Ecology and Evolution 2:3242–3268.
Zeuthen, E. 1953. Oxygen uptake as related to body size in organisms. The Quarterly review of biology 28:1–12.
Zhao, M., G. Eglinton, G. Read, and A. Schimmelmann. 2000. An alkenone (U37K′) quasi-annual sea surface temperature record (A.D. 1440 to 1940) using varved sediments from the Santa Barbara Basin. Organic Geochemistry 31:903–917.

4.6 Appendix
Supplemental Information for Chapter 4: Correlated trends and shifts in terminal shell size of foraminifera over the last 760 years

Sara S. Kahanamoku[1], Maya Samuels-Fair[1], Ivo Duijnstee[1], Jared C. Richards[2], Seth Finnegan[1]
1) Department of Integrative Biology and Museum of Paleontology, University of California, Berkeley, CA; 2) Department of Organismal Biology, Harvard University, Cambridge, MA

Supplemental Text

Relationships between reproductive mode and body size

To determine whether megalospheric body sizes may drive overall species means observed through time within *Bolivina* species with dimorphic reproductive mode variation, we fit a linear mixed model to predict overall species means with species-specific megalospheric mean sizes, with species as a random effect. Megalospheric size is a significant and positive predictor of mean size (conditional $R^2 = 0.63$, marginal $R^2 = 0.16$; beta = 0.83, $p << 0.01$). Taken alongside the tendency towards positive correlations in reproductive morph size (with notable exceptions; Table S4.4), these results suggest that size changes could be driven by reproductive mode, perhaps through correlated blooms across species.

Multi-predictor linear models of environmental proxies

To test for correlations between environmental variables, body size, and reproductive mode, we fit multiple linear mixed models with species as a random effect, and used model selection to determine best fit. In these models, $\delta^{15}N$ and reducing index (both oxygenation proxies) were significant and positively correlated with shell area. The conditional R^2 for model containing composite core data was 0.73 (while marginal R^2, related to the fixed effects alone, was much lower than species-specific linear regressions at 0.04). For the model containing box core data, $\delta^{15}N$ and reducing index were also significant and positive predictors of body size, with a conditional R^2 of 0.74 and a marginal R^2 of 0.01.

Supplemental Figures

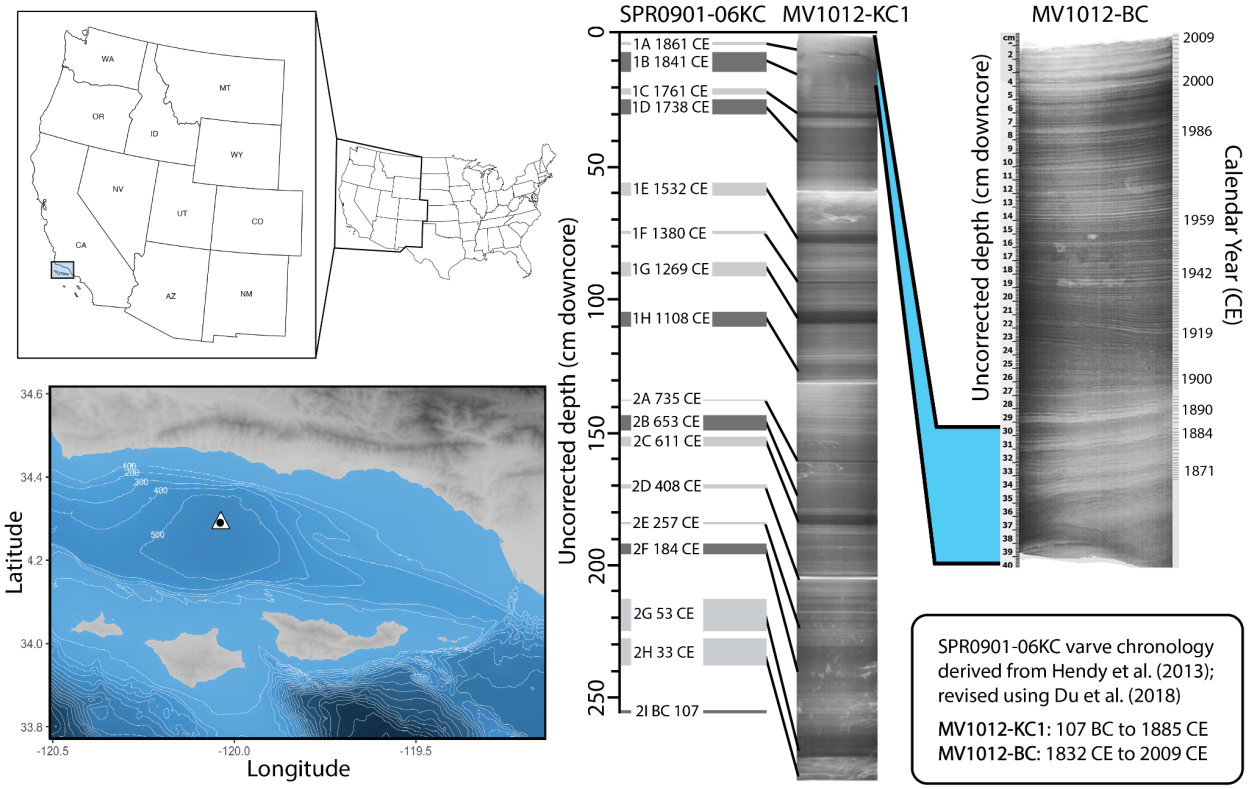

Supplementary Figure 4.1: Santa Barbara Basin setting and core chronology.

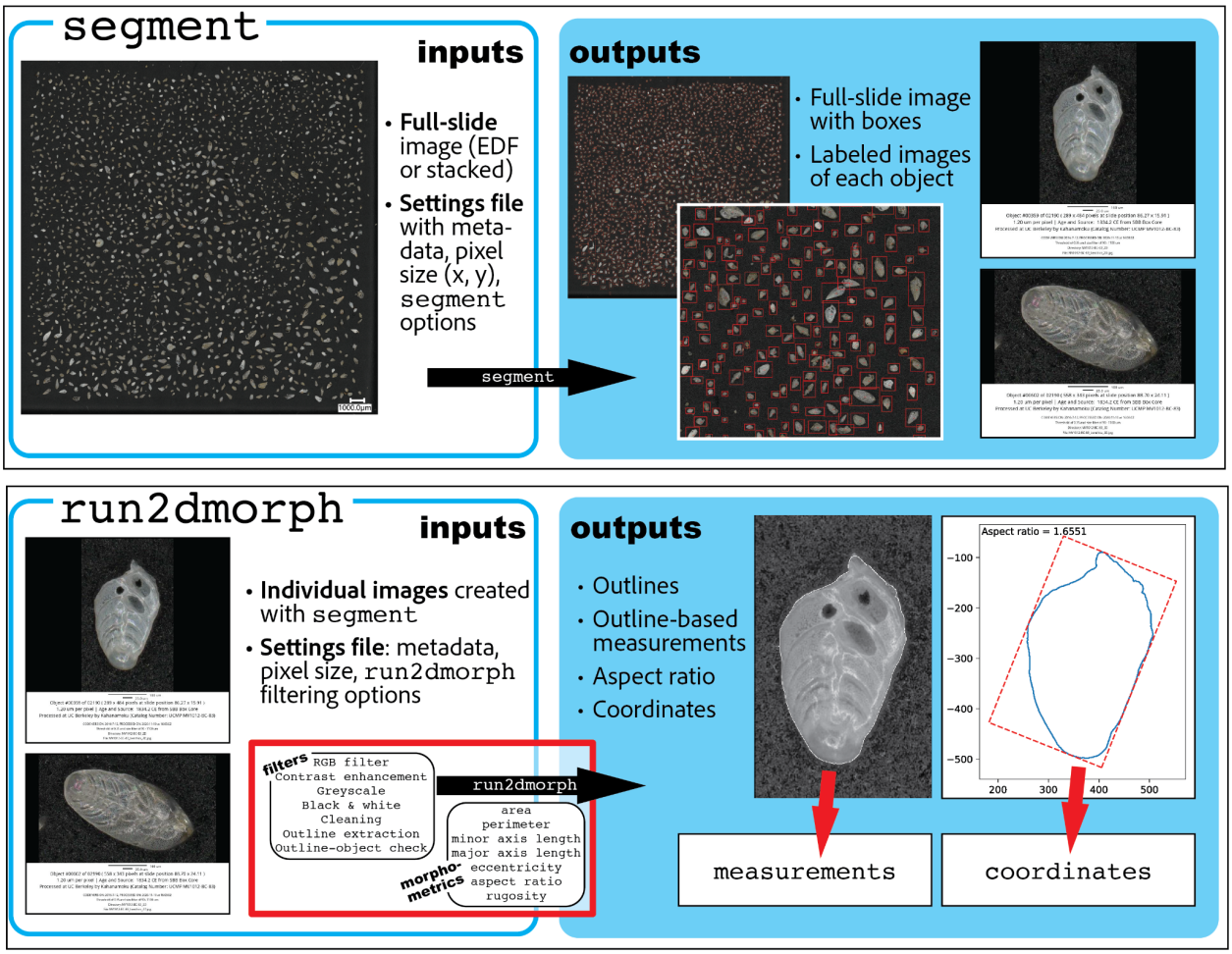

Supplementary Figure 4.2: Automorph Workflow.

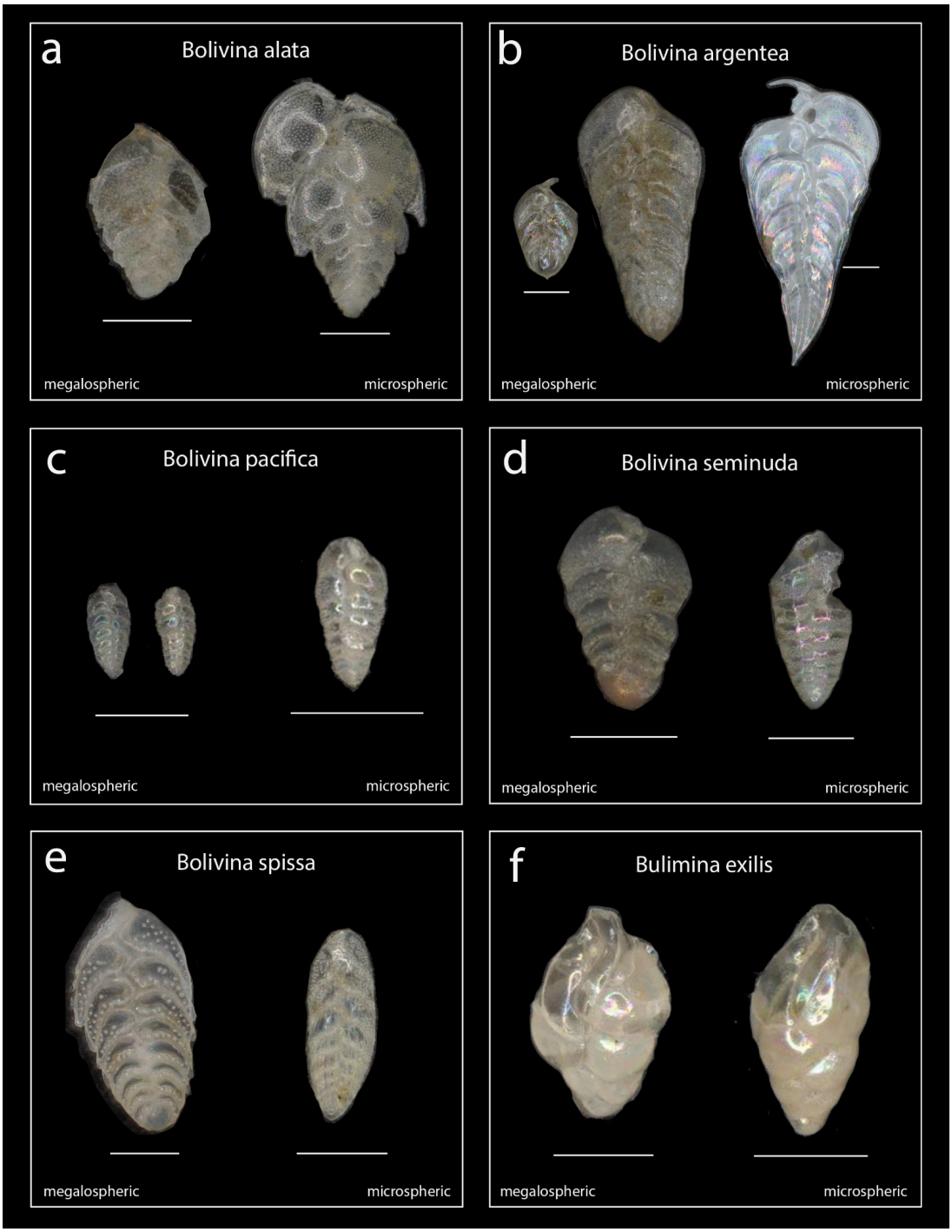

Supplementary Figure 4.3: Species identifications used in this study with morphological indicators of reproductive variation.
(a) Bolivina alata megalospheric and microspheric; (b) Bolivina argentea megalospheric and microspheric; (c) Bolivina pacifica megalospheric and microspheric; (d) Bolivina seminuda megalospheric and microspheric; (e) Bolivina spissa megalospheric and microspheric; (f) Bulimina exilis megalospheric and microspheric. Scale bars indicate 100 μm. Final chambers are missing from the outer two *B. argentea* specimens, and the microspheric *B. seminuda* and megalospheric *B. alata* and *B. exilis* are partially broken.

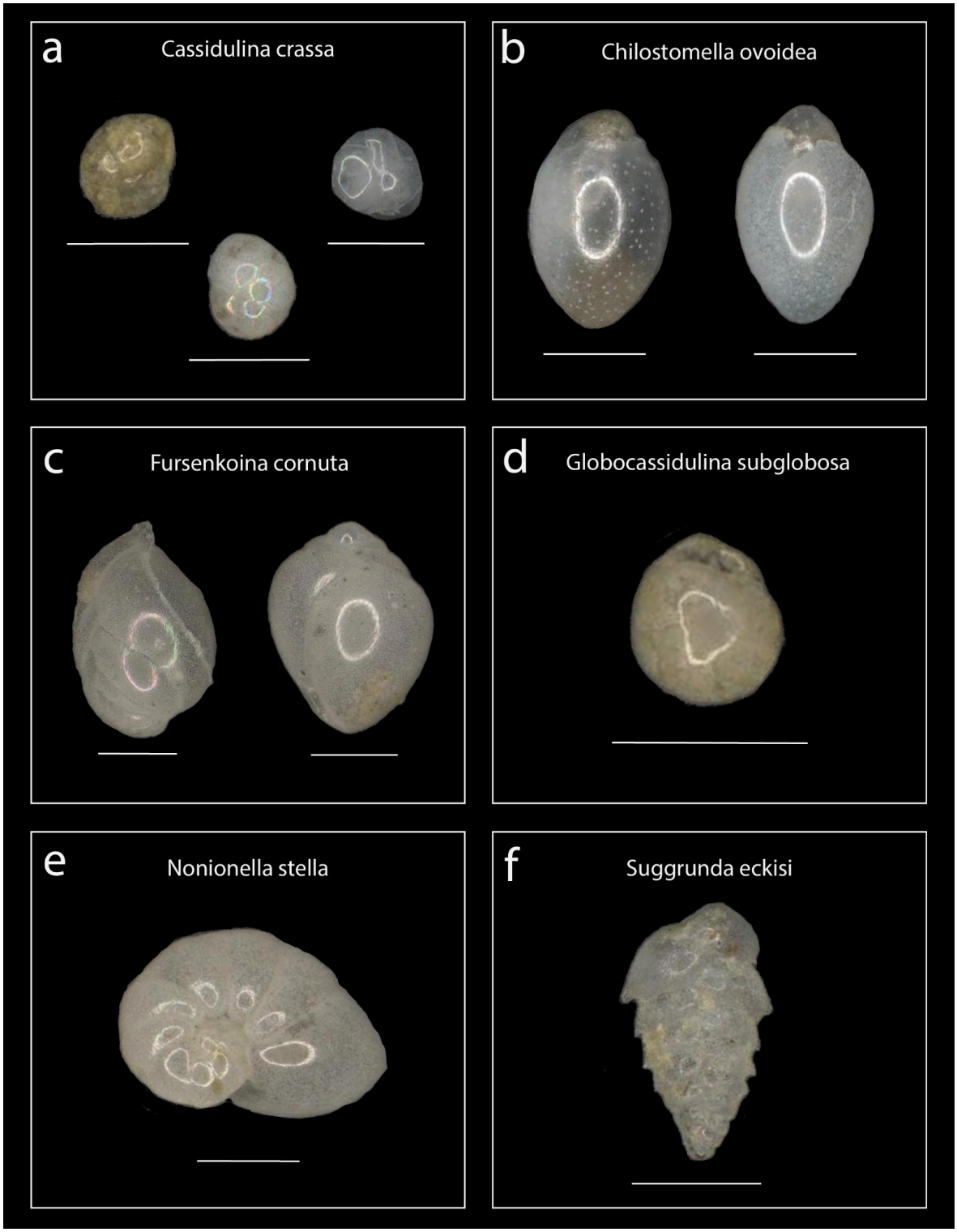

Supplementary Figure 4.4: Additional species identifications used in this study.
(a) Cassidulina crassa; (b) Chilostomella ovoidea; (c) Fursenkoina cornuta; (d) Globocassidulina subglobosa; (e) Nonionella stella; (f) Suggrunda eckisi. Scale bars indicate 100 μm.

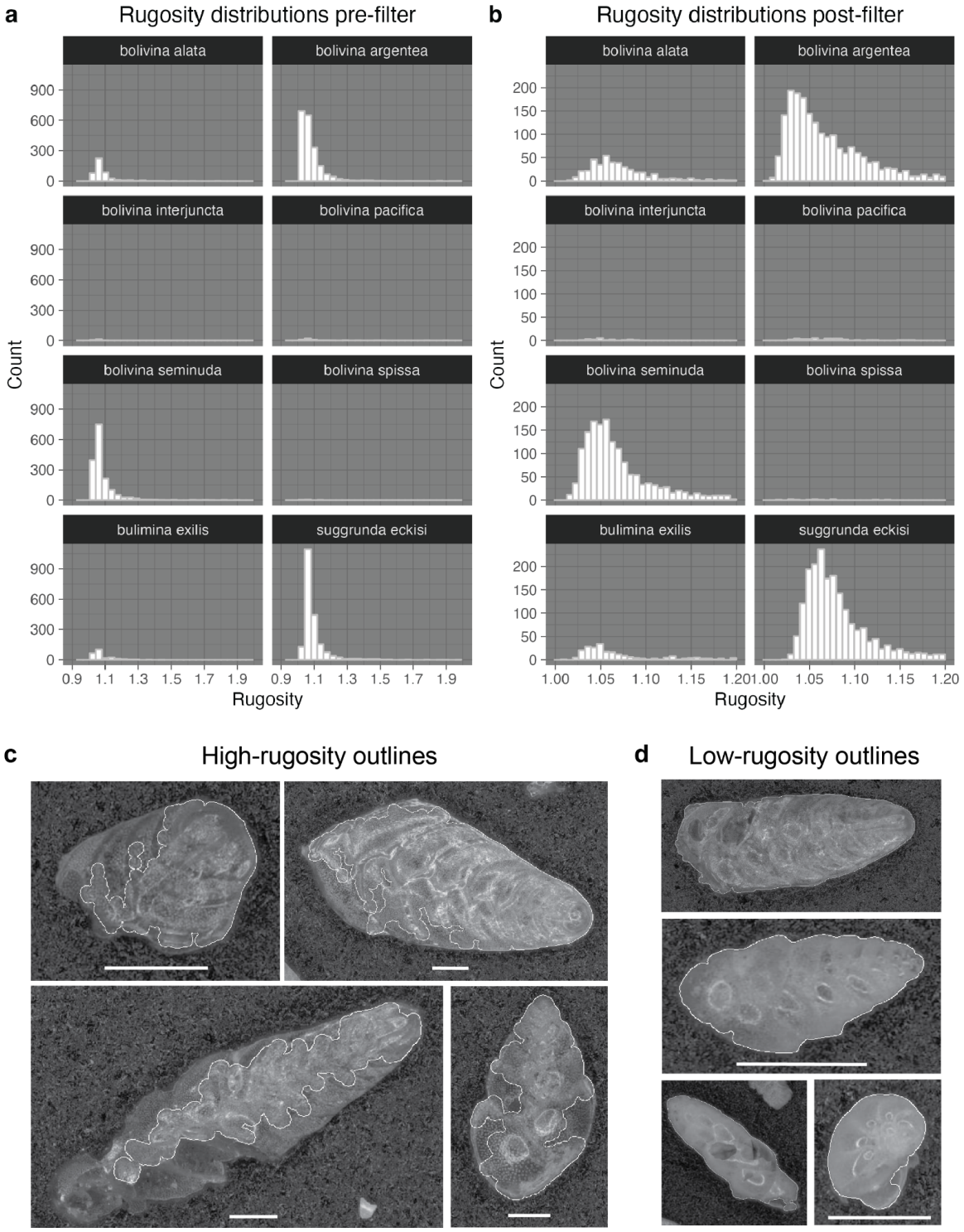

Supplementary Figure 4.5: Filtering for rugosity removes outliers with poorly-extracted outlines and fragments.

(a) Rugosity distributions across 6 common species prior to filter show long tails; (b) Removing high-rugosity individuals removes long tail; (c) examples of high-rugosity images, which show poorly-extracted outlines; (d) examples of low-rugosity images with well-extracted outlines.

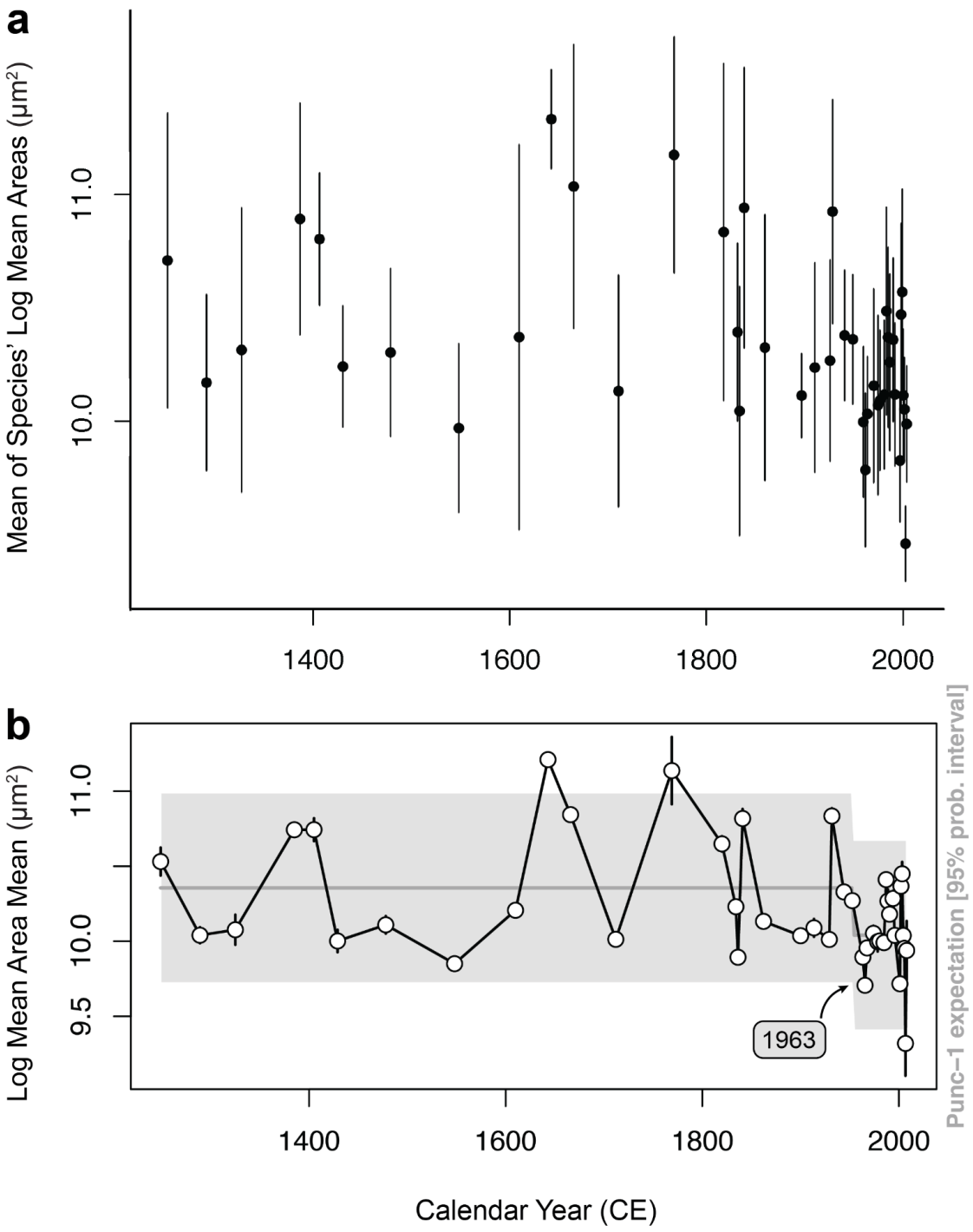

Supplementary Figure 4.6: Modes of change for species-specific mean areas through time. (a) Means, (b) Best-fit punctuated change model. Points indicate means, while lines indicate standard deviations; panel (b) shows 95% confidence intervals in light gray, while model means are denoted by a darker gray line. Overall means show a general decrease towards the recent. A punctuated change model is the best fit for these data, with a model breakpoint at 1963 CE.

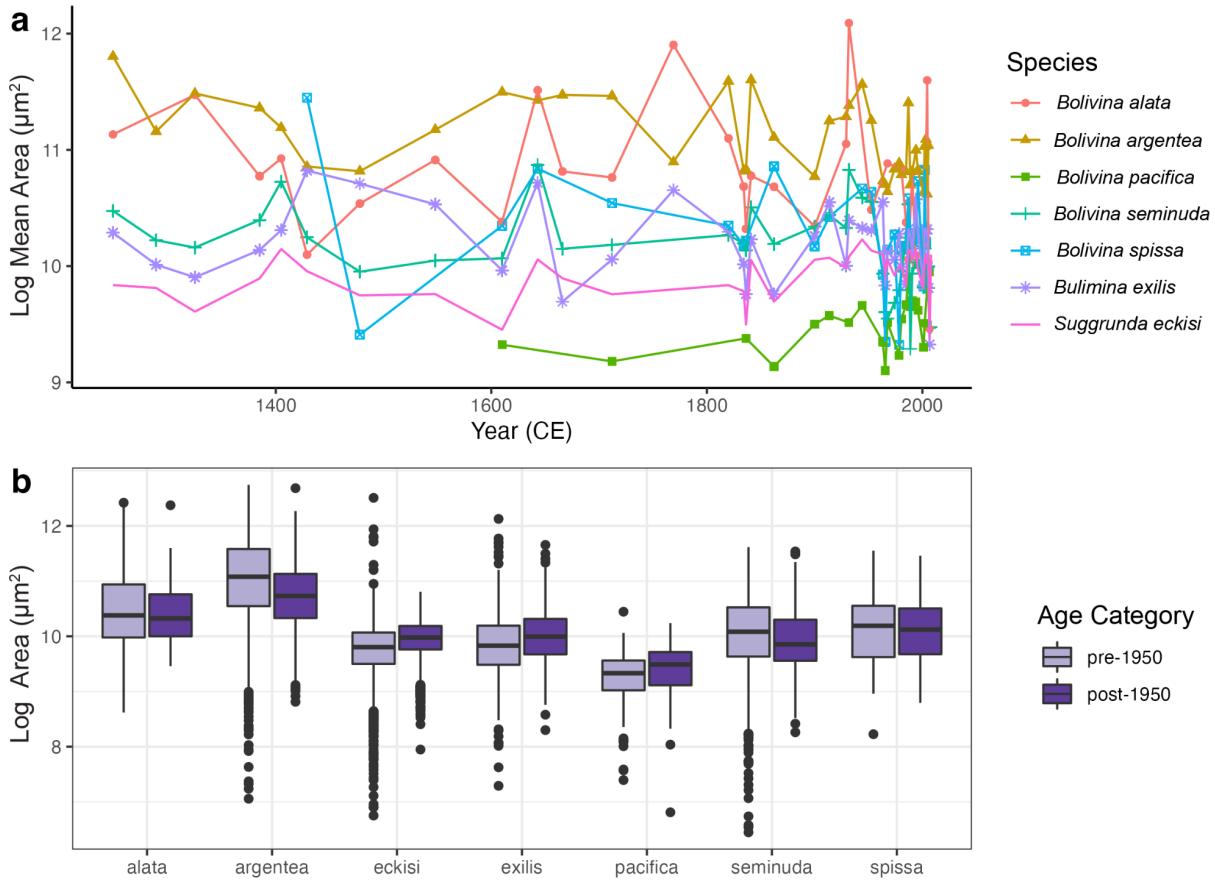

Supplementary Figure 4.7: Body sizes are significantly different in modern samples when compared to the longer core interval.
(a) Log-transformed mean area by species through time; color and point shape denotes species. Species sizes shift following ~1950 CE (breakpoint chosen to highlight both 19th and 20th century shifts), such that overall size distributions are smaller in the interval from 1950-2009 CE when compared to the interval from 1240-1949 CE ($p << 0.01$, two-sample t-test). (b) Boxplots of areas by species pre- and post-1950 CE show that some species increase in size following 1950 (*S. eckisi, B. exilis, B. pacifica*) while others decrease in size (*B. alata, B. argentea, B. seminuda, B. spissa*).

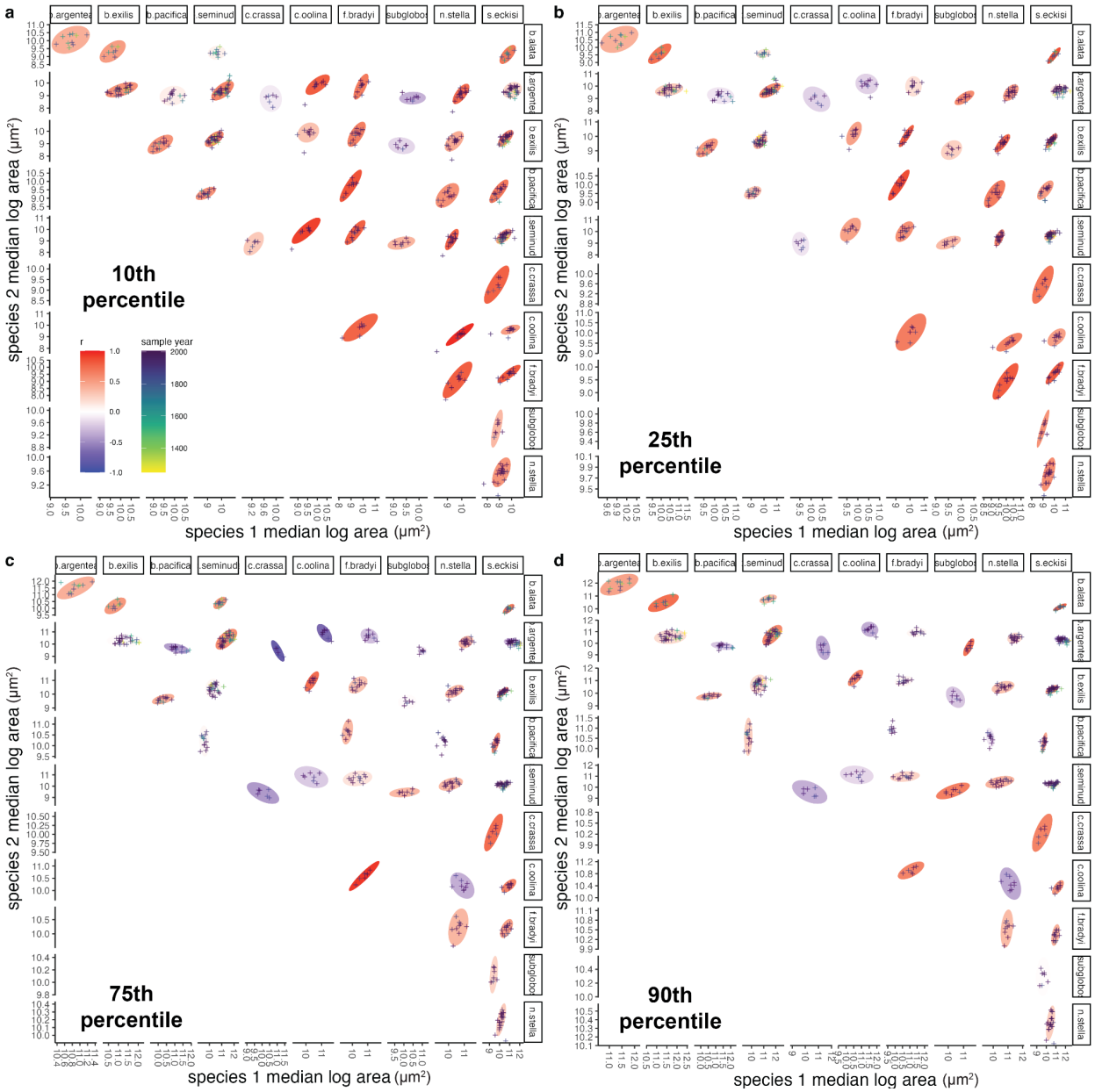

Supplementary Figure 4.8: Scatterplot matrices for correlation among median body size percentile.

(a) 10th percentile; (b) 25th percentile; (c) 75th percentile; (d) 90th percentile. Ellipse direction, aspect ratio, and color indicates the strength and direction of correlations between species pairs, with red colors denoting positive correlations (Spearman's ρ) and blue colors indicating negative correlations. Points indicate the number of samples in which species co-occur with sufficient numbers of individuals of both species, with point colors denoting the age of these samples (darker colors denote more recent samples, while lighter colors denote older samples). Missing ellipses denote species pairs for which samples were insufficient to calculate correlations.

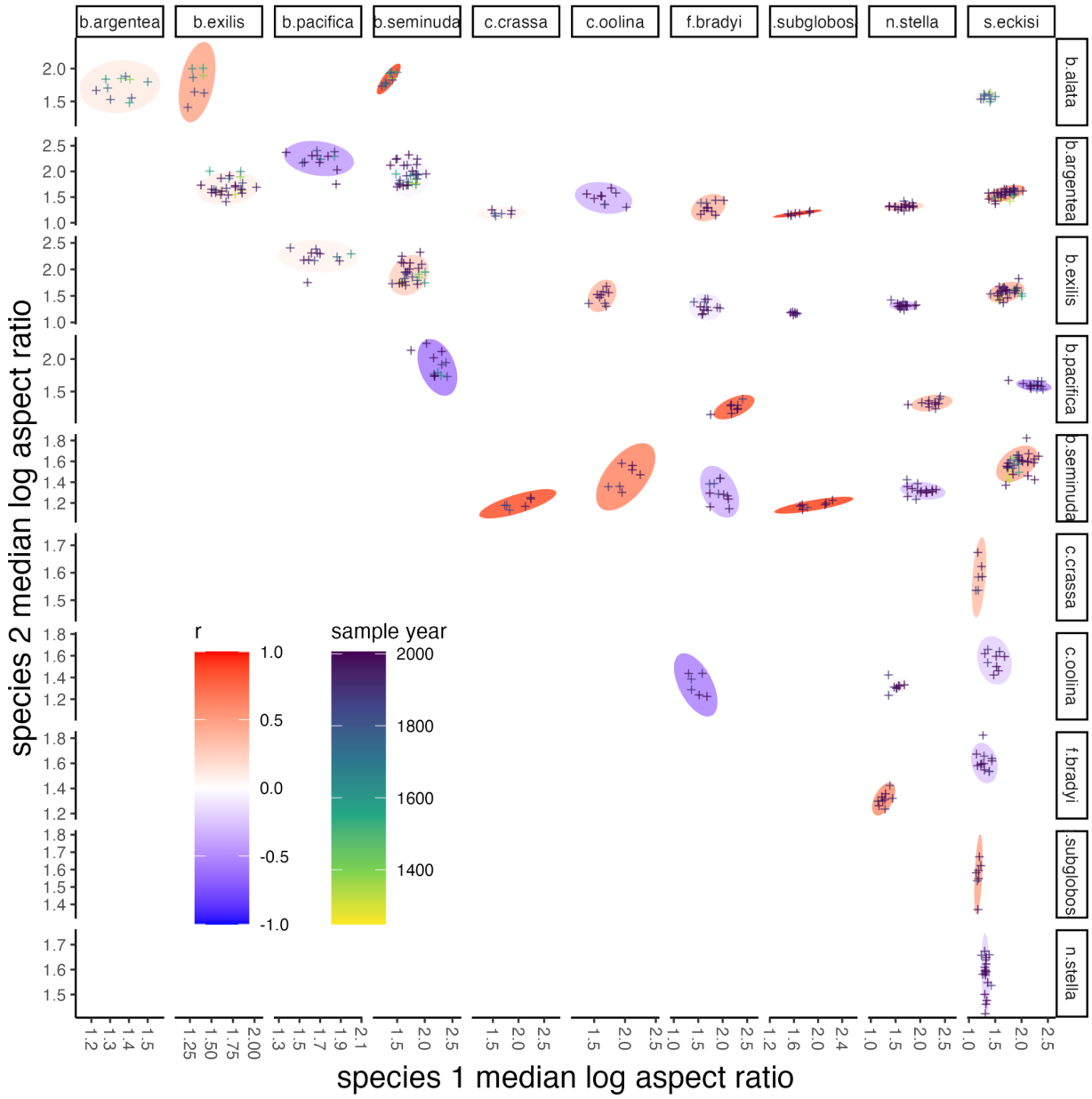

Supplementary Figure 4.9: Scatterplot correlation matrix for species' median body shapes. Here, shell aspect ratio is used as a proxy for shape. Ellipse direction, ellipse aspect ratio, and color indicates the strength and direction of correlations between species pairs, with red colors denoting positive correlations (Spearman's ρ) and blue colors indicating negative correlations. Points indicate the number of samples in which species co-occur with sufficient numbers of individuals of both species, with point colors denoting the age of these samples (darker colors denote more recent samples, while lighter colors denote older samples). Missing ellipses denote species pairs for which samples were insufficient to calculate correlations.

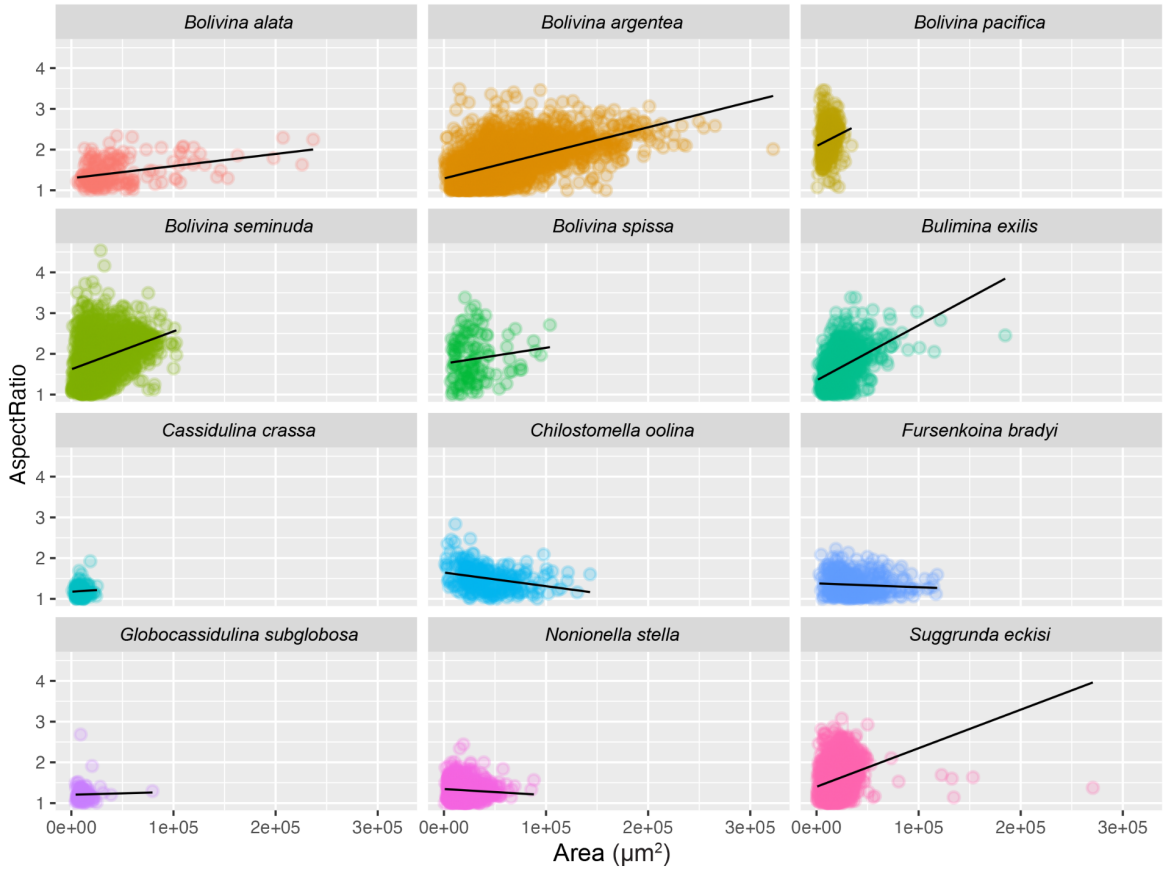

Supplementary Figure 4.10: Aspect ratio and area relationships by species.
Species with strong positive relationships between area and aspect ratio include species within the genus *Bolivina* as well as *Bulimina exilis* and *Suggrunda eckisi*, all of which are biserial benthic foraminifera which grow by adding chambers in an alternating chamber arrangement which creates two series of chambers with ~180˚ between consecutive chambers.

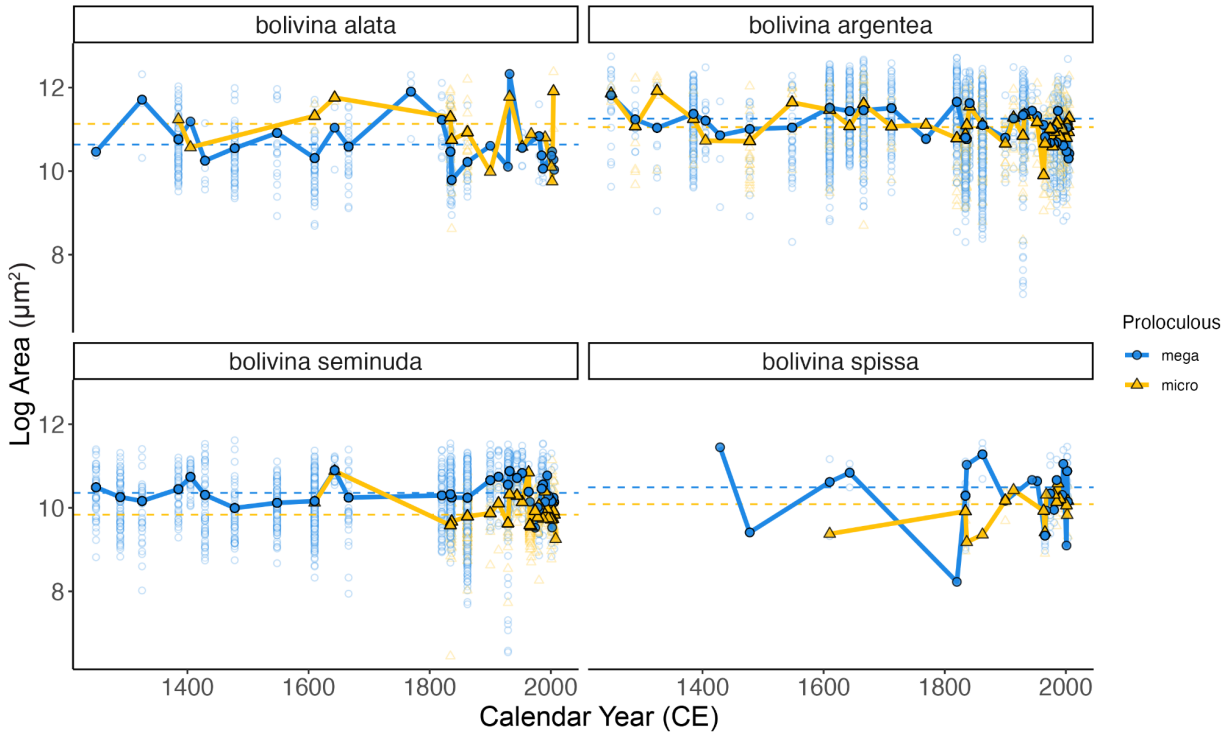

Supplementary Figure 4.11: SBB biserial benthic foraminifer species size means by proloculus size.
For each species, log-transformed size means are represented by bold lines and solid-filled shapes, while individual size measurements are represented by open shapes. Shape and color denote proloculus type: yellow triangles represent microspheric sizes, while blue circles represent megalospheric sizes.

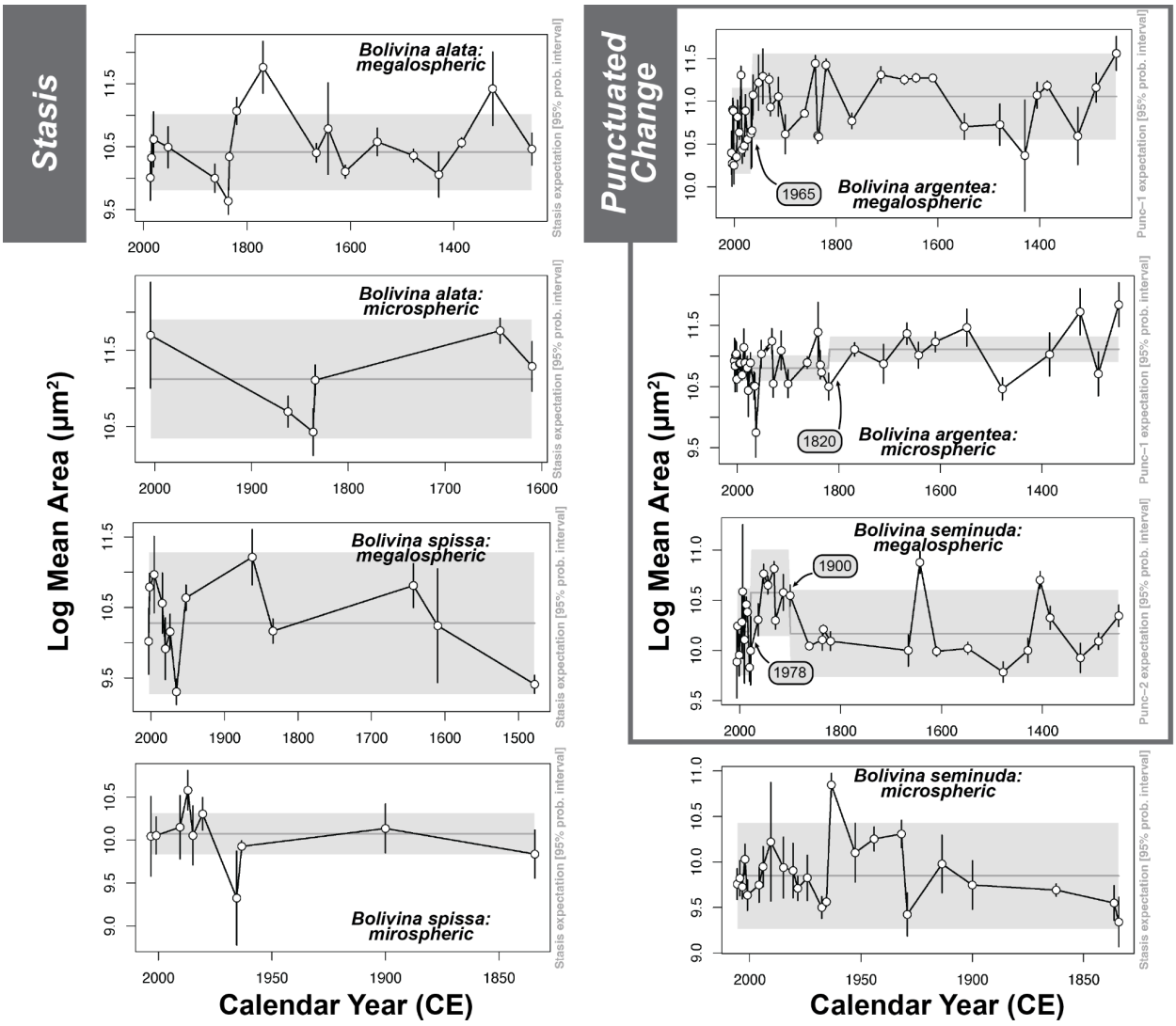

Supplementary Figure 4.12: Best-fit rate models for ~760-year temporal trends of species' mean areas by reproductive morph favor stasis and punctuated change.
Models were run only for those biserial benthic foraminifera with visible reproductive dimorphism in proloculus size (*B. alata*, *B. argentea*, *B. seminuda*, and *B. spissa*). Species-specific mean areas are denoted by open circles, with standard deviations marked by error bars. Solid grey lines indicate the overall model mean, while shaded grey areas denote 95% confidence intervals. Stasis is the best fit model for five of the eight reproductive morphotypes (megalospheric and microspheric *B. alata* and *B. spissa*, and microspheric *B. seminuda*). A 1-step punctuated change model is the best fit for two reproductive morphotypes (megalospheric and microspheric *B. argentea*), while a 2-step punctuated change model is the best fit for megalospheric *B. seminuda*. Estimated step-points are marked on each timeseries.

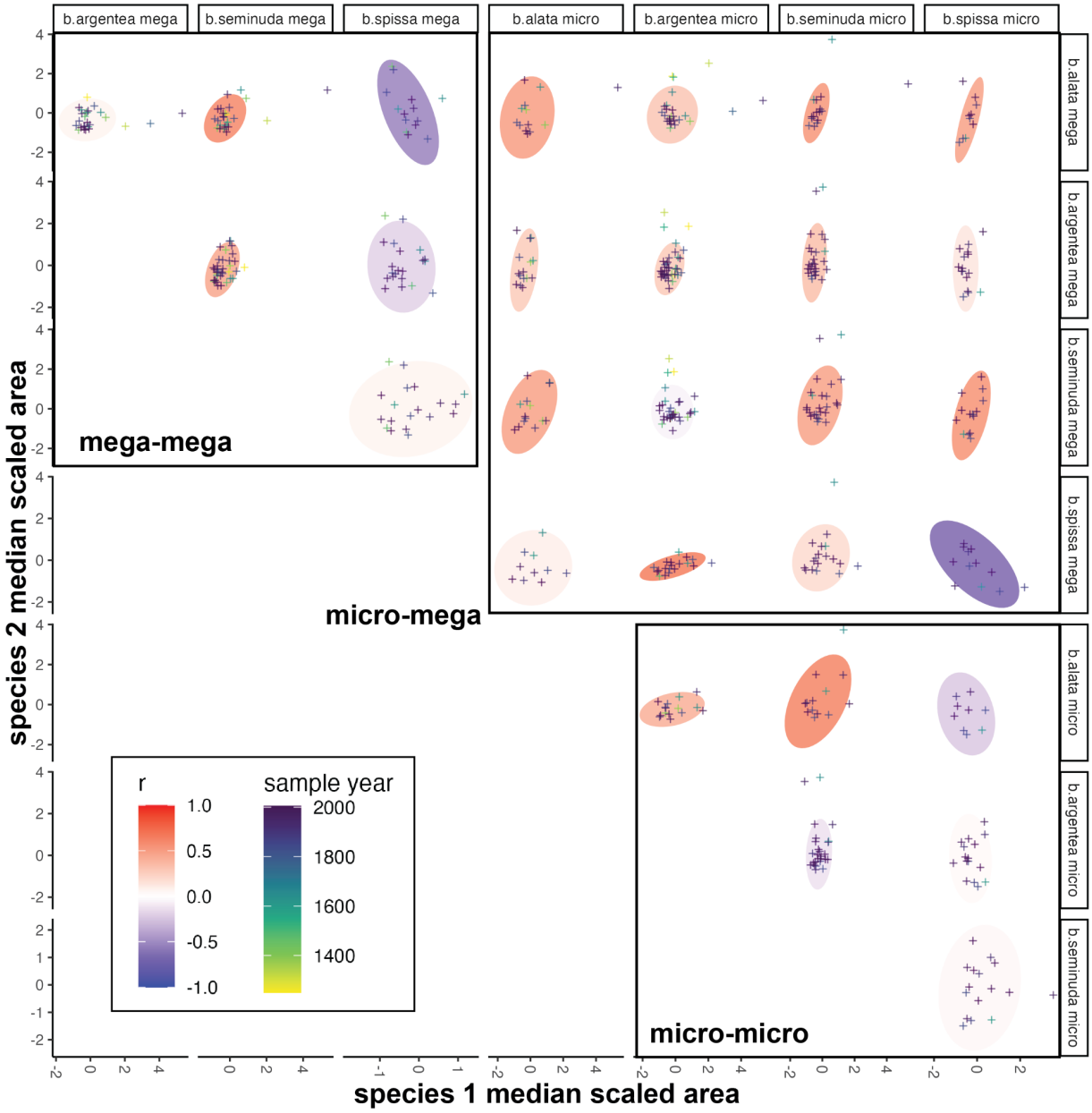

Supplementary Figure 4.13: Median body size across species reproductive morphs is weakly to moderately positively correlated for micro-mega morph pairings.
Ellipse direction, aspect ratio, and color indicates the strength and direction of correlations (Spearman's ρ) between species pairs. Points indicate the number of samples in which species co-occur, with point colors denoting the age of these samples. All correlations between reproductive morph species pairs are weakly to moderately positive, with the exception of correlations between *B. spissa* and *B. alata* (mega-mega and micro-micro); *B. spissa* and *B. spissa* (mega-micro); *B. spissa* and *B. argentea* (mega-mega, micro-micro) and *B. seminuda* and *B. argentea* (micro-micro).

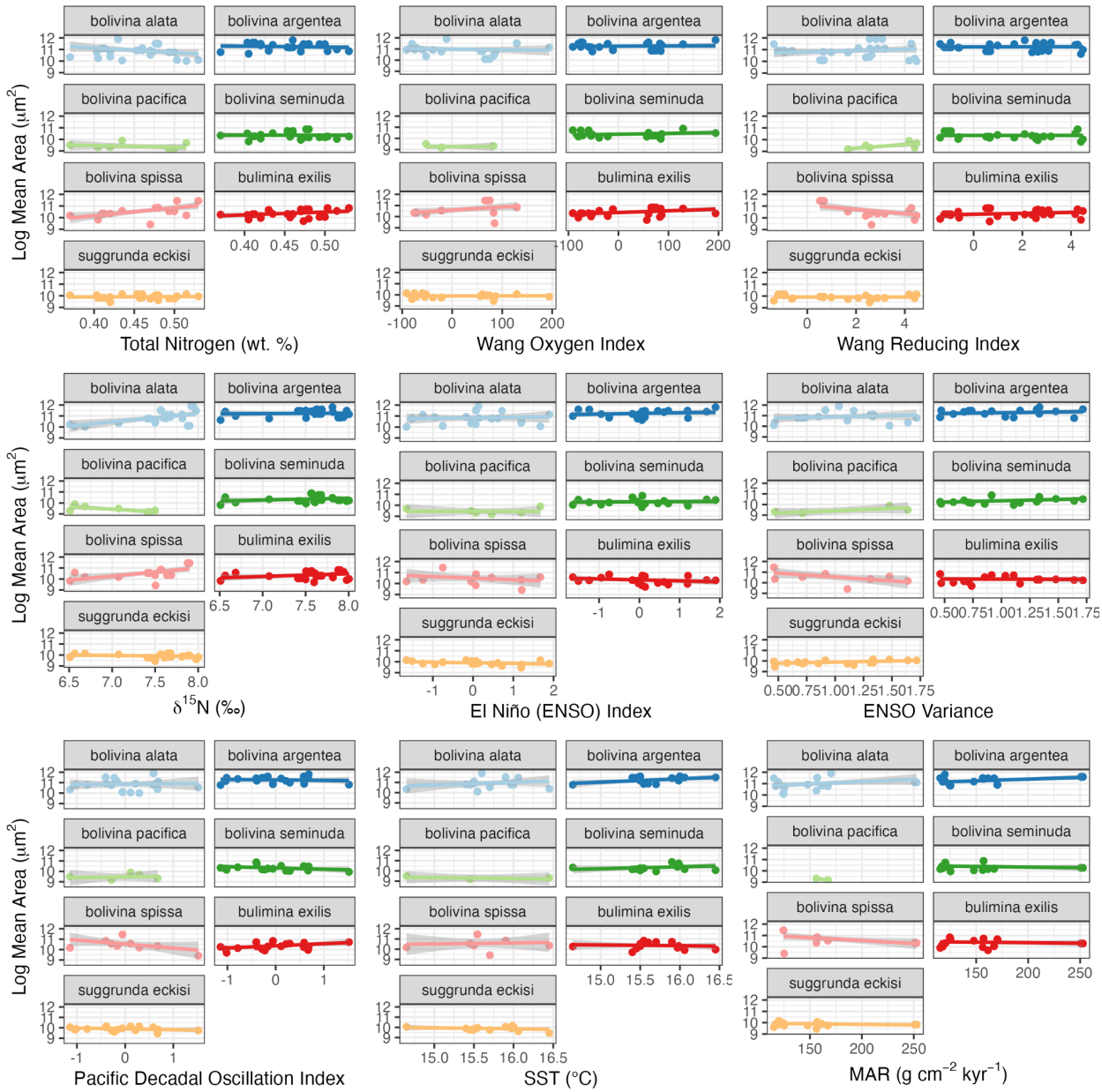

Supplementary Figure 4.14: Linear regressions by species for composite core data (1249-2008 CE).

Species picked from both core records are biserial benthic foraminifera. Species' log-transformed mean sizes are shown regressed against indicators of food availability (TN), oxygenation (an Oxygen and Reduction index from Wang et al. 2017, and $\delta^{15}N$), and major environmental proxies: El Niño Southern Oscillation (ENSO) Index and Variance, Pacific Decadal Oscillation (PDO) Index, Sea Surface Temperature (SST), and Mass Accumulation Rate (MAR).

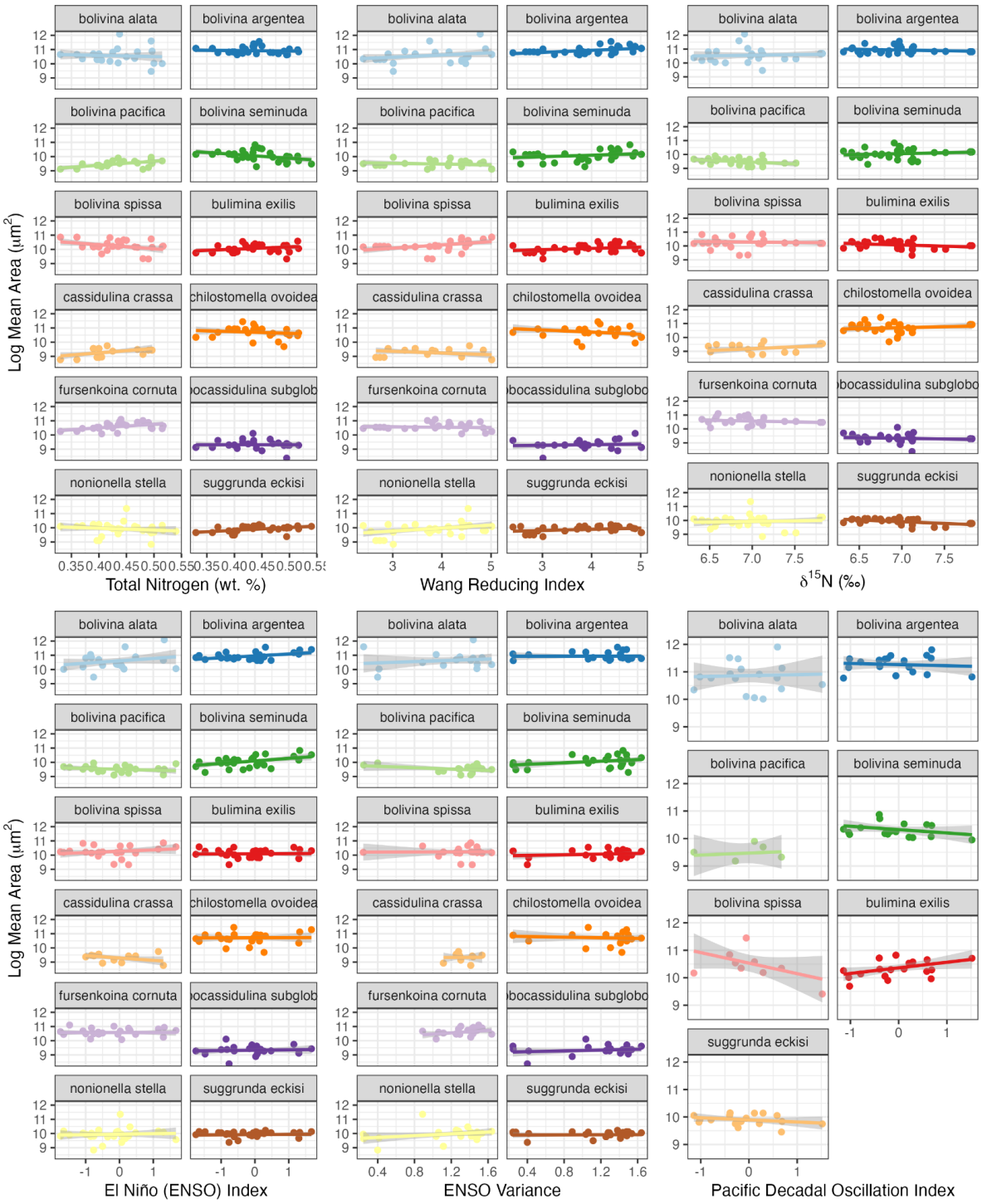

Supplementary Figure 4.15: Linear regressions by species for box core data (1834-2008 CE).

The 12 most common species are represented here. Species' log-transformed mean sizes are shown regressed against environmental indicators with data that spans into the 20th century: food availability (TN), oxygenation (represented by Reduction index from Wang et al. (2021) and $\delta^{15}N$), El Niño Southern Oscillation (ENSO) Index and Variance, and Pacific Decadal Oscillation (PDO) Index.

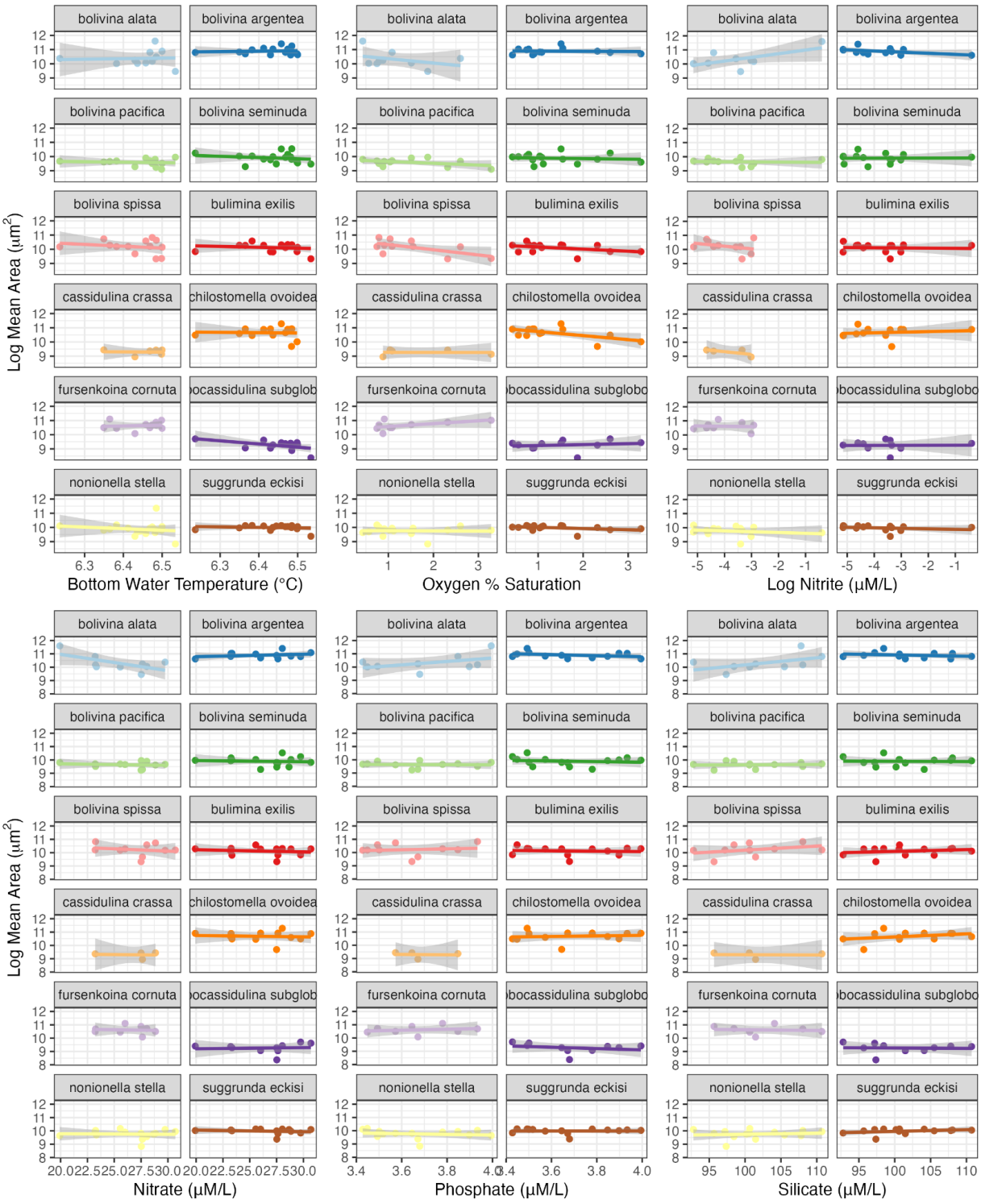

Supplementary Figure 4.16: Linear regressions by species for box core data from 1950-2008 CE.

The 12 most common species are represented here, and their log-transformed mean sizes are shown regressed against annual data from the California Cooperative Oceanic Fisheries Investigations Database CalCOFI from Station 081.8 046.9 between 500-599m water depth.

Supplemental Tables

Supplementary Table 4.1: Sample metadata.
Sample names and ages from both cores are reported alongside information on sample processing (which species were picked, split size)

Site	Core Type	Sample	Calendar Year CE	Assemblage Type	Split Size
MV1012	Box	MV1012-BC-2	2007.9	All	1
MV1012	Box	MV1012-BC-3	2006.7	All	1
MV1012	Box	MV1012-BC-4	2005.6	All	1
MV1012	Box	MV1012-BC-5	2004.4	All	1
MV1012	Box	MV1012-BC-6	2003.3	All	1
MV1012	Box	MV1012-BC-7	2002.1	All	1
MV1012	Box	MV1012-BC-8	2001	All	1
MV1012	Box	MV1012-BC-9-10	1998.4	All	1
MV1012	Box	MV1012-BC-11	1995.8	All	1
MV1012	Box	MV1012-BC-12	1994	All	1
MV1012	Box	MV1012-BC-14	1990.5	All	1
MV1012	Box	MV1012-BC-15	1988.8	All	1
MV1012	Box	MV1012-BC-16	1987	All	1
MV1012	Box	MV1012-BC-17	1984.8	All	1
MV1012	Box	MV1012-BC-19	1980.5	All	1
MV1012	Box	MV1012-BC-20	1978.4	All	1
MV1012	Box	MV1012-BC-22	1974.1	All	1
MV1012	Box	MV1012-BC-25	1967.6	All	1
MV1012	Box	MV1012-BC-26	1965.5	All	1
MV1012	Box	MV1012-BC-27	1963.3	All	1
MV1012	Box	MV1012-BC-32	1952.6	All	1
MV1012	Box	MV1012-BC-36	1944.1	All	1

Site	Core Type	Sample	Calendar Year CE	Assemblage Type	Split Size
MV1012	Box	MV1012-BC-41	1931.8	All	1
MV1012	Box	MV1012-BC-42	1929.2	All	1
MV1012	Box	MV1012-BC-48	1913.6	All	1
MV1012	Box	MV1012-BC-53	1900	All	1
MV1012	Box	MV1012-BC-57	1890.9	All	1
MV1012	Box	MV1012-BC-70	1862.3	All	1
MV1012	Kasten	KC1-1-25	1841	Biserial only	1/32
MV1012	Box	MV1012-BC-82	1836.3	All	1
MV1012	Box	MV1012-BC-83	1834.2	All	1
MV1012	Kasten	KC1-1-52	1820	Biserial only	1/32
MV1012	Kasten	KC1-1-64	1769	Biserial only	1/16
MV1012	Kasten	KC1-1-103	1712	Biserial only	1/128
MV1012	Kasten	KC1-1-117	1666	Biserial only	1/16
MV1012	Kasten	KC1-1-124	1643	Biserial only	1/32
MV1012	Kasten	KC1-2-9	1610	Biserial only	1/64
MV1012	Kasten	KC1-2-28	1548	Biserial only	1/32
MV1012	Kasten	KC1-2-49	1478	Biserial only	1/32
MV1012	Kasten	KC1-2-59	1429	Biserial only	1/32
MV1012	Kasten	KC1-2-64	1405	Biserial only	1/16
MV1012	Kasten	KC1-2-68	1385	Biserial only	1/128
MV1012	Kasten	KC1-2-80	1325	Biserial only	1/32
MV1012	Kasten	KC1-2-87	1289	Biserial only	1/16
MV1012	Kasten	KC1-2-103	1249	Biserial only	1/32

Supplementary Table 4.2: Taxonomic references and synonyms for the 12 common species used in this study.
Species life science identifier (Aphia ID) numbers are reported alongside common synonyms and taxonomic references.

Species	Life Science Identifier (Aphia ID)	Synonyms	Taxonomy References	Image References
Bolivina alata	112964	*Bolivina beyrichi var. alata* *Brizalina alata* *Vulvulina alata*	Seguenza 1862	Erdem and Schönfeld 2017, Palmer et al. 2020
Bolivina argentea	852154	*Brizalina argentea*	Cushman 1926	Lutze 1964, Erdem and Schönfeld 2017, Palmer et al. 2020
Bolivina seminuda	417913	*Bolivinella seminuda* *Bolivinellina seminuda* *Brizalina seminuda*	Cushman 1911	Erdem and Schönfeld 2017, Palmer et al. 2020
Bolivina seminuda var. humilis	816071	*Bolivina humilis* (accepted) *Bolivina seminuda var. humilis* *Bolivinella humilis* *Bolivinellina humilis* *Brizalina humilis*	Cushman & McCulloch 1942	Erdem and Schönfeld 2017
Bolivina spissa	814781	*Bolivina subadvena var. spissa* *Brizalina spissa*	Cushman 1926	Erdem and Schönfeld 2017, Palmer et al. 2020
Bolivina pacifica	112979	*Bolivina acerosa var. pacifica* *Bolivinellina pacifica* *Brizalina pacifica*	Cushman & McCulloch 1942	Erdem and Schönfeld 2017
Suggrunda eckisi	521635	-	Natland 1950	Bernhard et al. 1997
Nonionella stella	113604	*Nonionella miocenica var. stella*	Cushman & Moyer 1930	Bernhard et al. 1997
Bulimina exilis	417980	*Eubulimina exilis* (accepted)	Brady 1884	

Species	Life Science Identifier (Aphia ID)	Synonyms	Taxonomy References	Image References
		Bulimina elegans var. exilis		Erdem and Schönfeld 2017
		Bulimina exilis var. tenuata		
		Bulimina tenuata		
		Buliminella exilis var. tenuata		
		Buliminella subfusiformis var. tenuata		
		Buliminella tenuata		
		Eubulimina tenuata		
		Stainforthia exilis		
		Stainforthia exilis subsp. tenuata		
Fursenkoina cornuta	862715	*Virgulina cornuta*	Cushman 1913	Bernhard et al. 2012
Chilostomella ovoidea	113554	-	Reuss 1850	Erdem and Schönfeld 2017
Cassidulina crassa	397221	*Globocassidulina crassa* (accepted)	Orbigny 1839	Erdem and Schönfeld 2017
		Smymella crassa		

Supplementary Table 4.3: Environmental data used for regression analyses.
For each variable, its abbreviation, range of available data, data source, and interpolation type (if applicable) is reported.

Abbreviation	Variable	Calendar Range	Source	Interpolation used
ENSO	El Niño Southern Oscillation	910-2008 CE	Li et al. 2011 (1910-2000), NOAA NINO3 (2000-2008)	Linear interpolation
PDO	Pacific Decadal Oscillation	993-1996 CE	MacDonald and Case 2005	Linear interpolation
D15N	Bulk sedimentary d15N	170.5 BCE -1910 CE	Wang et al. 2019	Moving 5-point window
TN	Bulk sedimentary total Nitrogen	170.5 BCE -1910 CE	Wang et al. 2019	Moving 5-point window
TOC	Bulk sedimentary total organic carbon	170.5 BCE -1910 CE	Wang et al. 2019	Moving 5-point window
SST Uk37	Alkenone Sea Surface Temperature	1297-1941 CE	Zhao et al. 2000	Linear interpolation on yearly averages
OMZ	OMZ reconstruction using redox-sensitive metals (Mo, Re, Ba)	165 BCE - 1904 CE	Wang et al. 2021, Wang et al. 2017	Moving 5-point window
MAR	Mass Accumulation Rate	70000 BCE - 1834 CE	Du et al. 2018	-
O2 SAT	Oxygen percent saturation	1953-2008 CE	CalCOFI	-
NO2	Nitrite (micromoles per liter)	1953-2008 CE	CalCOFI	-
NO3	Nitrate (micromoles per liter)	1953-2008 CE	CalCOFI	-
PO4	Phosphate (micromoles per liter)	1953-2008 CE	CalCOFI	-
SiO3	Silicate (micromoles per liter)	1953-2008 CE	CalCOFI	-
BOTTOM T	Bottom water temperature	1953-2008 CE	CalCOFI	-

Supplementary Table 4.4: Correlations between megalospheric and microspheric morphs of Bolivina.

Species 1	Species 2	Species Pair	Correlation Coefficient
b.argentea mega	b.spissa mega	b.argentea mega.b.spissa mega	0.96
b.seminuda mega	b.alata micro	b.alata micro.b.seminuda mega	0.93
b.spissa mega	b.argentea micro	b.argentea micro.b.spissa mega	0.81
b.alata mega	b.alata micro	b.alata mega.b.alata micro	0.79
b.spissa mega	b.seminuda micro	b.seminuda micro.b.spissa mega	0.64
b.argentea micro	b.seminuda micro	b.argentea micro.b.seminuda micro	0.5
b.seminuda mega	b.seminuda micro	b.seminuda mega.b.seminuda micro	0.44
b.alata mega	b.argentea mega	b.alata mega.b.argentea mega	0.42
b.argentea mega	b.seminuda mega	b.argentea mega.b.seminuda mega	0.37
b.alata mega	b.seminuda micro	b.alata mega.b.seminuda micro	0.35
b.argentea mega	b.seminuda micro	b.argentea mega.b.seminuda micro	0.33
b.alata mega	b.seminuda mega	b.alata mega.b.seminuda mega	0.14
b.argentea mega	b.argentea micro	b.argentea mega.b.argentea micro	0.05
b.alata mega	b.argentea micro	b.alata mega.b.argentea micro	0.04
b.seminuda mega	b.argentea micro	b.argentea micro.b.seminuda mega	0.02
b.alata micro	b.seminuda micro	b.alata micro.b.seminuda micro	-0.29
b.argentea mega	b.alata micro	b.alata micro.b.argentea mega	-0.76
b.alata micro	b.argentea micro	b.alata micro.b.argentea micro	-0.86

5 170 years of variation in the community structure of Santa Barbara Basin benthic foraminifera

Sara S. Kahanamoku[1], Ivo Duijnstee[1], Seth Finnegan[1]

Affiliations:

1. Department of Integrative Biology and Museum of Paleontology, University of California, Berkeley

Abstract

Here we present an analysis of diversity and community structure within Santa Barbara Basin benthic foraminifera from a core spanning 1834-2008 CE. Each sample was picked for every individual benthic foraminifer present, such that our data represent a true fossil assemblage, including rare species. Using these data alongside measurements of size for each individual, we show that species' relative abundances and biomass are temporally structured, with major shifts in relative composition and the dominance of particular species through the ~170-year interval we examine. Assemblage compositions differ from Holocene-era records, and show that species considered to be indicators of severe hypoxia begin to dominate the record towards present, with some previously ephemeral species (*N. stella*) undergoing large increases in abundance in the 21st century. PCA ordinations indicate that variation in both species composition and biomass can be explained by variation in the amount of total organic carbon (TOC, a proxy for food availability) present in each sample, as well as ENSO variance (i.e., the strength of El Niño to La Niña fluctuations). No other environmental parameters examined were significant predictors of community change as summarized by PCA axes. We interpret the relationship between ordinations on species abundance and biomass, TOC, and ENSO variability as indicating the importance of food availability for structuring SBB benthic foraminifer communities. The timing of change we observe within the data corresponds with other biotic shifts seen in benthic foraminifera assemblages from this same record, suggesting that mid-19th and 20th century changes affected the benthic foraminifer communities, from individuals to populations.

5.1 Introduction

The Santa Barbara Basin (SBB) is an extreme environment. Persistent hypoxia within the center of the basin is responsible for the preservation of seasonal varve couplets (Reimers et al. 1990, Thunell et al. 1995, Schimmelmann and Lange 1996), which are formed via alternation between wintertime rainfall enhancing terrigenous sediment delivery, and spring-summertime increases in primary productivity driving biogenic sediment deposition (Hendy et al. 2015, Du et al. 2018). The dysoxic bottom waters of the SBB result in part from the bathymetry of the basin, where high southeastern and northwestern sills (200m and 475m, respectively) restrict the movement of waters into the basin's center, which lies at ~600m water depth. Basin-enhanced hypoxia (Moffitt et al. 2014) is further intensified by overlying surface productivity in the Santa Barbara Channel (Bray et al. 1999). Thus, while hypoxia is a common feature of sites along the California margin oxygen minimum zone (OMZ), it is intensified by the unique environment of the basin and is often more extreme than non-basinal sites within the broader California bight region (Moffitt et al. 2014).

Extreme hypoxia (<0.1 ml L^{-1}) within the SBB is most intense in the late summer and early fall. Yet seasonal mitigation of these low-oxygen conditions basin occurs via "spillover events,"

which increase dissolved oxygen in the deepest areas of the basin (Reimers et al. 1990, Bray et al. 1999, Bograd et al. 2002, Moffitt et al. 2014, Goericke et al. 2015, Myhre et al. 2017). Spillover events are thought to result from contributions of enhanced spring- and summertime equatorward flow to the movement of well-oxygenated California Margin waters over the northern sill of the basin, while mixing of more poorly-oxygenated waters is prohibited via poleward flow of the less dense overlying waters of the Davidson current (Myhre et al. 2017). As a result, while oxygen remains relatively low throughout the year, fluctuations in oxygenation resulting from seasonal stagnation and flushing events allow the deepest portions of the basin to range in dissolved oxygen content from <0.1 ml L^{-1} to ~0.5 ml L^{-1} (i.e., extreme to severe hypoxia; Bograd et al. 2002, Goericke et al. 2015).

Within the resource-limited environment of the SBB, multiple clades thrive in spite of persistent hypoxic conditions. The basin is considered a "symbiosis oasis" with meiofaunal abundances and biovolumes that are an order of magnitude higher than comparable aerated sites (Bernhard et al. 2000). In these communities, benthic foraminifera comprise the majority of the eukaryotic biovolume within the basin and are present at maximal abundances during peaks in hypoxia, often living on or within sulfidic sediments (Reimers et al. 1990, Bernhard and Reimers 1991, Bernhard et al. 2000). All of the benthic foraminifera present within the basin are at minimum tolerant of low oxygen, and a majority of the most abundant species are thought to possess the ability to carry out denitrification, a key strategy for surviving prolonged periods of extreme hypoxia (Piña-Ochoa et al. 2010). In fact, most Rotaliid foraminifera–the most well-represented clade within the SBB–likely possess a partial denitrification pathway, though the extent to which each species can denitrify varies depending on their specific gene set (Woehle et al. 2022). Some of these Rotaliids are hypoxic extremophiles, such as *Nonionella stella*, which has intracellular nitrate stores that allow for complete denitrification to N_2 and are hypothesized to be able to respire nitrate for up to a month (Risgaard-Petersen et al. 2006). Others are considered to be merely hypoxia tolerant, though recent studies have shown that even species considered to be indicators of well-oxygenated conditions (e.g., *Cibicidoides wuellerstorfi*) can do well under severe to extreme hypoxia (Woehle et al. 2022).

In other words, SBB foraminifera thrive in extreme environments, and they have done so for millennia. While rapid climate changes have occurred during the Holocene–such as fluctuations between drought and extreme rainfall (Hendy et al. 2015), oscillations in oxygenation during the Little Ice Age (Wang and Hendy 2021), and oscillations of the OMZ (Hendy 2010, Moffitt et al. 2014, Wang and Hendy 2021)–these shifts in the oceanographic and climatic conditions within the basin and the broader California system are relatively constrained. Previous studies have shown that Holocene benthic foraminiferal assemblages have remained relatively consistent–for example, in which species are present and their relative abundances (Moffitt et al. 2014)–over the past ~10 kyr. However, climate change and novel human impacts arising from the colonization and industrialization of California over the past ~200 years have impacted the California Current in complex ways, with changes to oxygenation (Ren et al. 2018, Pitcher et al. 2021), productivity (Black et al. 2014), and sediment delivery regimes (Rodriguez et al. 2020), among others (Kivenson et al. 2019, Brandon et al. 2019, Osborne et al. 2020), all of which have increased the variability of even the deepest environments within the basin. While other related taxa–such as planktic foraminifera, diatoms, and silicoflagellates (Field et al. 2006, Barron et al.

2013)–have been shown to undergo community-level changes in the 20th century, fewer California Current records for benthic foraminifera exist.

Here we use a dataset of benthic foraminifer species counts and body size data from more than 19,000 individuals sampled from a core ranging from 1834-2008 CE to examine trends in benthic foraminifer diversity, abundance, and biomass in the SBB over the past two centuries, during a period of significant environmental change. We ask: how has benthic foraminifer community structure in the deepest environments of the basin responded to increased environmental variation during the 19th through 21st centuries?

5.2 Materials and methods

5.2.1 Core sampling and sample processing

A box core was collected in 2010 aboard the R/V Melville from the center of the SBB at station MV1012-ST46.9 (34˚17.228'N, 120˚02.135'W; ~580m water depth; Figure 5.1). Established chronologies for SBB material were adapted to create an age model for core MV1012 that extended to the base of the box core. 0.5 cm transverse sections from each core were sampled and ages were assigned to the top and bottom of each sampled section, with a typical resolution of 2.2 ± 0.57 years (Table 5.1). Samples were dried and washed over a 63-μm mesh to create material for micropaleontological analysis. Prior to the present study, these samples were picked for plastic particles (Brandon et al. 2019) and fish otoliths (Jones and Checkley 2019). All other assemblages within the samples are thus considered ecologically representative.

For the present study, box core material was dry picked under a Leica dissecting microscope at 16x magnification for all benthic foraminifera within each sample. Samples were not split, but were picked in their entirety. As a result, the foraminifer assemblages we examine here capture the full range of variation present within each sample. Following picking, samples were arranged on brass-coated matte black picking plates and imaged in bulk using a Keyence VHX-7000 digital imaging microscope at 150x magnification with lighting settings held constant across samples for consistency in post-processing.

Full-sample images were processed using *AutoMorph*, an open-source suite of image processing software designed to extract outline-based measurements from full-assemblage images. Two *Automorph* modules were used for this study: `segment`, which identifies individual objects within full-assemblage images and creates individual 2D EDF images for each; and `run2dmorph`, which generates outline-based morphometric measurements for each individual object. Image outputs from `segment` were used for species identification and functional classification, while morphometric outputs from `run2dmorph` were used to compile biomass information for each species.

5.2.2 Species identification and functional classification

Individual images produced via `segment` formed the basis for species identification and related classifications. Both benthic foraminifera and non-foraminifer objects extracted by segment were visually identified and placed into the most appropriate classification category (see Chapter 2 of this dissertation). Benthic foraminifera were identified to species (Table 5.2); both complete and partially broken shells were used for species identifications, but heavily fragmented foraminifera

were placed into a separate "fragment" category and excluded from the analysis. These identification data were used to calculate relative abundance for each species within a given sample. Deposition rates for box core MV1012 (Brandon et al. 2019) were used to transform species counts into measurements of benthic foraminifer accumulation rate (BFAR; foraminifera per surface area per year; Table 5.1).

Functional classifications were assigned to each species to capture their oxygen tolerance category, minimum reported oxygenation threshold, denitrification ability, and maximum reported denitrification threshold (Table 5.2). These classifications were derived from previously published literature. Oxygenation marker taxa were classified following the approach of Jorissen et al. (2007) and Moffitt et al. (2014), and oxygen classifications were associated with the minimum reported oxygen threshold for each species. In cases where oxygen classifications differed from the minimum reported oxygen threshold for that species, classifications were kept consistent with previously published literature. Denitrification ability and maximum reported denitrification (mM NO_3^-) were classified following the approach of Piña-Ochoa et al. (2010) and Woehle et al. (2022) and maximum reported denitrification thresholds were updated with the most recent species-specific values wherever possible.

5.2.3 Morphometric analysis

Individual shell areas were measured from specimen images using *AutoMorph*'s `run2dmorph` module, which uses an outline-based approach to generate morphometric measurement. Measurements were filtered to exclude broken and poorly-extracted measurements by applying a rugosity filter following methods outlined in Chapters 2 and 4 of this dissertation. We approximated biomass using outline-based measurements of 2D shell area. Previous studies have shown that shell area is considered to scale relatively constantly with shell volume for most benthic foraminifera, including a subset of the species we examine here (Belanger 2022). Because of this, we used measurements of shell area as a proxy for biomass in all analyses.

5.2.4 Multivariate analysis

We used a Principal Components Analysis (PCA) to examine multivariate structure within both the relative abundance and relative biomass data. All analyses were performed in R (R Core Team 2013) using the package `vegan` (Oksanen et al. 2020).

PCA is an ordination technique that assumes that samples are linearly increasing or decreasing along a gradient, and is used to find gradients along which the majority of the variation with the data matrix is explained (i.e., maximizing spread of individual samples along the given direction in the multivariate space of species abundance; Ringnér 2008). Normalized data (where normalization was done for the dataset as a whole) were used in PCA analyses. Separate PCA analyses were performed on relative abundance and relative biomass, using two distinct datasets for each metric: one that included common species, and another including all species from each sample (to capture the impact of rare species on community-level abundance and biomass). In addition, we performed a PCA on a dataset that contained both relative abundance and relative biomass, for all species in each sample, to determine the relative importance of each metric for understanding community-level change.

As an alternative analysis, samples were also processed using Non-metric Multidimensional Scaling (NMDS). NMDS is an indirect gradient analysis approach used to produce an ordination which relies on rank order distances, optimizing the difference between distances in the reduced dimension compared to the complete multidimensional space (Faith et al. 1987). When data were analyzed using NMDS, similar temporal structure to the PCA was visible within the ordination space (Figure S5.1). However, the analysis resulted in a constant stress value of 0.105 in all runs attempted, with no improvement when run parameters were altered. While the analysis resulted in a high R^2 value (nonmetric fit: 0.98; linear fit: 0.94), NMDS axis 1 and 2 explained, respectively, only 28.3% and 20.4% of the variance within the data (Figure S5.1). As a result, we favored PCA over NMDS.

5.2.5 Environmental data collection

To examine how environmental change impacts community composition, we collected data from previously published literature on environmental parameters with the potential to influence foraminifer diversity, abundance, and life history. Two types of data were used: paleoceanographic data (typically produced via core records from adjacent sites within the SBB) and direct measurements of oceanographic parameters (obtained from the California Cooperative Oceanic Fisheries Investigations, or CalCOFI; CalCOFI 2022). Proxy data included information on total organic carbon (a proxy for food availability that strongly co-varies with total nitrogen; Wang et al. 2017), redox metals (proxies for oxygenation; Wang and Hendy 2021), and El Niño Southern Oscillation Index and Variance (ENSO; Li et al. 2011) (Table S5.1). All proxy data were sourced from core records that were sampled near to or at the sampling location of the cores used within these studies, all have comparable age models that allow for integration of these variables with our morphological and reproductive data.

Direct observational oceanographic data was obtained via the CalCOFI online database for samples from the center of the SBB (Station 081.8 046.9; ~34.28˚N, 120.02˚W). Data from 1953-2008 CE was compiled for bottom water temperature; oxygen saturation state; and concentrations of nitrate, phosphate, and silicate from bottles collected at or below 500m water depth. Monthly data were averaged to create a yearly record of each parameter at the deepest sections of the water column sampled by CalCOFI. Within-year minima and variance were also calculated for each of the variables of interest in order to capture a measure of sub-seasonal variability.

5.2.6 Statistical analysis

Hill diversities with $q = 0$ (richness), 1 (Shannon entropy), and 2 (inverse Simpson index) were calculated on raw species counts for benthic foraminiferal communities following Chao et al. (2014) using the R package `vegan` (Oksanen et al. 2013). Multivariate data were examined against environmental predictors in additive general linear models. We tested each environmental variable as predictors for PC1 and PC2 using the `vegan` function 'envfit,' which performs a multiple regression of environmental variables on ordination axes and assesses significance using a permutation test. Outputs were assessed using traditional linear regressions and model selection was performed with ANOVA.

5.3 Results

5.3.1 Species diversity and relative contributions are variable through time

The data we examine encompasses 30 samples, containing 19,684 individuals in ~56 species for a total of 19,684 individuals. Of these, 16,200 had successfully extracted morphometric data used for shell area approximations. These shell areas were used as a proxy for biomass in our analyses. The species represent 34 genera, the majority of which come from within the Rotaliid clade (Table 5.1).

Shifts in both biomass and abundance of the most common species occur throughout the interval we examine (Figure 5.2). When data are placed into time bins (1834-1850, 1850-1900, 1900-1950, 1950-2000, and 2000-2008 CE) and these composite data are used to calculate relative abundances, the directionality of changes in relative composition are apparent (Figure 5.3). Notably, *Bolivina argentea* comprises the majority of the assemblage at the beginning of the record, with a peak relative abundance of 40% and relative biomass of 60% (Figure 5.2, Figure 5.3). However, in all time bins following, *B. argentea* decreases in both relative abundance (Figure 5.3) and relative biomass, in some samples dropping to near absence (Figure 5.2). In contrast, *Nonionella stella* increases in compositional importance towards the present and becomes the dominant species within samples following ~1970 CE (Figure 5.2, Figure 5.3). *N. stella* is also observed to undergo "blooms" in 1998 and 2003 CE, where they comprise more than 50% of the assemblage in these years. Similar trends are observed in total abundances through time (Figure S5.2).

Other compositional shifts are less extreme but likewise show a temporal trend. For example, *Bolivina seminuda* decreases in both biomass and relative abundance towards the present, with extremely low abundances observed following the late 1980s (Figure 5.2, Figure 5.3). *B. pacifica* and *B. alata* follow a similar pattern, with their highest abundances and biomass seen in the earliest part of the record, after which they decrease in compositional importance. *S. eckisi* fluctuates in compositional importance, becoming dominant in the early- to mid-20th century, following which it becomes the second most common species behind *N. stella*. The remainder of the common species (*Bulimina exilis*, *Chilostomella ovoidea*, and *Fursenkoina cornuta*) are relatively stable in their abundances and biomass through time, with low compositional importance throughout the interval. When rare species (Table S5.2; defined as species with less than 10 total occurrences throughout the core record) are included, they comprise ~25% of samples from the earliest time bin (1834-1850 CE), following which their abundance drops and remains a relatively small contribution to overall assemblages (Figure S5.3).

Species richness (Hill number $q = 0$) and diversity (Hill number $q = 2$, or inverse Simpson index) fluctuate across the core interval (Figure 5.2). Peaks for both metrics occur at the very beginning of the record, following which an interval of relatively constant diversity and richness persists until the late 20th century CE, when variability in both diversity and richness increases until a large drop in both occurs towards the end of the record at ~2004 CE.

5.3.2 Changing assemblages may partially reflect changing oxygenation conditions

The relative contribution to each sample of species that represent strongly hypoxic conditions (oxygen threshold of <0.1 ml L^{-1}) increases towards the recent, becoming overwhelmingly dominant following the earliest time bin in our samples (Figure S5.4). There are stepped increases between 1900 and 2000 CE that show that faunal indicators of strong hypoxia do

increase in their contributions to overall assemblages towards the recent, with concomitant decreases in intermediate and strong hypoxia (0.3 ml L^{-1}) and intermediate hypoxia (0.6 ml L^{-1}) species. Oxic species (3 ml L^{-1}) remain rare throughout. When denitrification ability (Table 5.2) is assessed, our data show that denitrifiers are particularly abundant in SBB samples (Figure S5.5). Due to incomplete classification information, the true abundance of foraminifera which can carry out denitrification within our samples is likely higher than what we observe here.

5.3.3 Multivariate analyses show significant differences between oldest and youngest samples

The PCA ordination performed on relative abundance data is presented in Figure 5.4. PCA axis 1 accounted for 53% of the variation, while PCA axis 2 accounted for 30% (Figure S5.6). Species loadings show strong influences of *B. seminuda*, *B. exilis*, and *F. cornuta* within the ordination space. Similar results are obtained when only common species are included in the analysis (Figure S5.7). When PCA axis 1 is plotted against time, we find that this axis increases in variability following ~1950 CE (Figure S5.8).

The PCA ordination performed on relative biomass data is presented in Figure 5.5. PCA axis 1 accounted for 55% of the variation, while PCA axis 2 accounted for 28% (Figure S5.6). Likewise, as with the abundance dataset, similar results are obtained for a PCA ordination is performed on biomass dataset that only includes common species (Figure S5.9).

Both ordinations we performed–the PCA on relative abundance data and the PCA on relative biomass data–yield similarly structured results. Eigenvalues are similarly structured for each, and when temporal trends within these axes are compared, we find that PCA axis 2 for relative biomass data changes significantly following ~1950 CE, similar to trends observed in PCA axis 1 for abundance (Figure S5.8). Biomass PC1 and abundance PC2 are highly correlated in a linear regression (Figure S5.10, $R^2 = 0.91$), suggesting that they represent similar underlying structure in the dataset.

However, there are some notable differences between these metrics of ecological structure. There is significant spread between relative abundance and relative biomass measurements when they are compared within the same ordination space (Figure 5.6). Some samples are closely grouped, such that biomass and abundance data plot in the same PCA axis 1 and axis 2 coordinates, while other samples have significant and large offsets between abundance and biomass data. In addition to differences in spread, the directionality of the offsets observed is different between oldest samples (<1950 CE) and those from younger time periods (1950-2000 CE; 2000-2008 CE). Together, these trends suggest that samples (<1950 CE) are grouped separately from younger (>1950 CE) samples, and likely have distinct community characteristics.

When PCA axes are compared across these two datasets, older samples appear skewed towards relative biomass PC2, while younger samples are more skewed towards relative abundance PC1 (Figure S5.10). This temporal variation is more apparent when both datasets are plotted within the same ordination space (Figure 5.6); the oldest samples within the core (i.e, pre-1900 CE) are separated from the youngest samples when PCA axis 1 is compared with PCA axis 2 (Figure 5.7) and PCA axis 3 (Figure S5.11).

To determine whether these PCAs were impacted by negative correlation biases (Filzmoser and Hron 2008, 2009, Filzmoser et al. 2009), we ran an additional PCA on the 10 most common species within the relative abundance data using the R package `robCompositions` (Templ et al. 2011). In this analysis, PCA axis 1 accounted for 37% of the variation, while PCA axis 2 accounted for 28.9% (Figure S5.12). Temporal structuring remains apparent in this analysis, with the oldest samples grouping separately from those from younger time periods. Species loadings differ slightly, with *N. stella* emerging as strongly inversely related to both PCA axes. However, other common species loadings show relatively similar relationships to one another as those seen within the primary PCA analysis, both in their relative directions to one another and their absolute directions within the temporally-structured data (Figures S5.8, S5.11).

5.3.4 Food availability and ENSO variability are major predictor of sample variance

When environmental data were tested as predictors of major ordination axes (i.e., community composition), relative abundance and relative biomass PCA axes 1 and 2 were found to both be significantly correlated with TOC (Figure 5.7) and ENSO Variance (here, a 21-year running biweight variance; Li et al. 2011) (Figure 5.8; Table 5.3). No other proxy variables tested (ENSO Index and an index of reducing conditions) were significant. Similarly, no instrumental variables (CalCOFI 2022) were significant predictors of the primary PCA axes in any model tested. This includes both annually-averaged variables (i.e., annual temperature; oxygen saturation state; and nitrite, nitrate, phosphate, and silicate concentrations) as well as variables that capture sub-annual and seasonal trends (i.e., minima and variance of variables of interest; Table 5.3).

Plotting these environmental variables against principal components from ordinations suggests that even nonsignificant variables may play a role in structuring the community variation we observe. When environmental proxy variable vectors are placed on PCA ordinations for relative abundance, TOC and ENSO variance are parallel and similar in strength, yet have opposite signs (TOC is inversely related to abundance PCA axis 1, while ENSO variance is positively related; Figure 5.8A). ENSO Index shows a similar trajectory and strength to ENSO Variance. In contrast, the index of reducing conditions within the basin has the highest vector value of all variables examined, with a negative relationship to PCA axis 2 (Figure 5.8A). Instrumental variables also show strong loadings for temperature (positively related to PCA axis 2), bottom water oxygenation (inversely related to PCA axis 2), and total annual rainfall (positively related to PCA axis 1 and inversely related to PCA axis 2; Figure 5.8B). Environmental loadings on relative biomass PCA ordinations show similar trends, though loadings often differ slightly. When proxy data are examined, ENSO index has the highest loading strength (inversely related to PCA axis 2) and reducing index has the lowest (positively related to PCA axis 1), while ENSO variance and TOC are positively and inversely correlated, respectively, with PCA axis 1 (Figure 5.8C). Instrumental variables show strong loadings for bottom water oxygenation (positively related to PCA axis 1 and inversely related to PCA axis 2) and bottom water temperature and total annual rainfall (inversely related to PCA axis 1 and positively related to PCA axis 2; Figure 5.8D).

5.4 Discussion

5.4.1 Recent communities are distinctly different from older communities

Our data show that benthic foraminifer accumulation rate and the diversity of communities in the SBB decrease towards the recent (Figure 5.2). The data we use allow us to assess community composition from samples that are representative of full fossil assemblages within the basin, capturing the impact of rare species within the >63 μm fraction throughout the interval. In addition, we can use these data to capture trends in relative biomass and compare these with relative and absolute abundance trajectories through time. Using these data, we see that the earliest samples from this record (1834 and 1836 CE) have the highest proportion of rare species throughout the box core record (Figure S5.3). Rare species (Table S5.2) decrease significantly following the mid-19th century, after which they represent less than 10% of the relative composition of samples until the end of the core record in 2008 CE.

It is likely that the relatively high species diversity during the earliest part of the core is tied to the *Macoma* event in 1835-1840 CE, during which time a macrofaunal community (including pelecypod bivalves from the genus *Macoma*) flourished briefly in the SBB (Schimmelmann et al. 1992, Burke et al. 1996). It is suggested that the *Macoma* event represents a time of heightened oxygen levels, potentially due to decreased upwelling concurrent with a flushing event that allowed for a sustained influx of oxygen-rich waters to the basin (Schimmelmann et al. 1992). Previous studies suggest that benthic foraminifer diversity reaches a peak during this time, but corresponds with decreased abundance (Burke et al. 1996). We find that this trend holds within our samples, where common species' abundances drop during the event (Figures S5.2, S5.15). The samples we examine from this period have the highest proportion of oxic indicator species of all samples from the MV1012-BC core record; in addition, a number of the species we observe during this time interval do not reappear later in the record.

Following this anomalous, high-diversity interval, we find that species richness and Shannon diversity decreases after the mid-19th century, remaining relatively stable in this new state until another drop in the mid-20th century. Post-1950 CE samples show heightened variability in these diversity metrics, with a final major drop in richness and diversity occurring in the latest part of the core interval, at ~2004-2006 CE. While this interval corresponds with the coretop, it is considered to be undisturbed, suggesting that these recent drops in diversity are not necessarily taphonomic (Jones 2016, Brandon et al. 2019, Jones and Checkley 2019; see supplemental for more information).

Species composition within the SBB over the past 170 years differs from those observed over the broader Holocene interval. When our data are compared with longer-term records from nearby sites within the SBB, the composition of dominant species within the basin is substantially different in the modern era. *B. argentea* is compositionally dominant during the Holocene (11.7-0 kya), while *N. stella* is the most ephemeral (Moffitt et al. 2014). This trend reverses in our samples: *N. stella* becomes compositionally dominant following the mid-20th century CE, while *B. argentea* steadily declines in compositional importance across the 19th through 21st centuries. Other *Bolivinia* species undergo similar declines in their relative abundance within post-19th century SBB assemblages, mirroring findings in Chapters 1 and 2 of this dissertation. The compositional resurgence of *N. stella* is due to a large increase to its absolute abundance (rather than representing an overall decreased abundance at the community level; Figure S5.2).

5.4.2 Assemblages reflect changing environmental conditions

Species classifications show that there is an increasing prevalence of hypoxic-specialist species towards the present (Figure S5.4). These changes in benthic foraminifer assemblages over the past ~170 years broadly reflect oceanographic conditions as evidenced by proxy and instrumental records. Warming occurs in the SBB during the 20th century alongside reduced upwelling, which impacted water column stratification and decreased oxygenation at depth (Weinheimer et al. 1999, Field et al. 2006, Bringué et al. 2014).

Deoxygenation heightened following the mid-20th century. A large-scale oceanographic regime shift occurred in the North Pacific in the 1970s (Alfken et al. 2021), which resulted in reductions in the influence of the southward California Current and increases in the influence of the poleward California Undercurrent on the SBB system. These changing oceanographic conditions resulted in reduced mixing and heightened stratification in the basin, which increased the supply of warm, oxygen-poor tropical waters at deeper levels in the basin. This long-term trend of decreasing oxygen was continued by unprecedented increases in water column denitrification beginning in 2004 (White et al. 2019) due to the shoaling of the hypoxic boundary and declines in the rate or extent of flushing events within the SBB (Bograd et al. 2008, Goericke et al. 2015). Even more dramatic changes have occurred over the last decade, the most striking of which has been the increase in nitrite concentrations by over an order of magnitude (Goericke et al. 2015).

While our core period only goes up until 2008, these large-scale environmental impacts correspond with trends in our data, including the sharp diversity decrease observed in 2004 and *N. stella* "blooms," the largest of which is seen in 2003. Such blooms are reminiscent of repopulation events of anoxia-induced disturbance as observed, for instance, in Gullmar Fjord, Sweden since 1980 (e.g., Filipsson and Nordberg 2004). In the same time interval after the 1970s other taxa have similar short-lived blooms in different sub-decadal time intervals (e.g., *B. pacifica*, *C. ovoidea*, and *F. cornuta*; see Figure S5.2), producing the volatility in PCA scores after 1975 (Figure S5.8b and d). If these asynchronous blooms of multiple taxa indeed represent repopulation events after disturbance, the dominance of a few taxa may well be caused by founder-effect-like random events following the bottlenecks of disturbance. In this scenario, rapid, sub-decadal variation in species composition may actually represent repetition of very similar environmental conditions of temporary recovery following interpunctuating pulses of more severe hypoxia or anoxia. Additional data is needed to understand whether the trends we observe within our samples for benthic foraminifera within the SBB have remained consistent over the past ~15 years, or whether additional changes have occurred.

5.4.3 Abundance and biomass data show similar but offset trends

Ordinations for abundance and biomass are structured similarly, with PCA axes 1 and 2 explaining the majority (83%) of the variation within each dataset. One interpretation of these related ordinations–where the axis structuring the majority of the variation for one dataset is the secondary axis of variation for the other–is that abundance and biomass data are structured in slightly different ways. Offsets between these datasets can be seen both when relative abundance and biomass are plotted against time (Figure 5.2) and when they are examined in the same ordination space (Figure 5.6).

Abundance and biomass data both show temporal structuring, such that the oldest samples form a distinct group from the youngest samples we examine (Figures 5.4-5.6). When PCA axes for

the separate ordinations are compared, oldest samples are found to skew towards the relative biomass PCA axis, while younger samples skew towards the relative abundance PCA axis (Figure S5.10). There is also temporal grouping when the two datasets are treated as one and compared within the same ordination space (Figure 5.6), and an offset between relative abundance and relative biomass data is observed to change in both strength and direction through time (Figure 5.6). Interestingly, some samples from the middle of the core record (~1950 CE) show little to no offset between relative abundance and relative biomass data (Figure 5.6, Figure S5.10), suggesting that these datasets map nearly identically to one another during these times. While these multivariate results are difficult to interpret, they suggest that differences exist between biomass and relative abundance data which may impact how each data type captures variation in community structure through time.

5.4.4 Food availability and environmental variation as a driver of community composition

We find that TOC and ENSO variance are significant environmental predictors for PCA axes 1 and 2 for both abundance and biomass, potentially explaining ~30% and 40% of the variation in these axes, respectively (Figures 5.7 and 5.8). This suggests that both food availability and environmental variation structure the benthic foraminifer communities we examine, both in ordination space and through time. The oldest samples within the core–those from pre-1900, which have the highest diversity and species richness–are associated with lower values of TOC and higher values of ENSO variability, while the youngest samples show opposite relationships (Figures 5.7 and 5.8, Figure S5.13). Additionally, TOC (but not ENSO variance) is a significant predictor of abundance (i.e., time- and volume-normalized abundance, or BFAR; Table S5.3), with a majority of the common species having inverse relationships between their absolute abundance and TOC (Figure S5.14). A major exception to this trend is *N. stella*, which increases in absolute abundance with TOC; however, variation in *N. stella* abundance is poorly explained by TOC alone ($R^2 \approx 0$).

TOC is interpreted as primarily indicating export productivity in the basin, rather than simply measuring preservation due to reduced oxygen exposure time (Zhao et al. 2000, Hendy et al. 2015, Wang et al. 2017). As a result, this finding suggests that food availability is a major determinant of community composition within the basin. ENSO variance is more difficult to interpret as a predictor of community structure. ENSO phases (i.e., negative Southern Oscillation Index values) typically deepen the thermocline, dampening upwelling, and resulting in lessened export of nutrients to the seafloor, among other factors (Li et al. 2011, Jacox et al. 2015). ENSO variance (a moving-window estimate of variation in ENSO amplitude) may thus be thought of as representing the strength of fluctuations in ENSO over time. In our data, we see inverse relationships between TOC and ENSO variance and the PCA axes we examine, suggesting that ENSO variability is likely related to food availability in addition to other factors such as oxygenation (McPhaden et al. 2006).

One interpretation of the relationships between TOC and the uni- and multivariate measures of community structure we examine here is that increasing amounts of TOC lead to low-diversity assemblages dominated by a few taxa with high abundance (Gooday 1988, 1996). Our data also display this pattern, where intervals with decreased TOC often correspond with increases in species-specific relative abundance and increases in diversity metrics, and vice versa (Figure S5.15) which potentially mirror increases in abundance PC1 and biomass PC2 scores with

heightened TOC (Figure 5.7). This direct connection between TOC and abundance within our samples suggests that food availability is a major determinant of community structure within the SBB.

The impact of ENSO variability on biotic assemblages is less well-understood, but strong ENSO variability has been shown to drive heightened variation in the composition of benthic foraminifer communities (Kelmo and Hallock 2013). The youngest samples we examine (primarily 21st-century) exhibit the lowest amounts of ENSO variance and correspond with a period of low diversity. While this diversity drop may be related to TOC, as mentioned above, it is possible that it is also partially driven by lessened ENSO variability. Further research is needed to better understand the relationship between ENSO variance and community composition within the SBB.

Notably, similar trends are also observed in body size data from the same core record (Chapter 2 of this dissertation), where total nitrogen (TN; highly correlated with TOC, and another proxy for food availability) and ENSO variance are found to be significant predictors of biomass for some SBB species. Food availability is well-known to structure benthic foraminifer assemblages, with evidence from both experimental settings (Duijnstee et al. 2003, Nomaki et al. 2005, Ernst et al. 2005) and observational data (Gooday 1988, Loubere 1994, Lesen 2005, Belanger 2022), and is considered to be a primary control structuring foraminifer diversity over time periods similar to those captured within our samples (Ernst et al. 2005).

Studies of SBB conditions over past two centuries suggest that food availability is impacted by broader oceanographic, climatic, and land-use changes within the region. TOC in the SBB increases towards the recent (Figure S5.2), and are likely driven by increased delivery via heightened sedimentation, thus primarily indicating export productivity rather than simply measuring TOC preservation due to reduced oxygen exposure time (Zhao et al. 2000, Hendy et al. 2015, Wang et al. 2017). Within the SBB, TOC is likely delivered to the seafloor via marine snow events in the spring and summer (Thunell et al. 1995, Thunell 1998), but can also be deposited via storm-related river discharge (Warrick et al. 2008) and carried to the center of the basin via hyperpycnal currents (Warrick et al. 2008, Hendy et al. 2015). Large particulate delivery events–such as flooding in 1861-1862, the St. Francis Dam disaster of 1928, and an oil spill in 1969 CE (Schimmelmann and Kastner 1993, Engstrom 1996, Taylor and Taylor 2007, Hendy et al. 2015)–have been shown to impact TOC within the SBB. In the present study, we find some correlation between these events and the assemblage shifts we observe (Figure S5.15).

It is important to note that the relevant timescales of environmental impacts within the basin likely play a role in determining which variables resolve as significant predictors of species composition when using annually-resolved data. We find that no variables that capture sub-annual oceanographic variation (i.e., the minima and variance of oxygenation and food proxies) are significant predictors of community structuring in our samples, as represented by PCA ordinations. The lack of correlation between these datasets may be due in part to the nature of the benthic foraminifer record within the SBB. Benthic foraminifera often vertically migrate within sediment, contributing to mixing across layers and driving time averaging within samples (Alve and Bernhard 1995, Geslin et al. 2004). While vertical migration is much less pronounced within anoxic sediments like those in the SBB as opposed to more well-oxygenated sites (Moodley et al.

1998, Duijnstee et al. 2003, Koho et al. 2011), assemblages may still extend beyond their true seasonal layers and contribute to "ghosting" across samples. As a result, higher-resolution (i.e., sub-seasonal) studies are needed to fully capture the impact of sub-annual variation on benthic foraminifer community structure in the SBB.

5.4.5 SBB community change at all levels

The timing of the shifts in diversity and abundance we observe roughly corresponds with changes in reproduction (Chapter 1 of this dissertation) and body size (Chapter 2 of this dissertation) towards the recent. In the mid-19th and 20th centuries, benthic foraminifera within the SBB undergo crashes in abundance, drops in the relative frequency of asexual reproduction, decreases in test size, and downward trends in diversity. Following this time point, there is heightened variability in biological characteristics at all ecological scales–in reproductive life history; inter- and intraspecific biomass; and in species abundance, diversity, and community composition–that persists through the present day.

The changes we observe suggest that the SBB has become a different system towards the present than it has been throughout the majority of the late Holocene. Put simply, SBB benthic foraminifera experienced strong changes to individual- and population-level characteristics in the mid-19th and 20th centuries, after which time these characteristics became more readily variable. In other words, not only do SBB communities undergo change in the modern era, but they also become more changeable. The data we examine, taken together with evidence from previous work, suggests that modern benthic foraminifer ecosystems are significantly different from those of both the past ~1 kyr and over the longer Holocene interval (~11 kyr; Moffitt et al. 2014).

Given that the SBB is a complex system, the drivers of these changes may be difficult to pinpoint with certainty and precision. Yet the timing of the changes we observe aligns with major events in the history of California, as well as major changes to the climatic system that result from novel conditions that arise over the past few hundred years and intensify in the 20th and 21st century (Black et al. 2014, Pitcher et al. 2021). Our finding that food availability plays a large role in structuring SBB benthic foraminifer communities–and in particular that rising TOC drives decreases in diversity and abundance–suggests that under future climate scenarios where TOC is increases are projected to intensify (Xiu et al. 2018, Pozo Buil et al. 2021), benthic foraminifera will experience heightened change. Future work to examine the ongoing impact of California Current system changes–as well as less direct impacts from human-derived sources (e.g., Halpern et al. 2009, Yasuhara et al. 2012, Collins et al. 2019, Brandon et al. 2019, Broadman et al. 2022)–is needed to fully unravel the biotic history of SBB ecosystems and their future under a changing climate.

Chapter 5 Figures

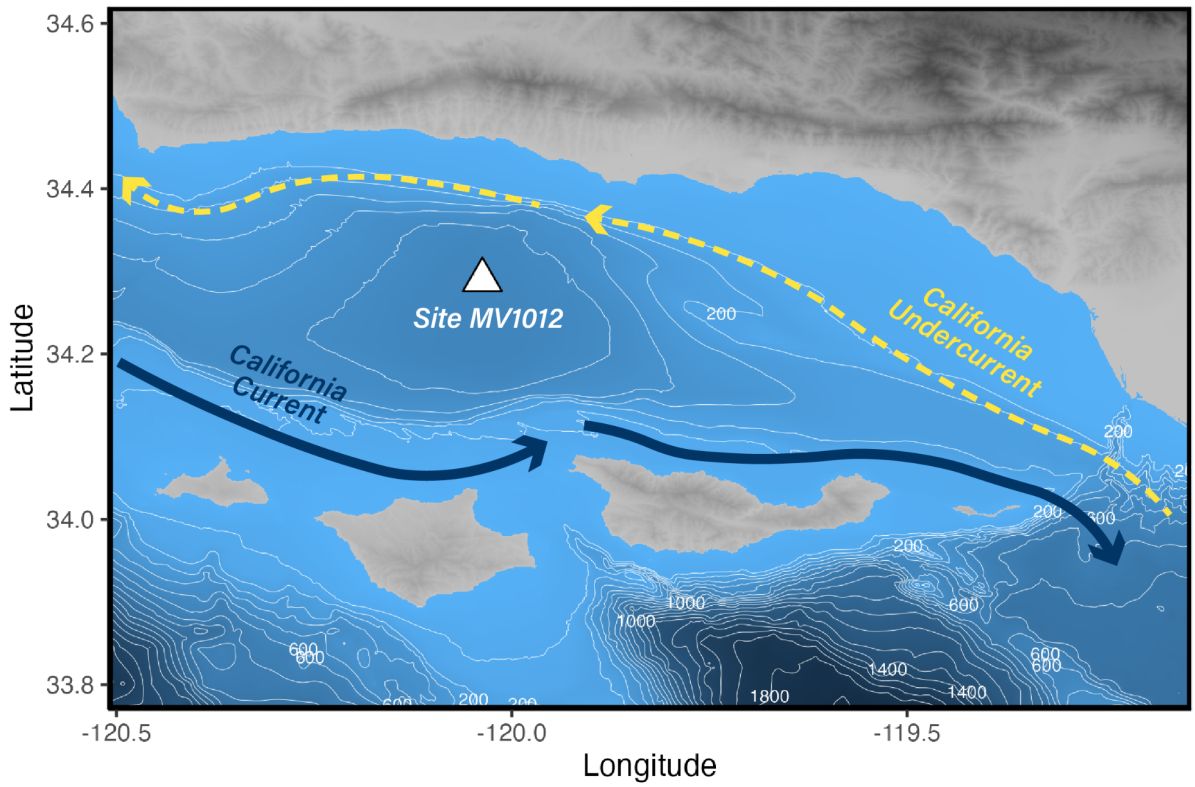

Figure 5.1: Setting and oceanographic influences on the Santa Barbara Basin.
Site MV1012 is in the center of the SBB (34˚17.228'N, 120˚02.135'W; ~580m water depth), and was chosen as a reoccupation of ODP site 893. The surficial California Current (CC) and deeper Undercurrent (CU) run in opposite directions through the SBB region, with the CC having a subarctic origin and the CU having a tropical origin.

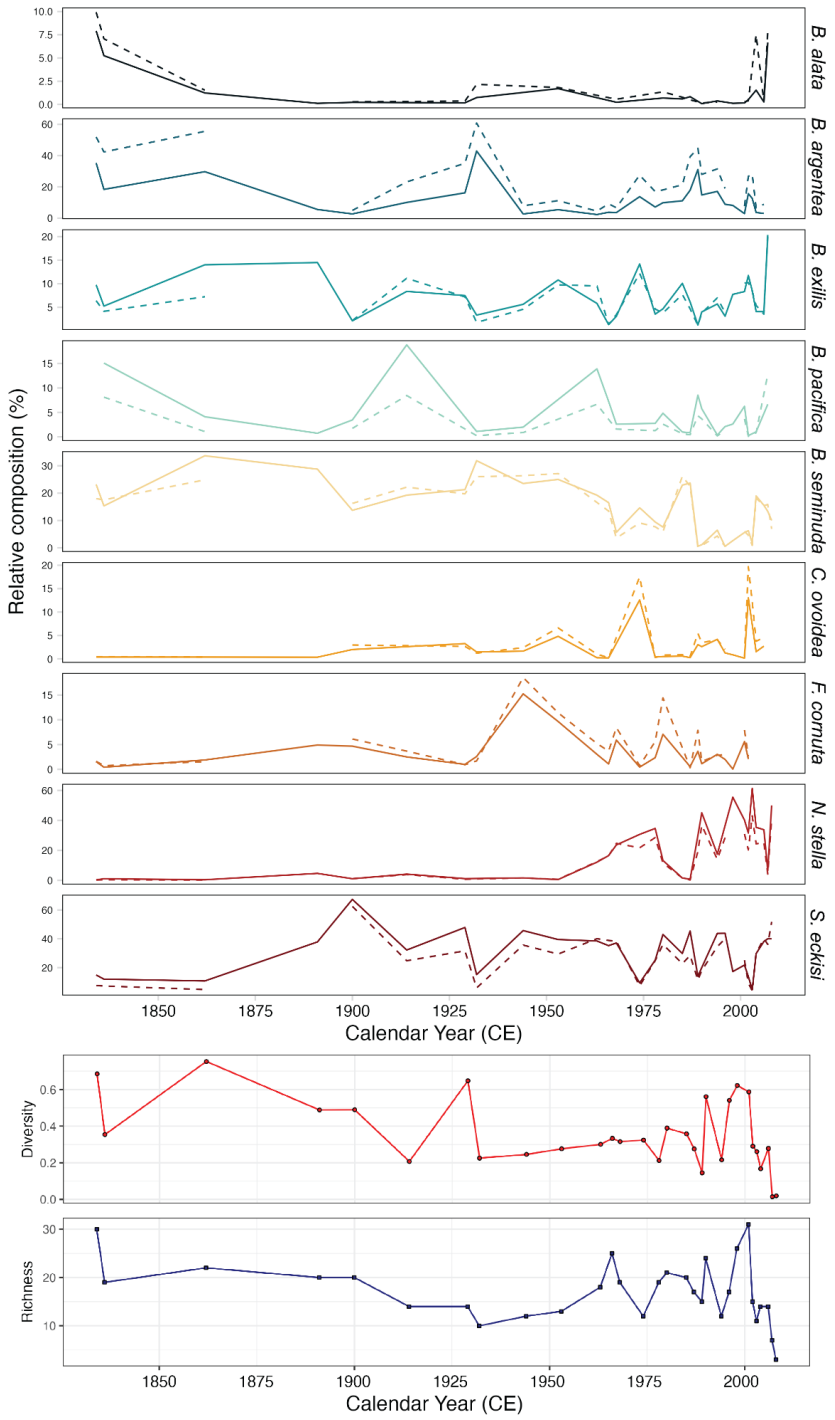

Figure 5.2: Relative composition and diversity metrics of SBB foraminifer assemblages, 1834-2008 CE.
Panel (a) shows relative composition for nine of the most common species across this interval. Solid lines indicate relative abundance, while dashed lines indicate relative biomass for each species. Panel (b) shows Hill numbers $q = 0$ and 2 calculated on absolute abundance for each sample. Top of panel (b) is the inverse Shannon index ($q = 2$; red line with circular points); bottom of panel (b) is species richness ($q = 0$; blue line with square points).

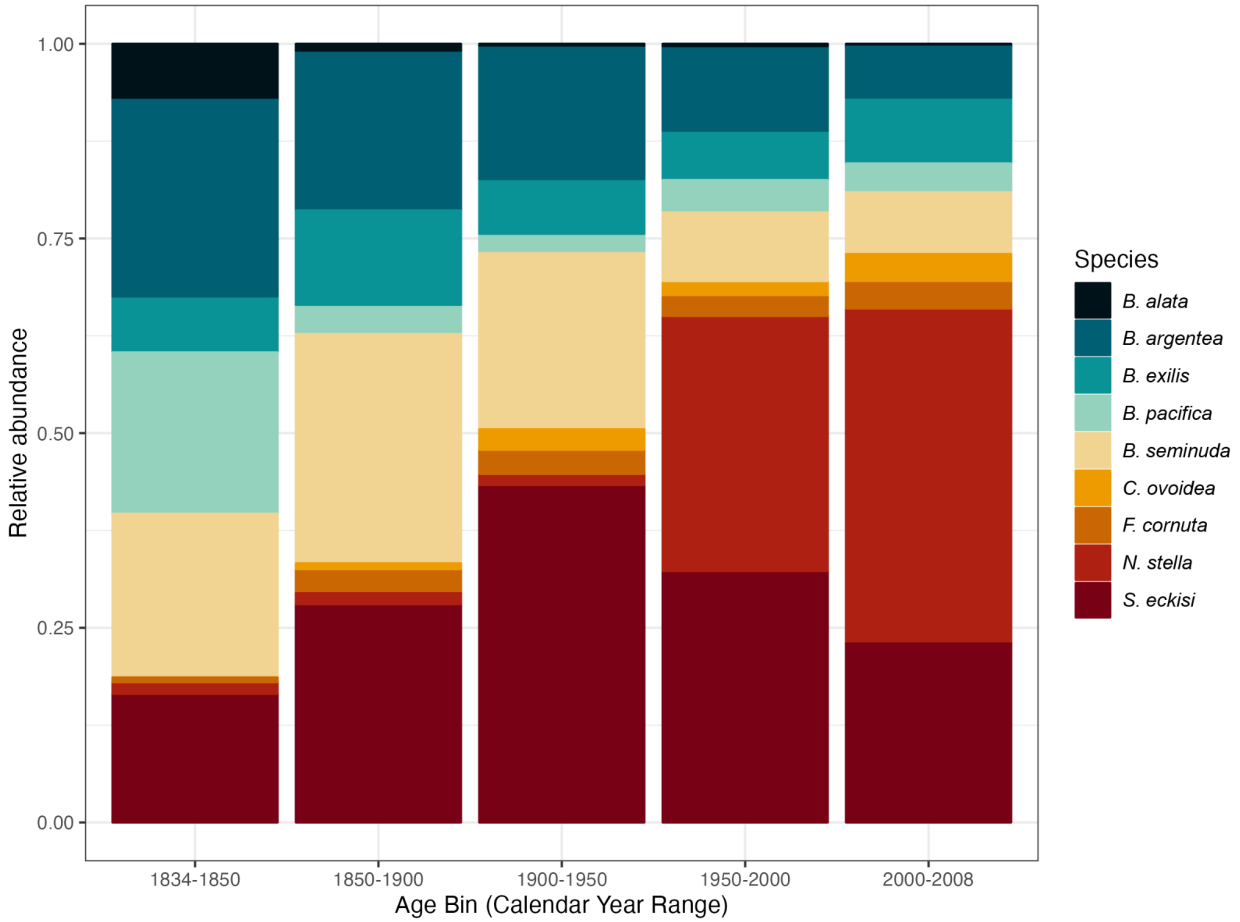

Figure 5.3: Relative abundance of common species, 1834-2008 CE.
Here, common species are those with more than ten total occurrences throughout the core interval. Relative abundances are calculated from total species counts when grouped into five age bins: 1834-1850 CE, 1850-1900 CE, 1900-1950 CE, 1950-2000 CE and 2000-2008 CE. Colors correspond to species identity.

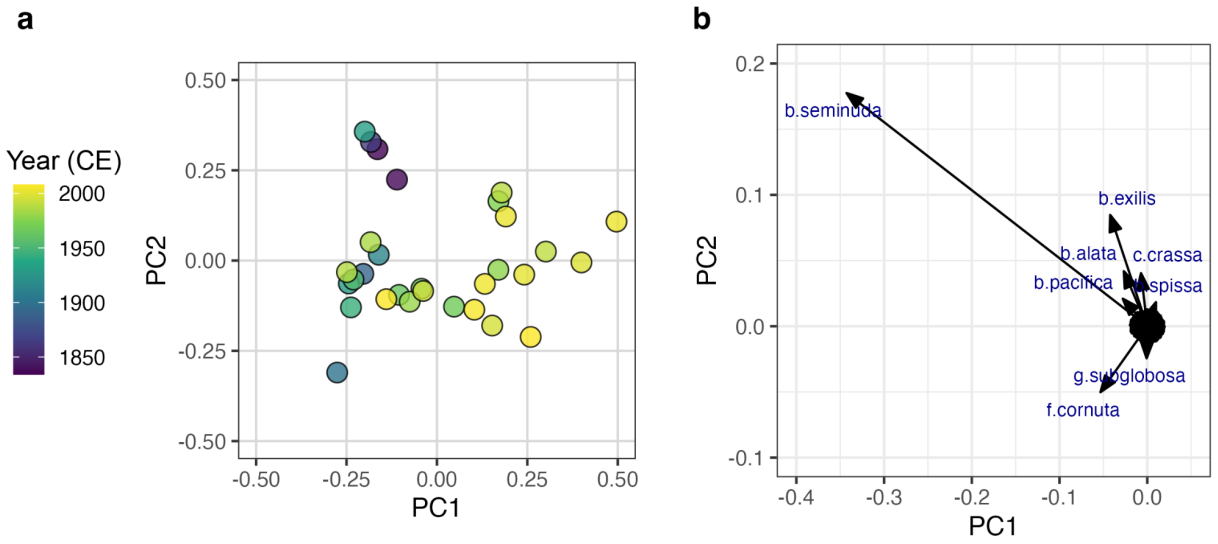

Figure 5.4: PCA of species relative abundance for all species.
Included specimens are summarized in Tables S5.2 and S5.3. (a) Sample scores; colors denote sample age in calendar years (CE). (b) Species loadings; length of vectors denote the degree of correlation between each given species and the principal components. Species with highly similar loading values close to the centroid are not labeled; see Figure 5.6 for more information on these groups.

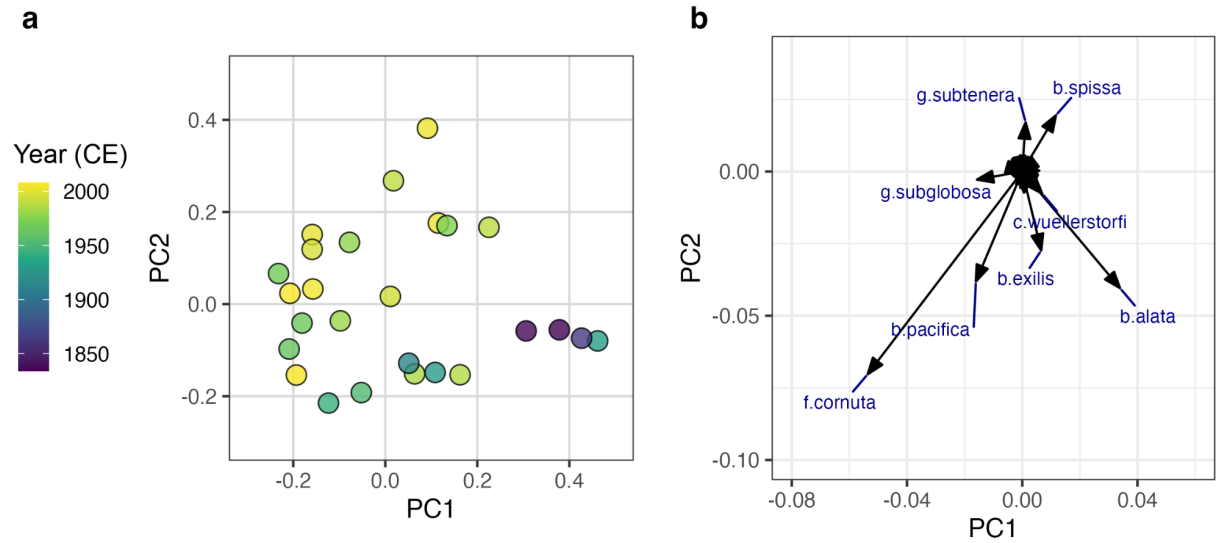

Figure 5.5: PCA of species relative biomass for all species.
Included specimens are summarized in Tables S5.2 and S5.3. (a) Sample scores; colors denote sample age in calendar years (CE). (b) Species loadings; length of vectors denote the degree of correlation between each given species and the principal components. Species with highly similar loading values close to the centroid are not labeled; see Figure 5.6 for more information on these groups.

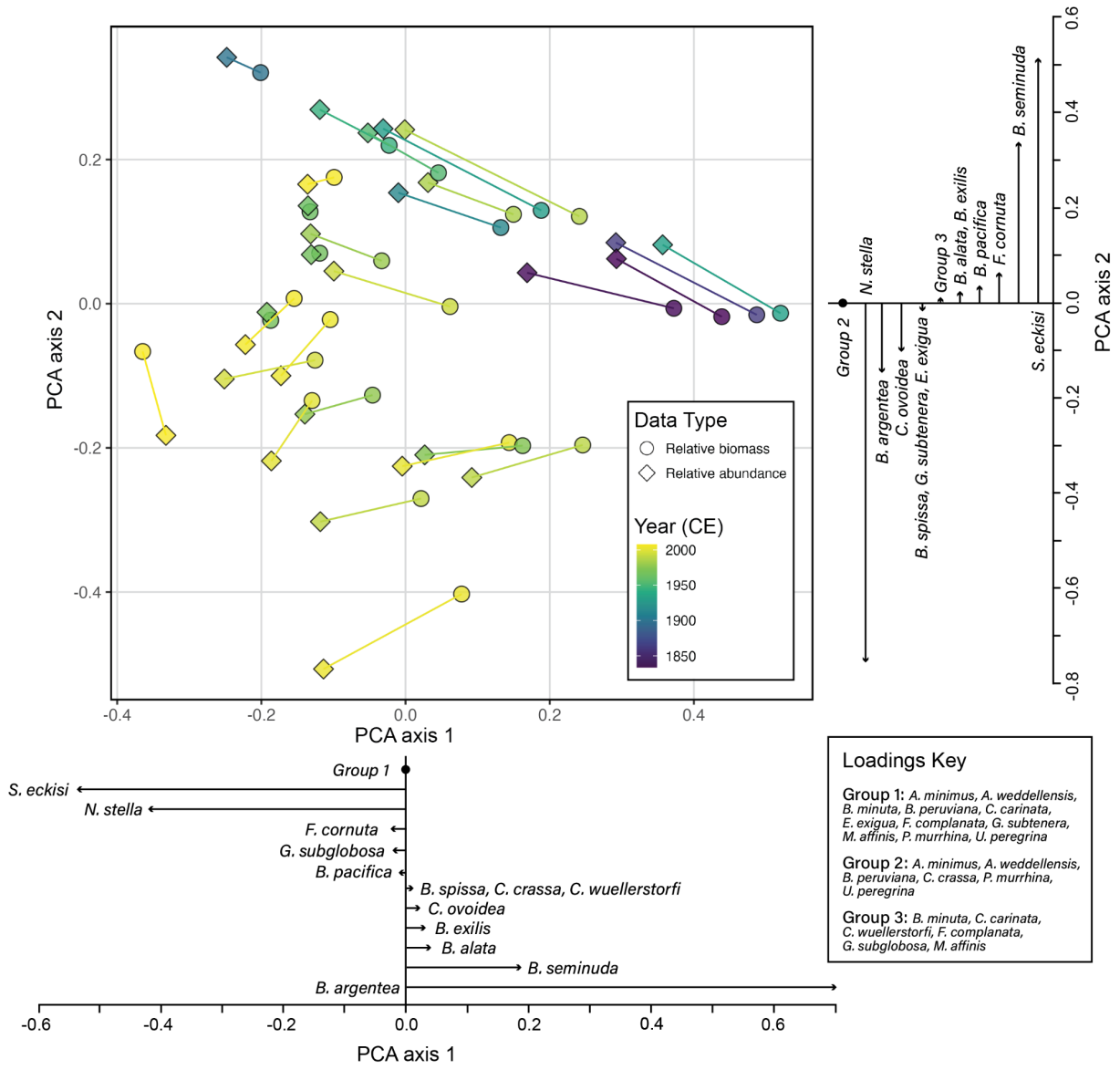

Figure 5.6: PCA of relative abundance and biomass analyzed in the same ordination space. Colors denote sample age in calendar years (CE). Lines connect samples from the same year; shape denotes measurement type (relative biomass vs. relative abundance). Species loadings on each PCA axis are shown on the bottom and right-hand side; length of vectors denote the degree of correlation between each species and the given principal component. Species with similar loading values are grouped together and denoted in the loadings key. Data shown here are from common species; when all species are included in the analysis, the results are highly similar.

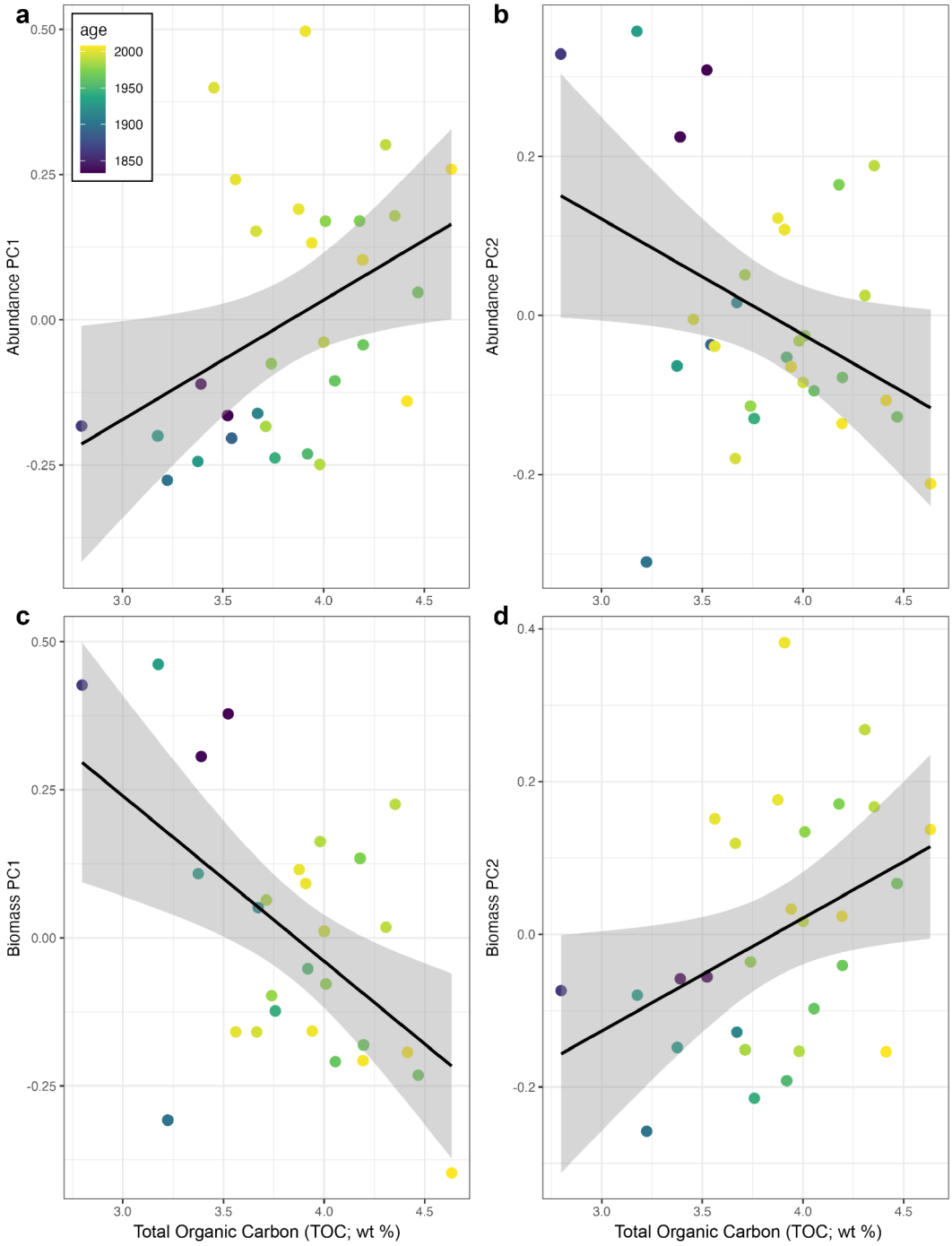

Figure 5.7: Biomass and abundance PCA axes 1 and 2 are partially explained by Total Organic Carbon concentrations.
(a) Biomass PC1 and (b) PC2; (c) Abundance PC1 and (d) PC2. Colors denote sample age; black lines denote linear regression models, where shaded gray windows represent 95% confidence intervals. Weight percent TOC from (Wang et al. 2017).

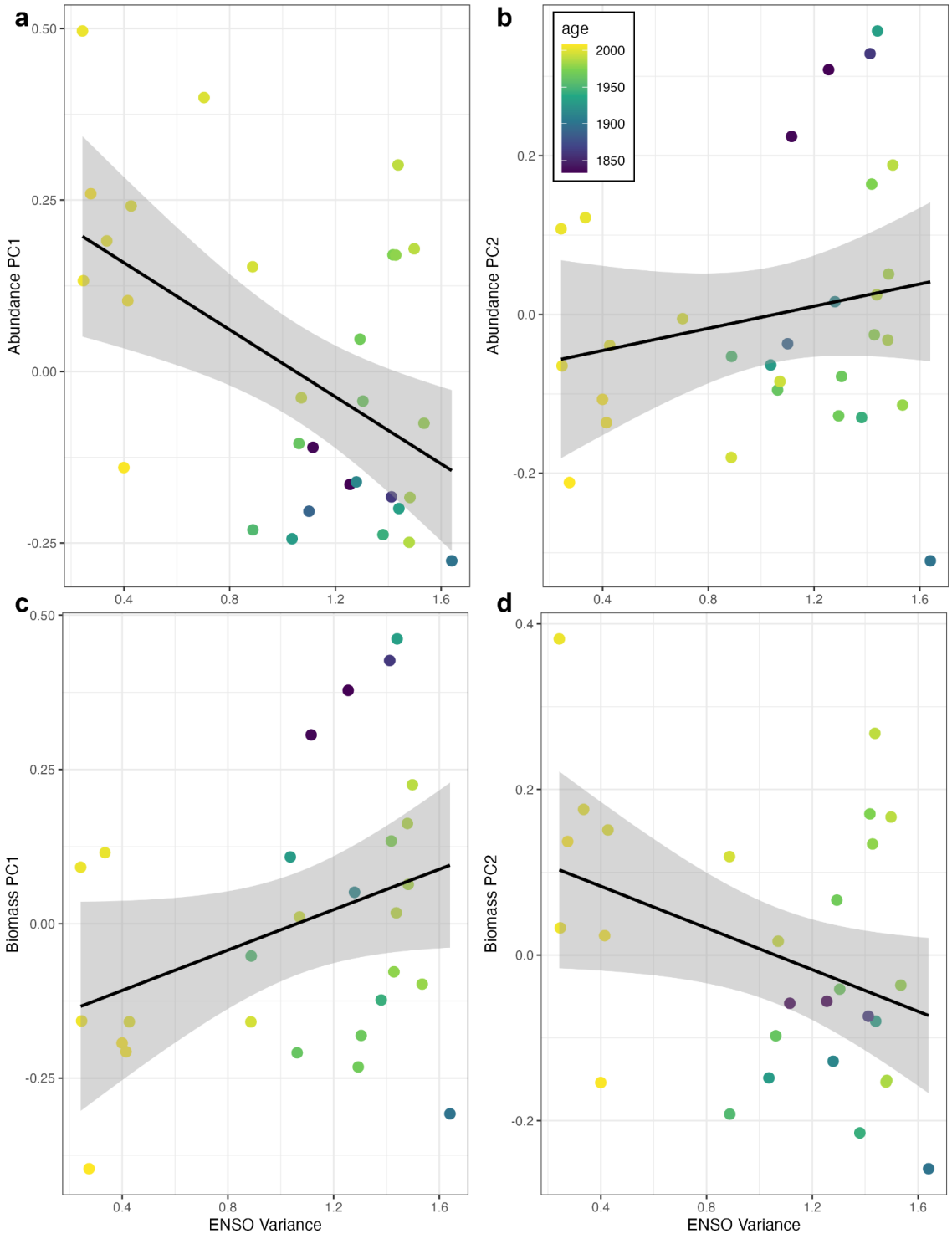

Figure 5.8: Biomass and abundance PCA axes 1 and 2 are partially explained by ENSO variability.
(a) Biomass PC1 and (b) PC2; (c) Abundance PC1 and (d) PC2. Colors denote sample age; black lines denote linear regression models, where shaded gray windows represent 95% confidence intervals. ENSO variance here denotes a 21-year running biweight variance on ENSO index (Li et al. 2011).

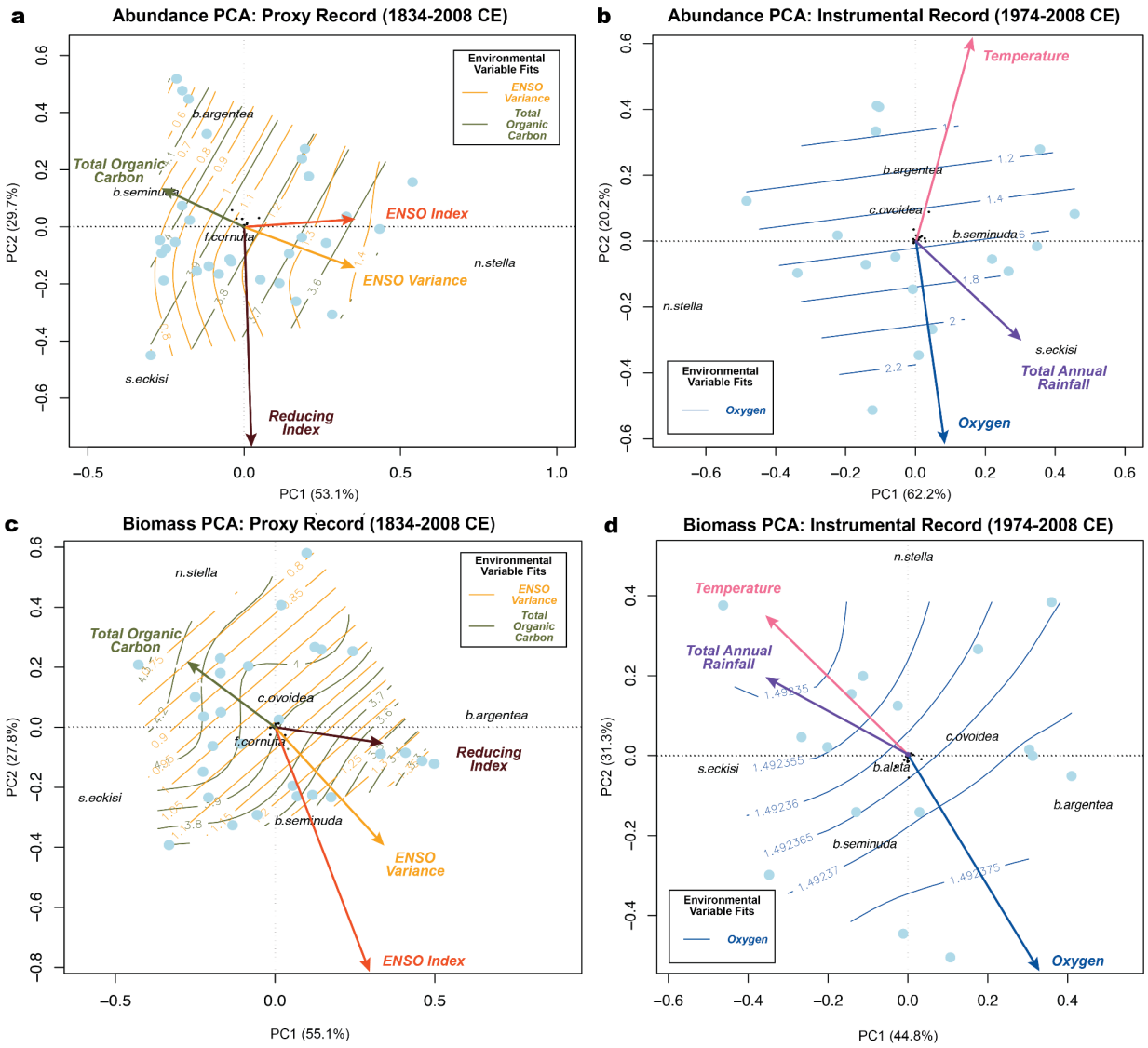

Figure 5.9: Abundance and Biomass PCA analysis with environmental variable loadings. Abundance PCA shown in panels (a, b); biomass PCA in panels (c, d). Proxy record variables (a, c) which encompass the entire core record include total organic carbon (TOC), ENSO index and variance, and a reducing index; instrumental record variables (b, d) from CalCOFI data and nearby monitoring sites include oxygen saturation state, bottom water temperature, and total annual rainfall. Some variables (NO_2, NO_3, SiO_3, PO_4) were excluded for ease of interpretation. Contour lines represent the surface of fitted environmental variables (denoted by color), produced using GAM models to illustrate potential non-linear relationships between the ordination axis and the given variable.

Chapter 5 Tables

Table 5.1: Ages, deposition rates, and total foraminifera and total biomass for each sample used in this study.
Deposition rates and ages were provided by Brandon et al. (2019); see supplemental for further information.

Sample Name	Age	Deposition Rate	Total Foraminifera	Total Biomass [combined shell area (μm^2)]
MV1012-BC-2	2008	1.14286	20	376362
MV1012-BC-3	2007	1.14286	15	163660
MV1012-BC-4	2006	1.14286	367	7736109
MV1012-BC-5	2004	1.14286	195	4348479
MV1012-BC-6	2003	1.14286	341	10006440
MV1012-BC-7	2002	1.14284	383	13404626
MV1012-BC-8	2001	2.625	1248	18727782
MV1012-BC-9-10	1998	2.625	1601	-
MV1012-BC-11	1996	1.75	1095	25465614
MV1012-BC-12	1994	1.75	263	8432851
MV1012-BC-14	1990	1.75	1147	29394349
MV1012-BC-15	1989	1.75	164	5057429
MV1012-BC-16	1987	2.15385	359	14159511
MV1012-BC-17	1985	2.15385	506	12345907
MV1012-BC-19	1980	2.15385	579	15015079
MV1012-BC-20	1978	2.15385	254	5651629
MV1012-BC-22	1974	2.15385	437	11085679
MV1012-BC-25	1968	2.15385	423	9423808
MV1012-BC-26	1966	2.15385	454	8261814
MV1012-BC-27	1963	2.15385	395	9201270
MV1012-BC-32	1953	2.125	352	11727544
MV1012-BC-36	1944	2.125	302	10696263
MV1012-BC-41	1932	2.5555555	270	16479200
MV1012-BC-42	1929	2.5555555	1682	34278802
MV1012-BC-48	1914	2.71429	239	6838949
MV1012-BC-53	1900	2.28571	897	22197995
MV1012-BC-57	1891	2.28571	814	-

Sample Name	Age	Deposition Rate	Total Foraminifera	Total Biomass [combined shell area (µm²)]
MV1012-BC-70	1862	2.1666	2746	85485823
MV1012-BC-82	1836	2.1666	457	10046409
MV1012-BC-83	1834	2.1666	1742	56337861

Table 5.2: Species' traits related to oxygen tolerance and symbiosis.
Species are grouped into clades as specified by Piña-Ochoa et al. 2009 and Woehle et al. 2022. Oxygen tolerances are reported via oxygenation categories alongside minimum reported oxygen thresholds (in ml L^{-1}). Denitrification ability is indicated and average denitrification is reported (in mM NO_3^-).

Clade	Species	Oxygenation Category	Lowest Reported Oxygen Threshold	Nitrate Collector ?	Reported mM NO3-	Endobionts	Vacuoles	O source	N Source	Symb Source
Rotaliids - Clade 1										
	Bolivina alata	Intermediate and strong hypoxia	0.3 ml L -1	Yes	37			Sen Gupta and Machain-Castillo 1993; Stefanelli 2004	Piña-Ochoa et al. 2009	
	Bolivina argentea	Intermediate and strong hypoxia	< 0.3 ml L -1	Yes	195	None	Yes	Moffitt et al. 2013	Bernhard et al. 2012	Risgaard-Petersen et al. 2006
	Bolivina interjuncta			Yes					Glock et al. 2012	
	Bolivina pacifica	Intermediate and strong hypoxia	0.3 ml L -1	-				Sen Gupta and Machain-Castillo 1993		
	Bolivina seminuda	Intermediate and strong hypoxia	< 0.1 ml L -1	Yes	118			Harman 1964	Piña-Ochoa et al. 2009	
	Bolivina spissa	Intermediate hypoxia	0.3 ml L -1	-				Moffitt et al. 2013		
	Bolivinita minuta			-						
	Cassidulina carinata			Yes	1				Piña-Ochoa et al. 2009	
	Cassidulina crassa			-						
	Cassidulina minuta			-						
	Suggrunda eckisi	Intermediate and strong hypoxia	< 0.1 ml L -1	-				Savrda et al. 1984; Harman 1964		
	Uvigerina	Intermediate	0.3 ml L -1	No				Moffitt et al.	Piña-Ochoa	

	peregrina	and strong hypoxia						2013	et al. 2009	
Rotaliids - Clade 2										
	Anomalinoides minimus			-						
Rotaliids - Clade 3										
	Bulimina exilis (= Stainforthia sp.?)			Yes	180				Risgaard-Petersen et al. 2006, Piña-Ochoa et al. 2009	
	Chilostomella oolina (= ovoidea?)	Intermediate and strong hypoxia	0.1 ml L -1	Yes	65			Cannariato and Kennett 1999	Piña-Ochoa et al. 2009	
	Cibicidoides wuellerstorfi			No					Woehle et al. 2022	
	Epistominella exigua			No					Piña-Ochoa et al. 2009	
	Melonis affinis			-						
	Nonionella stella	Strong hypoxia	< 0.02 ml L -1	Yes	35	Sequesterd plastids	No	Moffitt et al. 2013	Piña-Ochoa et al. 2009	Risgaard-Petersen et al. 2006
Rotaliids - Unknown Clade										
	Fursenkoina bradyi (Fursenkoina cornuta?)			Yes	125				Berhard et al. 2012	
	Fursenkoina complanata			-						
	Globocassidulina subglobosa			-						
	Gyroidina subtenera			-						
Lagenids										
	Oolina squamosa			-						
Miliolids										
	Pyrgo murrhina	Oxic conditions	>3.5 ml L−1	No				Myhre et al. 2017	Woehle et al. 2022	

Table 5.3: Regression output for linear models examining environmental variables as predictors for PCA ordinations.
Data types and their age ranges are indicated alongside which variables were tested from each dataset and their respective p- and R-squared values. Bolded values indicate those for significant predictors ($\alpha = 0.01$).

PCA Dataset Type	Age Range	Predictor Variable	p-value	R-squared
Abundance: Proxy Data	1834-2008 CE	**TOC**	**0.01**	**0.29**
		ENSO Index	0.42	0.06
		ENSO Variance	**0.001**	**0.42**
		Reducing Index	0.76	0.02
Biomass: Proxy Data	1834-2008 CE	**TOC**	**0.02**	**0.13**
		ENSO Index	0.16	0.07
		ENSO Variance	**0.003**	**0.24**
		Reducing Index	0.84	-0.03
Abundance: Instrumental Data	1974-2008 CE	O2 Saturation	0.04	0.37
		Temperature	0.77	0.04
		Nitrite	0.11	0.24
		Nitrate	0.4	0.13
		Phosphate	0.14	0.24
		Total Annual Rainfall	0.12	0.26
Biomass: Instrumental Data	1974-2008 CE	O2 Saturation	0.11	0.46
		Temperature	0.07	0.62
		Nitrite	0.04	0.84
		Nitrate	0.007	0.95
		Phosphate	0.06	0.67
		Total Annual Rainfall	0.17	0.3

5.5 Chapter 5 References

Alfken, S., L. Wörmer, J. S. Lipp, T. Napier, M. Elvert, J. Wendt, A. Schimmelmann, and K.-U. Hinrichs. 2021. Disrupted Coherence Between Upwelling Strength and Redox Conditions Reflects Source Water Change in Santa Barbara Basin During the 20th Century. Paleoceanography and Paleoclimatology 36:e2021PA004354.

Alve, E., and J. M. Bernhard. 1995. Vertical migratory response of benthic foraminifera to controlled oxygen concentrations in an experimental mesocosm. Marine Ecology Progress Series:137–151.

Barron, J. A., D. Bukry, D. B. Field, and B. Finney. 2013. Response of diatoms and silicoflagellates to climate change and warming in the California Current during the past 250 years and the recent rise of the toxic diatom Pseudo-nitzschia australis. Quaternary International 310:140–154.

Belanger, C. L. 2022. Volumetric analysis of benthic foraminifera: Intraspecific test size and growth patterns related to embryonic size and food resources. Marine Micropaleontology 176:102170.

Bernhard, J. M., K. R. Buck, M. A. Farmer, and S. S. Bowser. 2000. The Santa Barbara Basin is a symbiosis oasis. Nature 403:77–80.

Bernhard, J. M., and C. E. Reimers. 1991. Benthic foraminiferal population fluctuations related to anoxia: Santa Barbara Basin. Biogeochemistry 15:127–149.

Black, B. A., W. J. Sydeman, D. C. Frank, D. Griffin, D. W. Stahle, M. García-Reyes, R. R. Rykaczewski, S. J. Bograd, and W. T. Peterson. 2014. Six centuries of variability and extremes in a coupled marine-terrestrial ecosystem. Science 345:1498–1502.

Bograd, S. J., C. G. Castro, E. Di Lorenzo, D. M. Palacios, H. Bailey, W. Gilly, and F. P. Chavez. 2008. Oxygen declines and the shoaling of the hypoxic boundary in the California Current. Geophysical Research Letters 35.

Bograd, S. J., F. B. Schwing, C. G. Castro, and D. A. Timothy. 2002. Bottom water renewal in the Santa Barbara Basin. Journal of Geophysical Research: Oceans 107:9-1-9–9.

Brandon, J. A., W. Jones, and M. D. Ohman. 2019. Multidecadal increase in plastic particles in coastal ocean sediments. Science Advances 5:eaax0587–eaax0587.

Bray, N. A., A. Keyes, and W. M. L. Morawitz. 1999. The California Current system in the Southern California Bight and the Santa Barbara Channel. Journal of Geophysical Research: Oceans 104:7695–7714.

Bringué, M., V. Pospelova, and D. B. Field. 2014. High resolution sedimentary record of dinoflagellate cysts reflects decadal variability and 20th century warming in the Santa Barbara Basin. Quaternary Science Reviews 105:86–101.

Broadman, E., L. Reidy, and D. Wahl. 2022. Late Holocene human-environment interactions on the central California coast, USA, inferred from Morro Bay salt marsh sediments. Anthropocene 38:100339.

Burke, S., R. Dunbar, and W. Berger. 1996. Benthic and pelagic Foraminifera of the Macoma layer, Santa Barbara Basin. Oceanographic Literature Review 1:64–65.

CalCOFI. 2022. CalCOFI – California Cooperative Oceanic Fisheries Investigations. https://calcofi.org/.

Chao, A., N. J. Gotelli, T. Hsieh, E. L. Sander, K. Ma, R. K. Colwell, and A. M. Ellison. 2014. Rarefaction and extrapolation with Hill numbers: a framework for sampling and estimation in species diversity studies. Ecological monographs 84:45–67.

Collins, B. M., J. D. Miller, E. E. Knapp, and D. B. Sapsis. 2019. A quantitative comparison of forest fires in central and northern California under early (1911–1924) and contemporary (2002–2015) fire suppression. International Journal of Wildland Fire 28:138–148.
Du, X., I. Hendy, and A. Schimmelmann. 2018. A 9000-year flood history for Southern California_ A revised stratigraphy of varved sediments in Santa Barbara Basin. Marine Geology 397:29–42.
Duijnstee, I., S. Ernst, and G. Van der Zwaan. 2003. Effect of anoxia on the vertical migration of benthic foraminifera. Marine Ecology Progress Series 246:85–94.
Engstrom, W. N. 1996. The California storm of January 1862. Quaternary Research 46:141–148.
Ernst, S., R. Bours, I. Duijnstee, and B. van der Zwaan. 2005. Experimental effects of an organic matter pulse and oxygen depletion on a benthic foraminiferal shelf community. Journal of Foraminiferal Research 35:177–197.
Faith, D. P., P. R. Minchin, and L. Belbin. 1987. Compositional dissimilarity as a robust measure of ecological distance. Vegetatio 69:57–68.
Field, D. B., T. R. Baumgartner, C. D. Charles, V. Ferreira-Bartrina, and M. D. Ohman. 2006. Planktonic Foraminifera of the California Current Reflect 20th-Century Warming. Science 311:63 LP – 66.
Filipsson, H. L., and K. Nordberg. 2004. Climate variations, an overlooked factor influencing the recent marine environment. An example from Gullmar Fjord, Sweden, illustrated by benthic foraminifera and hydrographic data. Estuaries 27:867–881.
Filzmoser, P., and K. Hron. 2008. Outlier detection for compositional data using robust methods. Mathematical Geosciences 40:233–248.
Filzmoser, P., and K. Hron. 2009. Correlation analysis for compositional data. Mathematical Geosciences 41:905–919.
Filzmoser, P., K. Hron, and C. Reimann. 2009. Principal component analysis for compositional data with outliers. Environmetrics: The Official Journal of the International Environmetrics Society 20:621–632.
Geslin, E., P. Heinz, F. Jorissen, and Ch. Hemleben. 2004. Migratory responses of deep-sea benthic foraminifera to variable oxygen conditions: laboratory investigations. Marine Micropaleontology 53:227–243.
Goericke, R., S. J. Bograd, and D. S. Grundle. 2015. Denitrification and flushing of the Santa Barbara Basin bottom waters. Deep Sea Research Part II: Topical Studies in Oceanography 112:53–60.
Gooday, A. J. 1988. A response by benthic foraminifera to the deposition of phytodetritus in the deep sea. Nature 332:70–73.
Gooday, A. J. 1996. Epifaunal and shallow infaunal foraminiferal communities at three abyssal NE Atlantic sites subject to differing phytodetritus input regimes. Deep Sea Research Part I: Oceanographic Research Papers 43:1395–1421.
Halpern, B. S., C. V. Kappel, K. A. Selkoe, F. Micheli, C. M. Ebert, C. Kontgis, C. M. Crain, R. G. Martone, C. Shearer, and S. J. Teck. 2009. Mapping cumulative human impacts to California Current marine ecosystems. Conservation Letters 2:138–148.
Hendy, I. L. 2010. The paleoclimatic response of the Southern Californian Margin to the rapid climate change of the last 60ka: A regional overview. Quaternary International 215:62–73.
Hendy, I. L., L. Dunn, A. Schimmelmann, and D. K. Pak. 2013. Resolving varve and radiocarbon chronology differences during the last 2000 years in the Santa Barbara Basin sedimentary record, California. Quaternary International 310:155–168.

Hendy, I. L., T. J. Napier, and A. Schimmelmann. 2015. From extreme rainfall to drought: 250 years of annually resolved sediment deposition in Santa Barbara Basin, California. Quaternary International 387:3–12.
Jacox, M. G., J. Fiechter, A. M. Moore, and C. A. Edwards. 2015. ENSO and the California Current coastal upwelling response. Journal of Geophysical Research: Oceans 120:1691–1702.
Jones, W. A. 2016. The Santa Barbara Basin Fish Assemblage in the Last Two Millennia Inferred from Otoliths in Sediment Cores:1–141.
Jones, W. A., and D. M. Checkley. 2019. Mesopelagic fishes dominate otolith record of past two millennia in the Santa Barbara Basin. Nature Communications 10:4564.
Jorissen, F., C. Fontanier, and E. Thomas. 2007. Proxies in late cenozoic paleoceanography. Developments in Marine Geology 1:263–32.
Kelmo, F., and P. Hallock. 2013. Responses of foraminiferal assemblages to ENSO climate patterns on bank reefs of northern Bahia, Brazil: A 17-year record. Ecological Indicators 30:148–157.
Kivenson, V., K. L. Lemkau, O. Pizarro, D. R. Yoerger, C. Kaiser, R. K. Nelson, C. Carmichael, B. G. Paul, C. M. Reddy, and D. L. Valentine. 2019. Ocean Dumping of Containerized DDT Waste Was a Sloppy Process. Environmental Science & Technology 53:2971–2980.
Koho, K. A., E. Piña-Ochoa, E. Geslin, and N. Risgaard-Petersen. 2011. Vertical migration, nitrate uptake and denitrification: survival mechanisms of foraminifers (Globobulimina turgida) under low oxygen conditions. FEMS Microbiology Ecology 75:273–283.
Lesen, A. E. 2005. Relationship between benthic foraminifera and food resources in South San Francisco Bay, California, USA. Marine Ecology Progress Series 297:131–145.
Li, J., S.-P. Xie, E. R. Cook, G. Huang, R. D'Arrigo, F. Liu, J. Ma, and X.-T. Zheng. 2011. Interdecadal modulation of El Niño amplitude during the past millennium. Nature Climate Change 1:114–118.
Loubere, P. 1994. Quantitative estimation of surface ocean productivity and bottom water oxygen concentration using benthic foraminifera. Paleoceanography 9:723–737.
McPhaden, M. J., S. E. Zebiak, and M. H. Glantz. 2006. ENSO as an integrating concept in earth science. science 314:1740–1745.
Moffitt, S. E., T. M. Hill, K. Ohkushi, J. P. Kennett, and R. J. Behl. 2014. Vertical oxygen minimum zone oscillations since 20 ka in Santa Barbara Basin: A benthic foraminiferal community perspective. Paleoceanography 29:44–57.
Moodley, L., G. J. van der Zwaan, G. M. W. Rutten, R. C. E. Boom, and A. J. Kempers. 1998. Subsurface activity of benthic foraminifera in relation to porewater oxygen content: laboratory experiments. Marine Micropaleontology 34:91–106.
Myhre, S. E., D. Pak, M. Borreggine, J. P. Kennett, C. Nicholson, T. M. Hill, and C. Deutsch. 2017. Oxygen minimum zone biotic baseline transects for paleoceanographic reconstructions in Santa Barbara Basin, CA. Deep-Sea Research Part II:0–1.
Nomaki, H., P. Heinz, C. Hemleben, and H. Kitazato. 2005. Behavior and response of deep-sea benthic foraminifera to freshly supplied organic matter: a laboratory feeding experiment in microcosm environments. Journal of Foraminiferal Research 35:103–113.
Oksanen, J., F. G. Blanchet, R. Kindt, P. Legendre, P. R. Minchin, R. O'hara, G. L. Simpson, P. Solymos, M. H. H. Stevens, and H. Wagner. 2013. Package 'vegan.' Community ecology package, version 2:1–295.
Oksanen, J., G. Blanchet, M. Friendly, R. Kindt, P. Legendre, D. McGlinn, P. R. Minchin, R. B.

O'Hara, G. L. Simpson, P. Solymos, M. H. H. Stevens, E. Szoecs, and H. Wagner. 2020, December. vegan: Community Ecology Package version 2.5-7 from CRAN.
Osborne, E. B., R. C. Thunell, N. Gruber, R. A. Feely, and C. R. Benitez-Nelson. 2020. Decadal variability in twentieth-century ocean acidification in the California Current Ecosystem. Nature Geoscience 13:43–49.
Piña-Ochoa, E., S. Høgslund, E. Geslin, T. Cedhagen, N. P. Revsbech, L. P. Nielsen, M. Schweizer, F. Jorissen, S. Rysgaard, and N. Risgaard-Petersen. 2010. Widespread occurrence of nitrate storage and denitrification among Foraminifera and Gromiida. Proceedings of the National Academy of Sciences 107:1148–1153.
Pitcher, G. C., A. Aguirre-Velarde, D. Breitburg, J. Cardich, J. Carstensen, D. J. Conley, B. Dewitte, A. Engel, D. Espinoza-Morriberón, G. Flores, V. Garçon, M. Graco, M. Grégoire, D. Gutiérrez, J. M. Hernandez-Ayon, H.-H. M. Huang, K. Isensee, M. E. Jacinto, L. Levin, A. Lorenzo, E. Machu, L. Merma, I. Montes, N. Swa, A. Paulmier, M. Roman, K. Rose, R. Hood, N. N. Rabalais, A. G. V. Salvanes, R. Salvatteci, S. Sánchez, A. Sifeddine, A. W. Tall, A. K. van der Plas, M. Yasuhara, J. Zhang, and Z. Zhu. 2021. System controls of coastal and open ocean oxygen depletion. Progress in Oceanography 197:102613.
Pozo Buil, M., M. G. Jacox, J. Fiechter, M. A. Alexander, S. J. Bograd, E. N. Curchitser, C. A. Edwards, R. R. Rykaczewski, and C. A. Stock. 2021. A Dynamically Downscaled Ensemble of Future Projections for the California Current System. Frontiers in Marine Science 8.
Reimers, C. E., C. B. Lange, M. Tabak, and J. M. Bernhard. 1990. Seasonal spillover and varve formation in the Santa Barbara Basin, California. Limnology and Oceanography 35:1577–1585.
Ren, A. S., F. Chai, H. Xue, D. M. Anderson, and F. P. Chavez. 2018. A Sixteen-year Decline in Dissolved Oxygen in the Central California Current. Scientific Reports 8:7290.
Ringnér, M. 2008. What is principal component analysis? Nature biotechnology 26:303–304.
Risgaard-Petersen, N., A. M. Langezaal, S. Ingvardsen, M. C. Schmid, M. S. M. Jetten, H. J. M. Op den Camp, J. W. M. Derksen, E. Piña-Ochoa, S. P. Eriksson, L. Peter Nielsen, N. Peter Revsbech, T. Cedhagen, and G. J. van der Zwaan. 2006. Evidence for complete denitrification in a benthic foraminifer. Nature 443:93–96.
Rodriguez, A. B., B. A. McKee, C. B. Miller, M. C. Bost, and A. N. Atencio. 2020. Coastal sedimentation across North America doubled in the 20th century despite river dams. Nature Communications 11:3249.
Schimmelmann, A., I. L. Hendy, L. Dunn, D. K. Pak, and C. B. Lange. 2013. Revised ~2000-year chronostratigraphy of partially varved marine sediment in Santa Barbara Basin, California. GFF 135:258–264.
Schimmelmann, A., and M. Kastner. 1993. Evolutionary changes over the last 1000 years of reduced sulfur phases and organic carbon in varved sediments of the Santa Barbara Basin, California. Geochimica et Cosmochimica Acta 57:67–78.
Schimmelmann, A., and C. B. Lange. 1996. Tales of 1001 varves: a review of Santa Barbara Basin sediment studies. Geological Society, London, Special Publications 116:121–141.
Schimmelmann, A., C. B. Lange, W. H. Berger, A. Simon, S. K. Burke, and R. B. Dunbar. 1992. Extreme climatic conditions recorded in Santa Barbara Basin laminated sediments: the 1835–1840Macoma event. Marine Geology 106:279–299.
Taylor, W. L., and R. W. Taylor. 2007. The great California flood of 1862. The Fortnightly Club of Redlands, California,< http://www. redlandsfortnightly. org/papers/Taylor06. htm>(Feb. 1, 2013).

Team, R. C. 2013. R: A language and environment for statistical computing.
Templ, M., K. Hron, and P. Filzmoser. 2011. robCompositions: an R-package for robust statistical analysis of compositional data.
Thunell, R. C. 1998. Particle fluxes in a coastal upwelling zone: sediment trap results from Santa Barbara Basin, California. Deep Sea Research Part II: Topical Studies in Oceanography 45:1863–1884.
Thunell, R. C., E. Tappa, and D. M. Anderson. 1995. Sediment fluxes and varve formation in Santa Barbara Basin, offshore California. Geology 23:1083–1083.
Wang, Y., and I. L. Hendy. 2021. Reorganized Atmospheric Circulation During the Little Ice Age Leads to Rapid Southern California Deoxygenation. Geophysical Research Letters 48:e2021GL094469.
Wang, Y., I. Hendy, and T. J. Napier. 2017. Climate and Anthropogenic Controls of Coastal Deoxygenation on Interannual to Centennial Timescales. Geophysical Research Letters 44:11,528-11,536.
Warrick, J. A., J. Xu, M. A. Noble, and H. J. Lee. 2008. Rapid formation of hyperpycnal sediment gravity currents offshore of a semi-arid California river. Continental Shelf Research 28:991–1009.
Weinheimer, A. L., J. P. Kennett, and D. R. Cayan. 1999. Recent increase in surface-water stability during warming off California as recorded in marine sediments. Geology 27:1019–1022.
White, M. E., P. A. Rafter, B. M. Stephens, S. D. Wankel, and L. I. Aluwihare. 2019. Recent Increases in Water Column Denitrification in the Seasonally Suboxic Bottom Waters of the Santa Barbara Basin. Geophysical Research Letters 46:6786–6795.
Woehle, C., A.-S. Roy, N. Glock, J. Michels, T. Wein, J. Weissenbach, D. Romero, C. Hiebenthal, S. N. Gorb, J. Schönfeld, and T. Dagan. 2022. Denitrification in foraminifera has an ancient origin and is complemented by associated bacteria. Proceedings of the National Academy of Sciences 119:e2200198119.
Xiu, P., F. Chai, E. N. Curchitser, and F. S. Castruccio. 2018. Future changes in coastal upwelling ecosystems with global warming: The case of the California Current System. Scientific Reports 8:1–9.
Yasuhara, M., G. Hunt, D. Breitburg, A. Tsujimoto, and K. Katsuki. 2012. Human-induced marine ecological degradation: micropaleontological perspectives. Ecology and Evolution 2:3242–3268.
Zhao, M., G. Eglinton, G. Read, and A. Schimmelmann. 2000. An alkenone (U37K′) quasi-annual sea surface temperature record (A.D. 1440 to 1940) using varved sediments from the Santa Barbara Basin. Organic Geochemistry 31:903–917.

5.6 Appendix
Supplemental Information for Chapter 5: Community structure of Santa Barbara Basin benthic foraminifera

Sara S. Kahanamoku, Ivo Duijnstee, Seth Finnegan

Supplemental Text

Core chronology

Core MV1012-BC was closely aligned with SPR0901-06KC, the most recently and accurately dated sediment core from a central basin site (Hendy et al. 2013). ^{14}C dates from planktonic foraminifera and terrestrial-derived organic carbon from Kasten Core SPR0901-06KC were used by Hendy et al. (2013) and Schimmelmann et al. (2013) to corroborate the accuracy of the traditional varve counting record for modern sediments and demonstrate that varve counting decreases in accuracy prior to ~1700 CE. Box core MV1012-BC is sufficiently shallow that varve counting is accurate and does not require an age model correction (Brandon et al. 2019).

Taphonomic notes

Surficial sediments on the box core were considered intact due to the presence of an undisturbed bacterial mat observed following core sampling. As a result, we interpret coretop sediments as being reflective of real seafloor conditions at the time of sampling. However, we note that the diversity drops we observe near the top of the core may be a result of ecological factors that contribute to sample "ghosting," or the migration of living benthic fauna into deeper sediments such that they are incorporated into records from earlier years. In other words, the depauperate coretop we observe may reflect vertical distributions of foraminifera at the time of sampling; foraminifera from the top 0.5-1 cm of the core may have migrated deeper into the sediment, thus making the top two samples more sparse. Yet given that SBB is a low-oxygen system, the vertical distribution of foraminifera is considered to be more compressed than in aerated systems, such that vertical migration is significantly limited within the SBB versus more typical coring sites. As a result, it is also possible that the low abundances we observe reflect real trends. Additional work is needed using core records that span beyond 2008 CE (the top of the present core) to illuminate the diversity trajectory within the SBB over the past 15 years and determine whether the changes we observe in diversity and abundance beginning in ~2004 CE are maintained towards present.

It is also important to note that benthic foraminifera within the core record we utilize represent assemblages rather than living communities.

Supplemental Figures

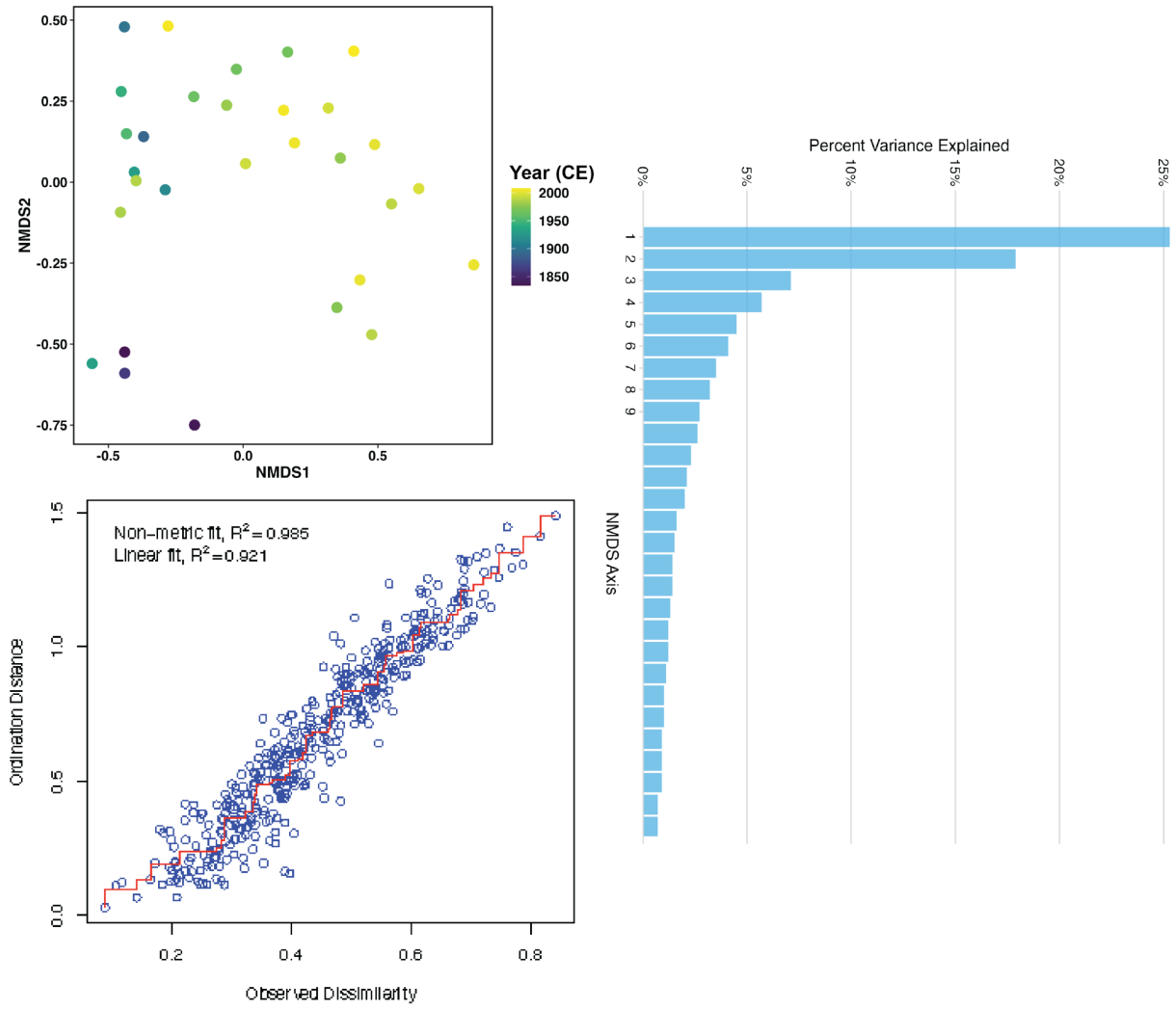

Supplementary Figure 5.1: Diagnostics for NMDS analysis on relative biomass data. Upper left: NMDS output for relative abundance data; colors denote sample age in calendar years (CE). Bottom left: stress plot showing goodness of fit. Right: proportion of variance within the data explained by each axis.

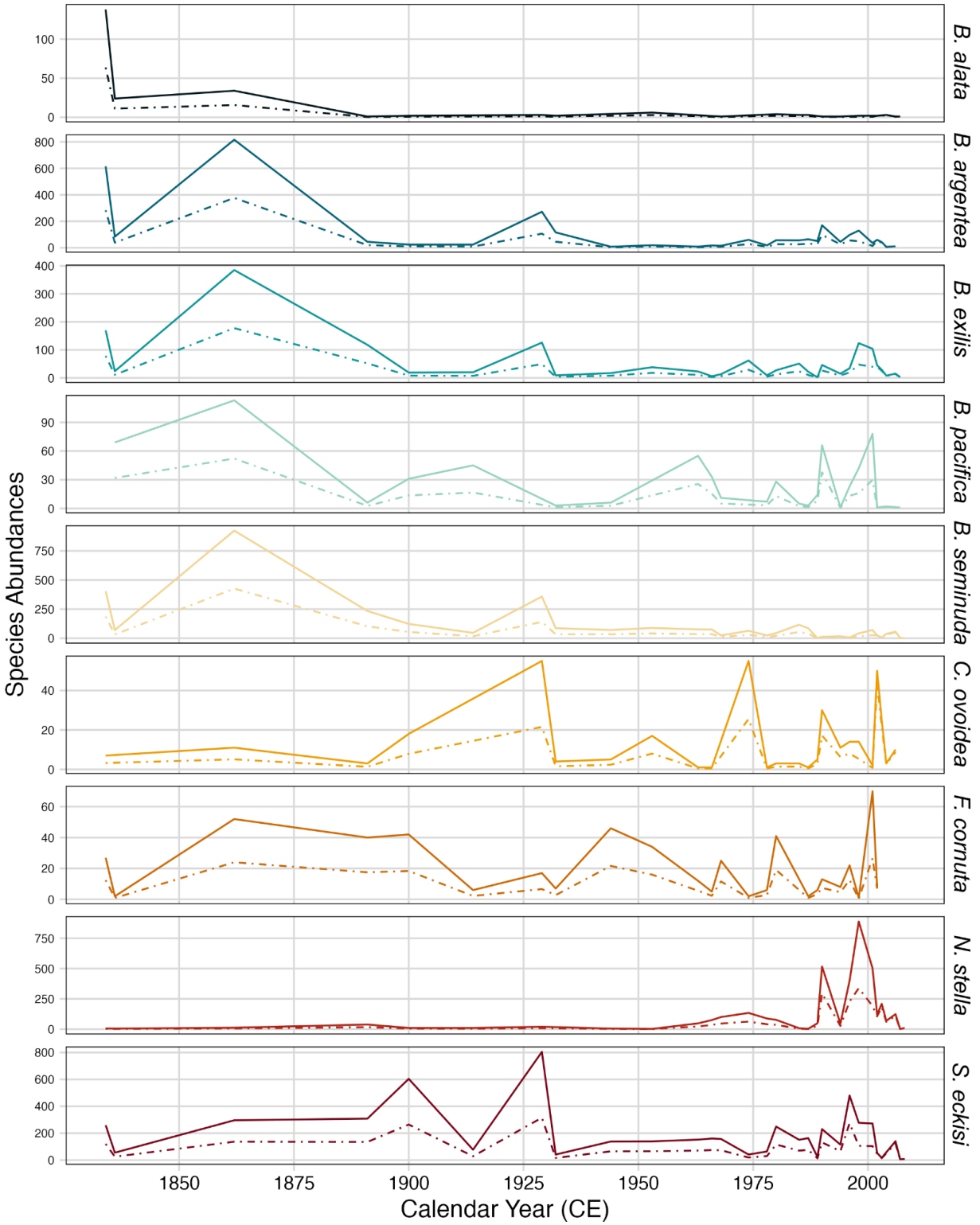

Supplementary Figure 5.2: Absolute abundance and benthic foraminifer accumulation rate for the most common species from core MV1012.
Solid lines denote absolute abundance; dashed lines indicate BFAR (foraminifera per surface area per year).

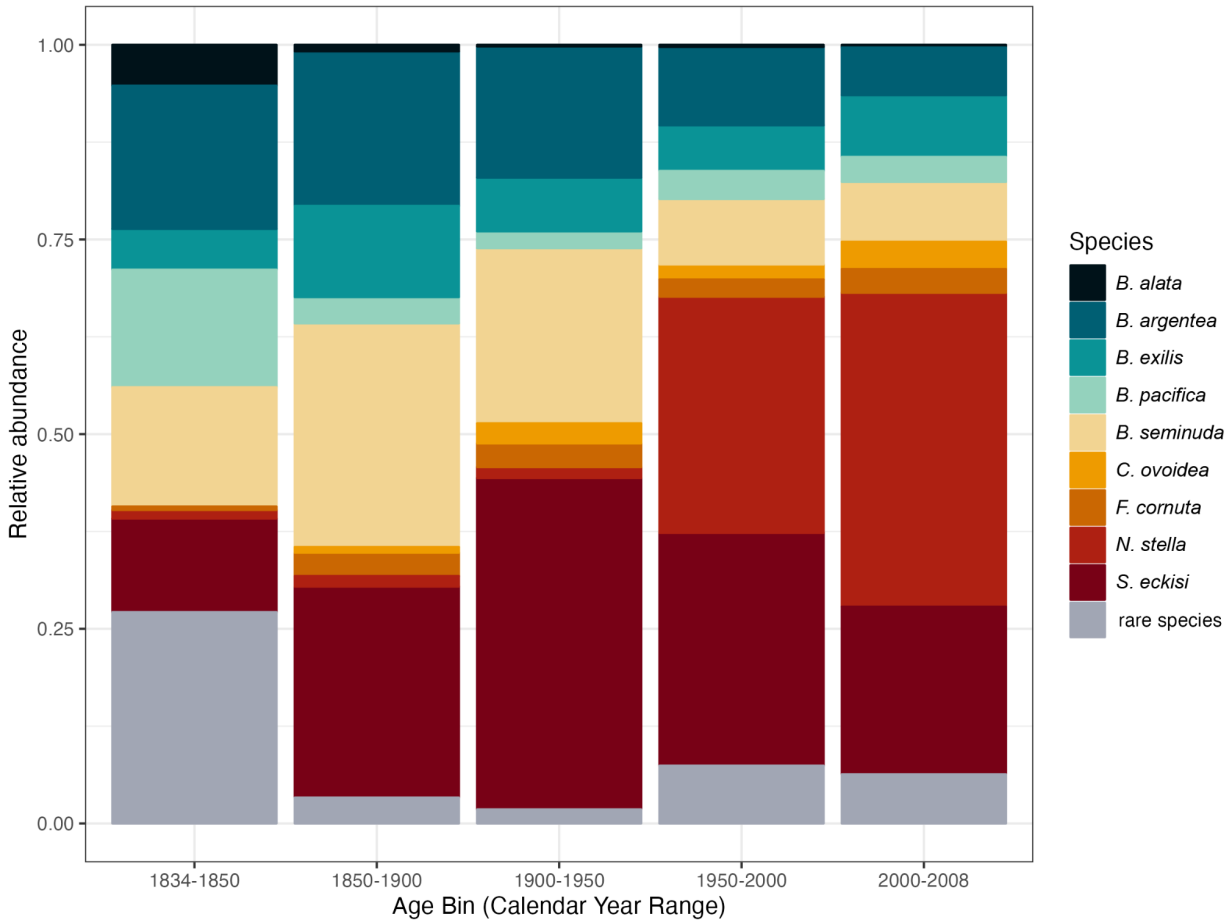

Supplementary Figure 5.3: Relative abundance of common and rare species.
Rare species are listed in Table S5.2. Colors denote taxonomic units (here, individual species and a combined category for rare species).

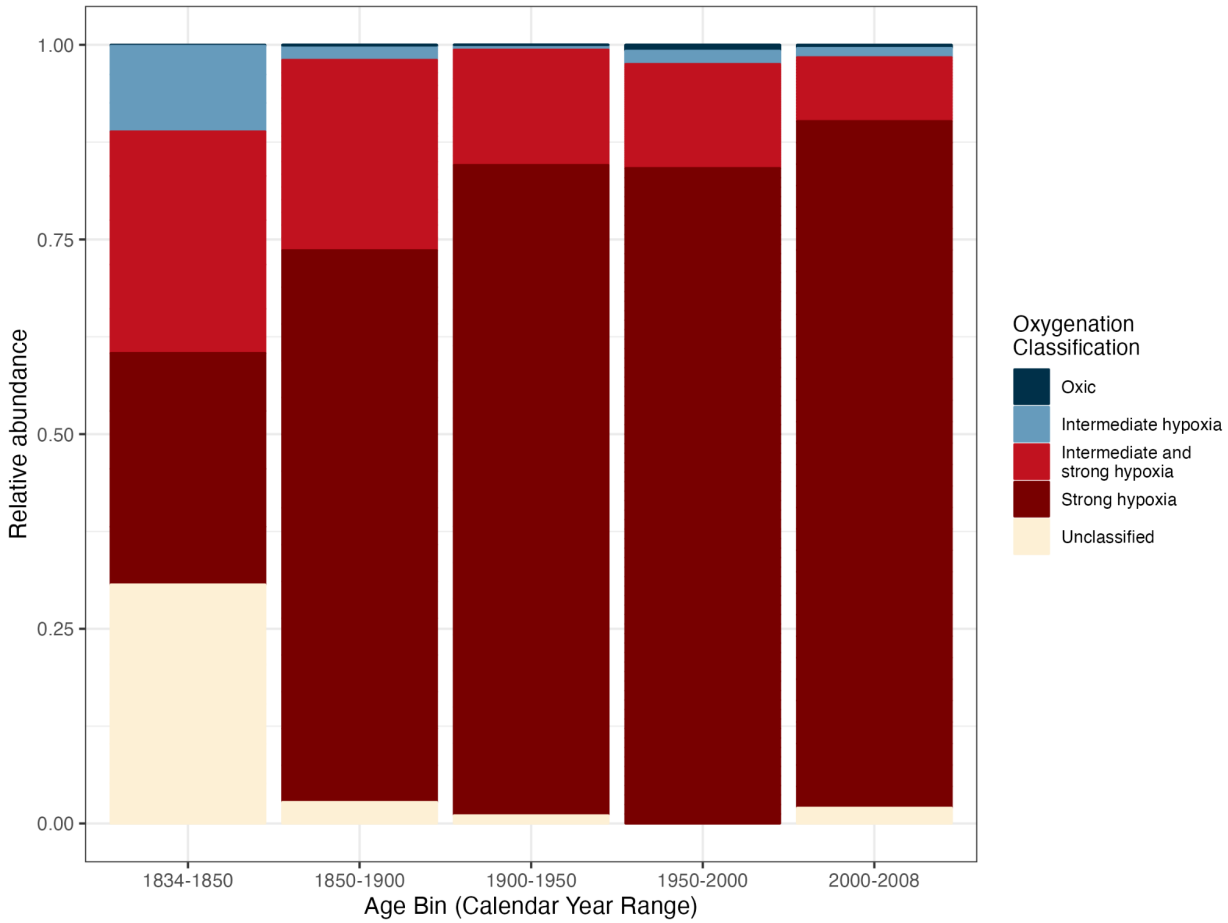

Supplementary Figure 5.4: Relative abundance of oxygen indicator species.
Colors denote oxygenation classifications (oxic, intermediate hypoxia, intermediate and strong hypoxia, and strong hypoxia) and include foraminifera that are not associated with an oxygenation classification (here, denoted as unclassified).

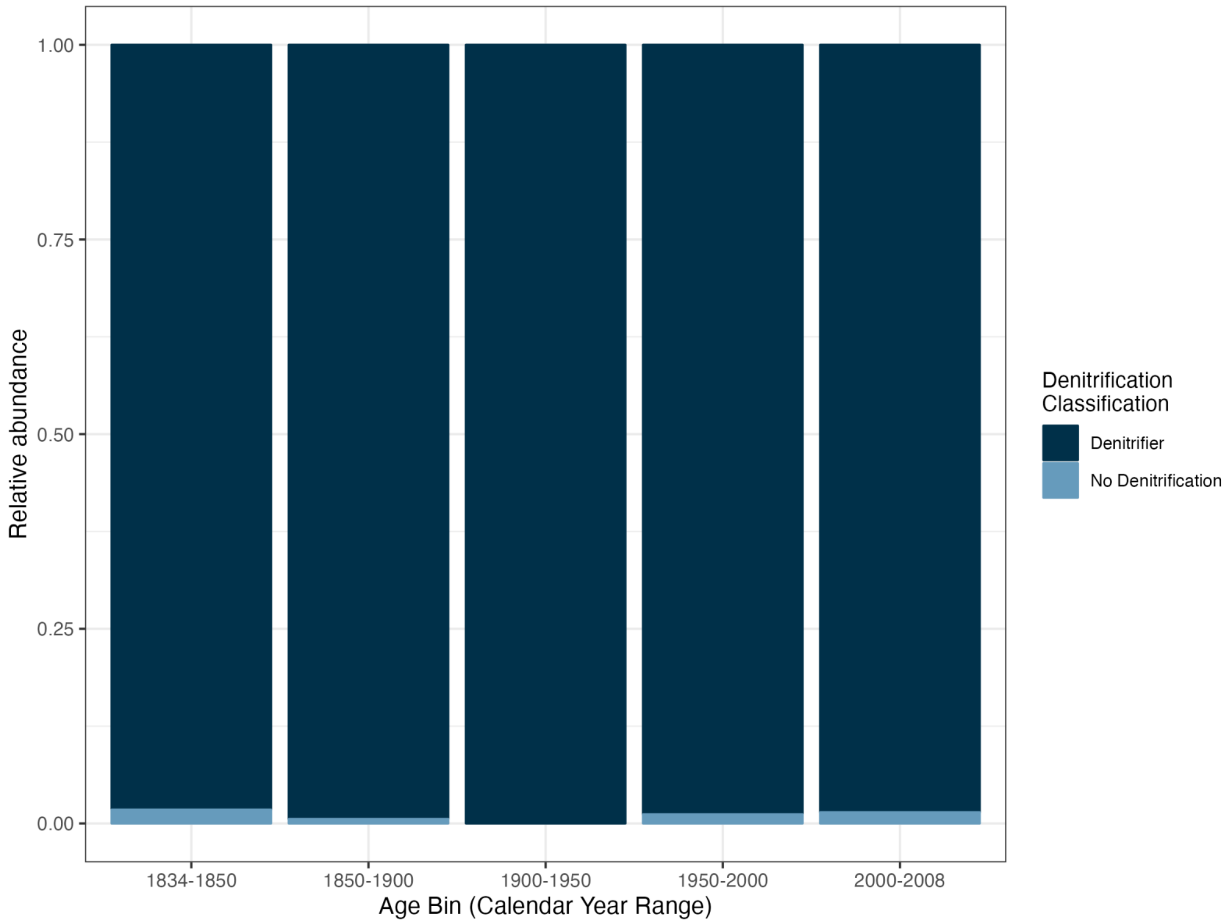

Supplementary Figure 5.5: Relative abundance of species that can undergo denitrification. Dark blue denotes species with known denitrification ability; light blue indicates species known to not undergo denitrification. Species without information on denitrification ability were excluded from this analysis.

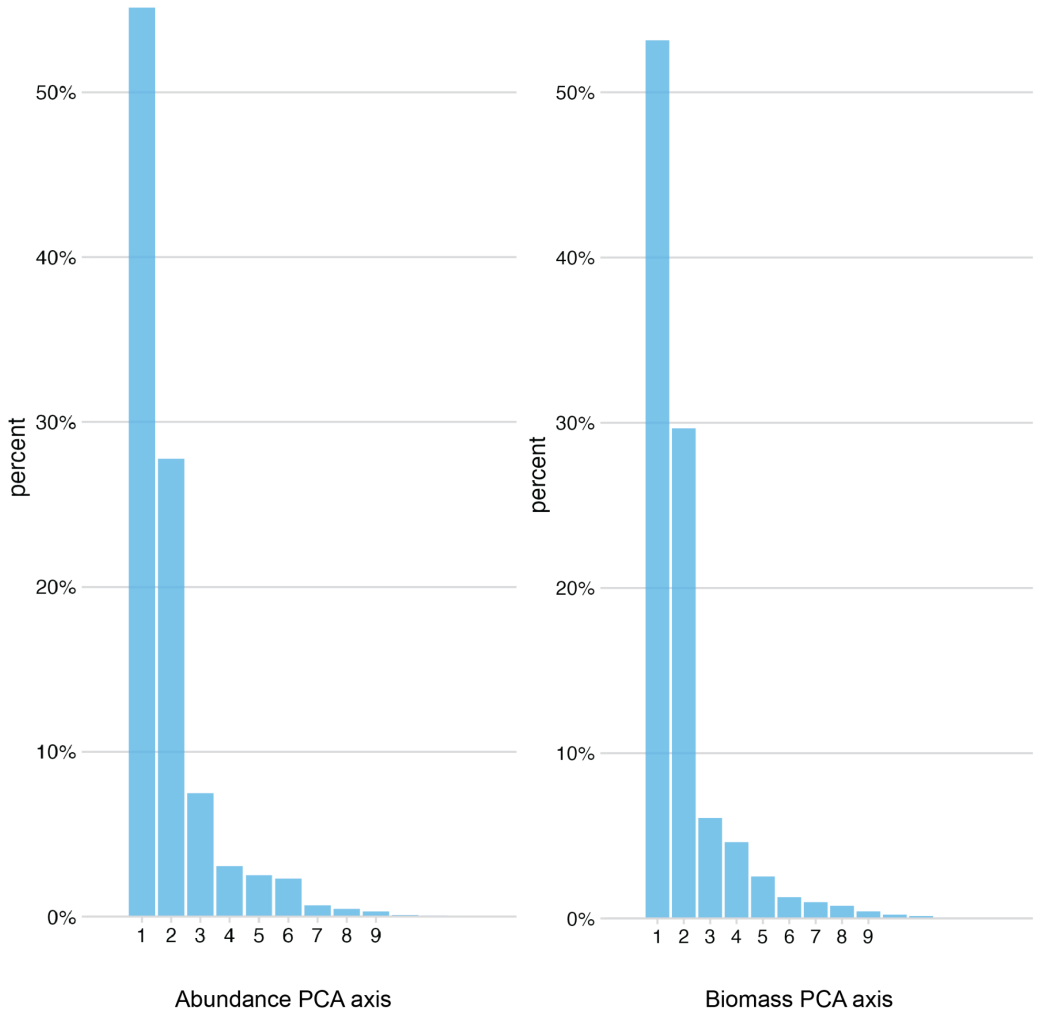

Supplementary Figure 5.6: Percent variation explained by each PCA axis for analyses done on abundance and biomass data.
Left: abundance; right: biomass. PCA axes 1 and 2 account for a majority of the variance explained by the PCA in both analyses, and indicate that there is similar underlying structure in each dataset.

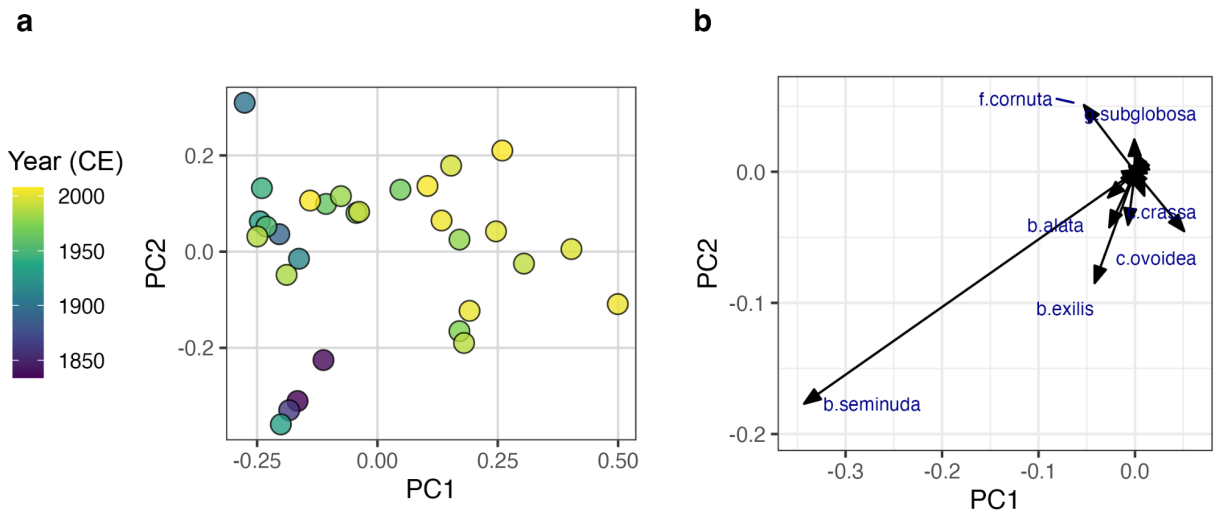

Supplementary Figure 5.7: PCA of species relative abundance for common species. See Table S5.2 for species excluded from this analysis. (a) Sample scores; colors denote sample age in calendar years (CE). (b) Species loadings; length of vectors denote the degree of correlation between each given species and the principal components. Species with highly similar loading values close to the centroid are not labeled.

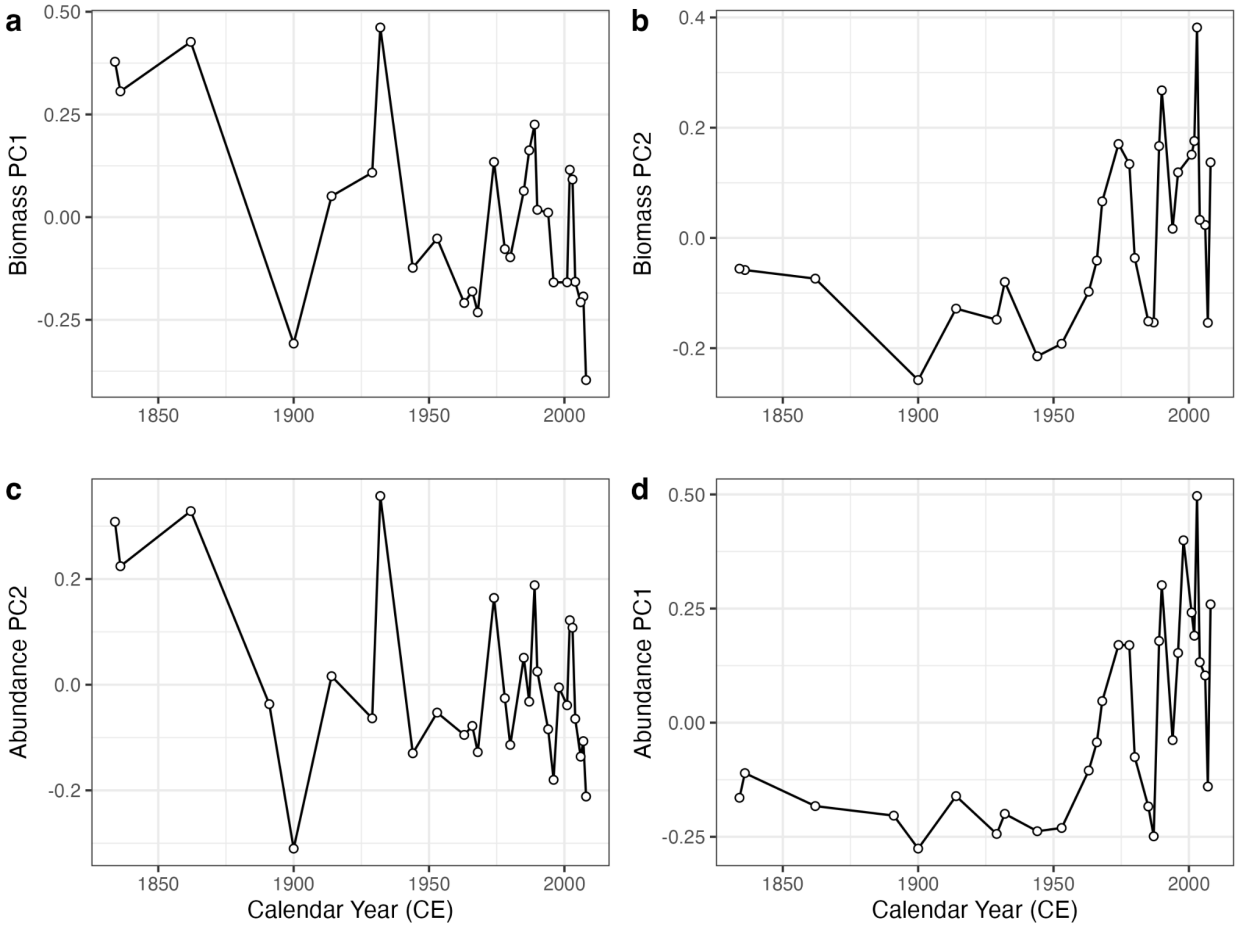

Supplementary Figure 5.8: PCA axes 1 and 2 from biomass and abundance data are similarly structured through time.
(a) Biomass PC1, (b) Biomass PC2, (c) Abundance PC2, and (d) Abundance PC1. Note similarities between biomass PC1 and abundance PC2 as well as biomass PC2 and abundance PC1 when plotted against sample age in calendar years (CE).

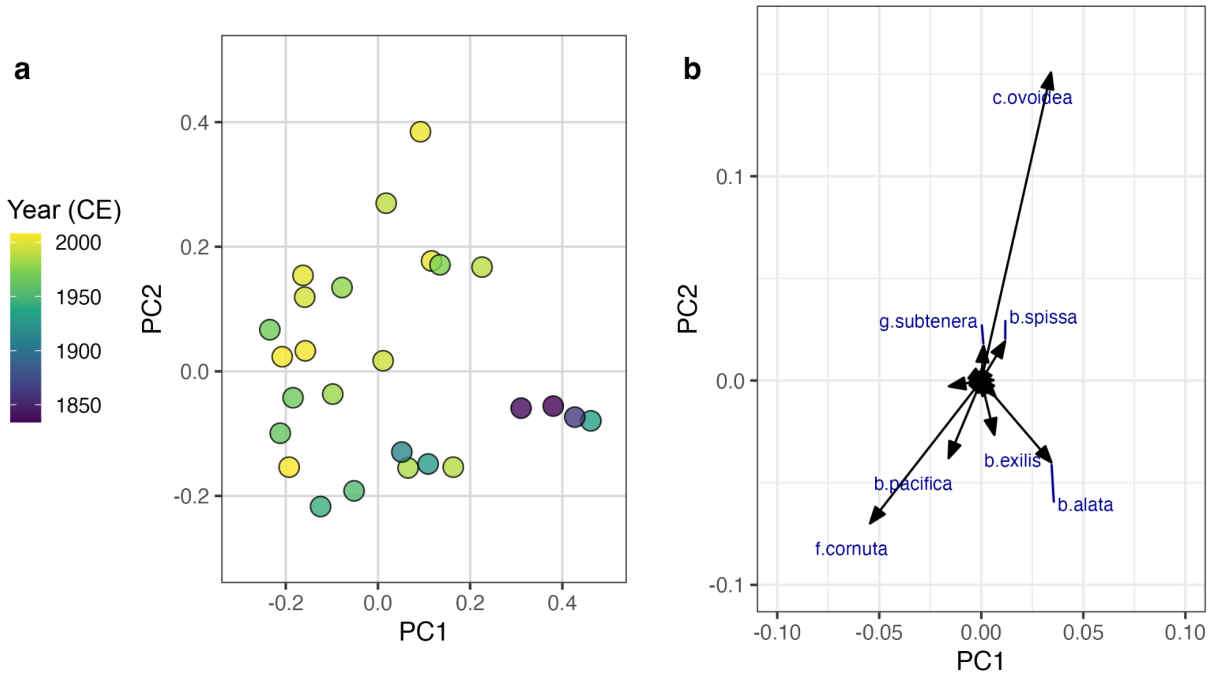

Supplementary Figure 5.9: PCA of species relative biomass for common species.
See Table S5.2 for species excluded from this analysis. (a) Sample scores; colors denote sample age in calendar years (CE). (b) Species loadings; length of vectors denote the degree of correlation between each given species and the principal components. Species with highly similar loading values close to the centroid are not labeled.

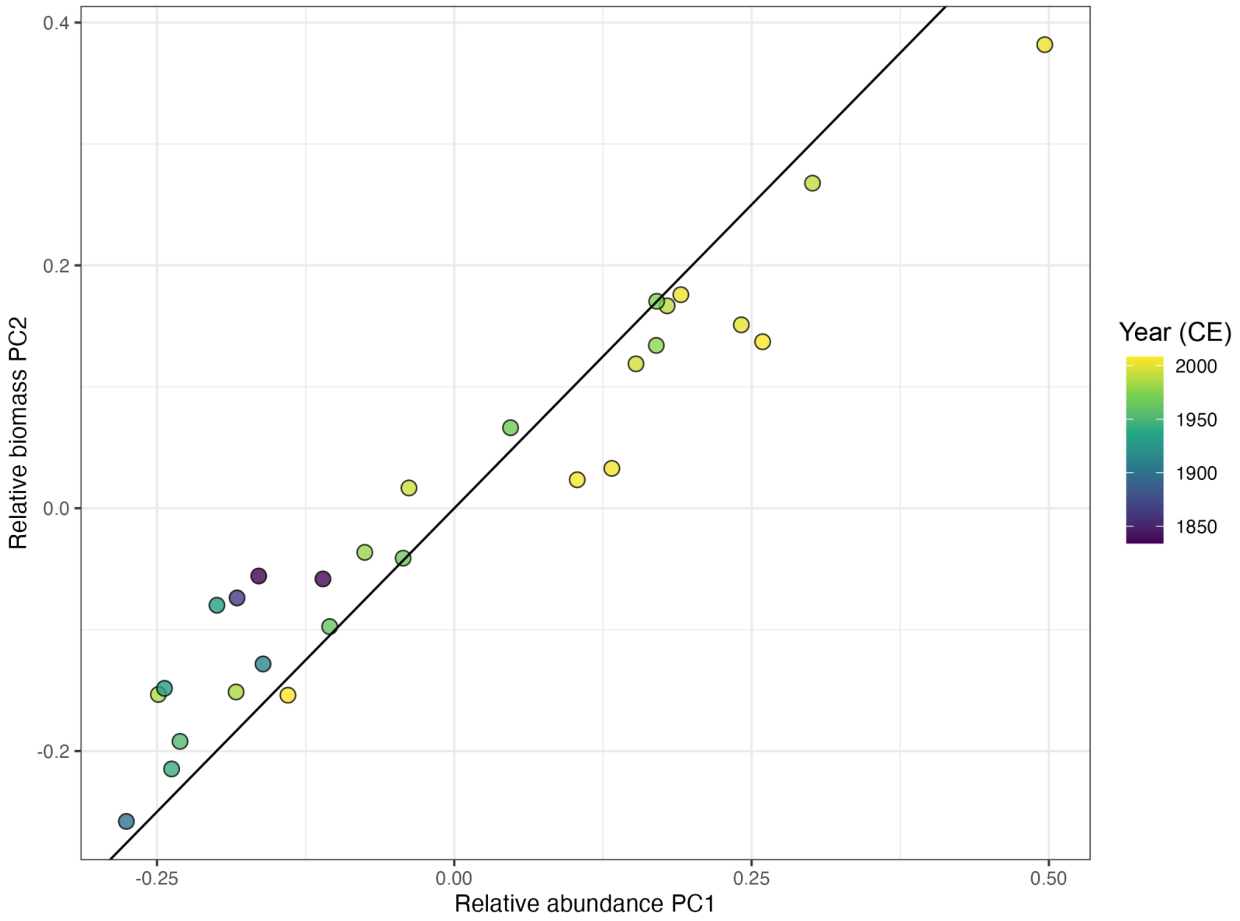

Supplementary Figure 5.10: Relative abundance PC1 vs. Relative biomass PC2.
The axes of variance for each dataset are highly correlated ($R^2 = 0.92$). Colors denote sample ages, while the solid black line denotes the line of unity.

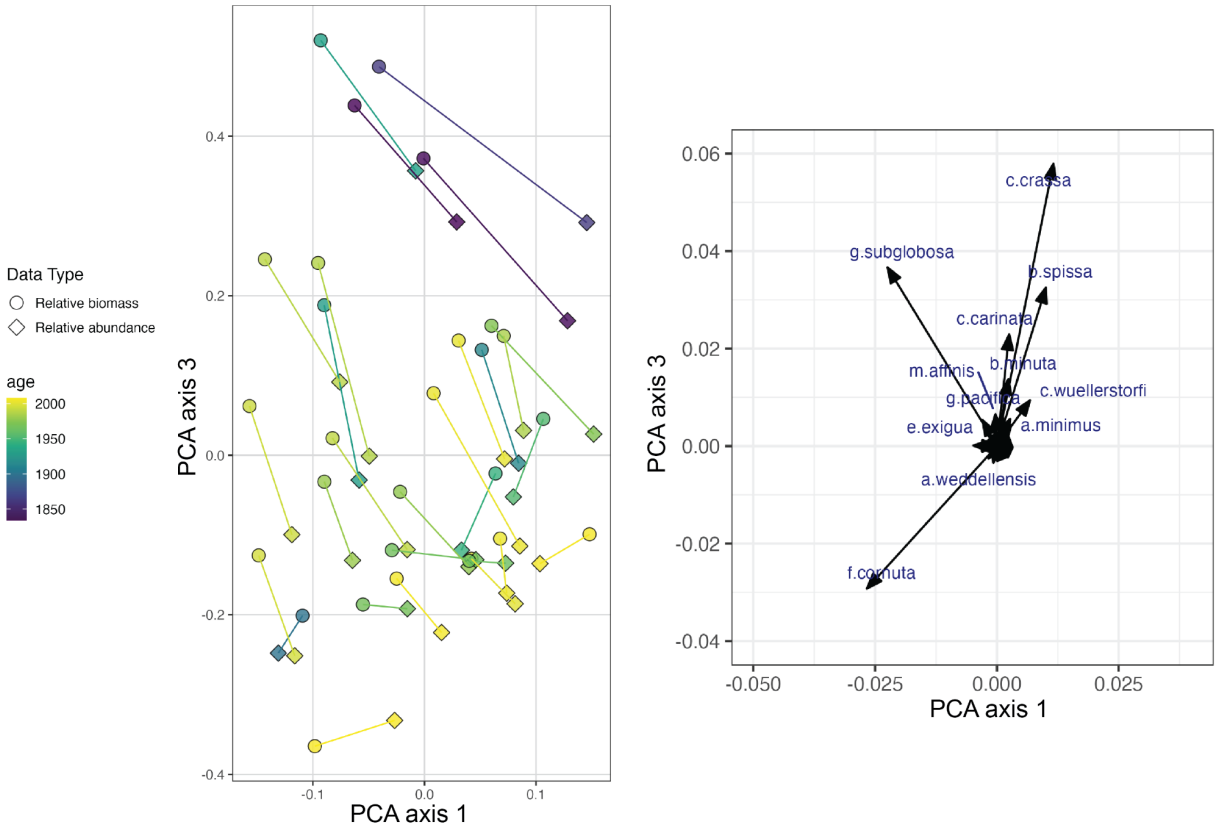

Supplementary Figure 5.11: PCA ordination results for a dataset containing both biomass and abundance counts.
PC1 and PC3 are shown here alongside species loadings. See Table S5.2 for species excluded from this analysis. (a) Sample scores; colors denote sample age in calendar years (CE). (b) Species loadings; length of vectors denote the degree of correlation between each given species and the principal components. Species with highly similar loading values close to the centroid are not labeled. Colors denote sample age in calendar years (CE). Lines connect samples from the same year; shape denotes measurement type (relative biomass vs. relative abundance). Data shown here are from common species; when all species are included in the analysis, the results are highly similar.

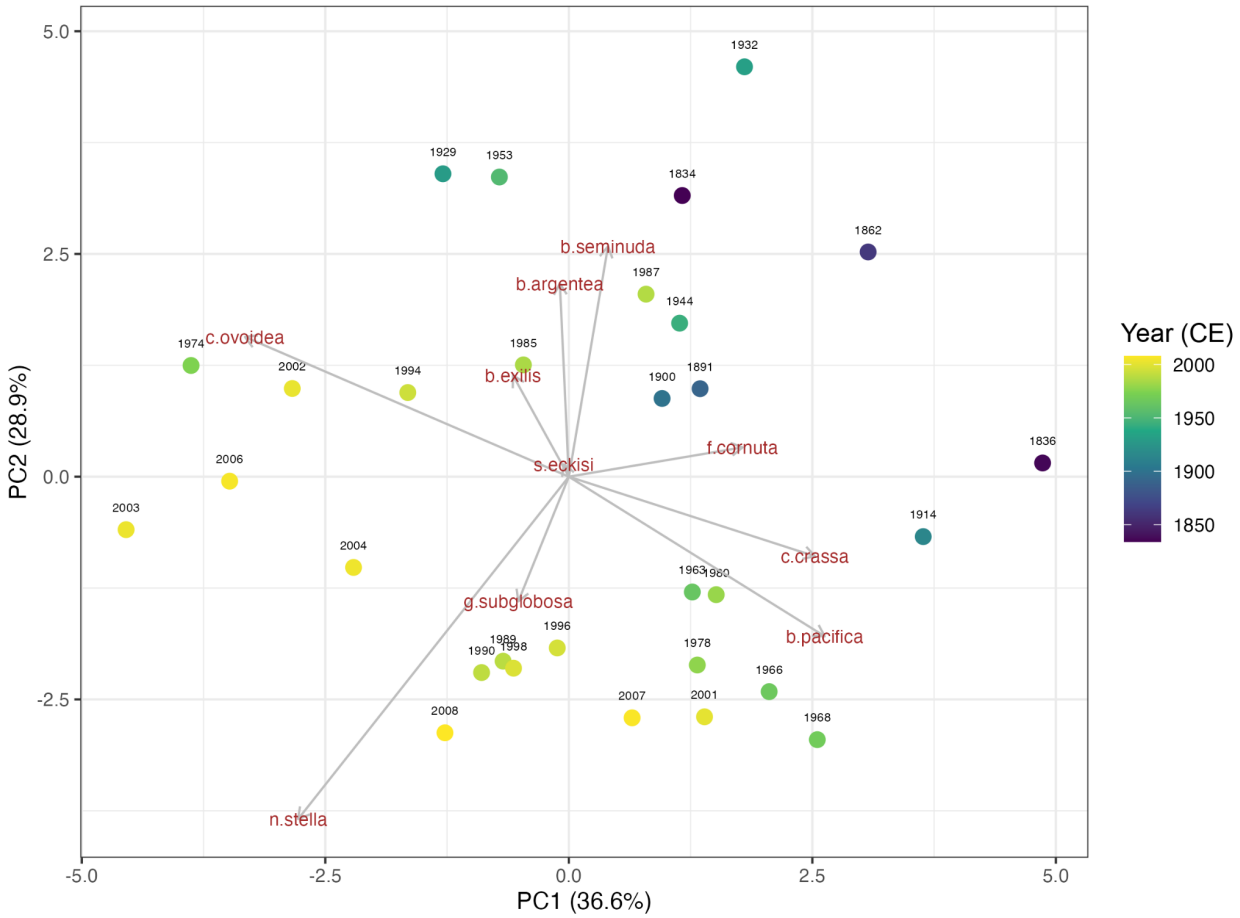

Supplementary Figure 5.12: PCA ordination results accounting for negative correlation bias.
Ordination results shown are for an alternative PCA analysis run on a dataset containing the 10 most common species. Points denote samples; colors indicate sample age in calendar years (CE). Vectors denote species loadings and are labeled by species

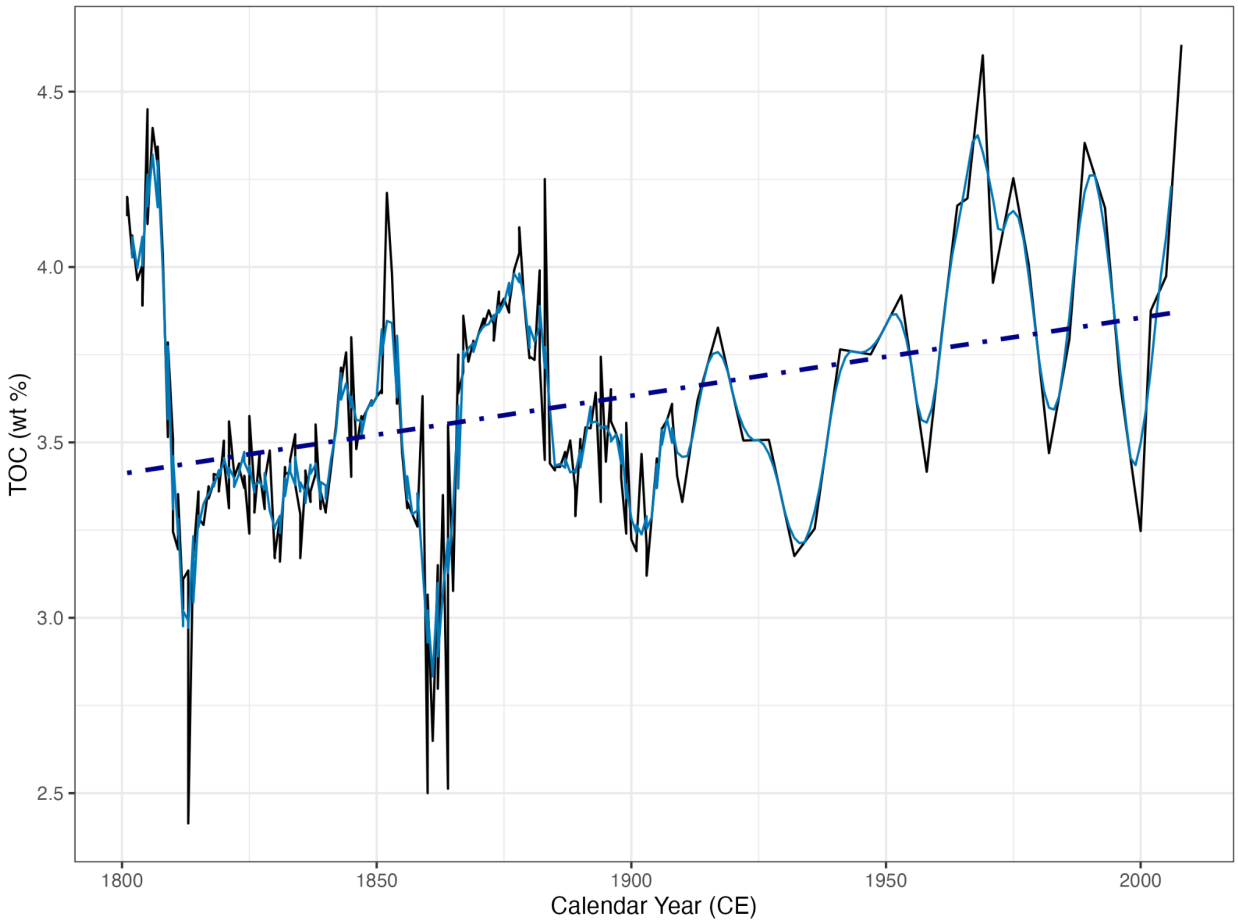

Supplementary Figure 5.13: Total organic carbon (TOC) values from proxy data for the box core interval (1834-2008 CE).
TOC measured by Hendy et al. (2015) is denoted by a solid black line; the solid light blue line denotes a 5-year running average, while the dotted line denotes the output of a regression of calendar year and TOC.

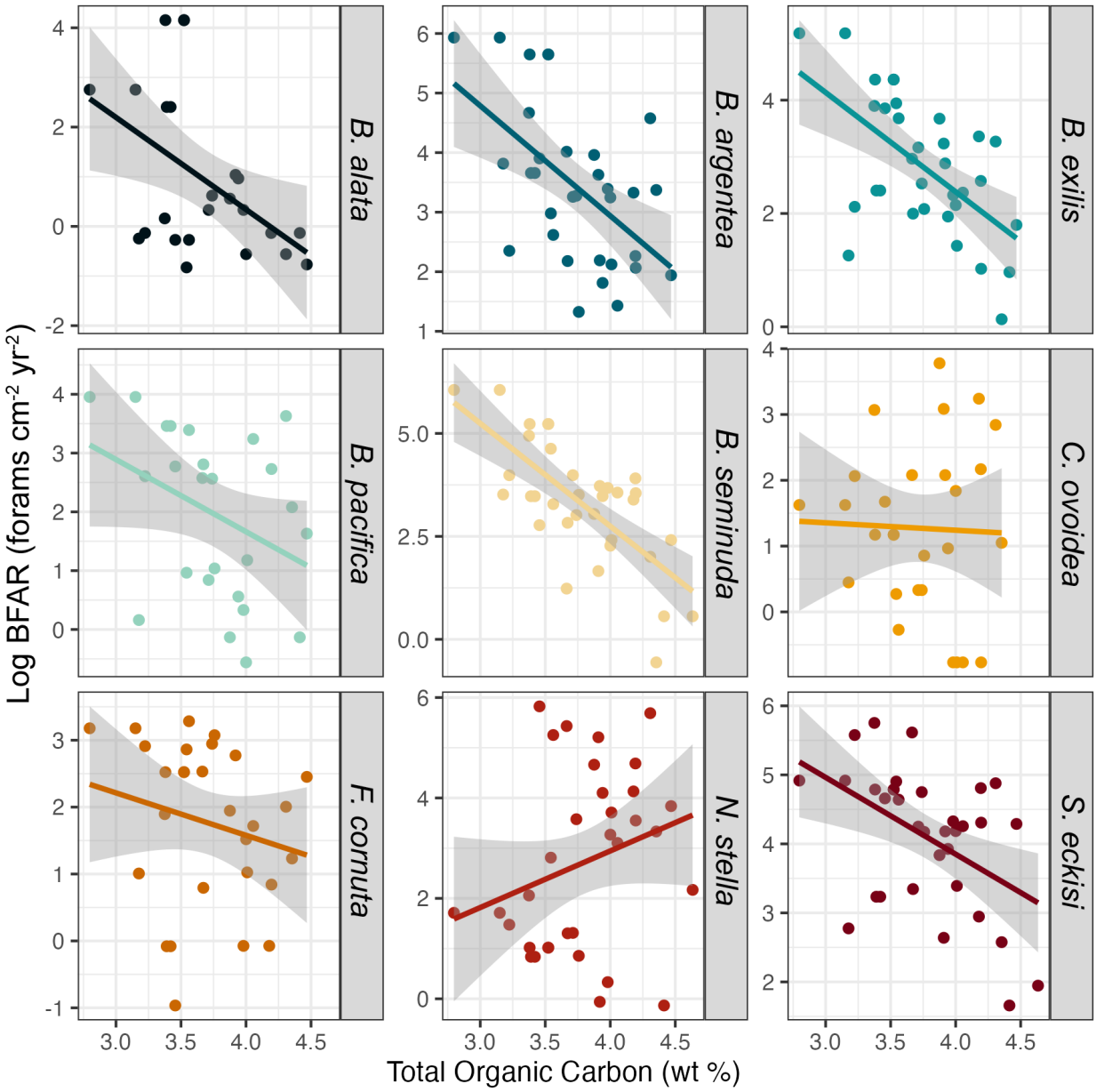

Supplementary Figure 5.14: The relationship between benthic foraminifer accumulation rate and total organic carbon for common species.
Log-transformed benthic foraminifer accumulation rate (BFAR; foraminifera per surface area per year).

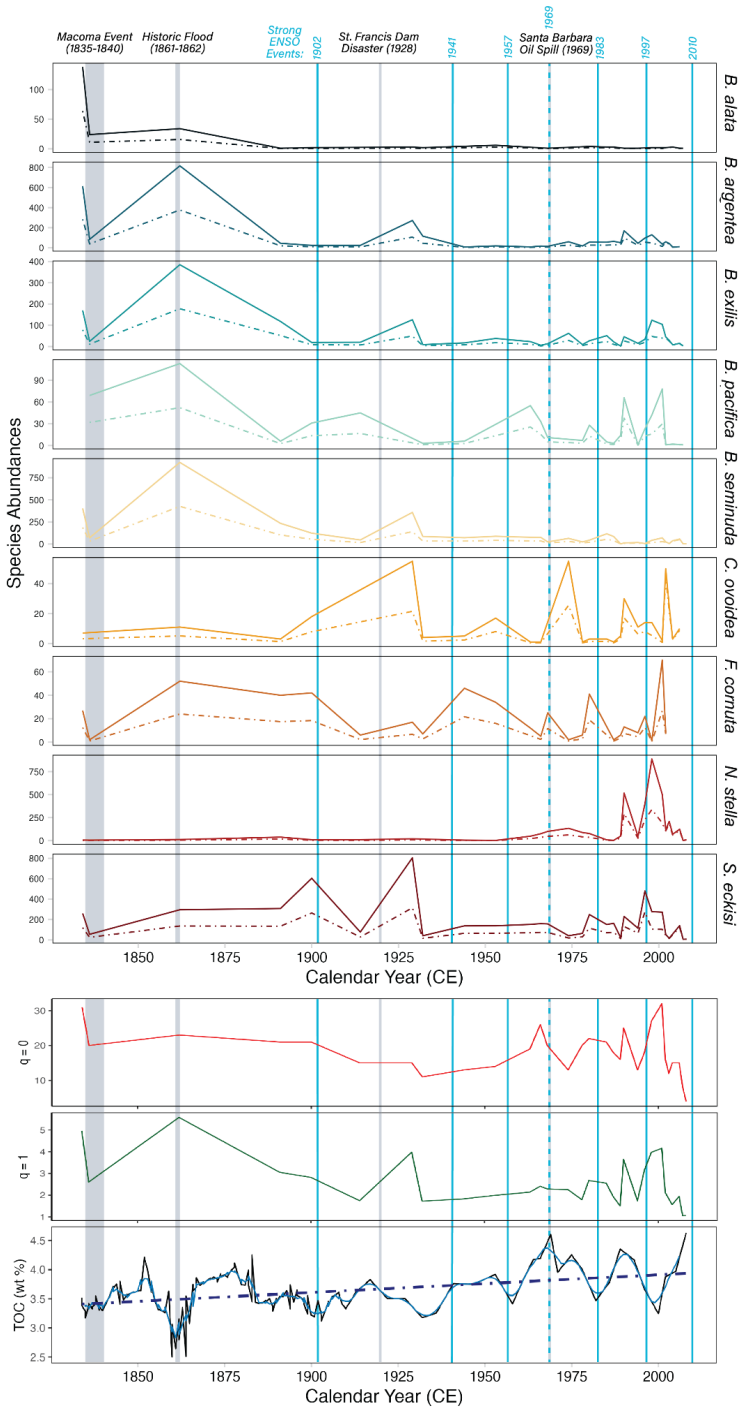

Supplementary Figure 5.15: Temporal trends in species' abundances and diversity metrics and their correlation with major climatic events and total organic carbon (TOC). Solid lines indicate abundance; dashed lines indicate benthic foraminifer accumulation rate (BFAR; foraminifera per surface area per year). Major regional events are denoted by gray bars, and strong ENSO events are denoted by blue lines. Diversity metrics shown are q = 0 (species richness) and q = 1 (Shannon diversity). Total organic carbon (TOC) is denoted by a solid black line; the solid light blue line denotes a 5-year running average, and the dashed line indicates the output of a linear regression between TOC and calendar year (CE).

Supplemental Tables

Supplementary Table 5.1: Environmental variables examined as predictors of PCA axes and species abundance.

Abbreviation	Variable	Calendar Range	Source	Interpolation used
ENSO	El Niño Southern Oscillation	910-2008 CE	Li et al. 2011 (1910-2000), NOAA NINO3 (2000-2008)	Linear interpolation
D15N	Bulk sedimentary d15N	170.5 BCE -1910 CE	Wang et al. 2019	Moving 5-point window
TOC	Bulk sedimentary total organic carbon	170.5 BCE -1910 CE	Wang et al. 2019	Moving 5-point window
SST Uk37	Alkenone Sea Surface Temperature	1297-1941 CE	Zhao et al. 2000	Linear interpolation on yearly averages
Reducing Index	OMZ reconstruction using redox-sensitive metals (Mo, Re, Ba)	165 BCE - 1904 CE	Wang et al. 2021, Wang et al. 2017	Moving 5-point window
MAR	Mass Accumulation Rate	70000 BCE - 1834 CE	Du et al. 2018	-
O2 SAT	Oxygen percent saturation	1953-2008 CE	CalCOFI	-
NO2	Nitrite (micromoles per liter)	1953-2008 CE	CalCOFI	-
NO3	Nitrate (micromoles per liter)	1953-2008 CE	CalCOFI	-
PO4	Phosphate (micromoles per liter)	1953-2008 CE	CalCOFI	-
SiO3	Silicate (micromoles per liter)	1953-2008 CE	CalCOFI	-
BOTTOM T	Bottom water temperature	1953-2008 CE	CalCOFI	-
O2 SAT Minimum	Annual minimum oxygen (percent saturation)	1953-2008 CE	CalCOFI	-
O2 SAT Variance	Annual variance in oxygen (percent saturation)	1953-2008 CE	CalCOFI	-
NO2 Minimum	Annual minimum nitrite concentration (micromoles per liter)	1953-2008 CE	CalCOFI	-
NO2 Variance	Annual variance in nitrite (micromoles per liter)	1953-2008 CE	CalCOFI	-
NO3 Minimum	Annual minimum nitrate concentration (micromoles per liter)	1953-2008 CE	CalCOFI	-
NO3 Variance	Annual variance in nitrate (micromoles per liter)	1953-2008 CE	CalCOFI	-

Abbreviation	Variable	Calendar Range	Source	Interpolation used
PO4 Minimum	Annual minimum phosphate concentration (micromoles per liter)	1953-2008 CE	CalCOFI	-
PO4 Variance	Annual minimum phosphate concentration (micromoles per liter)	1953-2008 CE	CalCOFI	-
SiO3 Minimum	Annual minimum silicate concentration (micromoles per liter)	1953-2008 CE	CalCOFI	-
SiO3 Variance	Annual variation in silicate (micromoles per liter)	1953-2008 CE	CalCOFI	-

Supplementary Table 5.2: Rare species.

Genus	Species
Alabaminella	weddellensis
Angulogerina	angulosa
Anomalinoides	minimus
Anomalinoides	larseni
Astrononion	stellatum
Bolivina	spissa
Bolivina	interjuncta
Bolivina	ordinaria
Bolivinita	minuta
Buccella	peruviana
Cassidulina	minuta
Cassidulina	carinata
Cassidulina	crassa
Cassidulina	auka
Cassidulina	delicata
Cibicidoides	wuellerstorfi
Epistominella	exigua
Epistominella	pulchella
Epistominella	pacifica
Epistominella	sandiegoensis
Epistominella	obesa
Epistominella	smithi
Fursenkoina	complanata
Fursenkoina	pauciloculata
Globobulimina	pacifica
Globobulimina	ovata
Globobulimina	barbata
Globocassidulina	subglobosa
Globocassidulina	neomargareta
Globocassidulina	pacifica
Gyroidina	subtenera
Lagena	striata
Melonis	affinis
Melonis	pompilioides
Nonionella	decora
Nonionella	digitata
Nonionoides	turgidus
Oolina	squamosa
Parafissurina	malcomsonii
Praeglobobulimina	spinescens
Pullenia	elegans
Pullenia	bulloides
Pyrgo	murrhina
Quinqueloculina	seminula
Triloculina	trihedra

Genus	Species
Uvigerina	auberiana
Uvigerina	peregrina
Uvigerina	senticosa
Uvigerina	interruptacostata

Supplementary Table 5.3: Regression output for a model examining TOC as a predictor for abundance for common species from core MV1012.
Here abundance is represented by benthic foraminifer accumulation rate (BFAR; foraminifera per surface area per year).

Model	Species	p-value	R-squared
BFAR ~ TOC	*Bolivina alata*	1.43E-01	0.095
	Bolivina argentea	3.48E-04	0.352
	Bulimina exilis	5.63E-05	0.412
	Bolivina pacifica	6.33E-03	0.282
	Bolivina seminuda	3.47E-05	0.42
	Chilostomella ovoidea	7.51E-01	0.004
	Fursenkoina cornuta	3.01E-02	0.168
	Nonionella stella	9.24E-01	0.0003
	Suggrunda eckisi	3.09E-03	0.243

Supplemental References

Brandon, J. A., W. Jones, and M. D. Ohman. 2019. Multidecadal increase in plastic particles in coastal ocean sediments. Science Advances 5:eaax0587–eaax0587.

Hendy, I. L., L. Dunn, A. Schimmelmann, and D. K. Pak. 2013. Resolving varve and radiocarbon chronology differences during the last 2000 years in the Santa Barbara Basin sedimentary record, California. Quaternary International 310:155–168.

Hendy, I. L., T. J. Napier, and A. Schimmelmann. 2015. From extreme rainfall to drought: 250 years of annually resolved sediment deposition in Santa Barbara Basin, California. Quaternary International 387:3–12.

Schimmelmann, A., I. L. Hendy, L. Dunn, D. K. Pak, and C. B. Lange. 2013. Revised ~2000-year chronostratigraphy of partially varved marine sediment in Santa Barbara Basin, California. GFF 135:258–264.

6 Conclusion of the Dissertation: If the past is the key to the future, which pasts do we recognize?

Every generation rewrites its history, as the saying goes. Besides, mainline history is only one way of reconstructing the past, which has no existence without reference to the present. How one reconstructs the past, as history or whatever, is a political act–a choice from valid alternatives made for particular purposes.

– Epeli Hau‘ofa (Tongan, Oceanian), 2008

6.1 Ecology on “invisible” timescales and the social contexts of global change

In conceptualizing this dissertation, my goal was to leverage extraordinary fossil records to examine how marine ecosystem change occurs over invisible timescales. I spent close to five years generating a dataset of benthic foraminifer species counts, reproductive mode information, and morphometric measurements, with the intention of amassing a dataset of individual measurements from a high-resolution site that would allow for nuanced investigation into ecological cycles across a period of time that includes both ecosystem stability and large-scale environmental change.

One of the major motivations behind this work was my desire to understand the natural variability present in marine ecosystems over ecologically-relevant timescales. Like all modern-day Earth systems, the ocean is changing at a rate rapid enough to be close to the limits of the resolving power of the fossil record (Kidwell 2015). Because rapid changes are unlikely to be preserved in geological archives, relatively few studies exist that can leverage past data at the timescales needed to determine how ecological processes evolve over decades to centuries (Estes et al. 2018). Neither can instrumental records fill this data gap; these typically begin in the late 1800s at the earliest, and long-term (i.e., multi-year) ecological monitoring projects rarely extend into the past beyond the 1970s. As such, critical information on the long-term, pre-industrial states of ecosystems is missing. This lack of information contributes to “shifting baseline” phenomena (Jackson et al. 2012) and limits our ability to identify the nature and extent of ecological responses to novel impacts and predict their near-term outcomes under future climate and global change scenarios.

Another major motivation of this work was my desire to understand how California’s oceans are affected by the accelerating socially-driven ecological impacts that occur in the 19th through 21st centuries. This is because over the past ~200 years, major social changes–colonialization, industrialization, and urbanization–resulted in massive landscape changes across the California coast. While the terrestrial impacts of genocide, forced removal, and other disruptions to and shifts in eco-social dynamics have been studied–though less extensively than other “anthropogenic[4]” climate change factors–fewer publications exist that detail how marine ecosystems were impacted by these changing landscape-use regimes.

[4] In the introduction to this dissertation I noted that I do not use the term “Anthropocene” due to its implication that there is a universal responsibility for the climate crisis (Todd 2015, Davis and Todd 2017, Whyte 2017, 2018). In a similar vein, I hesitate to use the term “anthropogenic” in my writing. While it is often simply taken to mean “human-induced,” I find its lack of specificity limiting at best; at worst, I find that it is used to bolster arguments that promote nihilistic attitudes about futures under climate change (Heglar 2019b), sometimes going so far as to call for

The resulting chapters in this dissertation leverage the dataset I generated throughout the course of my PhD to develop baselines for benthic foraminifer ecosystems from the common era of the Santa Barbara Basin and examine whether major changes to human-environment relationships that begin in the 19th century in California impact the reproductive, morphological, and diversity dynamics of these communities. Though much remains to be done with these data, the three major chapters I include in this dissertation provide a view of ecosystem trends at multiple scales through the past several centuries that offer expanded insights[5] into the dynamics of benthic foraminifer communities in the SBB and suggests promising avenues for future research.

Chapter 2 outlines the high-throughput methods I used to generate these data. These methods build on work by Pincelli Hull, Allison Hsiang, Leanne Elder, Kayli Nelson, Janet Burke, and myself and other collaborators at Yale University to develop software that allows for automated extraction of morphometric data from large, full-sample images of micro- and macrofossils (Hsiang et al. 2017). These automated techniques have revolutionized our ability to collect large datasets that capture the full range of individual variation from paleontological samples (Kahanamoku et al. 2018, Elder et al. 2018, Sibert et al. 2018, Hsiang et al. 2019), and are the primary reason I and the thirteen undergraduate researchers who collaborated on this work were able to digitize and measure over twenty thousand foraminifera and generate what is, to our knowledge, the largest dataset of benthic foraminifer images and morphometric measurements to date.

In Chapter 3, my collaborators and I used these data to document the reproductive life history of four species of *Bolivina* during the Common Era. We found that for the majority of the Common

---

removal of humans from ecosystems (Fletcher et al. 2021) or to urge "us" to seek "humanity's" future on other planets (Smiles 2020, Prescod-Weinstein 2022). My thinking is as follows: if the drivers of climate and biotic change can be ascribed to specific actions or social-environmental structures–such as colonialism, capitalism, industrialization, the burning of fossil fuels, the urbanization of landscapes, etc. (Wildcat 2010, IPCC 2014, 2018, 2019, Norton-Smith et al. 2016)–then specifically naming these causes is a necessary and critical part of socially-driven research. In fact, specificity is an obligation (Liboiron 2021a) and a signpost, both requiring us to identify the structures that are doing the most damage *and* allowing us to imagine what transformations are needed to ensure livable and diverse futures. A secondary benefit of specificity about the causes of global change is that it helps to contextualize its seemingly vast and diffuse ecological, climatic, and social manifestations, providing a path to realizing, as Mary Annaïse Heglar writes, that "this crisis didn't appear out of thin air. Someone did this do us: the fossil fuel industry… [which] was born of the industrial revolution, which was born of slavery, which was born of colonialism" (Heglar 2019a). Specificity is critical because, as Max Liboiron and Tiffany Lethabo King write, "colonialism is not an event, not an intent. It is 'not even a structure, but a milieu or active set of relations that we can push on, move around in, and redo from moment to moment'" (King 2019 in Liboiron 2021). In order to recognize the "specific horizon of possible action[s] before [us]" (Liboiron 2021a) we must first recognize the relations that we are engaged in. While it may seem excessive to be this distrustful of a single word (to paraphrase Todd 2015), defamiliarization (Liboiron and Lepawsky 2022) can be an invitation to examine our obligations and decide which horizon we wish to face.

[5] If the phrase "expanded insights" sounds a bit odd here, it is because this two-word snippet is the result of yet another trip down the anti-colonial theory rabbit hole. When I first wrote this sentence, I used the word "novel," (which has been written in this dissertation at least fourteen times), referring to the "novel insights" my work generated. Then I re-read Max Liboiron's blog post on "Firsting in Research" (Liboiron 2021b), which invited me to reconsider this act of firsting and consider the place of a hubristic statement like this in an essay which discusses how Western (dominant) scientific knowledge is not the first or the only, nor is it universal. This is another invitation to specificity, here "as a methodology of nuanced connection and humility rather than a way to substantiate uniqueness" (Liboiron 2021a).

Era, asexual blooms are a common feature, and are correlated with El Niño events, suggesting that these clonal blooms occur during permissive environmental conditions. Yet the fundamental relationship between abundance and asexual reproduction changes at the latter half of the 19th century, and all species undergo a crash in abundance (with declines of over an order of magnitude) between the mid-19th century and the beginning of of the 20th century. Asexual reproduction concurrently becomes much less common and reproductive mode increases in variability across all of the species we examine. Through this work, we uncover another biotic impact of modern-era change that adds to a growing evidence base of mid-19th century shifts in western North American ecosystems: even in the offshore, seemingly far-removed environment of the SBB, the reproductive life history of unicellular benthic organisms undergoes a state change in the late 1800s that continues to the present day.

In Chapter 4, we applied a dataset of over 21,000 individual measurements spanning ~760 years to examine trends in body size across all species within the Santa Barbara Basin. We found that body size within SBB benthic foraminifera is impacted by life history and environmental trends. Community-level mean size undergoes a stepped decrease in the mid-20th century, and is driven by intraspecific size shifts (both increases and decreases) which occur in the 19th and 20th centuries. Size changes observed within our samples are correlated across species and stronger at when individuals are smaller, suggesting that the community-level size decreases we observe towards the recent correspond with even stronger body size correlations. Reproductive mode plays a role in determining body size distributions in a given population, with some modern size decreases being partially driven by the drop in asexual individuals resulting from mid-19th century reproductive shifts. While food and oxygenation proxies predict size for some species within the basin, there are no shared community-level predictors of size, suggesting that the impacts of environmental change and life history on foraminifer size in the SBB are complex. Yet the timing of change is again placed in the 19th and 20th centuries, suggesting that the novel changes to the broader California system may also impact foraminifer body size within the basin.

Finally, in Chapter 5 we assessed how benthic foraminifer assemblage compositions differ across the ~200-year-long interval over which we observe life history and body size shifts. The data we use for this chapter span from 1834-2008 CE, and include information on the species identity of nearly every foraminifer present within each sample. With this information, we find that assemblage compositions differ from Holocene-era records, and that marked changes in community structure occur between the 19th and 21st centuries. Multivariate analyses show that variations in species composition and biomass are explained by total organic carbon and ENSO variance, suggesting that food availability and environmental variation structure communities within the basin. The timing of change we observe within these data again corresponds with the other biotic shifts we observe in the previous two chapters, with mid 19th and early 20th century assemblages being compositionally different from late 20th and 21st century assemblages.

Through this dissertation, I find that not only do Santa Barbara Basin benthic foraminifera communities change, but they also become more changeable, demonstrating heightened variability[6] in individual characteristics that have species- and community-scale ecological

[6] It is important to note that sampling density in this study is, by design, higher towards present. All else equal, we may expect to capture more short-term variability in individual characteristics simply due to uneven sampling.

consequences. The timing of change that we observe correlates with major shifts in human-environment interactions that accompanied the accelerating colonization of California, such as intensifications in fire (Williams et al. 2019) and sedimentation regimes (Rodriguez et al. 2020) that directly result from the implementation of colonial policy. Climate and oceanographic factors also undergo changes in the past several centuries that are attributed to colonialism: early onset-warming is placed in the mid-1800s in North America (Abram et al. 2016) and a suite of regional and global impacts are recorded as early as the 15th century and shown to intensify through the 19th and 20th centuries (Lewis and Maslin 2015). Climatic and biotic changes have continued through the present day, where the links to colonialism, capitalism, and altered social-environmental regimes are becoming even more apparent as impacts intensify.

Given the dataset I utilize–which records a select set of biological signals from a specific group of organisms living in a highly specialized environment–and the limitations inherent in the use of paleo data of any kind (Behrensmeyer et al. 2000, Kidwell 2013), it is difficult, in a scientific sense, to confidently draw conclusions about the specific links between social-environmental regime shifts and the ecological changes I observe in SBB foraminifera from my studies alone. Yet the broader context and the body of evidence that exists point, again and again, in a similar direction. While uncertainty is an inalienable part of the practice of science, it is important to ensure that recognizing uncertainty does not prohibit action, nor does it preclude a more relational engagement with those connected to the subject matters from which these uncertainties derive (Kearns 2021).

This conclusion chapter serves two purposes. First, it is a way to summarize my findings in a (somewhat[7]) more readable format for those who wish to engage with this work from a different academic or experiential background. Up to this point, I have recapitulated my research findings and attempted to place them into broader context, with the hope that this may serve useful to both scientists and interdisciplinary scholars. The sections that follow are my attempt to identify a path forward in spite of the uncertainty, to draw from the many academic and personal backgrounds that inform my work to determine which recountings of the past I recognize through my research, and which futures I hope to pursue.

6.2 Indigenous knowledges are historical archives

Aboriginal writing is concerned with history, with precise knowledge of the history of Aboriginal existence, gleaned, if necessary, from white records, and prised out of white archives [by the Aboriginal writer].

– Jackie Huggins (Bidjara, Birri Gubba, Juru), 1998

My dissertation research is situated within the Santa Barbara Basin, a place famous for being a repository of climate information, and from which a majority of past information utilized by

However, the magnitude of changes we observe—both in trait measurements and the variation within these measurements—highlights how modern foraminifer communities are distinct from those of the past.

[7] While I hope that the language in this chapter is more accessible than in previous chapters, it is still fairly academic and peppered with occasional bits of jargon that are specific to my field(s). (Sorry, mom!)

Western[8] scientists to build baselines and predict future scenarios is derived. The SBB is also an archive of colonial impacts, which emerge in the physical records stored within the basin. However, physical fossil records are not the only source of information about the ecological history of the Santa Barbara region. Nor are they always the best for understanding the true trajectory of the past.

Many additional, rich sources of information exist that can offer a glimpse into the region's past (Figure 6.1). These include instrumental records (such as the CalCOFI information I utilize in some chapters in this dissertation), which have daily to monthly resolution and can extend back into the early to mid 20th century; archival records, which have variable resolution but can reach into the early 19th century (McClenachan et al. 2015, Szabó 2015); as well as information from Indigenous knowledges, which extends back tens of thousands of years and includes place-based and -adapted holistic information that is an unparalleled source of knowledge on eco-social relationships and the impacts of colonization on regional ecosystems (McGregor 2004, Wildcat 2010, Simpson 2017, Liboiron 2021a, Hernandez 2022).

I have attempted to use my work in the SBB as a way to examine a small slice of the impacts of colonialism[9] on the ocean, using the tools that my training in Western science has equipped me with. As a paleoecologist trained to study the history of life and earth, I recognize that just as the rock record has preserved an archive of history, "ecological conditions are themselves living archives of past management actions; they represent a repository of traditional knowledge in the land" (Norgaard 2019). As an Indigenous scholar of Kanaka ʻŌiwi and Maʻohi lineages, I also recognize that there is an inherent compromise in my use of scientific tools, which is described by Max Liboiron (Métis) as the "compromise of doing both Indigenous and anticolonial work in science and academia" (Liboiron 2021a). This can mean that academia is often not an ideal place for Indigenous knowledges[10], as the incommensurabilities (Tuck and Yang 2012, Tuck and

[8] A note on "Western" and related terms: just as there is no single "Indigenous" science, "Western" science is also not a monolith (Guba and Lincoln 1994, Maffie 2009, Kimmerer and Kimmerer 2013). Western, here is used to indicate the scientific traditions that emerge from Western culture, the "heritage of social norms, ethical values, political systems, epistemologies, technologies, and legal structures and traditions heavily influenced by various forms of Chistianity and Judaism… which heavily influenced societies in Europe and beyond" (Liboiron 2021a). Further, I do not use "Western" here to serve as a foil to Indigenous science, as these diverse epistemologies are not diametrically opposed. Note that I sometimes use "dominant" in addition to "Western" to indicate the Eurocentric scientific tradition.

[9] While it may seem a bit late in the text to define colonialism, it is important to me that this section begin with a glimpse into my ideological footing. To me, Max Libroiron's writings on colonialism succinctly capture the essence of the relational phenomena that the term discusses, which is premised on "assumed entitlement to Indigenous Land" (Liboiron 2021a). They write: "While there are different types of colonialism–settler colonialism, extractive colonialism, internal colonialism, external colonialism, neoimperialism–they have some things in common. Colonialism is a way to describe relationships characterized by conquest and genocide that grant colonialists and settlers ongoing state access to land and resources… Colonialism is more than the intent, identities, heritages, and values of settlers and their ancestors. It's about genocide and access" (Liboiron 2021a).

[10] In fact, academia can and is often extractive, particularly when Eurocentric or Western sciences overlap with and seek to utilize Indigenous Knowledges (IK; Tuck and McKenzie 2014, David-Chavez and Gavin 2018, Liboiron 2021a). Many of us who work in both fields are familiar with discussions of "integration" and "synthesis" with Western scientists who typically seek to integrate Indigenous Knowledge *into* Western Science, and thus build a new amalgamation that remains inherently grounded in Western philosophy. Integration too often means assimilation; settler frameworks force IK into occupying arrangements, where IK is braided into processes and frameworks that remain rooted in Western science, thus ensuring that the unsettling potential of Indigenous

McKenzie 2014) of the relations inherent to each, and the hostility of academia to alternative ways of knowing (Smith 1999, Meyer 2001, Liboiron 2021a, Watego 2021) make this a difficult space in which to navigate as someone with obligations to place and people.

As a result of these many pressures, my dissertation work is limited. Of course, like all dissertations, these limitations are numerous, perhaps too numerous to recount here. But in this conclusion I wish to focus on one particularly impactful limitation of my research: that the projects I report on here only encompass methods that fall under the domain of Western scientific training. As a result, there is the lack of holistic information included in my work. While this may be viewed by some as a strength, I view it as another result of the compromises inherent in present-day academic spaces. Put simply, my research is limited because it did not include engagement with the Chumash people, who have studied the region currently known as Santa Barbara through relationship since time immemorial, generating rich, complex, culturally-grounded oceanographic, ecological, and biological knowledge which provides critical and irreplicable context for understanding how the oceans in this place have changed over many thousands of years. This relational information has been curated, cared for, and perpetuated for millennia, but is all too often excluded from conventional scientific works, including my own.

While in this piece I will not delve more deeply into the reasons for this exclusion (though see Smith 1999, Tuck 2018, Liboiron 2021a, Watego 2021, McAllister et al. 2022), I hope to use this conclusion as a place where I can lay the groundwork for future where I am able to appropriately include Land[11] relations and obligations at the center of my work. As with many Indigenous scientists who have come before me (Smith 1999), I am motivated to do anticolonial research because of my background. I seek to understand the world in its cultural contexts–to embrace the richness of an understanding of knowledge as not acultural, but as always situationally and contextually grounded to the places and the people from whom that knowledge is derived (Guba and Lincoln 1994, Smith 1999, Meyer 2001, Kahakalau 2004, Akena 2012, Tuck and McKenzie 2014, Morishige et al. 2018, Alegado and Hintzen 2021, Liboiron 2021a, 2021c). In recognizing the linkages between people, culture, and place, our understanding of the historical trajectories of ecosystems can become not only richer but also more accurate (Huggins 1998, Watego 2021) and grounded in justice-oriented outcomes (Whyte 2020, McGregor et al. 2020).

I am also motivated to do this work because of the continued ways in which Western science ignores the social drivers of global change, often choosing instead to view colonialism, capitalism, and racism as being within the domain of the social sciences and humanities. While writing this dissertation, it was difficult to find scientific publications specific to the Santa Barbara region that discuss one of the largest climate change impacts of the Holocene: the abrupt shift from ecosystems managed by Indigenous peoples through relationships crafted over millennia to a new ecological regime founded on land disposession and Indigenous genocide that

knowledge is nullified in the process. There are, of course, examples of beneficial overlaps, which typically result when Indigenous peoples have the power to design, implement, and manage outcomes of projects that involve IK (as well as refuse to participate; (Bartlett et al. 2012, Kimmerer and Kimmerer 2013, Tuck and Yang 2014, David-Chavez and Gavin 2018, Kahanamoku et al. 2020, Liboiron 2021a).

[11] Here I capitalize Land when referring to it as a proper name indicating a primary relationship, following Styres and Zinga (Indigenous and settler; 2013) and Liboiron (2021a). To me this is the best depiction in English of the ʻŌiwi relation to ʻāina (Land, lit. "they who feed;" Pukui and Elbert 1986).

not only disrupted traditional ecological-social connections but introduced novel, often harmful, behaviors that have shaped the land- and seascapes we know today. It was even rarer to find studies discussing this period that explicitly name colonialism as a potential driver.

To me, the paucity of studies connecting the knowledges of Indigenous science to research questions about colonialism is disconcerting in no small part because I know that Indigenous knowledges are historical archives. As the quote at the beginning of this section from Aborigial scholar Jackie Huggins emphasizes, Indigenous peoples are distinctly concerned with history, and are the experts on the history of our own existence (Huggins 1998). We use any information necessary–including oral traditions, written records, settler state archives, and instrumental and fossil climatic and biological data–to reconstruct historical events, revitalize biocultural conservation and resource management traditions (e.g., McGregor 2007, Vaughan 2018, Morishige et al. 2018). Through this holistic research, we can develop a full picture of the impacts of colonialism on the trajectory of Indigenous life and ecosocial relations (Simpson 2004, 2017). In contrast, "colonial literature, despite its long tradition of domination, is not a historical one" (Watego 2021).

While such critiques of the historical canon may seem harsh[12], they speak to the positioning of all fields of academia as stemming from dominant culture. This epistemological foundation may be more commonly recognized within the fields which explicitly position humans or the "human condition" as their study subject–such as literature, anthropology, or sociology–yet they are similarly present within the sciences (Kimmerer and Kimmerer 2013). Science, as both a compilation of methodologies and a philosophy, does not stand on neutral ground; rather, it is inherently the domain of dominant culture (Smith 1999, Liboiron 2021a). The scientific method has long been used, whether or not with the explicit knowledge or consent of those involved in the process of science, as a tool with which to craft narratives and define what is considered as fact (Arvin 2019). Histories are defined in this way; the history of Earth itself is no exception.

While there has been admirable and growing pushback against the positioning of the Native as a "subject" rather than a "knower," the knowledges of Indigenous science remain on the margins (Smith 2006, Louis 2007), and the title of "knower" remains a conditional one. Indigenous peoples are "relegated to being the primary informer at best to the professional person who then argues the story on their behalf" (Wright 2017). This positioning is continually remade; Indigenous scientists have continually found ourselves facing outdated notions of objectivity within the academy and elsewhere from our earliest involvement in academia (Smith 1999, Watego 2021). Yet it is Indigenous peoples–academics, researchers, scholars, activists, cultural knowledge-holders, and practitioners of all kinds–who are leading the work of making the connection between intensifying colonialism and deteriorating ecosystem and Earth system states, as well as leading the efforts to remedy these impacts to the benefit of all (Jones 2021). Meanwhile, dominant science, which has yet to meaningfully engage with these ideas, writes Earth history, and overwhelmingly used to decide what actions are to be taken for the future (Mohamed et al. 2022).

[12] Though see Tuck (2018), "Biting the university that feeds us."

Through my training scientific training, use of the phrase "the past is the key to the future[13]" has grown in popularity among paleo scientists seeking to communicate the importance of their research. Yet I cannot help but notice which knowledges are often omitted from this work, and the power dynamics that remain at play even when these knowledges are included (Smith 1999, Cartier 2019). My experiences have led me to ask: when we speak of using past knowledge to develop solutions to mitigate climate change and ensure a liveable future, which knowledges do we include? In other words, whose pasts and futures are we discussing?

6.3 If climate change is colonialism, Indigenous peoples must lead in conservation science and climate adaptation

Indigenous imaginations of our futures in relation to climate change—the stuff of didactic science fiction—begin already with our living today in a post-apocalyptic situation. Had someone told our ancestors a story of what today's times are like for Indigenous peoples, our ancestors would surely have thought they were hearing dystopian tales… so for Indigenous peoples, 'the Anthropocene epoch,' as a concept some people invoke often to envision the future, does not present us, at first glance, with the specter of unprecedented changes.

– Kyle Powys Whyte (Neshnabé), 2017

We have it all over the western scientists when it comes to adapting to climate change. We've been adapting to a changing climate for thousands of years.

– Lisa Hillman (Karuk), 2020

A notable example of *which* pasts are included in dominant discourse is the divide that exists between Indigenous perceptions of colonialism as an apocalyptic event and the more credulous attitudes of dominant science fields, which have only recently begun to discuss climate change as a new phenomenon that represents a global crisis. Perhaps this is because the experience of the colonial period was asymmetric (Whyte 2017, 2020). Due to demographics in science, technology, engineering, and mathematics (STEM; Bernard and Cooperdock 2018), "the shockwaves of the consequences of colonialism" (Davis and Todd 2017) are only more recently being felt among a majority of scientists. As a result, these scientists may be more likely to ascribe universal blame to humanity for causing the climate "crisis" (Whyte 2018).

As an Indigenous scientist, it is not a new idea to me that colonialism is a driver of global change that has pushed global ecosystems towards a tipping point (Whyte 2020). My own ancestors in Hawai'i already survived an apocalypse, where ridge-to-reef biocultural management systems that sustained over a million people were systematically eradicated by Europeans and Americans at the same time that the Native Hawaiian population declined by approximately ninety percent in less than a century. In California, the lands on which I study, tens of thousands of years of Indigenous management of land and oceans through fire, planting, harvesting was violently interrupted by the genocide and forced removal of California Natives and suppression of

[13] As you may guess, this is not a new idea; in Hawai'i, this idea is captured in the saying "I ka wa ma mua ka wa ma hope." For select readings on this topic, see Kame'eleihiwa 1992, Hau'ofa 2008, or Wilson-Hokowhitu 2019. As Epeli Hau'ofa writes, "Where time is circular, it does not exist independently of the natural surroundings and society. It is very important for our historical reconstructions to know that the Oceanian emphasis on circular time is tied to… natural phenomena" (2008).

biocultural management techniques like cultural burning (Bauer Jr 2016). These legacies are written on the landscape across the colonized world, where colonists and settlers sought to terraform Earth in a Eurocentric image.

We cannot truly tackle the global problems of climate change without first understanding its history, and this history is inextricably linked to colonialism. Within the field of Indigenous Environmental Studies, climate change is well understood as the latest intensification in a long continuum of colonial impact (Wildcat 2010, Norton-Smith et al. 2016, Whyte 2016, 2020, Davis and Todd 2017, McGregor et al. 2020, Liboiron 2021a, Hernandez 2022). Outside of academia, Indigenous peoples around the world have long viewed colonialism as an ecocidal event, one that disrupts the carefully-crafted ecosocial relationships that were established, refined, and maintained over tens of thousands of years. The changes induced by colonialism are perhaps even "more extreme than what many nonindigenous persons fear most about moving beyond 2˚C" (Whyte 2020).

It can feel trivial–and exhausting (McAllister 2022)–to recapitulate the same arguments that many generations of accomplished Black and Native scholars and scientists have made before me. Yet nearly a decade of experience has made it clear to me that the natural sciences remain, to their detriment, a space that is insulated from these discussions. In other words, scientists have much to learn from the Indigenous traditions of scholarship, stewardship, and activism.

As we move into an era where climate futures are at stake, it is critical that all scientists whose expertise relates to climate and ecosystems recognize the historical impacts of colonialism and work to remedy the inequities that it continually perpetuates. While scientists increasingly understand that the practice of science does not benefit all equally (Edge 2020, Stevens et al. 2021, Chen et al. 2022), as transformative measures are proposed for our disciplines and the policymaking spheres they influence, we must take care to ensure that these do not perpetuate harm against Indigenous peoples (Whyte 2020, Liboiron 2021c). Indeed, if our efforts are not explicitly anticolonial, work to mitigate climate change and implement sustainable practices will fall short of professed equity goals.

As I envision possible futures, I turn to Max Liboiron's writings about the practice of anticolonial science. They ask us to consider: "How would scientific practices in the Americas and other colonized regions change if all labs were required to understand what it is to do science in a settler-colonial context–to understand that the practice of science extends from colonialism and feeds into it? And how might those changes feed into anticolonial research practices, scientific and otherwise?" (Liboiron 2021a).

While I do not have the answers to these questions–they will look different to different people, in different places–I can offer some suggestions for those looking to do anticolonial science. First, I ask us to recognize that knowledge is not universal: that place-based knowledge is specific, rich, and, more often than not, generated outside of the academy (Tuck and McKenzie 2014, Haraway 2020, Alegado and Hintzen 2021). Differing epistemological frameworks will result in different research questions, methodologies, and outcomes (Guba and Lincoln 1994); these differences can be a benefit to science, but only as long as the power dynamics at play are appropriately recognized and overturned (Hofstra et al. 2020).

Secondly, I ask us to follow Indigenous peoples' lead in conservation science and climate adaptation work. As Lisa Hillman (Karuk) notes in the above quote, Indigenous peoples have long been adapting to climate change, and face disproportionate impacts that mean that we are on the leading edge of sustainable practice (Norton-Smith et al. 2016, Jones 2021, Mohamed et al. 2022). While local, federal, and international bodies are also working to address the ecological crisis, without justice-oriented approaches to climate adaptation and mitigation–including self-determination for Indigenous peoples, reciprocity between settler governments and Native nations, and accountability for wrongdoing–the cross-societal coordination needed to enact locally-developed climate responses will be exceedingly difficult to achieve. Put succinctly, if sustainability efforts "fail Indigenous peoples, they fail all life" (McGregor et al. 2020)

Of course, regardless of which future trajectory humanity takes, Indigenous peoples will continue to act, as we have always done (Simpson 2017, Whyte 2020). Rather than ignoring both Indigenous history and modern-day actions, dominant science should support these beneficial efforts by supporting these communities in leading the design, development, and implementation of climate-related research (Latulippe and Klenk 2020).

Finally, I ask us to recognize that truly anticolonial research supports Indigenous sovereignty. In fact, Indigenous sovereignty–via governance or through other more subversive mechanisms–is a critical aspect of sustainability, both of ecosystems and of Indigenous cultures and lifeways (Nelson and Shilling 2018). Without sovereignty over decision-making processes, Indigenous peoples are too often dehumanized or are seen as of secondary importance, with our needs placed behind those that are "shared by humanity" (Kahanamoku et al. 2020). In contrast with the dehumanizing regimes of settler colonialism, when Indigenous sovereignty is enacted and asserted "over environs and destinies," it leads to "resistance, resilience, and innovation in… economies of wellbeing" (Wolfgramm-Rolfe et al. 2018).

The research I report on in this dissertation has implications for our understanding of the past, providing additional insights into the individual- to community-level variability of some of the most abundant benthic microorganisms in the global ocean, and how this variability shifted as a result of a changing environment. Yet there is much more that can be expanded on if I were to include additional epistemological frameworks in attempting to understand the impacts of colonialism on marine ecosystems. I envision my future work as doing just that–implementing the lessons learned from my training and experience as an Indigenous scientist to see the multifaceted legacies of colonialism with enough clarity to address them (Liboiron 2021c).

Chapter 6 Figures

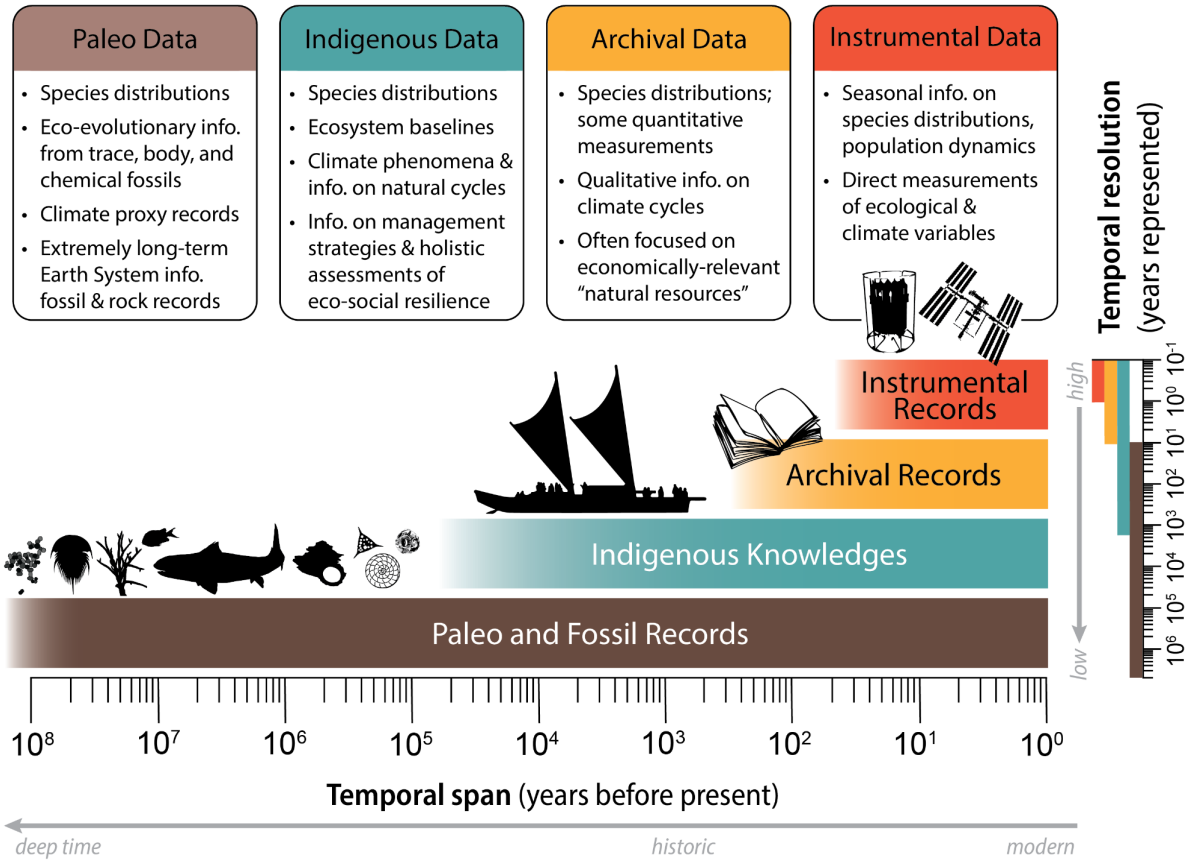

Figure 6.1: Types of information on past ecosystem states.

6.4 Chapter 6 References

Abram, N. J., H. V. McGregor, J. E. Tierney, M. N. Evans, N. P. McKay, and D. S. Kaufman. 2016. Early onset of industrial-era warming across the oceans and continents. Nature 536:411–418.

Akena, F. A. 2012. Critical Analysis of the Production of Western Knowledge and Its Implications for Indigenous Knowledge and Decolonization. Journal of Black Studies 43:599–619.

Alegado, R., and K. Hintzen. 2021. Kūlana Noiʻi: a kanaka ʻōiwi-centered indigenist axiology for conducting research with communities. Page *in* J. Stephens and L. Pipe, editors. IGNITE: A Justice-Forward Approach to Decolonizing Higher Education through Space, Place, and Culture. Vernon Press, Wilmington.

Arvin, M. R. 2019. Possessing Polynesians: The Science of Settler Colonial Whiteness in Hawai`i and Oceania. Duke University Press.

Bartlett, C., M. Marshall, and A. Marshall. 2012. Two-eyed seeing and other lessons learned within a co-learning journey of bringing together indigenous and mainstream knowledges and ways of knowing. Journal of Environmental Studies and Sciences 2:331–340.

Bauer Jr, W. J. 2016. California through Native eyes: Reclaiming history. University of Washington Press.

Behrensmeyer, A. K., S. M. Kidwell, and R. A. Gastaldo. 2000. Taphonomy and paleobiology. Paleobiology 26:103–147.

Bernard, R. E., and E. H. G. Cooperdock. 2018. No progress on diversity in 40 years. Nature Publishing Group 11:1–4.

Cartier, K. 2019. Keeping Indigenous Science Knowledge out of a Colonial Mold. Eos 100.

Chen, C. Y., S. S. Kahanamoku, A. Tripati, R. A. Alegado, V. R. Morris, K. Andrade, and J. Hosbey. 2022. Systemic racial disparities in funding rates at the National Science Foundation. eLife 11:e83071.

David-Chavez, D. M., and M. C. Gavin. 2018. A global assessment of Indigenous community engagement in climate research. Environmental Research Letters 13:123005–123018.

Davis, H., and Z. Todd. 2017. On the Importance of a Date, or Decolonizing the Anthropocene:20.

Edge, L. 2020. Science has a racism problem. Cell 181:1443–1444.

Elder, L. E., A. Y. Hsiang, K. Nelson, L. C. Strotz, S. S. Kahanamoku, and P. M. Hull. 2018. Sixty-one thousand recent planktonic foraminifera from the Atlantic Ocean. Scientific Data 5:180109.

Estes, L., P. R. Elsen, T. Treuer, L. Ahmed, K. Caylor, J. Chang, J. J. Choi, and E. C. Ellis. 2018. The spatial and temporal domains of modern ecology. Nature Ecology & Evolution 73:1–10.

Fletcher, M.-S., R. Hamilton, W. Dressler, and L. Palmer. 2021. Indigenous knowledge and the shackles of wilderness. Proceedings of the National Academy of Sciences 118:e2022218118.

Guba, E. G., and Y. S. Lincoln. 1994. Competing paradigms in qualitative research. Handbook of qualitative research 2:105.

Haraway, D. 2020. Situated knowledges: The science question in feminism and the privilege of partial perspective. Pages 303–310 Feminist theory reader. Routledge.

Hauʻofa, E. 2008. Our Sea of Islands. Pages 27–40 We Are the Ocean: Selected Works. University of Hawai'i Press, Honolulu.

Heglar, M. A. 2019a, August 20. The Fight for Climate Justice Requires a New Narrative. Inverse.

Heglar, M. A. 2019b. Home is always worth it. Medium.
Hernandez, J. 2022. Fresh banana leaves: healing Indigenous landscapes through Indigenous science. National Geographic Books.
Hofstra, B., V. V. Kulkarni, S. Munoz-Najar Galvez, B. He, D. Jurafsky, and D. A. McFarland. 2020. The Diversity–Innovation Paradox in Science. Proceedings of the National Academy of Sciences 117:9284–9291.
Hsiang, A. Y., A. Brombacher, M. C. Rillo, M. J. Mleneck-Vautravers, S. Conn, S. Lordsmith, A. Jentzen, M. J. Henehan, B. Metcalfe, and I. S. Fenton. 2019. Endless Forams:> 34,000 modern planktonic foraminiferal images for taxonomic training and automated species recognition using convolutional neural networks. Paleoceanography and Paleoclimatology 34:1157–1177.
Hsiang, A. Y., K. Nelson, L. E. Elder, E. C. Sibert, S. S. Kahanamoku, J. E. Burke, A. Kelly, Y. Liu, and P. M. Hull. 2017. AutoMorph: Accelerating morphometrics with automated 2D and 3D image processing and shape extraction. Methods in Ecology and Evolution 9:605–612.
Huggins, J. 1998. Sister girl: The writings of Aboriginal activist and historian Jackie Huggins. UQP.
IPCC. 2014. Climate Change 2014: Synthesis Report. Contribution of Working Groups I, II and III to the Fifth Assessment Report of the Intergovernmental Panel on Climate Change. Page 151 (R. K. P. Core Writing Team and L. A. Meyer, Eds.). Geneva.
IPCC. 2019. IPCC Special Report on the Ocean and Cryosphere in a Changing Climate. Page (D. C. R. H.-O. Pörtner V. Masson-Delmotte, P. Zhai, M. Tignor, E. Poloczanska, K. Mintenbeck, M. Nicolai, A. Okem, J. Petzold, B. Rama, N. Weyer, Ed.).
IPCC, V. Masson-Delmotte, P. Zhai, H.-O. Pörtner, D. Roberts, J. Skea, P. R. Shukla, A. Pirani, W. Moufouma-Okia, C. Pean, R. Pidcock, S. Connors, J. B. R. Matthews, Y. Chen, X. Zhou, M. I. Gomis, E. Lonnoy, T. Maycock, M. Tignor, and T. Waterfield. 2018. Global warming of 1.5˚C. Pages 1–32.
Jackson, J. B. C., K. E. Alexander, and E. Sala. 2012. Shifting Baselines: The Past and the Future of Ocean Fisheries. Island Press.
Jones, B. 2021, June 11. Indigenous people are the world's biggest conservationists, but they rarely get credit for it. Vox.
Kahakalau, K. 2004. Indigenous heuristic action research: Bridging western and indigenous research methodologies. Hulili: Multidisciplinary research on Hawaiian well-being 1:19–33.
Kahanamoku, S., R. Alegado, A. Kagawa-Viviani, K. L. Kamelamela, B. Kamai, L. M. Walkowicz, C. Prescod-Weinstein, M. A. de los Reyes, and H. Neilson. 2020. A Native Hawaiian-led summary of the current impact of constructing the Thirty Meter Telescope on Maunakea. arXiv preprint arXiv:2001.00970.
Kahanamoku, S. S., P. M. Hull, D. R. Lindberg, A. Y. Hsiang, E. C. Clites, and S. Finnegan. 2018. Twelve thousand recent patellogastropods from a northeastern Pacific latitudinal gradient. Scientific Data 5:170197.
Kame'eleihiwa, Lilikalā. 1992. Native Land and Foreign Desires: Pehea Lā E Pono Ai? Bishop Museum Press, Honolulu.
Kearns, F. R. 2021. Getting to the Heart of Science Communication: A Guide to Effective Engagement. Island Press, Washington.
Kidwell, S. M. 2013. Time-averaging and fidelity of modern death assemblages: building a taphonomic foundation for conservation palaeobiology. Palaeontology 56:487–522.
Kidwell, S. M. 2015. Biology in the Anthropocene: Challenges and insights from young fossil

records. Proceedings of the National Academy of Sciences 112:4922–4929.
Kimmerer, R. W., and R. W. Kimmerer. 2013. The Fortress, the River and the Garden. Pages 49–76 *in* A. Kulnieks, D. R. Longboat, and K. Young, editors. Contemporary Studies in Environmental and Indigenous Pedagogies. SensePublishers, Rotterdam.
King, T. L. 2019. The Black shoals: Offshore formations of Black and Native studies. Duke University Press.
Latulippe, N., and N. Klenk. 2020. Making room and moving over: knowledge co-production, Indigenous knowledge sovereignty and the politics of global environmental change decision-making. Current Opinion in Environmental Sustainability 42:7–14.
Lewis, S. L., and M. A. Maslin. 2015. Defining the Anthropocene. Nature 519:171–180.
Liboiron, M. 2021a. Pollution is colonialism. Page Pollution Is Colonialism. Duke University Press.
Liboiron, M. 2021b, January 18. Firsting in Research.
Liboiron, M. 2021c. Decolonizing geoscience requires more than equity and inclusion. Nature Geoscience 14:876–877.
Liboiron, M., and J. Lepawsky. 2022. Discard studies: Wasting, systems, and power. MIT Press.
Louis, R. P. 2007. Can You Hear us Now? Voices from the Margin: Using Indigenous Methodologies in Geographic Research. Geographical Research 45:130–139.
Maffie, J. 2009. 'In the end, we have the Gatling gun, and they have not': Future prospects of indigenous knowledges. Futures 41:53–65.
McAllister, T. 2022. 50 Reasons Why There Are No Māori in Your Science Department. Journal of Global Indigeneity 6:1–10.
McAllister (Te Aitanga a Māhaki), T., S. Naepi (Naitasiri/Palagi), L. Walker (Whakatōhea), N. Gillon (Ngāti Awa Ngāiterangi), Ashlea, P. Clark (Ngāpuhi), N. T. Lambert (Ngāti Mutunga Emma, A. B. McCambridge, N. T. Thoms (Ngāi Tahu -Ngāti Kurī Channell, N. T. Housiaux (Ātiawa ki Whakarongotai Ngāti Raukawa, Te Atihaunui a Pāpārangi), Jordan, N. P. Ehau-Taumaunu (Ngāti Uepōhatu Te Ātiawa, Te Whānau-ā-Apanui), Hanareia, N. T. Waikauri Connell (Atihaunui a Pāpārangi Tūwharetoa), Charlotte Joy, T. Keenan (Te Atiawa Rawiri, T. Ā. Thomas (Ngāti Mutunga o Wharekauri Ngāi Tohora, Rapuwai), Kristie-Lee, A. Maslen-Miller (Samoan), N. T. Tupaea (Ngāti Koata Ngāti Kuia, Te Aitanga a Māhaki, Ngāti Mūtunga), Morgan, N. T. Mauriohooho (Ngāti Raukawa ki Wharepuhunga Ngāti Maniapoto, Waikato), Kate, C. Puli'uvea, H. Rapata (Kāi Tahu), S. A. Nicholas (Ngā Pū Toru -'Avaiki Nui), R.-N.-A.-R. Pope (Ngā Ruahine), S. A. F. Kaufononga, T. R. Reihana (Nga Puhi Te Whakatōhea, Ngai Tūhoe), Kiri, T. Fleury (Te Atiawa Kane, N. Camp (Samoan), G. M. Rangikahiwa Carson (Ngāti Whakaue), J. L. Kaulamatoa (Tongan/Pālangi), Z. L. Clark (Tongan/Pālangi), M. Collings (Te Rarawa), P. H. Bell (Ngāti Maniapoto Georgia M., T. A. Henare (Te Rarawa Kimiora, R. Reiri (Ngāti Kahungunu Ngāi Tahu), Kylie, P. Walker (Whakatōhea), S. Escott (Ngāti Kahungunu Palagi), Kirita-Rose, J. Moors, B.-J. Wilson (Ngāti Tūwharetoa), G. Laita (Samoan Olivia Simoa, T. W.-A. Maxwell (Te Whakatōhea Ngāitai, Ngāti Porou, Ngāti Tūwharetoa), Kimberley H., S. Fong (Ngā Puhi), K. T. Parata (Te Atiawa ki Whakarongotai Kati Mamoe, Kati Kuri), Riki, M. Meertens, N. R. Aston (Tangahoe Connor, N. R. Taura (Ngāi Te Rangi Ngāti Hauā, Ngāti Tūwharetoa, Ngāti Uenuku), Yvonne, N. Haerewa (Ngāti Porou), H. Lawrence (Samoan/Tokelauan/Pālangi), and T. Alipia. 2022. Seen but unheard: navigating turbulent waters as Māori and Pacific postgraduate students in STEM. Journal of the Royal Society of New Zealand 0:1–19.
McClenachan, L., A. B. Cooper, M. G. McKenzie, and J. A. Drew. 2015. The importance of

surprising results and best practices in historical ecology. BioScience 65:932–939.
McGregor, D. 2004. Coming full circle: Indigenous knowledge, environment, and our future. American Indian Quarterly 28:385–410.
McGregor, D. P. 2007. Nā kua ʻāina: Living Hawaiian culture. University of Hawaii Press.
McGregor, D., S. Whitaker, and M. Sritharan. 2020. Indigenous environmental justice and sustainability. Current Opinion in Environmental Sustainability 43:35–40.
Meyer, M. A. 2001. Acultural assumptions of empiricism: A native Hawaiian critique. Canadian Journal of Native Education 25:188.
Mohamed, J., P. Anderson, and V. Matthews. 2022, March 28. Indigenous peoples across the globe are uniquely equipped to deal with the climate crisis - so why are we being left out of these conversations? The Conversation.
Morishige, K., P. Andrade, P. Pascua, K. Steward, E. Cadiz, L. Kapono, and U. Chong. 2018. Nā Kilo ʻĀina: Visions of Biocultural Restoration through Indigenous Relationships between People and Place. Sustainability 10:3320–3368.
Nelson, M. K., and D. Shilling. 2018. Traditional ecological knowledge: Learning from Indigenous practices for environmental sustainability. Cambridge University Press.
Norgaard, K. M. 2019. Salmon and acorns feed our people: Colonialism, nature, and social action. Rutgers University Press.
Norton-Smith, K., K. Lynn, K. Chief, K. Cozzetto, J. Donatuto, M. H. Redsteer, L. E. Kruger, J. Maldonado, C. Viles, and K. P. Whyte. 2016. Climate change and indigenous peoples: a synthesis of current impacts and experiences. Gen. Tech. Rep. PNW-GTR-944. Portland, OR: US Department of Agriculture, Forest Service, Pacific Northwest Research Station. 136 p. 944.
Prescod-Weinstein, C. 2022, January 11. Becoming Martian. The Baffler 61.
Pukui, M. K., and S. H. Elbert. 1986. Hawaiian Dictionary: Hawaiian-English English-Hawaiian Revised and Enlarged Edition. University of Hawaii Press.
Rodriguez, A. B., B. A. McKee, C. B. Miller, M. C. Bost, and A. N. Atencio. 2020. Coastal sedimentation across North America doubled in the 20th century despite river dams. Nature Communications 11:3249.
Sibert, E., M. Friedman, P. Hull, G. Hunt, and R. Norris. 2018. Two pulses of morphological diversification in Pacific pelagic fishes following the Cretaceous–Palaeogene mass extinction. Proceedings of the Royal Society B: Biological Sciences 285:20181194.
Simpson, L. B. 2017. As We Have Always Done: Indigenous Freedom through Radical Resistance. U of Minnesota Press.
Simpson, L. R. 2004. Anticolonial Strategies for the Recovery and Maintenance of Indigenous Knowledge. American Indian quarterly 28:373–384.
Smiles, D. 2020, October 26. The Settler Logics of (Outer) Space. Society and Space.
Smith, L. T. 1999. Decolonizing Methodologies. University of Otago Press, Dunedin.
Smith, L. T. 2006. Researching in the Margins Issues for Māori Researchers a Discussion Paper. AlterNative: An International Journal of Indigenous Peoples 2:4–27.
Stevens, K. R., K. S. Masters, P. I. Imoukhuede, K. A. Haynes, L. A. Setton, E. Cosgriff-Hernandez, M. A. Lediju Bell, P. Rangamani, S. E. Sakiyama-Elbert, S. D. Finley, R. K. Willits, A. N. Koppes, N. C. Chesler, K. L. Christman, J. B. Allen, J. Y. Wong, H. El-Samad, T. A. Desai, and O. Eniola-Adefeso. 2021. Fund Black scientists. Cell 184:561–565.
Styres, S., and D. Zinga. 2013. The Community-First Land-Centred Theoretical Framework: Bringing a ‘Good Mind’ to Indigenous Education Research? Canadian Journal of Education /

Revue canadienne de l'éducation 36:284–313.
Szabó, P. 2015. Historical ecology: past, present and future. Biological Reviews 90:997–1014.
Todd, Z. 2015. Indigenizing the anthropocene. Art in the Anthropocene: Encounters among aesthetics, politics, environments and epistemologies:241–54.
Tuck, E. 2018. Biting the university that feeds us. Dissident knowledge in higher education:149–167.
Tuck, E., and M. McKenzie. 2014. Place in research: Theory, methodology, and methods. Routledge.
Tuck, E., and K. Yang. 2012. Decolonization is not a metaphor. Decolonization: Indigeneity, education & society, 1 (1), 1–40.
Tuck, E., and K. W. Yang. 2014. R-words: Refusing research. Humanizing research: Decolonizing qualitative inquiry with youth and communities 223:248.
Vaughan, M. B. 2018. Kaiaulu: Gathering Tides. Oregon State University Press, Corvallis.
Watego, C. 2021. Another day in the colony. University of Queensland Press.
Whyte, K. 2017. Indigenous climate change studies: Indigenizing futures, decolonizing the Anthropocene. English Language Notes 55:153–162.
Whyte, K. 2020. Too late for indigenous climate justice: Ecological and relational tipping points. WIREs Climate Change 11:e603.
Whyte, K. P. 2016. Is it colonial déjà vu? Indigenous peoples and climate injustice. Pages 102–119 Humanities for the Environment. Routledge.
Whyte, K. P. 2018. Indigenous science (fiction) for the Anthropocene: Ancestral dystopias and fantasies of climate change crises. Environment and Planning E: Nature and Space 1:224–242.
Wildcat, D. R. 2010. Red alert!: Saving the planet with indigenous knowledge. ReadHowYouWant. com.
Williams, A. P., J. T. Abatzoglou, A. Gershunov, J. Guzman-Morales, D. A. Bishop, J. K. Balch, and D. P. Lettenmaier. 2019. Observed Impacts of Anthropogenic Climate Change on Wildfire in California. Earth's Future 7:892–910.
Wilson-Hokowhitu, N. 2019. The past before us: Moʻokūʻauhau as methodology. University of Hawaii Press.
Wolfgramm-Rolfe, R., M. Spiller, C. Houkamau, and M. Henare. 2018. Home: Resistance, Resilience, and Innovation in Māori Economies of Well-Being. Traditional Ecological Knowledge: Learning from Indigenous Practices for Environmental Sustainability.
Wright, A. 2017, March 15. What Happens When You Tell Somebody Else's Story? https://meanjin.com.au/essays/what-happens-when-you-tell-somebody-elses-story/.